The role of cannabinoid receptors in modulation of GABAergic neurotransmission in the rat medial entorhinal cortex *in vitro*.

Nicola Helen Morgan

Doctor of Philosophy

Aston University

June 2008

Aston University

The role of cannabinoid receptors in modulation of GABAergic neurotransmission in the rat medial entorhinal cortex *in vitro*.

Nicola Helen Morgan, Doctor of Philosophy.

Year of submission 2008.

Summary

Type 1 cannabinoid receptors (CB_1R) have a well established role in modulating GABAergic signalling with the central nervous system, and are thought to be the only type present at GABAergic presynaptic terminals. In the medial entorhinal cortex (mEC), some cortical layers show high levels of ongoing GABAergic signalling (namely layer II) while others show relatively low levels (layer V). Using whole-cell patch clamp techniques, I have, for the first time, demonstrated the presence of functional CB_1R in both deep and superficial layers of the mEC. Furthermore, using a range of highly specific ligands for both CB1R and CB2R, I present strong pharmacological evidence for CB_2Rs being present in both deep and superficial layers of the mEC in the adult rat brain.

In brain slices taken at earlier points in CNS development (P8-12), I have shown that while both CB_1R and CB_2R specific ligands do modulate GABAergic signalling at early developmental stages, antagonists/ inverse agonists and full agonists have similar effects, and serve only to reduce GABAergic signalling. These data suggest that the full cannabinoid signalling mechanisms at this early stage in synaptogenesis are not yet in place. During these whole-cell studies, I have developed and refined a novel recording technique, using an amantidine derivative (IEM1460) which allows inhibitory postsynaptic currents to be recorded under conditions in which glutamate receptors are not blocked and network activity remains high.

Finally I have shown that bath applied CB_1 and CB_2 receptor antagonists/ inverse agonists are capable of modulating kainic acid induced persistent oscillatory activity in mEC. Inverse agonists suppressed oscillatory activity in the superficial layers of the mEC while it was enhanced in the deeper layers. It seems likely that cannabinoid receptors modulate the inhibitory neuronal activity that underlies network oscillations.

Key words; G-protein coupled receptors, temporal lobe, cannabis

Acknowledgements

Great thanks to my supervisor Dr G. Woodhall, for all his support and guidance, during my sometimes fraught PhD.

Thank you to all my work colleges for all their support and friendship throughout my PhD.
Thanks also to all my friends who where there with liquid support, laughter and, a little craziness on the days research was too much.

Finally a massive thank you to my lovely Dad and sisters, for always being there, and a special thank you to my mum, for teaching me to never stop asking questions

Table of Content

List of figures and tables

Abbreviations

KA Kainate

EC Entorhinal Cortex

PHR Parahippocampal Region

lEC Lateral Entorhinal Cortex

mEC Medial Entorhinal Cortex

THC Δ 9-tetrahydrocannabidol

CB_1R cannabinoid receptor type 1

CB_2R Cannabinoid receptor type 2

2-AG 2-arachidonyl glycerol

GABA γ-aminobutyric acid

AEA Anandamide

GP Globus pallidus

sIPSCs Spontaneous Post Synaptic Inhibitory Currents

eIPSCs Evoked inhibitory post synaptic currents

mIPSCs Mini inhibitory post synaptic currents

mEPSC Miniature excitatory post synaptic current

AD Alzheimer's disease.

Ca^{2+} Calcium

CNS Central Nervous System

GluRs Glutamate Receptors

AMPA *α*-amino-3-hydroxy-5-methyl-4-isoxazolepropionate receptors

NMDA N-methyl-D-aspartate

mGluRs metabotropic glutamate receptors.

DSI depolarisation suppression of inhibition

DSE Depolarisation suppression of excitation

IEI Inter event interval

2-AP5 D-(-)-2-Amino-5-phosphonopentanoic acid

CNQX 6-Cyano-7-nitroquinoxaline-2,3-dione

IEM 1460 N,N,N,-Trimethyl-5-[(tricyclo[3.3.1.13,7]dec-1-ylmethyl)amino]-1-pentanaminiumbromide hydrobromide.

aCSF artificial cerebrospinal fluid.

NT Neurotransmitter

ACPA Arachidonylcyclopropylamide

AM-251 N-(Piperidin-1-yl)-5-(4-iodophenyl)-1-(2,4-dichlorophen yl)-4-methyl-1H-pyrazole-3-carboxamide

JWH-133 (6aR,10aR)-3-(1,1-Dimethylbutyl)-6a,7,10,10a-tetrahydro -6,6,9-trimethyl-6H-dibenzo[b,d]pyran

AM-630 6-Iodo-2-methyl-1-[2-(4-morpholinly)ethyl]-1H-indol-3-y l](4-methoxyphenyl) methanone

JTE-907 N-(1,3-Benzodioxol-5-ylmethyl)-1,2-dihydro-7-methoxy-2- oxo-8-(pentyloxy)-3-quinolinecarboxamide

ICT Inhibitory Charge Transfer

NICT Normalised Inhibitory Charge Transfer

TA Temporoammonic

TPMPA 1, 2, 5, 6-tetrahydropyridin-4-yl)methylphosphinic acid

NAPE N-arachidonoylphosphatidylethanolamine

PI Phosphatidylinositol

POMC neurones Proopiomelanocortin neurones

TTX Tetrotoxin

GD Gestational Day

P Postnatal day

CHAPTER 1
General Introduction

1.0 INTRODUCTION

1.1 The Entorhinal Cortex

The entorhinal cortex (EC) is found within the temporal lobe and is part of a complex in the brain known as the parahippocampal region (PHR) (Witter & Wouterlood, 2002). As interest in the PHR grows amongst researchers, the important roles played by the EC in many aspects of brain function are becoming increasingly apparent. For example, the EC has been linked with learning and memory, especially spatial memory (Steffenach *et al.,* 2005; Brun *et al.,* 2005; Brun *et al.,* 2008; Moser 2006), and, through connectivity with the amygdala, with emotional memory (Meunier and Bachevalier, 2002; Meunier *et al.,* 2006). Damage to, or altered function in, the EC have also been linked to various brain disorders, including epilepsy (Du *et al* 1995., Fountain *et al* 1998., Wozny *et al* 2005; Jamali *et al.,* 2006), Alzheimer's disease (AD; Gómez-Isla *et al.,* 1996; Price *et al.,* 2001) and schizophrenia (Akil & Lewis 1997; Krimer *et al.,* 1997). Many studies have investigated the anatomy and connectivity of the EC (see below) and now an increasing amount of work is being done to enhance the understanding of the physiological properties of both EC neurones (Glovelli *et al.,* 1997, 1999) and neuronal networks (Cunningham *et al.,* 2003; 2006).

As part of the PHR, the EC is strongly interlinked with the hippocampal formation, including the dentate gyrus, subicular complex and the hippocampus proper. The EC plays an important role, mediating and modulating information flow between neocortex and the hippocampal formation. (Witter *et al.,*1989; Insausti *et al.,* 1997*)*. The work of Witter *et al.* (1989) and others such as Burwell (2000) and Insausti *et al.,* (2002) has shown that the human (Mikkonen 1999) rodent and monkey (Insausti *et al.,* 1997) entorhinal cortices are similar in connectivity and in the architecture of different cell types and their organisation into layers.

1.1.1 THE ANATOMY OF THE EC

The EC is located on the ventromedial surface of the temporal lobe (**Fig.1.1**; Garey, 1994; Insausti *et al.*, 1995). Rostrally, the EC associates with the amygdaloid complex while caudally, it associates with the hippocampal formation.

Fig 1.1 Schematic diagram of the left side of the rat brain.

Diagram showing the approximate position of the EC (shaded area). **EC** entorhinal cortex **OB** olfactory bulb; **FL** Frontal Lobe; **CB** cerebellum; **PL** parietal lobe; **TL** temporal lobe; **OL** occipital lobe.

Over the years, the EC has been subdivided in several different ways, however, for the purpose of this thesis, the subdivisions are as described by Witter *et al.*, (1989). Hence, if we consider the EC as having two major subdivisions, then in an intact brain the lateral entorhinal cortex (lEC) is identified as a triangular shape in the rostrolateral part of the brain and the medial entorhinal cortex (mEC) makes up the caudiomedial section of the EC (**Fig.1.2**).

Fig 1.2 Schematic diagram of a ventral view of left hemisphere of a rat brain.

Diagram illustrating the subdivisions of the EC. **LEC** lateral entorhinal cortex **MEC** medial entorhinal cortex; **OB** olfactory bulb; **PPC** prepiriform cortex; **CB** cerebellum.

Nominally, the EC has six layers with layer I being a molecular layer where very few cells are present, and layers II, III, V and VI being cellular layers. Layer IV is considered to be relatively sparsely populated, and has been termed *lamina dessicans*. The arrangement of the cells in specific layers differs between the lEC and the mEC (Lopes da Silva *et al.,* 1990). In the lEC, cells of layers II and III are easily distinguished, with layer II neurones being arranged in clusters or 'island' formations while layer III neurones are more evenly dispersed. In the mEC the distinction between layers II and III is harder to discern as layer II neurones do not show clustering (Lopes da Silva *et al.,* (1990). However, this writer has noted that while layer II of the mEC shows a random cell dispersal it appears that in layer III the neurones tend to align vertically. The transition between layer III and IV is clear in the mEC but less noticeable in the lEC (Lopes da Silva *et al.,* 1990). In both lEC and mEC, layers V is densely packed with relatively small neurones compared to superficial layers.

1.1.2 Entorhinal Cortex Connectivity

It was long believed that the EC was a simple transitional area between the allocortical organisation of hippocampus and the isocortical structure of neocortex, and it has been termed periallocortex, as well as periisocortex. However, anatomical research has revealed that it is a highly organised area showing a wealth of both extrinsic and intrinsic connections, and playing a key role in shaping cortical input to hippocampus and hippocampal output to cortical regions.

1.1.2.1 Extrinsic Connections: Inputs

The majority of inputs to the EC come from cortical areas, and Burwell & Amaral (1998) estimate that the EC receives approximately a quarter of its inputs from temporal cortical areas. Furthermore, Burwell & Amaral (1998) identify the perirhinal, postrhinal and ventral temporal associational cortices as providing the majority of these temporal inputs. This is further substantiated by the work of Van Hosen *et al.,* (1972); Van Hosen & Pandya (1975) and Insausti *et al.,* (1997) who confirmed the perirhinal and parahippocampal as providing the majority of inputs to the EC. Temporal inputs to EC appear to terminate in superficial layers (layers I-III; Naber *et al.,* 1999; Witter & Gröenewegen 1984). Room & Gröenewegen (1986), working in the cat, showed that fibres from olfactory related areas, the hippocampus and other parts of the limbic cortex project to the EC. As with other inputs to the EC these afferents show a high degree of organisation with the fibres from the olfactory structures terminating predominantly superficially, whereas hippocampal and limbic cortical afferents are directed mainly to layers deep to the *lamina dessicans* (namely layers V and VI). Afferents from mesocortical areas of the brain terminate in both deep and superficial layers of the EC.

Insausti *et al.,* (1987), working in the monkey, identified projections to the EC arising from several subcortical regions including the amygdaloid complex,

claustrum, basal forebrain, thalamus hypothalamus and the brain stem, as well as other structures from within the PHR such as the subiculum. Kloosterman *et al.,* (2003) used anteroreterograde tracers to show that subicular projections to the EC terminate mainly in the deep layers (V and VI) with only a minority of subicular projections terminating in superficial layers (II and III) of the EC. Kloosterman *et al., (*2003) also showed that there was topographical organisation of the projections from the subiculum to the EC.

1.1.2.2 Extrinsic Connections: Outputs

The EC reciprocates the majority of its connections, hence, the predominant outputs of the EC go to the limbic, paralimbic and olfactory areas, but it also sends projections to the neocortex (Lopes da Silva *et al.,* 1990).

The superficial layers (layers II and III) are the point of origin of efferents that make up the most important inputs to the hippocampal formation. The perforant path (PP) is an excitatory pathway that runs from the EC to the hippocampus. Projections that give rise to the PP can be split into two subdivisions, determined by their point of origin. Projections arising from layer III of the EC terminating in CA1 of the hippocampus form the temporoammonic path, while layer II EC projections terminating in the dentate gyrus, CA2 and CA3 of the hippocampus comprise the perforant path proper, Steward & Scoville, (1976); Witter and Groenwegen (1984).

Projections from the EC to the postrhinal cortex and perirhinal cortex show the same organised sites of origin and termination as seen with other inputs and outputs of the EC. Projections arising from the mEC and lEC have different sites of termination in the postrhinal and perirhinal cortices. The majority of the outputs arising from the mEC terminate in the caudal region of the postrhinal cortex, while the majority of the EC projections to the perirhinal cortex arise from the lEC,

however, 1-2% of the EC-perirhinal projections arise from the mEC (Burwell & Amaral 1998).

In the rat, the EC projects predominantly to the allocortical and periallocortical limbic areas including parts of the subicular complex (Witter & Groenwegen, 1984), it would appear that the majority of connections to the subiculum come from the LEC as Köhler *et al.,* (1986) showed that the mEC had sparse connections to the presubiculum, parasubiclum and subiculum the ventral retrosplenial and infralimbic cortices and olfactory related areas.

Working in the cat entorhinal cortex, Witter & Gröenwegen (1986) showed projections form the entorhinal cortex to dorsal and ventral striatum, parts of the amygdala and the claustrum. The majority of the subcortical projections arise from the LEC while mEC provides a much smaller output and sends no fibres to the amygdala. The subcortical projections from the EC are topographically organised along the mediolateral axis of the parahippocampal cortex, these projections arise from the deep layers of the EC. It has been noted that the EC distributes fibres to widespread subcortical and cortical structures, e.g. the EC projects too many regions of the forebrain including the septum the diagonal band of Broca, the striatum, substantia innominata, the amygdaloid complex and the claustrum. Witter & Groenwegen (1986) also noted that projections from the EC have a topographical and laminar organisation within target structures.

Insausti *et al.,* (1997) further defined EC connectivity and identified projections from the EC to lateral frontal (motor) parietal (somatasensory) temporal (auditory) occipital (visual) anterior insular and cingulate cortices. In general, the terminals of these projections from the EC are found in the superficial layers of the target cortices. A summary of the extrinsic connectivity of the EC is shown in **Fig. 1.3**.

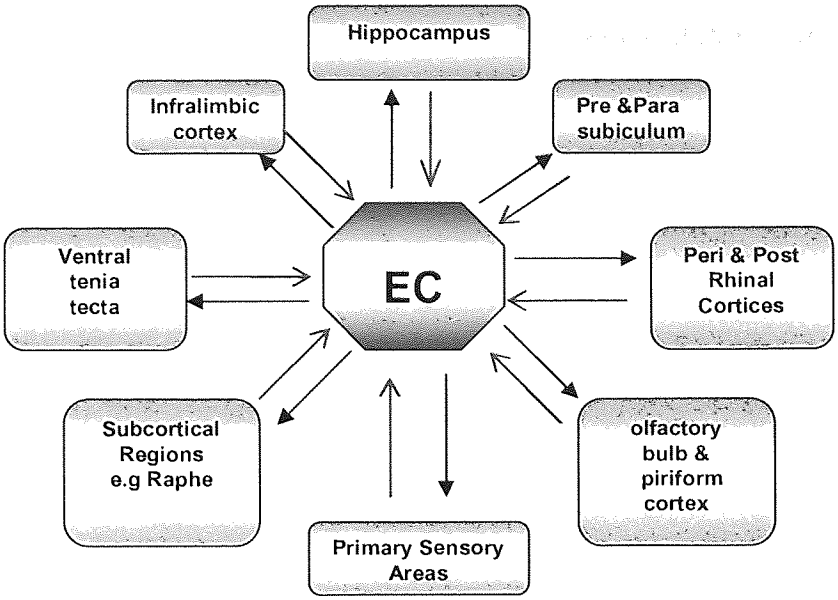

Fig 1.3 Summary of connections.

Summary of the main extrinsic connections of the entorhinal cortex, Red = inputs black = outputs

1.1.2.3 Intrinsic connections of the EC

Köhler *et al.,* (1986) used injections of phytoheamagglutinin from *phaseolus vulgaris* (PHA-L) to trace neurones and their projections. With this technique, these authors identified that in layer II of the mEC, neurones had axons that ran horizontally throughout the layer but there were also vertical projections to layer I of the MEC. Köhler *et al.,* (1986) also identified axons from the superficial layers (mainly II and III) that projected towards the deep layers, however, no sites of termination (synapse formation) were identified for these projections in the deep layers and it was concluded that they are merely passing on route to their intended targets in the dentate gyrus and hippocampus.

Projections originating from the deep layers are far more divergent than those originating in superficial layers. Hence, in layer II the majority of intraentorhinal projections stay within the layer, while those from deeper layers appear to traverse all layers of the entorhinal cortex. It has long been known that neurones from the deep layers of the EC have projections that run to the superficial layers. The work of Golveli *et al.,* (1999) and Köhler *et al.,* (1986), showed that manipulation of deep layer EC neurones brought about a change in the activity of neurones in the superficial layers.

A detailed study of the types of synapses formed by deep to superficial projections in the EC and the types of postsynaptic targets of these connections was made by van Haeften *et al.* (2003). This study showed that the majority of synapses formed by layer V projections to the superficial layers are asymmetrical (97% of synapses formed by layer V to layer I/II) suggesting that the input from the deep to superficial layers is almost exclusively excitatory, since only excitatory synapses are believed to show asymmetry at the ultra-structural level. The remaining 3% of the projections terminating in layer I/II were symmetrical, suggesting that deep layers only provide a weak inhibitory input to superficial

layers. When postsynaptic targets of deep to superficial projections were studied, van Haeften *et al.* (2003) concluded that 37.5% of the layer I/II asymmetrical synapses terminating in layer I/II connected with smooth dendritic shafts, suggesting that the postsynaptic target was a GABAergic interneurone, since principal (excitatory) neurones in EC are spiny, and inhibitory neurones aspiny (Germeroth *et al.,* 1989; Wouterlood *et al.,* 1995, 2000). Ca. 56.5% of the total asymmetrical synapses seen had a dendritic spine as its post synaptic target indicating a principal neuronal target. The remaining 6% of synapses are symmetrical and are believed to be inhibitory. All symmetrical synapses had a dendritic shaft as the postsynaptic target.

The distribution of asymmetric *versus* symmetric synapses would seem to indicate that the majority of the input from deep to superficial areas in the mEC is excitatory. This fits with the findings of Gloveli *et al.,* (2001) that neurones projecting from deep to superficial layers are immunohistochemically negative for GABA.

1.2 Cell of the entorhinal cortex

The cells of the entorhinal cortex were first identified by Lorente de Nó in 1933, using the Golgi-silver impregnation technique. Lorente de Nó identified neurones in the entorhinal cortex by their morphology alone. Since 1933, techniques have advanced and now neurones can be identified by their morphology, chemical markers and electrophysiological characteristics. Here I will give a brief outline of the cell types present in the EC based on their morphology, chemical markers and electrophysiological characteristics. In addition to this I shall review that intrinsic connectivity shown by the neurones of the EC.

1.2.1 Layer I

Lorente de Nó (1933) and Germeroth *et al.,* (1989) identified two cell types within layer I of the EC. These were spiny multipolar cells and horizontal cells, the projections of both these cell types appear to stay within layer I. Of the neurones in layer I some are positive for GABA and these neurones are believed to act as interneurones for layer I providing feedforward inhibition to principal cells (Finch *et al.,* 1988). Surprisingly, a significant proportion of layer I neurones appear to comprise excitatory interneurones which express calbindin but not GABA.

1.2.2 Layer II of the EC

Layer II of the EC has various cell types, the main principal neurones being stellate cells and horizontal cells. When Lorente de Nó (1933) first identified stellate cells he termed them star cells due to their morphology. In the mEC, stellate cells account for the largest proportion of neurones present in the mEC at approximately 65% (Klink & Alonso (1997); Alonso & Klink (1993); Buckmaster *et al.,* (2004).

In addition to morphological identification, Alonso and Klink (1993) used electrophysiological techniques to identify different cell types in the mEC. Two different groups of projection neurones were identified within layer II using this method. These two groups were termed stellate and non-stellate neurones. The two groups showed distinctly different electrophysiological behaviour during intracellular recording. In 1997, Klink and Alonso were able to further differentiate between the stellate and non stellate cells previously identified, by using *in vitro* injections of biocytin to fill neurones in layer II of the mEC. This technique revealed that within the EC there were the stellate cells which made up 65% of the projection cells in the EC and the group of cells that had previously been

determined non stellate cells could be subdivided into pyramidal like morphology 32% and horizontal morphology 2%. Stellate cells are the main projection neurones of layer II and are considered to be principal neurones. Germroth *et al.,* (1989), Wouterlood *et al.,* (1995) and Wouterlood *et al.,* (2000) have all shown that principal neurones in the superficial layers of the EC (such as stellate cells) tend to be spiny and as such tend to be excitatory in nature (interneurones are usually aspiny). The horizontal cells seen in layer II are so named due to the horizontal orientation of the somata, dendrites and axons. These neurones appear smooth in nature as opposed to the spiny description of principal cells. All the projections of these horizontal neurones remain within layer II (Jones & Bühl (1993; Germeroth *et al.,* 1991), and these neurones are believed to be inhibitory in nature. Jones & Bühl (1993) showed that basket cells (a type of interneurone) were present in layer II of the EC.

1.2.3 Layer III of the EC

Gloveli *et al.,* (1997) split the cell types of layer III of the mEC into four different types. Types one and two were excitatory projection cells that can be differentiated by their electrophysiological characteristics. These projection neurones give rise to the layer III contribution to the perforant path which is more commonly known as the temporoammonic path (TA), projecting to CA1 of the hippocampus Witter *et al.,* (1989). The apical process of both type 1 and type 2 projection neurones both reached the cortical surface where they showed a branching distribution in the superficial layers. Based on the structure of the two projections cells Gloveli *et al.,* suggest that type 1 cells receive largely excitatory inputs while type 2 cells predominantly receive inhibitory inputs. Finally when it came to projections to deeper layers of the EC it was found the basal dendrites of

type one cells extended in to layer IV of the EC while the basal dendrites of type 2 projection cells remained within layer III.

The other two cell types identified by Gloveli *et al.,* (1997) have small pyramidal cell bodies and are believed to have projections that remain with in the EC, based on this it is presumed that they play a role in the local circuitry of the EC. The two cell types in this group appear to have different orientation of their projections such that the type 3 neurones had two branches, one that went to the deeper layers of the EC and one which ramified within layer III itself. Finally, the type four neurones showed axonal projections only to the superficial layers namely layers I and II.

1.2.4 Layer IV

As already discussed, layer IV is known as the *lamina dessicans* and is usually known as the layer that separates the deep and superficial layers of the EC, however while it is cell sparse that is not to say it has no cells at all. Scattered pyramidal cells and fusiform cells have been identified with in the layer (Lingenhöhl, & Finch 1991). It is important to note that while layer IV is mainly a dense bundle of fibres it does not prevent the apical dendrites of layers V and VI projecting to the superficial layers of the EC as shown in the work of van Haeften *et al.,* (2003).

1.2.5 Layer V of the EC

Lorenete de Nó (1933) described two main cell types in layer V of the mEC. These were horizontal polygonal neurones and pyramidal type neurones. More recently these findings were confirmed in the work of Gloveli *et al.,* (2001) and van Haeften *et al.,* (2003). Of these two neuronal types it appears that the dendrites of the horizontal neurones remain in the deep layers while the

dendrites of the pyramidal neurones traverse all layers of the mEC (deep to superficial) forming synapses in all the superficial layers (layers I, II and III, van Haeften *et al.*, (2003).

1.2.6 Layer VI

Application of neurobiotin to layer VI revealed neurones with a small pyramidal cell body and apical projections that cross the *lamina dessicans* and terminate throughout the superficial layers (I, II, and III).

1.3 Glutamate Receptors of the EC

Although for the purpose of this work the focus is on GABAergic signalling, it is important to note that there is also excitatory signalling with in the entorhinal cortex, and this provides the stimulus for endogenous cannabinoid release. The primary excitatory neurotransmitter in the central nervous system is L-glutamate.

There are 2 broad groups of groups of glutamate receptors (GluRs). The ionotropic glutamate receptors (iGluRs) which are subdivided into 3 further groups N-methyl-D-aspartate (NMDA) receptors and the non NMDA receptors α-amino-3-hydroxy-5-methyl-4-isoxazolepropionate (AMPA) receptors and kainate receptors. In addition to the iGluRs there is also a G-protein coupled receptor group of GluRs known as metabotropic receptors (mGluRs; Conn & Pin, 1997; Ozawa *et al.,* 1998).

1.3.1 AMPA receptors

AMPA and kainate receptors mediate the fast excitatory neurotransmission at most synapses in the central nervous system (for review, see Ozawa *et al.,* and 1998). AMPA receptors are made up of 4 subunits, namely GluR1-4, and these can exist in two forms known as flip and flop. In addition, splice variants of the

GluR1-4 subunits exist creating even more variation within the AMPA receptor family. Depending on the subunits present in the receptor homo- or heterooligomer, the permeability of AMPA receptors to various ions is altered. Hence, AMPA receptor subtypes display different functional properties (Dingledine *et al.,* 1997; Bettler & Mulle, 1995 for full reviews). The most notable difference in ion permeability relates to Ca^{2+}. Homomeric receptors made up of GluR2 subunits display little permeability to Ca^{2+} while GluR1, GluR2 or GluR3 homomeric AMPA receptors are highly permeable to Ca^{2+}.

AMPA receptors are distributed thorough out the central nervous system where they are believed to mainly be located postsynaptically (Dingledine *et al.,* 1999) however there is also evidence for presynaptic location as well (Satake *et al.,* 2000). It appears that the different variants of AMPA receptor are differentially distributed through out the brain (Keinänen *et al.,* 1990).

1.3.2. Kainate receptors

Like AMPA receptors, kainate receptors (KAR) mediate the rapid phase of excitatory transmission, these receptors can exist in both heteromers and homomeric forms. The homomeric channels are believed to be made of GluR5, GluR6 and GluR7 subunits and show a low affinity for [^{3}H]-Kainate, while the heteromeric kinate channels are believed to have KA1 and KA2 subunits and have a high affinity for [^{3}H]-Kainate (for full review see Bettler & Mulle 1995) The KA1 and KA2 subunits are co expressed with GluR7 and they are unable to form functional channels on their own (Bettler *et al.,* 1992; Werner *et al.,* 1991). Kainate receptors are located both presynaptically (Represa *et al.,* 1987) and postsynaptically (Petralia *et al.,* 1994) and are found throughout the brain.

It has also been shown that kainate receptors play a metabotropic role in the modulation of transmitter release via G protein coupled and PKC dependent mechanisms. (Cunha *et al.,* 1999, Rodriguez-Moreno & Lerma 1998).

1.3.3 NMDA receptors

NMDA receptors are heteromers that consist of one NR1 subunit and then one or more of the NR2A-D subunits, in total it is believed that each heteromeric receptor contains a total of 5 subunits (for full reviews see Ozawa *et al.,* 1998; McBain & Mayer, 1994). NMDA receptors are distributed through out the brain appear to be most dense in the forbrain areas (see Ozawa *et al.,* 1998 for full review).The NMDA receptor appears to mediate the slower aspects of excitatory signalling are characterised by their relatively high permeability to Ca^{2+} (MacDermot *et al.,* 1986), and a voltage dependent block by Mg^{2+} (Mayer, *et al.,* 1984; Nowak *et al.,* 1984). Pharmacologically, NMDA receptors are blocked and activated by a range of chemicals the most common blockers being the antagonist 2-AP5 and the channel blocker MK801 while well know activators of NMDA receptors are NMDA, and glutamate (for a full review see McBain & Mayer, 1994).

1.4 GABA receptors

γ-amino butyric acid (GABA), is the primary inhibitory neurotransmitter in the central nervous system (CNS). There are three main receptors for GABA in the CNS, $GABA_A$ and $GABA_C$ receptors which are both ionotropic receptors (which act via ligand gated ion channels) and metabotropic $GABA_B$ receptors which (which act via G-protein coupling and second-messenger signalling mechanisms).

1.4.1 $GABA_A$ and $GABA_C$ receptors

$GABA_A$ receptors gate chloride ion channels and can be differentiated from $GABA_B$ receptors based on their sensitivity to antagonism by bicuculline and their insensitivity to baclofen (Hills & Bowery, 1981). These receptors appear to be complex in nature and can consist of a range of protein subunits. It appears that functional $GABA_A$ receptors are pentameric heteromers (Johnston, 1996b). A functional $GABA_A$ receptor must have at least 1 α and 1β subunit and at least one of the γ ,δ or ε subunits, (a number of protein subunits have been identified for $GABA_A$ receptors (α1-6, β 1-4, γ 1-4, δ, ε, ρ 1-3). Although it is thought that the ρ 1-3 may belong to the $GABA_c$ receptor (see Johnston 1996a for full review of $GABA_A$ receptors). Pharmacologically, $GABA_A$ receptors interact with a range of ligands, and these can be broadly grouped into the benzodiazepines, (which can either enhance GABA binding at $GABA_AR$ or hinder it) and barbiturates and neurosteriods which act to potentate the effects of GABA (see Johnston 1996a for full review).

Like $GABA_A$ receptors, $GABA_C$ receptors are ligand gated chloride channels however unlike $GABA_A$ receptors $GABA_C$ are not responsive to bicuculline and are not modulated by benzodiazepines. Instead $GABA_C$ receptors have their own selective ligands: (1, 2, 5, 6-tetrahydropyridin-4-yl) methyl-phosphonic acid; TPMPA) acts as an agonist at $GABA_C$ receptors and *cis*-4-aminocrotonic (CACA) activates $GABA_C$ (see Johnston 1996b for full reviews.) $GABA_C$ receptors show different response to that of $GABA_A$ receptors in their response to GABA. They bind GABA at lower concentrations than $GABA_A$ receptors , and in addition to this they do not become desensitized to GABA and their channels show a longer opening time (see Johnston 1996b for full review). $GABA_C$ receptors are formed of ρ1, ρ2, ρ3 (Johnston 1986b: Enz & Cutting 1998

for reviews), these subunits can form homomers and heteromers (Enz & Cutting 1998) using RT PCR López-Chávez *et al.,* (2005) have shown that $GABA_C$ are found throughout the CNS.

1.4.2 $GABA_B$ receptors

$GABA_B$ receptors are seven transmembrane region containing g-protein coupled receptors. To be a functional receptor the $GABA_B$ receptor must be made up of its two subunits $GABA_{B(1)}$ and $GABA_{B(2)}$ variation with the $GABA_B$ receptor is due to the various splice variants of the two subunits that exist, (for a full review see Billington *et al.,* 2001). It appears that subtypes of receptor may also determine whether the receptor is located pre or post synaptically (for a full review see Billington *et al.,* 2001). In addition to being found both pre-and post synaptically it has been shown that while $GABA_B$ receptors are distributed throughout the brain, there is evidence that the different subtypes are located in different regions (for review see Couve *et al.*, 2000). The $GABA_B$ receptors are identified by their sensitivity to baclofen, a selective agonist of $GABA_B$ receptors.

1.5 Cannabinoid Receptors

The effects of using derivatives from *Cannabis sativa* have been known an documented for centuries, but it was not until 1964 that the structure of the active ingredient Δ9-tetrahydrocannabidiol (THC) was identified due to work done in the laboratory of Mchoulams (for review see Wilson & Nicholl, 2002; Piomelli, 2003). However, isolation of the active compound did not directly lead to the discovery of cannabinoid receptors. The hydrophobic nature of THC misled researchers into thinking it was acting on cell membranes as opposed to there being specific receptors for it to interact with (Piomelli, 2003).

It was not until the development of more selective THC analogues that specific cannabinoid sensitive sites in the brain (and elsewhere) were identified by Devane *et al.,* (1988). In 1990, Matsuda *et al.* described the structure of the cannabinoid receptor now known as type 1 cannabinoid receptor (CB_1R). In 1993 another subtype of cannabinoid receptor was identified and in now known as type 2 cannabinoid receptor (CB2R) (Mackie & Hille 1992).

CB1R and CB2R are both G-protein coupled receptors (Matsuda *et al.,* 1990; Mackie & Hille 1992) and have been shown to interact with G_i, G_o and G_s proteins.

Since the discovery of specific cannabinoid receptors, much work has been done on identifying endogenous ligands (endocannabinoids), investigating the location of these receptors and learning more about how they modulate synaptic signalling, all of these areas are discussed below.

1.5.1 Endogenous Cannabinoids

In 1992 Devane *et al.* identified the first of the endocannabinoids, which they named anadamide (AEA). Then in 1995, Meachoulam *et al.* identified a second endocannabinoid that was named 2-arachidonyl glycerol (2-AG). Both AEA and 2-AG are derived from arachidonic acid and as such represent a novel class of neuromodulator that are derived from fatty acids (McAlister & Glass, 2002).

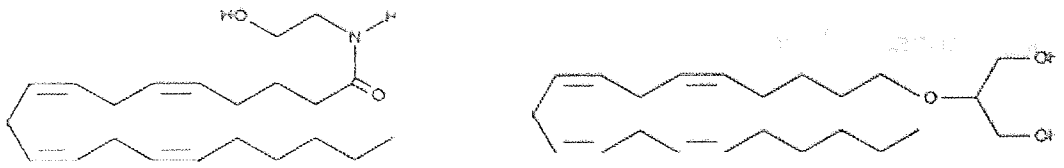

AEA 2-AG

Fig 1.4 Structure of endocannabinoids.

The structure of the endocannabinoids anandamide (arachichodonyl ethanolamine) and 2-AG (2-arachidonyl glycerol).

1.5.2 Activation and Synthesis of endocannabinoids

Neither AEA nor 2-AG is stored in intracellular compartments (unlike other neurotransmitters), instead they appear to be synthesised on demand in response to neuronal activity). Di Marzo *et al.*, (1994) showed that AEA synthesis occurred in response to stimulation in rat cortical and striatal neurones. AEA is synthesised from the precursor molecule 1,2-*sn*-di-arachidonoyl-phosphatidylcholine is transformed to N-arachidonoylphosphatidylethanolamine (NAPE) by N-acyltransferase (Hansen *et al.*, 2000 ;Di Marzo *et al.*, 1994; Sugiura *et al.*, 1996), NAPE is then transformed by the phospholipase D enzyme N-acylphosphatidylethanolamine (NAPE)-specific phospholipase D enzyme (NAPE-PLD; Okamoto *et al.*, 2004) which cleaves NAPE to give anandamide and phosphatidic acid (Di Marzo *et al.*, 1994). (for full reviews see Di Marzon *et al.*, 1998; Piomelli, 2003). 2-AG is present in the brain at levels that are 200-fold higher that AEA, however that is not to say it is a more important than AEA in terms of signalling. 2-AG happens to be an intermediate in various lipid metabolism pathways, thus at any given time there appears to be more of it in

brain tissue. Due to the fact that 2-AG is an intermediate in various pathways it is harder to ascertain the route it is synthesised by for cannabinoid signalling, however, two possible routes have been identified. The first of these routes begins with phosphatidylinositol (PI) which is hydrolysed to give 1,2, diacylglycerol (DAG) (this reaction is carried out by a phospholipase enzyme phospholipase C (PLC). DAG is then hydrolysed by the enzyme *sn*-1-DAG lipase to give the monoacylgycerol 2-AG (Stella *et al.,* 1997; Farooqui *et al.,* 1989). In 2003 two different isoforms of DAG lipase were characterised with the α isoform of the enzyme being predominantly present in adult brain while the β isoform is found predominantly in developing brains (Bisogno *et al.,* 2003). The second potential route of 2-AG synthesis again starts with PI and this is converted to a lyso-PI by phospholipase A1 (PLA1; Higgs & Glomset 1994) the enzyme lyso-PLC then hydrolyses lyso-PI to yield 2-AG (for a full review see Piomelli, 2003).

So far we have discussed how the endocannabinoids are synthesised now we shall consider what initiates their synthesis. It appears that endocannabinoid synthesis is activated by more than one route. A number of G-protein coupled receptors, namely muscarinic acetylcholine receptors (mAChRs; the M_1 and M_3 subtypes, Ohno-Shosaku 2003). Group I metabotropic glutamate receptors (mGluR1; Maejima *et al.,* 2001) and finally dopamine D2 receptors (Giuffrida *et al.,* 1999) have been linked with stimulation of cannabinoid signalling. For example D2 receptor activation leads to production and release of AEA (Giuffrida *et al.,* 1999) It would appear that activation of the group I mGluRs (namely the mGluR1 and mGluR5 subtypes) results in activation of cannabinoid signalling and leads to the suppression of both GABA and glutamate signalling (for full review see Doherty & Dingledine 2003). Activation of the postsynaptic mGluRs leads to activation of PLC as already discussed, and PLC has been implicated in the metabolic pathway that results in the formation of 2-AG and thus it is proposed

that this is possible route for interaction between mGluRs activation and cannabinoid synthesis and subsequent signalling. As both increase in intracellular Ca^{2+} and activation of PLC are needed for 2-AG production, and as activation of the group I mGluRs results in both of these events, this scenario seems plausible (Conn & Pin 1997; for full review see Doherty and Dingledine 2003). Finally it appears that endocannabinoid signalling follows two distinct routes, one of which is dependent on an increase in intracellular Ca^{2+}, and one which appears to be relatively independent of increase in Ca^{2+}. These various routes are discussed below.

1.5.2.1 AEA and 2-AG as CBR Ligands

AEA was first identified as a CBR ligand in 1992 (Devane *et al.,* 1992), concentrations of AEA in the brain are relatively low. Bazinet *et al.*, 2005 estimate that brain AEA levels in the rat were 2.45 ± 0.39pmol/g while Arai *et al.,* 2000 estimate rat brain AEA levels as being 3.37 ± 0.73 pmol/g, these differences can be attributed to different techniques used to measure brain AEA levels most notable of which being the route by which brain tissue was obtained as Bazinet *et al.*, (2005) have refined their method as they believe decapitation can cause an increase in the levels of AEA similar to that reported to occur in ischemia, and post-mortem delay. Either way these studies illustrate the relatively low levels of AEA present in "normal" whole brains. The low levels of AEA are not surprising as already stated it is believed AEA is synthesised on demand as opposed to being stored in neurones.

1.5.2.2 Reuptake and degradation of endocannabinoids.

The termination of AEA and 2-AG activity is due to removal from receptors by its reuptake in to neurones and glia cells and its subsequent intracellular degradation. Reuptake of AEA appears to occur via a selective transporter (Beltramo *et al.,* 1997; Hillard *et al.,* 1997; Ligresti *et al.,* 2004). Although properties of this transporter have been identified its molECular structure is not yet known (for a full review see Wang *et al.,* 2006; Piomelli, 2003). Once inside the cell, AEA is hydrolysed by the enzyme fatty acid amide hydrolase (FAAH) which is a membrane bound enzyme (for full reviews see Wang *et al.,* 2006; Piomelli 2003). Degradation gives arachidonic acid and ethanolamine (Cravatt *et al.,* 1996; Bracy *et al.,* 2002).

2-AG is believed to have the same transporter as AEA for reuptake into neurones (Beltramo *et al.,* 2000; Hájos *et al.,* 2004; see Wang *et al.*, 2006 for full review of endocannabinoid reuptake). However while 2-AG shares the same transporter as AEA and it can be hydrolysed by FAAH, it is not believed that FAAH is the main enzyme responsible for the intracellular degradation of 2-AG as Hájos *et al.,* 2004 showed that levels of 2-AG remains unaltered in the presence of FAAH inhibitors, which suggests that uptake and hydrolyses of 2-AG are still occurring. In addition to this, Lichtman *et al.,* (2002) showed that mice lacking FAAH can not hydrolyse AEA but still hydrolyses 2-AG. In 1999, Goparaju *et al.,* identified a specific enzyme in the porcine brain capable of hydrolyzing 2-AG, this enzyme is known a as monoacylglycerol lipase (MAGL). In addition to being present in porcine brain MAGLs have been isolated in rat (Dinh *et al.*, 2002) and human brains (Ho *et al.*, 2002). MAGLs differ from FAAH as they appear to have a cytosolic location (Dinh *et al., 2002*) in the cells rather than being attached to a membrane. Thus it appears that the endocannabinoid are synthesised and degraded via different routes although some overlap does occur.

1.5.3 Retrograde signalling

It is known that cannabinoid signalling works via a retrograde signalling method. Here, the arrival of neurotransmitters at a postsynaptic element causes depolarisation and Ca^{2+} influx into the neurone. This rise in intracellular Ca^{2+} activates the synthesis of endocannabinoids, which then leave the neurone and diffuse back to the presynaptic site where they bind with cannabinoid receptors. Binding of the cannabinoid receptors alters the influx of Ca^{2+} into the presynaptic terminal and this, in turn, alters neurotransmitter release.

1.6 DSI and Cannabinoids

Depolarising induced suppression of inhibition (DSI) was first identified as from of retrograde signalling by Llano *et al.,* (1991) working on cerebellar purkinje cells, and Pitler & Alger (1994) in pyramidal cells in the hippocampus. However it was not until the work of Wilson & Nicoll (2001) and Ohno-Shosaku *et al.,* (2001b) that endocannabinoids were identified as the signalling molecule responsible for DSI. DSI occurs when a brief depolarisation (with or without synaptic stimulation) of the postsynaptic neurone causes a transient suppression of GABA release in both spontaneous (s) and evoked (e) IPSCs during the period of DSI. Wilson & Nicoll, (2001) identified 3 properties of DSI that suggested it was mediated by endocannabinoids:

i) DSI and endocannabinoid synthesis both require calcium influx into the postsynaptic neurone to occur.

ii) DSI appears to be presynaptically mediated.

iii) DSI is blocked by pertussis toxin which implies that G-protein coupled receptors play a role. (For a full review see Wilson & Nicoll 2001)

In addition to this Ohno-Shosaku *et al.,* (2002a) showed that in CB_1R knock out mice no DSI occurred further supporting the theory that DSI is mediated by cannabinoid signalling.

1.7 Cannabinoids and Glutamatergic Signalling (DSE)

Depolarisation induced suppression of excitation (DSE), is similar to DSI described above. That is to say a brief period of depolarisation is followed by an inhibition of excitatory post-synaptic currents (EPSCs). DSE has been shown to occur in various sites through out the brain, such as the Purkinje cells (Kreitzer & Regeher, 2001), at glutamatergic inputs onto CA1 neurones (Ohno-Shosaku *et al.*, 2002a) and in the ventral tegmental area of the rat (Melis *et al.,* 2004). Like DSI, it has been shown that cannabinoids appear to mediate DSE. Both DSE and cannabinoid production require calcium influx into the post-synaptic cell to occur, using a calcium chelator such as BAPTA prevents DSE (Kreitzer & Regehr, 2001) and the CB_1R antagonists AM-251 and SR141716A prevent DSE (Kreitzer & Regehr 2001; Ohno -Shosaku *et al.,* 2002 a), while the CB_1R agonist WIN 55,212-2 occludes DSE (Kreitzer and Regehr 2001), and finally Ohno-Shosaku *et al.,* 2001 showed that no DSE occurred in CB_1R knockout mice.

As well as mediating DSE, it has been demonstrated that cannabinoids can affect glutamate signalling in general. Takahashi & Castillo (2006) showed WIN 55-212-2 decreased field EPSPs showing a decrease in glutamate release in the mouse hippocampus, and Ameri *et al.,* (1999) showed that in the rat hippocampus both WIN 55,212-2 and the endogenous cannabinoid, anandamide, reduced the amplitude of post-synaptic population spikes and that these effects could be blocked by SR141716A. Hajos *et al.,* (2001) showed WIN 55, 212-2 decreased the amplitude of evoked EPSCs in the hippocampus and that this effect could be reversed by application of the CB_1R antagonist SR141716A. Robbe *et al.,* (2001)

measured the effects of WIN 55,212-2 on evoked glutamate release in the nucleus accumbens by measuring field EPSPs and found that WIN 55,212-2 suppressed the field EPSPs and its effects could be overcome by SR 141716A (CB_1R antagonist). Robbe *et al., (2001)* also showed that WIN 55,212-2 caused an increase in the paired pulse ratio and decreased miniature excitatory post synaptic current (mEPSC) frequency but not amplitude compared to control indicating that the effects of WIN 55,212-2 on glutamate signalling were presynaptic. Application of WIN 55,212-2 also increased the paired plus ratio for glutamate signalling in the dentate gyrus (Kirby *et al.*, 1995) indicating a presynaptic location.

1.8 LOCATION OF CB_1 RECEPTORS

Autoradiography studies using the cannabinoid receptor ligand CP55,940 (Glass *et al.,* 1997., Herkenham *et al.,* 1989, 1991) shows that CB1Rs are distributed throughout neuronal tissue. These studies report a dense binding of CP55,940 in the basal ganglia, specifically the substantia nigra *pars reticulata* the globus pallidus (GP) and cerebellum. In the temporal lobe, the hippocampal formation and the EC show the highest density of staining within the cerebrum. Low density to no labelling was seen in the brain stem and spinal cord. The location of these receptors in areas that control movement and cognition helps explain the effects of THC in humans. In addition to autoradiography studies the location of CB1Rs has been investigated using immunohistochemical techniques. Studies such as those done by Tsou *et al* (1998), Moldrich & Wenger (2000) and Pettit *et al.,* (1998) concur with autoradiography studies as to the main sites of CB_1R distribution within the brain. However, immunohistochemical techniques not only allow general identification of the areas where receptors are present but it also allows identification of particular neuronal cells and fibres that possess the

cannabinoid receptors (Tsou *et al.,* 1998). Identification of the position of CB1Rs on specific neuronal types or at specific compartmental locations, positional information allows us to develop a better idea of how the receptors may mediate neuronal signalling. CB1R immunoreactivity has been shown near cell bodies, axons and dendrites of neuronal cells (Tsou *et al.,* 1998; Pettit *et al.,* 1998), however, the morphology and location of the neurones and processes expressing CB1Rs suggests that all receptors are located presynaptically on terminals of GABAergic and glutamatergic neurones (Tsou *et al.,* 1998., Katona *et al.,* 1999, 2001). More specifically, CB1Rs have been identified as being present on presynaptic terminals of GABAergic neurones in the hippocampus Hajos *et al.,* 2000; Hoffman & Lupica, 2000). In the Hajos study, CB1Rs were never found on glutamatergic neurones or terminals, but this does not mean that CB1Rs do not modulate glutamatergic signalling as well as GABAergic signalling. For example, In 2004, Melis *et al.* reported cannabinoid mediated suppression of glutamatergic transmission in the ventral tegmental area.

It has been suggested that CB_1Rs are highly likely to be found at the synapses on a specific subset of GABAergic interneurones, namely those that are immunopositive for cholecystokinin (CCK). This has been shown by Katona *et al.,* 2001, for the amygdala, and by Katona *et al.,* (1999) and Marscicano & Lutz (1999) in the hippocampus. This link between CCK positive cells and CB1 expression also occurs in many other brain regions (see Freund *et al.,* 2003 for full review). Interestingly, Katona *et al.,* (2000) also showed the CB_1Rs were located presynaptically on CCK positive interneurones in human tissue.

1.9 Location of CB_2 receptors

CB_2R are also known as peripheral cannabinoid receptors due to the long held belief that they are only expressed in immune cells and some peripheral neurones, while CB_1Rs are thought to be mainly expressed in the CNS.

CB_2R mRNA has predominantly been found in immune tissue such as the tonsils, spleen and bone marrow. More specifically CB_2R mRNA has been found in monocytes, microglial mast cells and many other immune specific cells. (see Howlett, 2002 and Cabral & Dove Pettit (1998) for reviews). Until recently it was believed that expression of CB_2Rs was limited to these areas, however development of more specific antibodies has led to the identification of CB_2Rs in the brain in relation to some disease states. Núñez *et al.,* (2007) showed that in Down's syndrome microglial and astroglia cells begin to express CB_2Rs and the FAAH enzyme involved in the hydrolyses of AEA. CB_2Rs and FAAH have also been found to be expressed in glial cells that are associated with the neuritic plaques found in suffers of Alzheimer's disease (Benito *et al.,* 2003). While the evidence for CB_2R expression in association with brains is growing, researchers such as Schatz *et al.,* (1997) and Griffin *et al.,* (1999) have been unable to show the presence of CB_2Rs in the normal CNS. However, in 2005 expression of functional CB_2Rs was shown in neurones of the brain stem (Van Sickle *et al.,* 2005) and in 2006 Gong *et al.,* used RT-PCR and immunohistochemical techniques to show that some degree of CB_2R expression was present throughout the rat brain. While the RT-PCR showed levels of CB_2R mRNA were lower than those of CB_1Rs it was still present and the immunohistochemisty indicated that CB_2Rs were present in nerve cell bodies, neuronal processes and glial cells and their processes through out the brain (Gong *et al.*, 2006). Onaivi *et al.*, (2006) working *in vivo* showed the CB_2R agonist JWH015 showed a trend for decreasing locomotor activity in mice and effects on behaviour when the performance of mice

placed in black white boxes was assed, However Onaivi *et al.,* 2006 do report some differences in the effects of JWH015 in different mouse strains and between males and females.

The majority of studies to date indicate that cannabinoid receptors are located presynaptically although postsynaptic CB_1Rs have been reported in the in the spinal cord (Hohmann *et al* 1999, Salio *et al.,* 2002). In the brain, only one group have reported the possibility of postsynaptic CB_1Rs (Endoh, 2006) in juvenile (P7-18) dissociated rat nucleus tractus solitarius neurones., As this is currently the only evidence for postsynaptic CB_1Rs, for th purpose of this thesis it will be presumed that the majority of the effects seen in response to CBR ligands are due to presynaptic CBRs.

1.10 Cannabinoid Receptor Pharmacology

The location of CB_1Rs on GABAergic neurones and the fact that the endocannabinoids AEA and 2-AG have been found in the brain indicates that they may be involved in the modulation of GABAergic signalling. Presently much work is being done to investigate the role CB_1Rs in GABAergic signalling in many of the brain regions identified as containing these receptors.

Application of the synthetic cannabinoid WIN 55,212-2 reduced the amplitude of $GABA_A$ receptor mediated eIPSCs and sIPSCs in the amygdala (Katona *et al.,* 2001; Hajos *et al.,* 2000; Hoffman & Lupica, 2000) report that in hippocampal neurones the agonist WIN 55,212-2 reduced the amplitude of eIPSCs, sIPSCs were also reduced in frequency in the presence of WIN 55,212-2 Hoffman & Lupica (2000). It appears that CB_1Rs only modulate action potential generated events, since miniature inhibitory post synaptic currents (mIPSCs), are unaffected by both the CB1R agonists CP55,940 (Hajos *et al.,* 2000; Hoffman & Lupica 2000).

The effects of WIN 55,212-2 on eIPSCs could be prevented or reversed by the synthetic CB1R antagonists SR141716A and AM-251 (Hajos *et al.,* 2000; Hoffman & Lupica, 2000) and SR141716A also blocked the effects of WIN 55,212-2 on sIPSCs. As well as using CB_1R antagonists to block the effects of WIN 55,212-2 on IPSCs, Hoffman & Lupcia (2000) reported that the effects of WIN 55,212-2 could be negated by the blockade of voltage-dependent calcium channels using cadmium. CB_1Rs only appear to act on $GABA_A$ IPSCs, as when $GABA_B$ mediated IPSCs were evoked WIN 55,212-2 had no effect on them (Hoffman & Lupica, 2000). Overall, the studies done in the hippocampus by Hajos *et al.,* (2000) and Hoffman & Lupica (2000) suggests that activation of CB_1Rs causes a decrease in calcium-dependent GABA release. Twitchell *et al.,* (1997) working in cultured rat hippocampal neurones showed that cannabinoids inhibit N and P/Q type calcium channels furthering supporting the theory that CB1Rs play a role in modulating synaptic transmission through alteration of calcium-dependent neurotransmitter release.

Much work has been done to investigate how *endocannabinoids* modulate $GABA_A$ receptor signalling. Three main effects of endocannabinoids at GABAergic terminals have been identified from work done looking at the interneuron synapses in CA1 of the hippocampus: **1)** a rise in postsynaptic intracellular calcium causes an endocannabinoid mediated suppression of GABA release this is known as DSI. **2)** Enhanced DSI (ΔDSI) this is caused by a moderate activation of postsynaptic mAChRs or group I mGluRs, and **3)** activation of mAChRs or mGluRs with a higher concentration of agonist causes a persistent relatively Ca^{2+} insensitive endocannabinoid mediated suppression of eIPSCs (Edwards *et al.,* 2005). Hence, it would appear that endocannabinoid signalling can be activated by two distinct routes, one is an increase of intracellular Ca^{2+} following depolarization of the postsynaptic neurone and the second is Ca^{2+}-independent

mechanism whereby endocannabinoid signalling is initiated by activation of group I mGluRs (Wilson & Nicoll 2002).

In the hippocampus there is much electrophysiological evidence to support the argument that CB1Rs modulate $GABA_A$ signalling via a presynaptic mechanism. Hoffman & Lupica (2000), Katona *et al.,* (1999) and Hájos *et al.,* (2000) have reported that synthetic CB_1R agonist WIN 55,212-2 reduces GABA release, and that the effects of WIN 55,212-2 can be blocked by pre-treating the slice with the CB_1R antagonist SR141716A. Hoffman & Lupica (2000) and Katona *et al.,* (1999) both suggest that WIN 55,212-2 is indeed acting at CB_1 receptor. In these studies, WIN 55,212-2 did not significantly alter mIPSCs providing evidence that cannabinoid signalling is indeed a presynaptic mechanism. Hoffman & Lupica also show that it is likely that CB_1R inhibition of $GABA_A$ synaptic transmission occurs through inhibition of voltage-dependent calcium channels in the hippocampus. Katona *et al.,* (1999) showed that the inhibitory effect of WIN on GABA release was not due to a reduced glutamatergic (excitatory) drive to the presynaptic GABAergic neurone as WIN 55,212-2 reduced GABA release by the same amount as in control when it was applied in the presence of NMDA and non NMDA glutamatergic receptor antagonists.

The results in the hippocampus suggesting that CB1Rs are located presynaptically on CCK-positive interneurones which form symmetrical GABAergic synapses with their postsynaptic targets are backed up by work done in the amygdala (Katona *et al.,* 2001). In this study, WIN 55,212-2 reduced GABA release (both eIPSCs and sIPSCs) while mIPSCs were again unaffected. Further more they provide evidence that WIN 55,212-2 is acting on CB_1 receptors as when experiments were repeated in nuclei of the amygdala that were shown to be negative for CB_1Rs WIN 55,212-2 had no effect on GABA release. Furthermore, WIN 55,212-2 was also shown to be ineffective in CB1R knock out mice. Ferraro

et al., (2001) confirmed the *in vitro* findings already discussed showing that *in vivo* WIN 55,212-2 decreased cortical GABA levels and that this effect could be blocked by the CB_1R antagonist SR141716A.

It has been shown that within both the deep and superficial layers of the mEC all sIPSCs are mediated by $GABA_A$ receptors and not, for example, glycine receptors (Woodhall *et al.*, 2005). Furthermore, while inhibitory signalling does occur in both deep and superficial layers of the mEC, the nature of this signalling appears to be very different between deep and superficial layers. Layer II shows a high degree of inhibitory input, the majority of which is known to be action potential independent while layer V shows comparably less inhibitory input of which a much larger percentage is action potential dependent (Woodhall *et al.*, 2005). The deep and superficial layers of the mEC receive a range of inputs from other brain regions that show great specificity for their targets within the EC. Some of the extrinsic connections are inhibitory in nature and as such will contribute to the inhibition in both deep and superficial layers along with intrinsic inhibitory synapses. Studies have shown that the inhibitory synapses found with in the entorhinal cortex do not belong to just one type of interneurone. With various studies showing the presence of such interneurones as those specifically stain positive for parvalbumin (PV: Wouterlood *et al.*, 1994), calretinin (Wouterlood *et al.*, 2000) and cholecystokinin (CCK; Köhler & Chan-Palay, 1982). Of these interneurones it has been shown that there is a high probability of expression of CB_1Rs at the synapses of the CCK positive interneurones.

Based on these known facts it was decided to investigate if CB_1Rs play in modulating inhibitory signalling in both deep and superficial layers (layers II and V) of the mEC and if that was the case how did the role of CB_1R modulation of $GABA_A$ mediated sIPSCs vary between these two very differently inhibited layers.

CHAPTER 2
Materials and Methods

2.1 Brain slice preparation and storage for patch clamp experiments

Combined entorhinal-hippocampal slices were prepared from male Wistar rats aged 25-30 days, or 8-12 days. The rats were anaesthetised with isoflurane gas and then decapitated. The brain was rapidly removed and placed in chilled sucrose cerebrospinal solution (composition below).

The cerebellum was removed and the brain hemisected. The dorsal surface of the cortex was removed in a plane parallel to the base of the brain. The cut surface was then glued to the steel platform (angled at approximately 12°) of a Vibroslice (Campden Instruments, UK) using cyanoacrylate glue. The brain was positioned so that the base of the brain was uppermost. The platform was then placed in the bath of the Vibroslice where it was immersed in chilled sucrose solution that was bubbled with carbogen. Chilled sucrose solution in the vibroslice bath was topped up during slicing. Horizontal slices 450μM or 350μM thick were cut using a (ceramic blade) and then discarded until the ventral end of the hippocampus and the start of the rhinal fissure began to show as this indicates the start of slices that contain ventral hippocampus, dentate gyrus, parahippocampal regions plus the entorhinal and perirhinal cortices, from this point on slices were dissected away from the rest of the brain as they were cut and placed in specialised storage beaker containing artificial cerebrospinal fluid (aCSF). Following cutting, slices were left for approximately 1 hour to recover prior to being placed in the recording chamber.

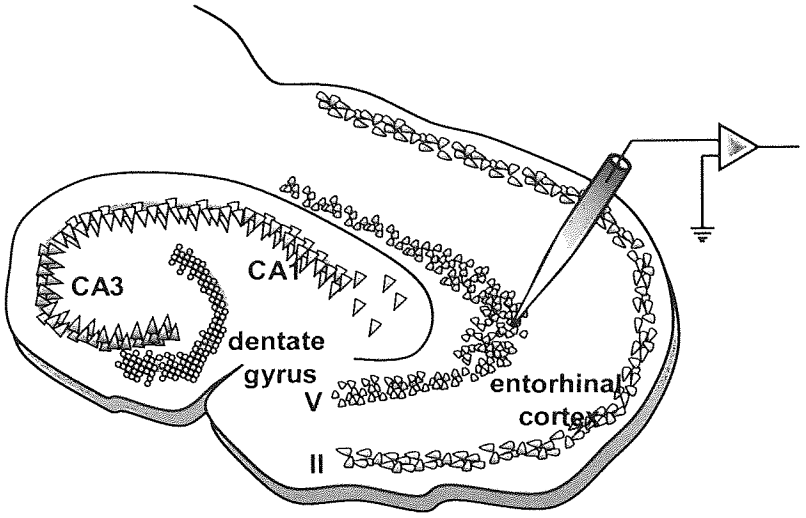

Fig 2.1 Entorhinal slice.

The combined entorhinal-hippocampal slice.

Slices were stored in a specialised container designed such that each slice has its own 'mini chamber'. The custom-built holding chamber was mad from a barrel of a 5ml syringe cut into 1cm segments. The segments were then glued together in a circular arrangement with one central piece surround by 6 further segments. A section of material from a pair of nylon tights was then stretched until it was tight and glued across the base of the circular arrangement. A "chimney" was made from a section of the barrel of a 10ml syringe wrapped with laboratory film to obtain an appropriate width. The chamber and the "chimney" were then placed in a 250ml beaker arranged in such a way so that the "chamber" was suspended halfway down the beaker held in place by the "chimney". Once the "chimney" and "chamber" were in placed the beaker was filled with aCSF.

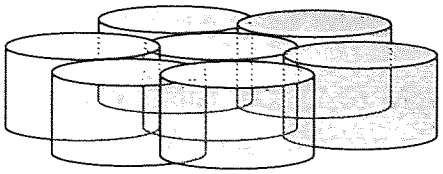

Fig 2.2 Holding chamber for slices.

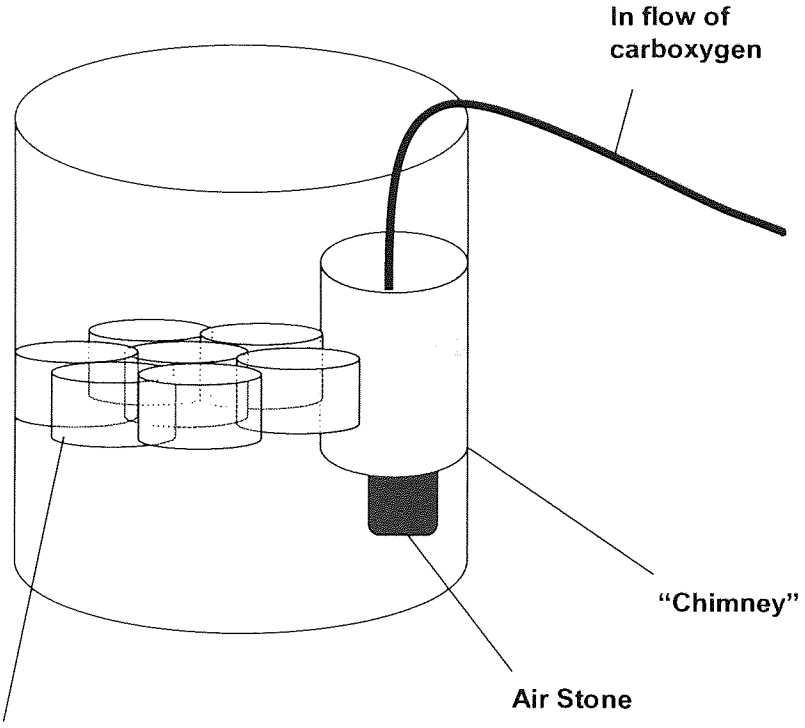

Fig 2.3 Storage beaker.
Holding Chamber secured in beaker ready for slice storage.

The aCSF in the beaker was bubbled continuously with carboxygen (95%O_2 5% CO_2) with the chimney providing a path for rising bubbles, giving circulation of the aCSF. In addition to the aCSF, the holding chamber also contained indomethacin (45μM) and uric acid (300μM) the storage setup was maintained at room temperature.

2.1.1 Sucrose aCSF (cold cutting solution) mM

Sucrose (240) KCl (2.5) $MgCl_2$ (1), $NaHCO_3$ (26), NaH_2PO_4 (1), Glucose (10), $CaCl_2$ (2.5), Pyruvate (5), indomethacin (0.045), Uric Acid (0.3). 310 mOsm.

2.1.2 aCSF in mM

NaCl (126), KCl (2.5), $MgCl_2$ (1), $NaHCO_3$ (26), NaH_2PO_4 (2), Glucose (10), $CaCl_2$ (2.5) pH 7.4 at room temperature at 310 mOsm.

Uric acid and indomethacin were added for their neuro-protective properties in an attempt to extend slice viability.

2.2 Visualisation and patching of neurones.

Once rested, slices were transferred to a recording chamber mounted on the stage of an Olympus BX50WI microscope. The microscope had an X40 water immersion objective for viewing slices. The holding chamber received a continuous supply of aCSF at room temperature (20-25°C) and a pump was used to remove the aCSF from the chamber (flow rate ~2ml/min). It was found for best patching results the slices needed 5-10 minutes in the recording chamber after transfer before patching was attempted.

The neurones of the EC were visualised in the slices by use of differential interface contrast optics and infrared camera. Neurones were selected for recording based on their size, morphology and position in the slice. In layer II of the EC it was found the larger neurones with a well defined shape and clear membranes gave the best patch. In layer V of the EC the smaller rounder shaped neurones with clear membranes seemed to give the best patch. In both layers II and V it was found to be better to patch neurones that lay a little way blow the surface of the slice as these gave longer more stable recordings, neurones close

to the surface tended to be more fragile when patched and tended to give a less stable recording.

2.2.1 Whole-cell patch clamp recordings.

As already discussed in the introduction, this study was investigating the effects of presynaptic CB1Rs in the EC Although it is possible to make pre-synaptic recordings in some preparations such as the Calyx of Held preparation (Takahashi *et al.,* 1996) the presynaptic terminal of the EC are too small to visualise and therefore it is not possible to record presynaptically in the EC. Therefore the best method of studying presynaptic effects on neuronal signalling in the EC was to make whole-cell patch clamp recordings of the post synaptic neurone at use it to act as a reporter of spontaneous and miniature release of neurotransmitter (NT) from the pre-synaptic terminal.

Whole cell patch clamping has many advantages over sharp intracellular recordings. These advantages include allowing the experimenter to alter the internal environment of the postsynaptic neurone from which the recording is being made. A second advantage of the whole cell patch clamp technique is that I provides higher resolution recordings that those given using intracellular method.

Electrodes for use in patch clamping were pulled from borosilicate glass (Harvard) a Sutter P-87 electrode puller that was set to give electrodes with an approximate tip diameter of 1μm and an open tip resistance of 3.5-5MΩ. Electrodes were filled with intracellular IPSC solution (see below). When patching it was found that a more stable patch was achieved when the seal between the electrode tip and the neurone membrane was allowed to reach a minimum of 2GΩ preferably more before breaking through, doing so tended to result in a better seal and more stable recordings. On patching a neurone it was left on seal test for 5-20 minutes to allow the neurone to fill with the intracellular solution from the

electrode. Using this method gave a much more stable recording than if recording was started as soon as the cell was patched.

2.2.2 IPSC intracellular solution mM

CsCl (90), HEPES (33), QX-314 (5), EGTA (0.6), MgCl2 (5.0), TEA-Cl (10), phosophocreatine (7) ATP (4), GTP (0.4) IEM (1) osmolarity of final IPSC solution was set to 275mOsmol and pH 7.3 at 290 mOsm. CsCl and TEA-CL are potassium channel blockers and were included in the intracellular solution to reduce the amount if current lost during its propagation from dendrites to the soma where the recording takes place.

2.2.3 IEM 1460

IEM 1460 (1 mM) was added to the internal solution to block AMPA and NMDA receptors from inside the neurone. This method removed the need to use bath application of CNQX and 2-AP5, thus enabling network effects to be studied.

2.3 Selection and bath application of drugs.

Initially WIN 55,212-2 (a synthetic CB_1R agonist) was used for experiments, however its lipophillic nature meant it was difficult to dissolve or keep in solution, leading to problems with ensuring delivery to the neurones and leading to questions about some results obtained while using it. To overcome this problem I switched to using arachidonylcyclopropylamide (ACPA) another synthetic CB_1 agonist. ACPA is available from Tocris in Tocrisolve™ which makes it a water soluble emulsion, as such there are no issues getting ACPA into solution for delivery to the slice. To block effects of the agonist (ACPA) the CB1R antagonist SR141716A (now called AM-251) was used.

During the course of the research, other CB_1R agonists and antagonists were employed, these were LY320135 a selective CB_1 antagonist/inverses agonist. 2-Arachidonylglycerol (2-AG) endogenous cannabinoid agonist. JWH-133 in tocrisolve™ selective CB_2R agonist. AM-630 CB_2 antagonist/inverse agonist, JTE-907 selective CB_2 antagonist/inverse agonist. For summary see table 2.1 below.

Cannabinoid Ligand	**Role at CBR**	**K_i CB_1R**	**K_iCB_2R**
WIN 55,212-2	Agonist	62.3nM	3.3nM
ACPA	Agonist	2.2nM	
AM-251	Antagonist/ inverse agonist	7.49nM	306 times more selective for CB_1R over CB_2R
2-AG	Agonist	472nM	1400nM
AEA	Agonist	89nM	371nM
LY320135	Antagonist/ inverse agonist	141nM	>10μM
JWH-133	Agonist	200 fold selective for CB_2 over CB_1	3.4nM
AM-630	Antagonist/ inverse agonist at CB_2Rs	165 fold more selective for CB_2R over CB_1R	31.2nM
JTE-907	Inverse agonist		0.38 (nM: rat CB_2Rs)

Table 2.1 CBR ligands.

All drugs were applied to slices via bath application whereby 50ml reservoirs of aCSF containing the drugs at the desired concentrations were set up on a tap

system so they could be switched into the general flow of aCSF that was constantly running around the rig.

All the cannabinoid receptor ligands are lipophillic substances so a long application time was needed to ensure the drugs got to their intended target. In this study I found that 20-30 minutes application was enough time for effects to be seen. Also due to the lipophillic nature of the drugs, it was not always possible to totally wash them out of the slice. However, this was achievable in younger animals, which is presumably due to reduced myelination.

2.4 Data acquisition and analysis.

Voltage clamp recordings were made from layer II and layer V neurones of the EC using multiclamp 700A amplifier (Axon Instruments). To record IPSCs neurones were voltage clamped at -80mV. Signals were filtered at 4Khz and digitized at 10 KHz. During recording access resistance was monitored. Monitoring of access resistance is very important because if it changes it can cause changes in the measured amplitudes and kinetics of the recorded currents. For example, a decrease in access resistance can make it appear that the amplitude of recorded IPSCs has decreased suggesting an effect that has not really occurred. Thus it is important to monitor access resistance throughout an experiment to avoid the possibility of it affecting results. Mean access resistance of experiments was found to be 21.36 MΩ (range 13MΩ - 32.5MΩ). Access resistance was uncompensated for all experiments. Recordings were rejected for analysis if the access was found to have changed by more than 20%.

Recordings from the neurones were made straight to the hard drive of a computer using Clampex 9.2 and Multiclamp commander (Molecular Devices, USA). Two backups of the recorded data were made on separate CDs using Deep Burn software. Minianalysis (Synaptosoft, USA) software was used to carry

out analysis of the spontaneous and evoked events. Minianalysis (Jaejin, USA) was used to look at frequencies, and kinetics of events. Sigma Plot 8.0 (Jandel, USA) and Excel (Microsoft) were used to carry out statistical analysis of the raw data.

When analysing the raw data detection parameters were set in the MiniAnalysis software, these parameters were a set of values that defined which deflections away from the baseline were considered genuine events (sIPSCs). Parameters for event detection were set for each neurone analysed to allow for any variation between cells, parameters were decided by first selecting a number of events in the trace by hand then using there characteristics to set the parameters for peak detection. (these parameters included, threshold for peak amplitude, and area, direction of the event and minimum or maximum periods to search for rise and decay times. Events were sometimes allocated extrapolated decay times by software integration algorithms, such that multiple peaks could be differentiated within complex bursts. In the early experiments a group of 200-300 events was determined as being enough for each sample. However, once NICT (see below) was selected as the characteristic being used to look for change in response to drug application, then epochs of time were used as the measure of the sample, it was decided to use 10 second epochs for layer II neurones and 20 second epochs for layer V. It is important to mention that when data was collected using epochs of time instead of a set number of events, although similar numbers of events were collected form each cell. Once all the events had been detected Minianalysis was instructed to remove any duplicates and sort the data by time. The raw analysis was then transfer to Sigmaplot into pooled spreadsheets to allow further statistical. Significance level of 0.05 or less was set for all statistical analysis

Inhibitory charge transfer (ICT; in pA·ms) is a measure of how much charge has crossed the membrane and this is representative of the amount of neurotransmitter that has been released. It can be calculated by measuring the area under the curve of an event (Hollrigel & Soltesz 1997) and is directly proportional to the amplitude multiplied by the decay time of an event. In our analysis we used normalised ICT which allows the determination of changes in GABA release over time upon application of our CB ligands

2.5 Extracellular experiments

2.5.1 Tissue preparation and storage

Adult wistar rats weighing 50-70g were use for the extracellular experiments. Brains were removed and prepared using the same methods and solutions described above, except for slice thickness which was set at 450 μm. As slices were cut they were places on small squares of lens tissue and stored at room temperature in an interface chamber which contained aCSF bubbled continuously carboxygen the top of which was covered with parafilm to maintain a humid environment inside the chamber.

2.5.2 Extracellular Recording.

Slices were placed in an interface recording chamber (BSC-1, SSD, Canada) and visualised using a dissecting microscope (Leica, Germany). The underside of the interface recording chamber contained water that was warmed to 32°C and continually bubbled with carboxygen.

A continuous stream of aCSF warmed to 32°C was washed around, but not over, the slice. To induce oscillations, kainic acid at 200-400nM was added to the bath aCSF. Once a slice was placed in the recording chamber it was left to equilibrate for 45-60 minutes to allow oscillatory activity to be induced and reach

full power before any recordings were started. The cannabinoids were bath applied to the slice. Due to the lipophillic nature of the cannabinoid ligands being used, it was decided that a minimum of 30 minutes was needed for the drugs to take affect.

Glass microelectrodes were made from filamented 1.2mm O.D. borosilicate glass (Sutter) and were pulled using a Flaming-Brown Puller (Sutter, USA), and were set to a resistance of 2-4MΩ. Electrodes were then filled with aCSF and placed on electrode holders positioned on opposite sides of the bath. Electrodes were lowered in to layers II and V of the slice. Oscillations were recorded using an NPI EXT-01 extracellular amplifier and Clampex software.

Data was analysed off-line using Clampfit and Sigmaplot. To study changes in the power of oscillations a 60s epoch of time was selected on the trace and then filtered for the appropriate frequency (initially this was 0-100Hz). To obtain a clearer picture of how specific frequency bands were changing we also filtered at 30-90 Hz for gamma oscillations and 15-29Hz for beta oscillations. Area under the curve (± the standard error of the mean) was then used as the measure of power for the oscillations. The students T-test was used to look for significant changes in the power of the oscillations in the different drug periods.

CHAPTER 3
The effects of synthetic cannabinoid agonists on GABAergic signalling in layers II and V of the mEC

3.1 INTRODUCTION.

Results in this chapter were collected from layer II and layer V neurones using whole-cell patch-clamp recording techniques as previously described (chapter 2). In addition to the methods laid out in chapter 2, when ACPA and AM-251 were used, the drug reservoirs for bath delivery were wrapped in aluminium foil and work was carried out at low light levels due to the photo-sensitive nature of the drugs.

3.1.1 WIN 55,212-2 has dual effects on layer II sIPSC frequency

Previous studies (Katona *et al.,* 1999, 2000; Wilson & Nicoll., 2001; Nakatsu *et al.,* 2003) in various brain areas have shown that the CB_1R agonist WIN 55,212-2 (1-10 μM) caused a decrease in sIPSC frequency and amplitude, and decreased eIPSCs amplitude. This was usually interpreted as an overall decrease in GABA release induced by CB_1R activation. Nakatsu *et al., (*2003) showed that WIN 55,212-2 suppressed both the frequency and amplitude of sIPSCs in human dentate gyrus, and the work of Katona *et al.,* (2000) showed WIN 55,212-2 suppressed GABA release in human hippocampal neurones. It has also been shown that WIN 55,212-2 reduced the amplitude of both evoked and spontaneous IPSCs in the amygdala (Katona *et al.,* 2001). Application of WIN 55,212-2 reduced stimulation evoked release of GABA in the hippocampus Katona *et al.,* (1999). Wilson & Nicoll, (2001) showed endogenous cannabinoids mediated similar effects on inhibitory synaptic function in the hippocampus.

Initially, we aimed to replicate the observations of Katona *et al.,* (1999) and others using the CB1R agonist WIN 55,212-2. We recorded sIPSCs in the presence of CNQX (20 μM) and D-2-amino-5-phosphonovalerate (2-AP5; 50 μM), to block ionotropic glutamate receptors. When WIN 55,212-2 (10 μM) was bath applied to entorhinal cortical slices, it was found that in layer II it caused a

significant decrease in sIPSC frequency and amplitude (although this effect was highly variable, and in some recording we noted an increase in frequency, amplitude or both of these parameters – *see 3.2 below*).

Experiments with WIN 55,212-2 in layer II saw an increase in sIPSC frequency in 50% of neurones and a decrease in frequency in the other 50% of neurones tested.

3.1.2 WIN 55,212-2 decreases sIPSC frequency and amplitude in layer II

Fig 3.1A and B show sIPSCs from a single layer II neurone during **(A)** control and **(B)** 20 minutes after application of WIN 55,212-2 (10μM). When the control and WIN 55,212-2 periods are compared it can be seen that in the presence of WIN 55,212-2, the number of large sIPSCs has been greatly reduced, suggesting that a decrease in GABA release has occurred. However, there are still a large number of smaller sIPSCs presents making it difficult to tell if sIPSC frequency has greatly decreased. **Fig 3.1C** shows the cumulative probability plot for sIPSC amplitudes during control (black) and WIN 55,212-2 (red) periods. In these plots, overlapping distributions (which indicate little or no change in the measured parameter) are seen as overlap between the cumulative probability curves. However, when separation between the curves is seen, this can be representative of change in the distribution, and this is usually confirmed using the non-parametric Kolmogorov-Smirnov (KS) test. For example, in **Fig. 3.1C**, there is separation between the plots 50-400 pA, indicating that following application of WIN 55,212-2 there is less likelihood of observing sIPSCs with these amplitudes. This correlates well with the gross distribution of events as seen in **Fig. 3.1A & B**, and this change in distribution of sIPSC amplitudes between control and WIN 55, 212-2 periods was significant ($P \leq 0.0001$, KS test, n=3). When the mean amplitudes were compared, and overall decrease from 64.88 ± 1.95 pA in control

to 47.66 ± 1.6pA in WIN 55, 212-2 was seen, and was also found to be significant ($P \leq 0.0001$, ANOVA).

Fig 3.1D shows the cumulative probability for sIPSC IEIs during control (black) and WIN 55,212-2 (red) periods. The two plots lie close together suggesting there is no difference in the distribution of sIPSC IEI times between control and WIN 55,212-2 periods however when a KS test is performed on the IEIs a significant change towards larger IEIs is evident in the distribution ($P \leq 0.0001$, KS test n=3). When the mean median IEI values were compared, IEI was found to have increased from 48.07 ± 8.43ms in control to 63.39 ± 14.76ms in WIN 55,212-2. This increase in IEI indicates that an overall decrease in sIPSC frequency has occurred between control and WIN 55,212-2 periods; however the change in mean median IEIs was not significant ($P \geq 0.39$, ANOVA n=3).

Fig 3.1E shows the cumulative probability plot for sIPSC areas. Here, the WIN 55,212-2 (red) plot lies below control indicating a lower probability of measuring sIPSC areas above 500 pA·ms in WIN 55,212-2 than control (black). This change in distribution of sIPSC area was significant ($P \leq 0.0001$, KS test).

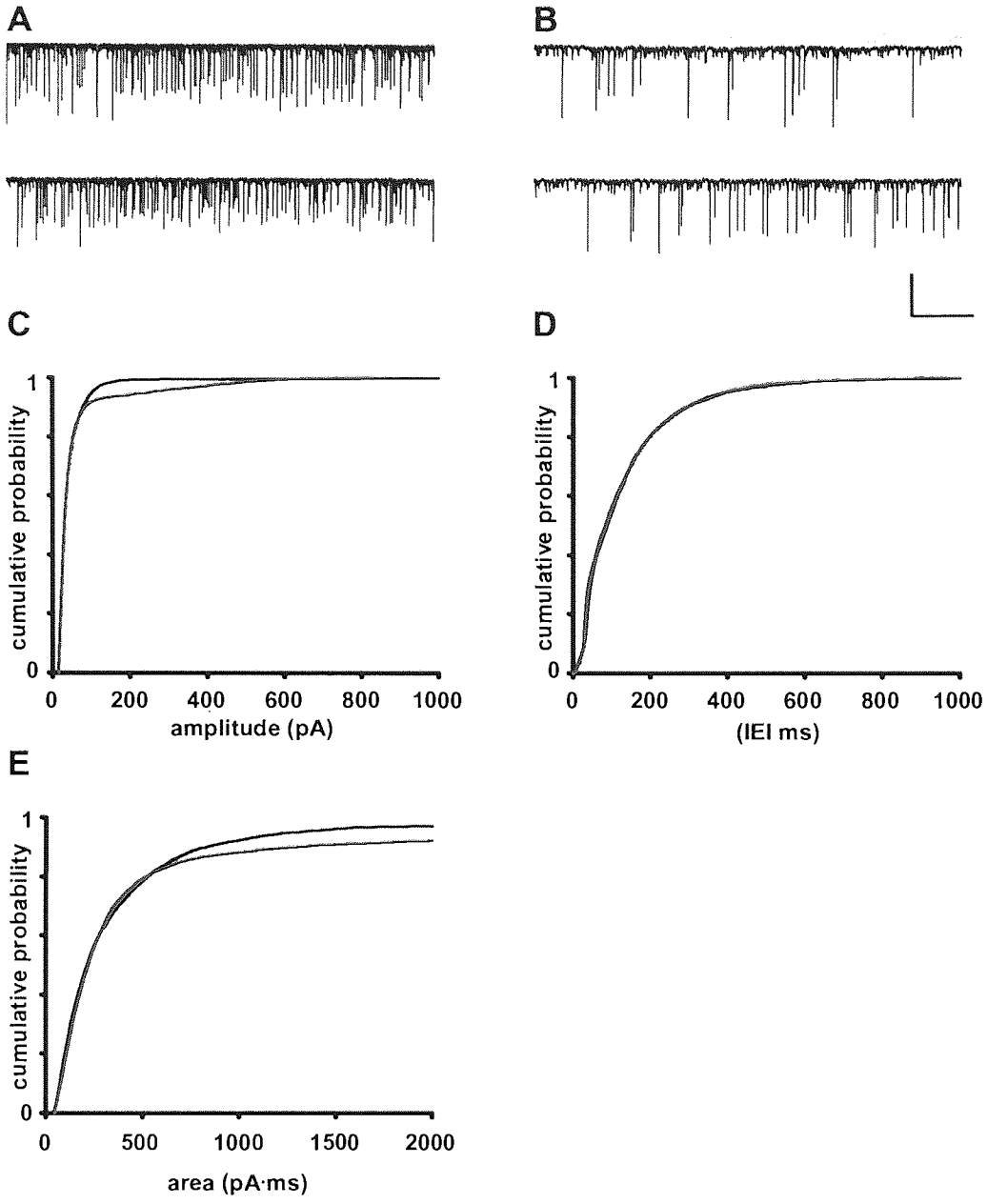

Fig 3.1 Suppressing effects of WIN 55,212-2 on sIPSCs in layer II mEC in CNQX and 2-AP5. Example sIPSCs from a single layer II neurone during **A.** Control and **B.** WIN 55,212-2. (10μM) **C** Pooled cumulative probability sIPSC amplitude in control and WIN 55,212-2 **D.** Pooled cumulative probability for sIPSC IEI in control and WIN 55,212-2. **E.** Pooled cumulative probability sIPSC area in control and WIN 55,212-2. Scale bar **X** 5000ms **Y** 500pA, Holding potential was -80mV in all experiments in CNQX, 2-AP5 (n=3).

Overall, in this small sample of sIPSCs recorded in layer II, it appears that WIN 55,212-2 caused a shift towards reduction in sIPSC amplitude and frequency, but only in a subset of IPSCs, meaning that gross statistical parameters were largely unchanged. This difficulty in measuring the effects of WIN 55,121-2 on sIPSCs in layer II may relate to the fact that CB1Rs are known to modulate action potential (AP)-dependent GABA release, and >90% of release in layer II is AP-independent (Woodhall *et al.,* 2005). Hence, even large changes in the amplitude and IEI of the minority AP-dependent sIPSCs may well be masked by the preponderance of miniature IPSCs or by subtle changes in their associated parameters. In addition, while the above data broadly agree with previous research indicating that WIN 55,212-2 decreases sIPSC activity this was not the only result seen. In some experiments it appeared that application of WIN 55,212-2 quite clearly caused an increase in sIPSC frequency and amplitude.

3.1.3 WIN 55,212-2 increases sIPSC frequency and amplitude in layer II

Fig 3.2A&B show sIPSCs recorded from a single layer II mEC neurone during control **(A)** and WIN 55,212-2 **(B)** application periods. When the sIPSCs recorded in the presence of WIN 55,212-2 are compared to control it is clear that the frequency of larger amplitudes sIPSCs has increased compared to control. In addition, the larger sIPSCs seen in WIN 55,212-2 appear to be interspersed within a population of very low amplitude sIPSCs, while under control conditions this population of background IPSCs has greater amplitude.

Fig 3.2C shows the cumulative probability plot for sIPSC amplitude. The WIN 55,212-2 plot (red) lies to the right of the control plot (black), indicating the greater likelihood of observing larger amplitude sIPSCs in WIN 55,212-2 compared with control. This change in distribution of sIPSC amplitude between control and WIN 55,212-2 was significant ($P \leq 0.0001$, KS test, n=3). In addition to

a change in the distribution of sIPSC amplitudes, application of WIN 55,212-2 caused a significant increase in mean sIPSC amplitude from 46.59 ± 0.36 pA in control to 56.67 ± 1.49 pA. This increase in amplitude was highly significant ($P \leq$ 0.0001, ANOVA).

Fig 3.2D is the cumulative probability plot for sIPSC IEI. Here the control (black) plot and the WIN 55,212-2 (red) plot lie very close together suggesting very little change in the distribution of IEIs. However, the KS test showed that a significant change in the distribution of sIPSC IEIs has occurred between control and WIN 55,212-2 periods. ($P \leq 0.0001$). When the mean median IEIs were compared it was found to decrease from 50.08 ± 1.23 in control to 45.56 ± 0.85ms in WIN 55,212-2 the overall decrease in IEI times was significant showing that an increase in sIPSC frequency occurred during WIN 55,212-2 application ($P \leq$ 0.012, ANOVA n=3).

Fig 3.2E shows the cumulative probability plot for sIPSC areas. The control (black) plot and the WIN 55,212-2 (red) plot lie directly on top of each other suggesting no change in sIPSC area distribution has occurred between control and WIN 55,212-2 periods, This was confirmed by a non-significant KS test (P= 0.041)

Despite the relatively low n-numbers in the experiments described above, we found robustly opposing effects of WIN 55,212-2 on sIPSCs in layer II of mEC. Indeed, we observed dual effects in a further 12 recordings which have unfortunately been lost due to a data storage failure. Give the inconsistency of the data in relation to the CB_1R agonist WIN 55,212-2; we determined to use a structurally different agonist to exclude the possibility of ligand-specific non-CB1R receptor dependent effects. We also attempted to avoid dimethyl sulphoxide (DMSO) based solutions of highly lipophillic compounds like WIN 55,212-2, since it was possible that the inconsistent effects we observed on sIPSC frequency and

amplitude may have been due to the drug precipitating out of solution before reaching the slice.

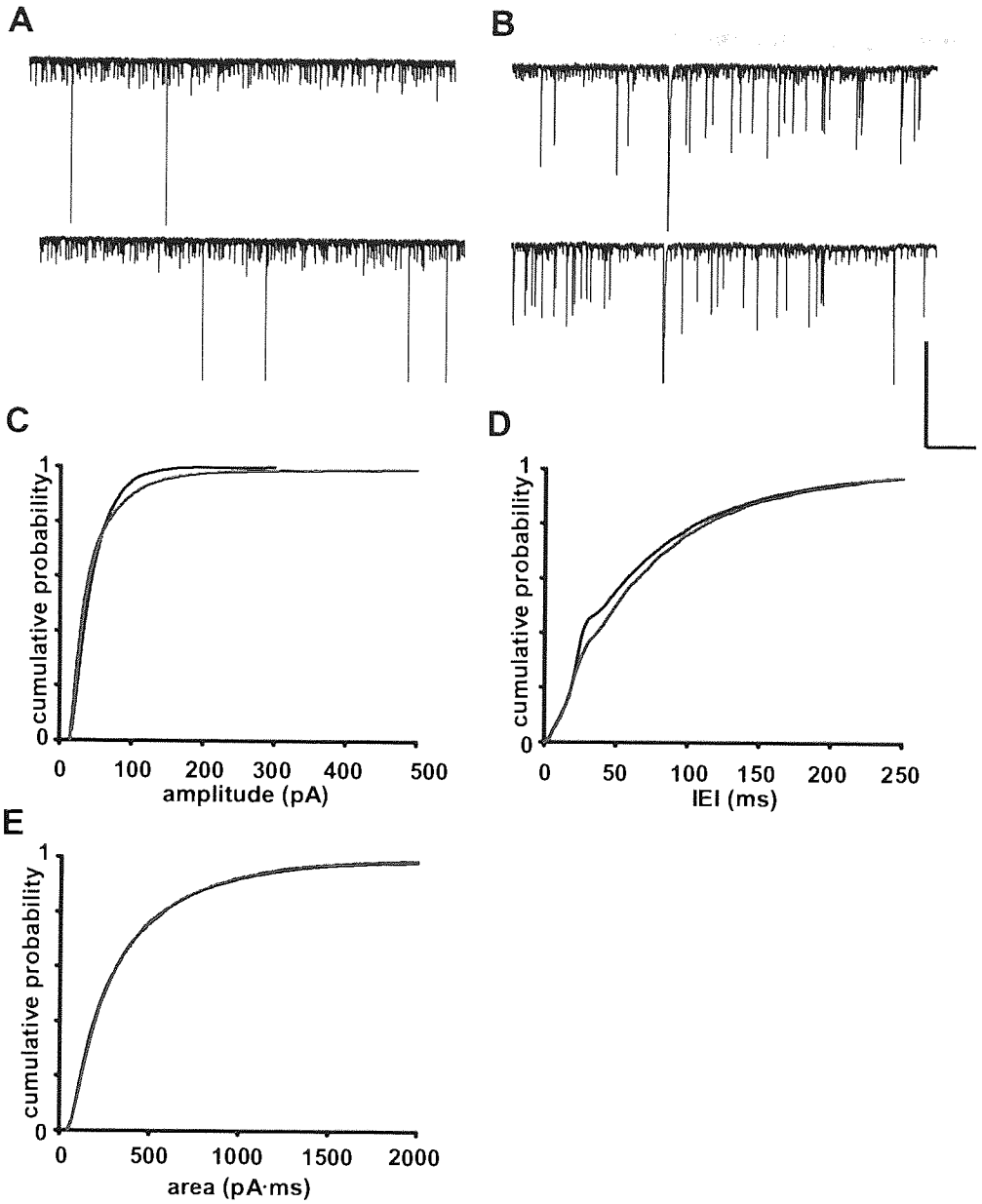

Fig 3.2 WIN 55,212-2 increases sIPSCs inlayer II mEC in CNQX and 2-AP5
sIPSCs from a single layer II neurone during **A.** Control and **B.** WIN 55,212-2 (10μM).
C. Pooled cumulative probability sIPSC amplitudes during control and WIN 55,212-2
D. Pooled cumulative probability sIPSC IEIs in control and WIN 55,212-2.**E** Pooled cumulative probability sIPSC area. All experiments performed at -80mV in CNQX and 2-AP5.
Scale **X** 5000ms **Y** 100pA Control = black, WIN 55,212-2 = red.

3.2 ACPA has dual effects on sIPSCs in layer II of the mEC.

To overcome potential drug delivery and specificity problems, a new synthetic CB1 agonist was selected, namely arachidonylcyclopropylamide (ACPA). ACPA is a selective CB_1R agonist, with a K_i of 2.2 nM at rat CB1Rs (Hillard *et al.*, 1999). An additional reason for selecting ACPA from the CB1R agonists available was its preparation in Tocrisolve™. Tocrisolve™ is an emulsion-based delivery system for lipophillic ligands such as the cannabinoids, comprising a 1:4 ratio mix of Soya oil to water which is then mixed with a block co-polymer. This meant that there were no problems dissolving ACPA for bath application, reducing the probability of the drug precipitating out of solution during the course of the experiment. As with the WIN 55,212-2 experiments, CNQX and D-AP5 were bath applied throughout in order to block AMPA and NMDA receptors and thus ensure that only GABAergic signalling was studied.

In these experiments a decrease in sIPSC frequency was seen in 18.2% of neurones while 81.8% showed an increase in sIPSC frequency during ACPA application.

3.2.1 ACPA decreases sIPSC amplitude and frequency in layer II

Fig 3.3 A&B show sIPSCs recorded from a single layer II mEC neurone during control and ACPA (10μM) periods. When the control sIPSCs **(A)** are compared to sIPSCs recorded during ACPA **(B)** application then it appears that the amplitude of sIPSCs has been greatly reduced. The base-line is also more apparent in the sIPSCs recorded from the ACPA periods when compared to control suggesting a decrease in frequency.

Fig 3.3C shows the cumulative probability plot for sIPSC amplitude during control and ACPA (10μM) periods. The ACPA (red) plot lies to the left of control (black) plot for amplitudes between 25 and 520pA suggesting that in ACPA there

is a higher probability of lower amplitude sIPSC amplitude. A gap between the two pots indicates a change in the distribution of sIPSC amplitudes between the two periods, this change in distribution was highly significant. ($P \leq 0.001$, KS test). As well as a change in the distribution of sIPSC amplitudes the mean amplitude decreased from 76.79 ± 4.31pA in control to 50.36 ± 5.35pA in ACPA. This decrease in amplitude was also very significant ($P \leq 0.0001$, ANOVA n=3).

Fig 3.3D is the cumulative probability plot for sIPSC IEIs, the ACPA plot (red) lies to the right of the control plot (black) for IEIs between 50ms and 400ms showing a lower probability for the lower IEIs during ACPA application, the ACPA plot also continues along the X axis after the control plot has finished showing that in ACPA there are IEIs that are larger than any seen in control. These differences in the two plots suggest that a change in the distribution of sIPSC IEIs occurs between control and ACPA. A KS test confirms that this change in distribution is highly significant ($P \geq 0.0001$). The mean median IEI confirms a decrease in sIPSC frequency during ACPA application with the mean median IEI increasing from 54.12 ± 10.13ms in control to 79.25 ± 3.58ms and this decrease was significant ($P \leq 0.003$, ANOVA n=3).

Fig 3.3E is the cumulative probability plot for sIPSC area, the control (black) and ACPA (red) plot are separated for the entire graph with the ACPA plot lying to the right of control indicating a higher probability of an sIPSC with any of these areas in ACPA than in control. The large gap between the two plots suggests that a change in sIPSC area distribution occurs between control and ACPA periods. This change in distribution was highly significant ($P \leq 0.0001$, KS test).

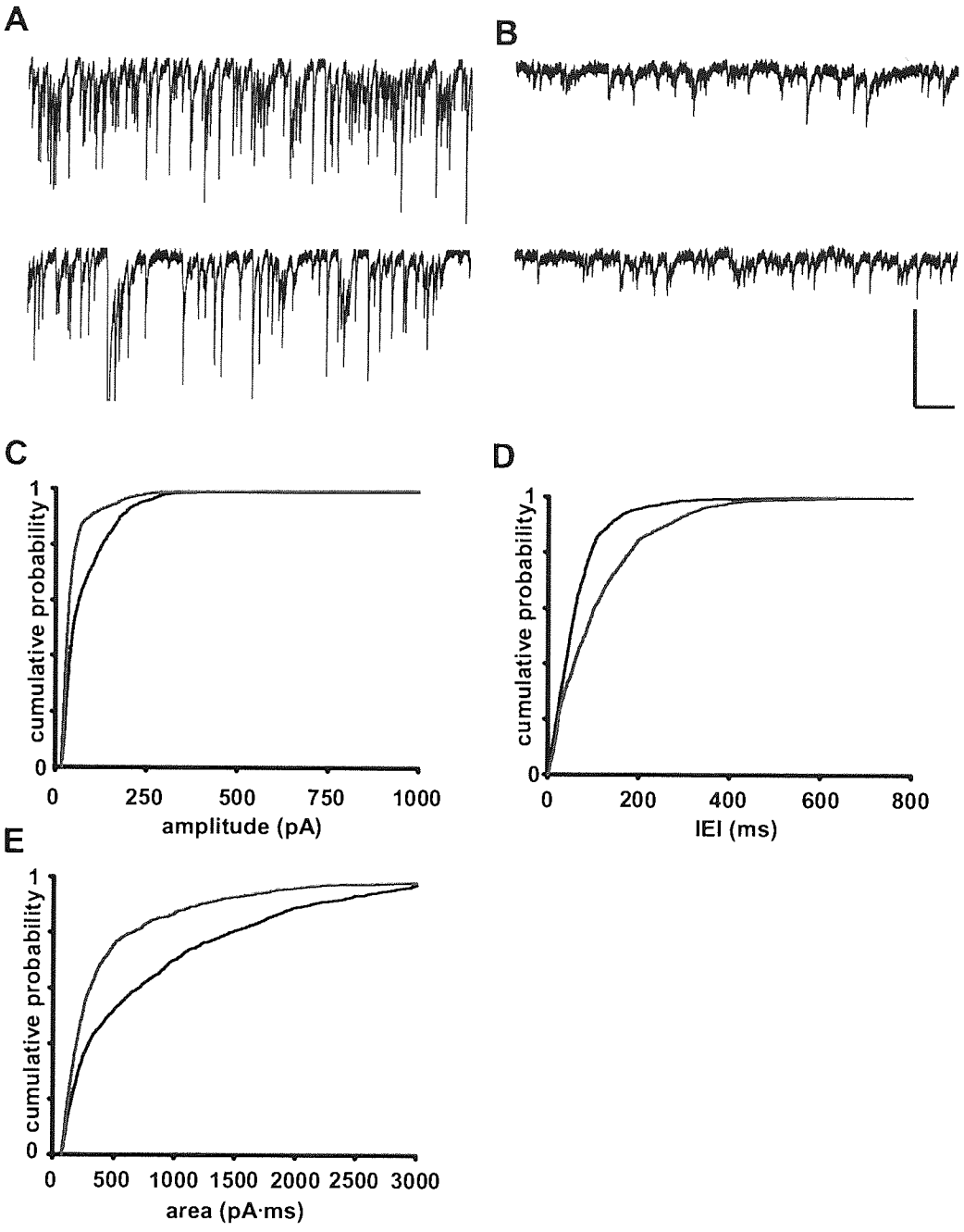

Fig 3.3 ACPA suppresses sIPSCs in layer II mEC in CNQX and 2-AP5
sIPSCs from a single layer II neurone during **A.** Control and **B.** ACPA (10μM) periods. **C.** Cumulative probability for sIPSC amplitudes in control and ACPA. **D.** Pooled cumulative probability for sIPSC IEIs in control and ACPA. **E. Pooled** cumulative probability for sIPSC area during control and ACPA all experiments in CNQX and 2-AP5 at -80mV. Scale **X**100ms **Y** 200pA, Control=black, ACPA =red C-E pooled data n=2

As with the WIN 55,212-2 experiments in layer II not all the neurones showed a decrease in sIPSC frequency when ACPA (10μM) was applied, indeed in the majority of recordings (70%), application of ACPA appeared to cause an increase in sIPSC frequency.

3.2.2. ACPA increases sIPSC frequency and amplitude in layer II

Fig 3.4 A&B show sIPSCs recorded from a single layer II neurone during control **(A)** and ACPA (10μM) application **(B)**. Comparing the traces, it appears that in ACPA there is a greater number of larger sIPSCs compared to control, indicating a possible increase in sIPSC frequency. **Fig 3.4C** is the cumulative probability plot for sIPSC amplitude, the ACPA plot lies to the right of the control (black) plot indicating a change in the distribution of sIPSC amplitudes induced by ACPA towards larger values. This change in distribution was significant ($P \leq 0.020$, KS test). In addition to an overall change is sIPSC amplitude distribution the mean amplitude also increased from 57.48 ± 1.65pA in control to 82.89 ± 2.69pA in ACPA this increase in mean amplitude was highly significant ($P \leq 0.0001$, ANOVA, n=5).

Fig 3.4D shows the cumulative probability plot for sIPSC IEI times. Here, the ACPA (red) plot lies to the left of control (black) for IEI times between 50ms and 300ms. The change in distribution of sIPSC IEI times was highly significant ($P \leq 0.0001$, KS test), and when mean median IEI times for control and ACPA were compared then the time was found to show a highly significant decrease in sIPSC IEI had occurred with the mean median IEI decreasing from 58.87 ± 1.42ms in control to 42.96 ± 0.86ms in ACPA. ($P < 0.0001$, ANOVA, n=5).

Fig 3.4E shows the cumulative probability for sIPSC area. Here, the ACPA (red) plot lies slightly to the right of the control (black) plot for areas between 125

and 500 pA·ms, indicating that there is a lower probability of low area sIPSCs during ACPA application than in control. The change in sIPSC area distribution between control and ACPA periods was highly significant ($P \leq 0.0001$, KS test).

In summary, it is clear that ACPA had similar, dual effects on sIPSCs recorded in layer II of the mEC to those seen with WIN 55,212-2. Since ACPA is structurally dissimilar to WIN 55,212-2, it seems unlikely that the dual effects we observed were related to intrinsic properties of the drugs used. As previously discussed, using the methods described, >90% of IPSCs in layer II would be AP-independent, and therefore, presumably under little influence from cannabinoid receptors, which act primarily at presynaptic calcium channels and would thus be expected to affect AP-dependent sIPSCs to a much greater extent. We tested this hypothesis by boosting AP-dependent GABA release by using high Ca^{2+}/low Mg^{2+} ACSF and/or the cholinergic agonist pilocarpine (10μM) to enhance excitability. We saw no consistent ACPA effect on sIPSCs in layer II (decreased IEI in 4/5 recordings, increased IEI in 1/5 with variable results on sIPSC amplitude, data not shown). Similarly, in a series of experiments in layer V, where AP-dependent activity is much greater than in layer II (Woodhall *et al.,* 2005), introduction of the sodium-channel blocker tetrodotoxin (TTX, 1 μM) into the bathing medium prevented all cannabinoid drug effects. **Fig. 3.5A** shows the effects of various CBR ligands (both agonists and antagonists) on sIPSCs recorded in mEC layer V in the presence of TTX. It is readily apparent that no change occurs under any drug condition. When data from 5 recordings were pooled, as shown in **Fig. 3.5B**, there was no effect of any drug on IEI, sIPSC area or amplitude. As discussed above, layer II has a much lower proportion of AP-dependent IPSCs; hence we did not attempt these experiments in layer II. Together, these data strongly suggested that our main observations were restricted to changes in the minority of AP-dependent sIPSCs in layer II of the mEC.

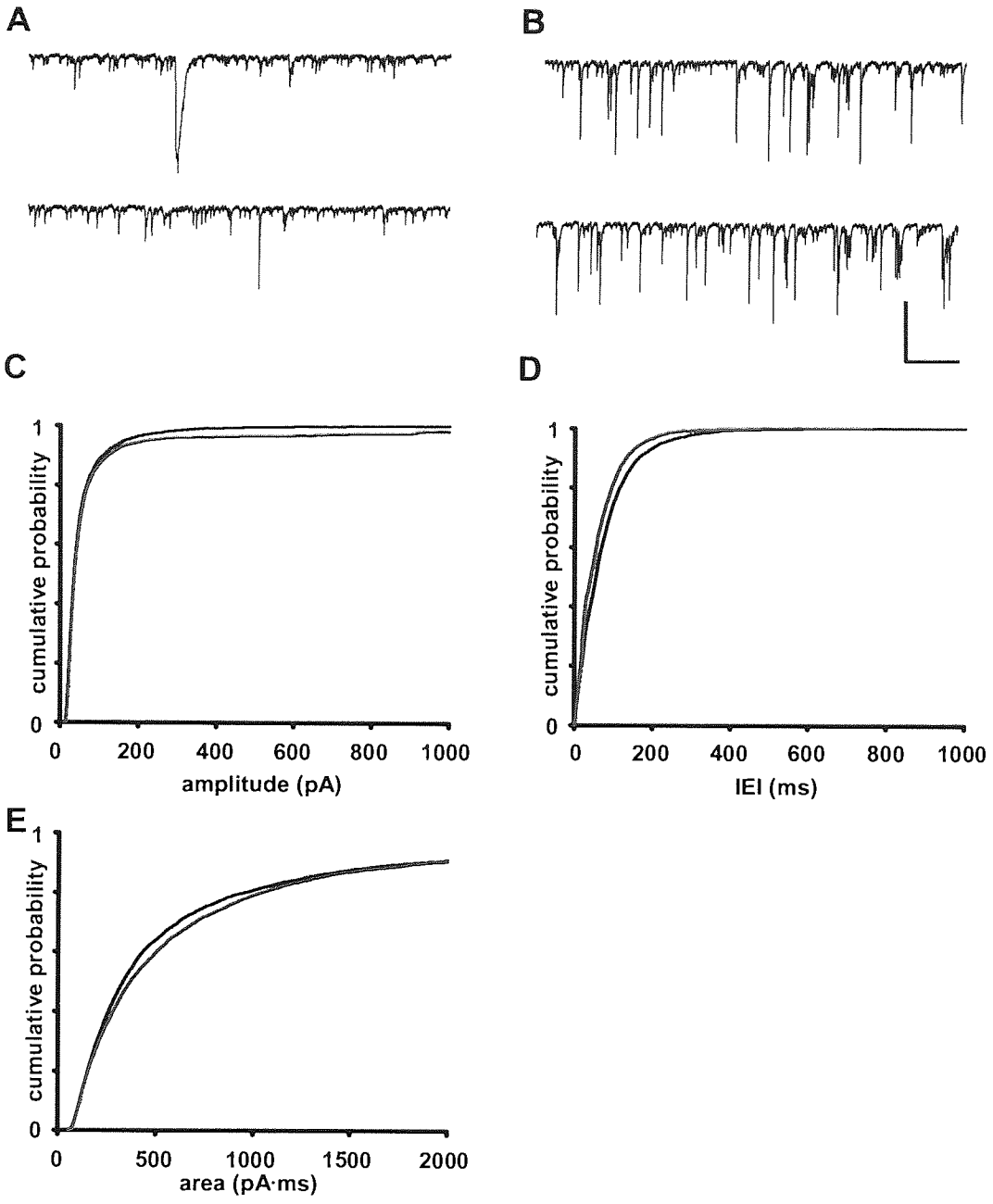

Fig 3.4 ACPA increases sIPSCs in layer II mEC in CNQX and 2-AP5
sIPSCs from a single layer II neurone during **A** Control and **B** ACPA (10μM). **C** Pooled cumulative probability plots sIPSC amplitude in control and ACPA. **D.** Pooled cumulative probability sIPSC IEIsin control and ACPA. **E**. Cumulative probability sIPSC areas in control and ACPA all in CNQX and 2-AP5 at -80mV. Control=black, ACPA=red Scale Bar **Y** 500pA, **X** 1000ms, n=9.

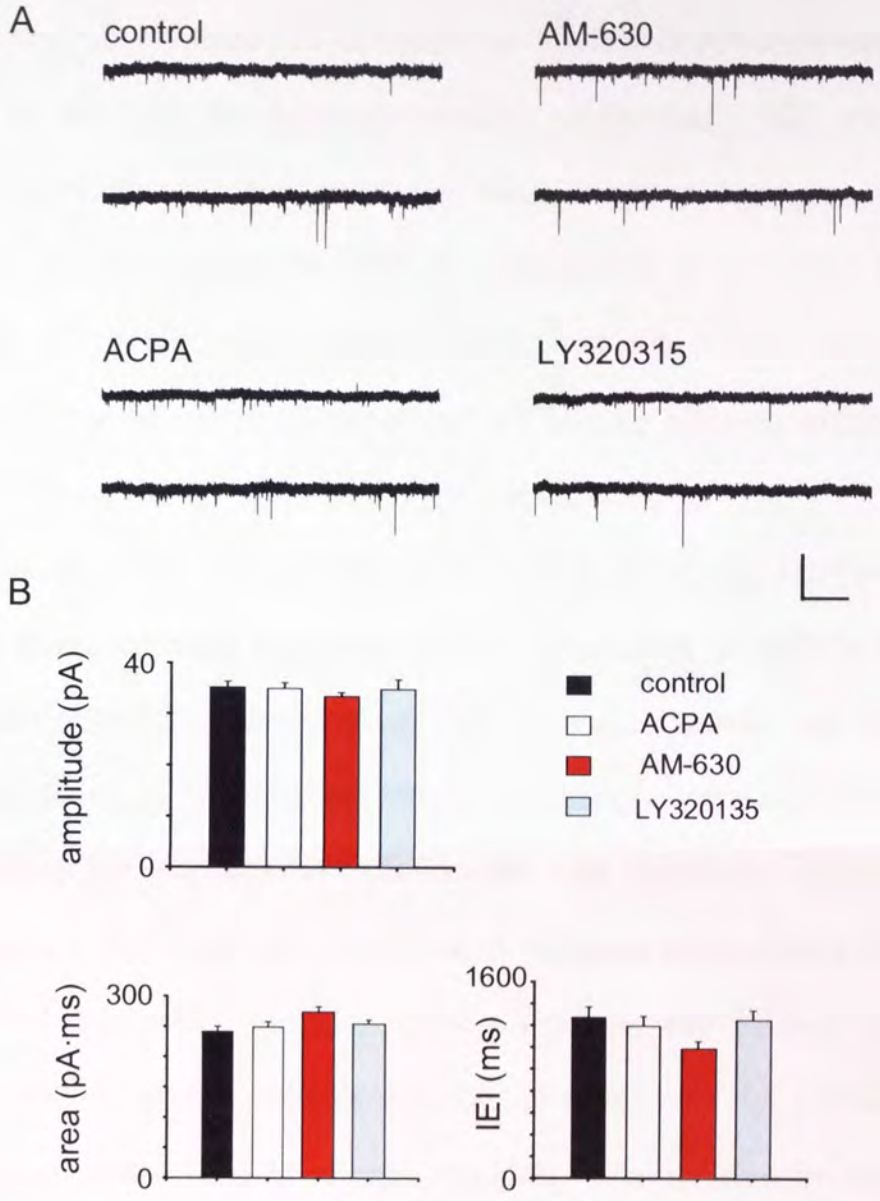

Fig 3.5 The effects of cannabinoid ligands in the presence of TTX in layer V of the mEC.
A. sIPSCs from a single layer V neurone in TTX during various drug applications **B.** The effects of cannabinoid ligands on sIPSC amplitude, area and IEI in the presence of TTX. AM-630 = CB_2R inverse agonist / antagonist, LY320135 CB_1R inverse agonist / antagonist

In an attempt to obtain the best possible measure of the effects of CB_1R activity in layer II of the mEC, we took a dual approach:

Firstly, we attempted to enhance the number of AP-dependent sIPSCs in the slice by removing the glutamate receptor antagonists CNQX and 2-AP5 from the bathing medium. In their place, we used an intracellularly acting ionotropic glutamate receptor antagonist, IEM1460 (Magazanik *et al.,* 1997; Buldakova *et al.,* 1999), at 1 mM. Hence, without driving network activity we were able to optimize the frequency of AP-dependent sIPSCs by allowing excitatory network activity to function in the absence of GluR antagonists.

Analysis of the data collected using WIN 55,212-2 and ACPA indicated that at times, these agonists increased IEI and amplitudes of sIPSCs and at other times, both of these parameters were decreased. However, we also observed mixed responses, in which IEI and amplitude changes were opposite in sign, and we could find no valid reason to favour IEI over amplitude when deciding the 'response' to a CB_1R agonists. To attempt to mitigate these issues, we calculated the inhibitory charge transfer (ICT; Hollrigel & Soltesz 1997; Bai *et al.,* 2001). Due to area variation between cells we actually normalised the ICT values (NICT) and used this as a measure of charge transfer). Charge transfer represents the amount of charge crossing the membrane and is the product of postsynaptic current amplitude and area values for a given epoch. We measured area and amplitude of sIPSCs over 20s epochs. All units presented in the figures below are normalized to control values in our paired experiments. Using this method, it was possible to ascribe definitive responses to drug application (increased or decreased NICT) even when IEI and amplitude values were changing in opposite directions. **Fig 3.6** Shows NICT calculated from the mean area under the curve for any given IPSC (**fig 3.6A, C, E** for layer II and **G for layer V)** while **Fig 3.6 B, D and F** show the NICT calculated for the entire total area in a given epoch of time.

These graphs show that there is very little difference between plotting the mean area or total area and as such for this work, when NICT is calculated the mean area will be used.

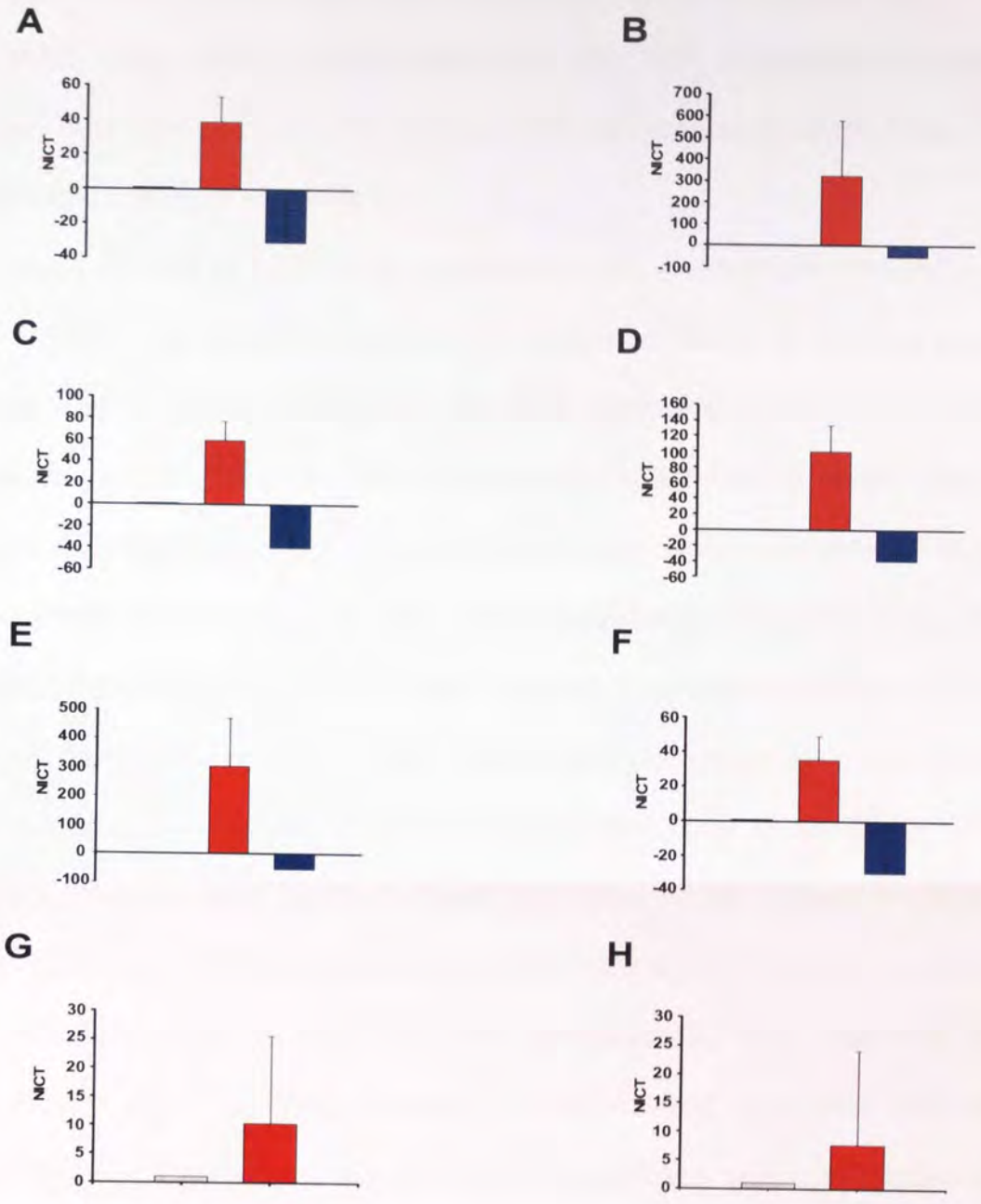

Fig 3.6 Comparing mean NICT and total NICT
Bar charts plotting change in NICT in layer II mEC in CNQX + 2AP-5 during WIN 55,212-2 application in both mean areas **A.** and total area **B**. **C. & D.** Bar charts plotting changes in NICT in layer II mEC I CNQX + AP-5 during ACPA application for both mean (**C**) and total areas (**D**). **E. &F.** Bar charts plotting change in NICT in layer II with IEM during ACPA application for both Mean (**E**) and total (**F**) areas. **G.** & **H.** Bar charts plotting change in NICT in layer V mEC in IEM during ACPA application for both mean (**G**) and total (**H**) area. Black bars =normalised control of 1, Red bar represents cells were NICT increased in response to CBR agonist Blue bars represent pooled cells where NICT decreased.

3.3 Using IEM1460, ACPA again has dual effects on sIPSCs in layer II

While using ACPA in conjunction with IEM 1460 a decrease in sIPSC frequency was seen in 44.44% of neurones while an increase in sIPSC frequency was seen in 55.56 % of neurones.

Since the use of intracellular blockade of both AMPAR and NMDAR is a novel technique, we sought to underpin its utility and validity in isolating purely GABAergic postsynaptic currents. **Fig. 3.7 A&B** shows the effects of the $GABA_A$ receptor antagonist picrotoxin (50 μM) on sIPSCs recorded in layer II in the presence of intracellular IEM 1460. As can be seen, $GABA_A$ receptor blockade reduces sIPSC frequency to near-zero. Further confirmation that sIPSCs recorded in layer II using IEM 1460 consist of nearly all $GABA_A$ receptor mediated inhibitory sIPSCs is the observation that 10-90% rise times, decay times, IEI and amplitude are all similar to the values reported previously (Woodhall *et al.,* 2005), when glutamate receptors were blocked. **Table 3.1** shows kinetic values for layer II sIPSCs measured in the presence of either IEM 1460 or CNQX/2-AP5. As can be seen, sIPSCs recorded in IEM 1460 have comparatively large amplitude and lower IEI with respect to those recorded in CNQX/2-AP5, consistent with their greater AP-dependent origin, but rise times, decay time and area values are consistent. By contrast, excitatory events in layer II have much more rapid decay (3-5 ms, Berretta and Jones, 1996, Woodhall *et al.,* 2000; 2001) and IEI on the order of 1000 ms. Hence, even assuming that 1 Hz sEPSCs in layer II were, for example reduced by only 50% in frequency, then with sIPSCs at 16 Hz, they account for > 97% of measured events.

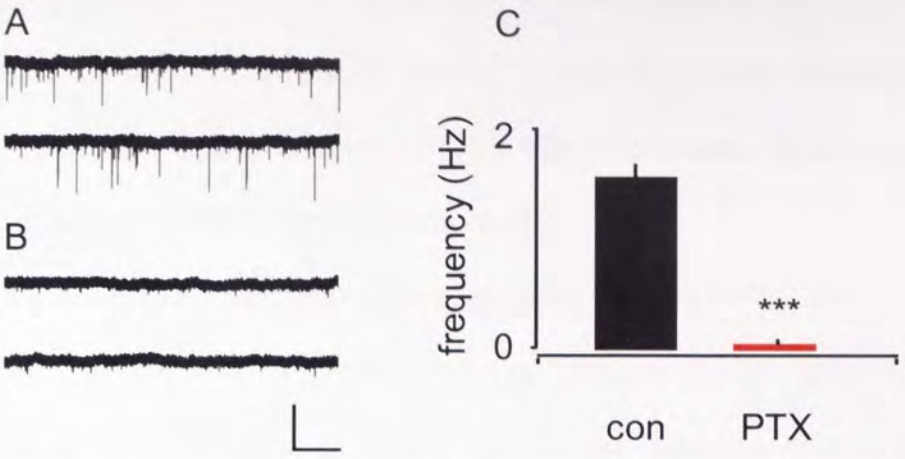

	Amplitude (pA)	rise time (ms)	Decay time (ms)	Area (pA·ms)	IEI (ms)
+IEM1640	184.8 ±7.5	2.9 ± 0.04	15.5 ± 0.46	371 ± 10	63.2 ± 1.7
CNQX+2-AP5	60.8 ±1.7	3.75 ± 0.08	13.3 ± 0.33	354 ± 15	90.2 ± 2.2

Fig 3.7 IEM allows only $GABA_A$ mediated GABAergic signalling.
sIPSCs from a single layer II neurone recorded in the presence of intracellular IEM 1460 during **A.** Control and **B.** In the presence of picrotoxin. **C.** Bar chart representing the decrease in sIPSC frequency during picrotoxin application. Black bar (control) red bar picrotoxin.

Table 3.1 Shows the mean kinetics for various layer II sIPSC parameters Recorded either in the presence of bath applied CNQX and 2AP-5 or intracellular IEM 1460.

Fig 3.8 A&B show sIPSCs recorded from a single layer II neurone during control **(A)** and following application of 10μM ACPA **(B)** in the presence of IEM 1460. During periods of ACPA application it would appear that the number of larger amplitude sIPSCs is roughly similar to that of control, however, it would seem that the numbers of smaller sIPSCs that intersperse these larger events have decreased in ACPA compared to control.

Fig 3.8C shows the cumulative probability plot for sIPSC amplitude during control (black) and ACPA (red). While the gap between the two plots is small, the overall change in distribution of sIPSC amplitudes between control and ACPA periods is significant ($P \leq 0.021$ KS test). In addition to a change in the distribution of amplitude, the mean amplitude showed a slight increase from 101.75 ± 3.25 pA in control to 108.27 ± 3.43pA in ACPA, this increase in amplitude was not significant ($P = 0.168$, ANOVA). **Fig 3.8D** is the cumulative probability for sIPSC IEI. The ACPA (red) plot lies to the right of control (black), indicating that the distribution of IEI has shifted towards larger values (decreased frequency) between control and ACPA periods. This change in distribution was highly significant ($P \leq 0.0001$, KS test). The increase in IEI was confirmed statistically, with the mean median IEI increasing from 34.64 ± 1.37 ms in control to 47.64 ± 1.31 ms in ACPA, this increase in IEI times was highly significant and shows that application of the CB1R agonist ACPA leads to a decrease in sIPSC frequency ($P \leq 0.0001$, ANOVA, n=4). As **Fig 3.8E** shows, in the cumulative probability for sIPSC area, the ACPA (red) plot lies to the right of the control (black) plot, indicating a change in sIPSC distribution had occurred and this change was also significant ($P \leq 0.006$, KS test).

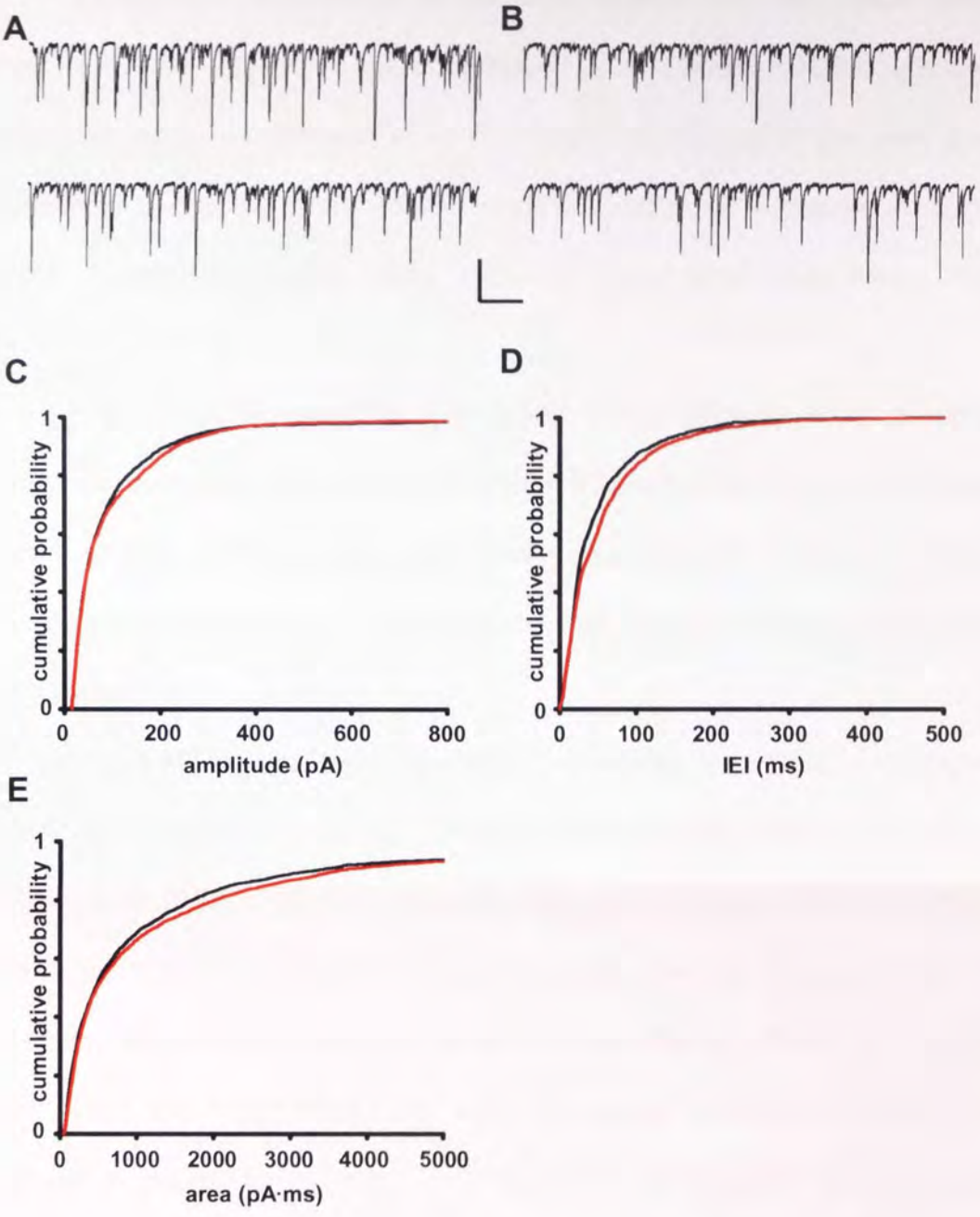

Fig 3.8 ACPA decreases sIPSCs in layer II mEC in the presence of IEM 1460
sIPSCs from a single layer II neuron during **A.** Control and **B.** ACPA periods. **C.** Pooled cumulative probability sIPSC amplitudes in control and ACPA. **D.** Pooled cumulative probability sIPSC IEI during control and ACPA **E.** Pooled cumulative probability sIPSC area in control and ACPA. Control = black, ACPA=red all experiments done in the presence of IEM at-80mV. Scale bar **X** 500ms **Y** 250pA, n=4.

As with the experiments in the layer II neurones with CNQX and 2-AP5 when ACPA was applied in the presence of IEM1460 (in layer II neurones) it was found that while a decrease in sIPSC frequency did occur (as was predicted) there were also some neurones where sIPSC frequency increased in response to ACPA. These recordings were analysed separately from those described immediately above.

Fig 3.9 A&B show sIPSCs recorded from a single layer II neurone during control **(A)** and ACPA **(B)** periods. In ACPA it appears that there are group of very closely spaced sIPSCs (presynaptic bursts, denoted with *) that do not appear in the control recordings and these suggest that overall increase in frequency has occurred.

Fig 3.9C shows the cumulative probability for sIPSC amplitudes. The ACPA plot (red) shows a large leftward shift between 200pA and 800pA. The large degree of separation between the two plots indicates definite change in the distribution of sIPSC amplitudes has occurred. The KS test confirmed that the change in distribution towards lower amplitudes was significant. ($P \leq 0.0001$, KS test). When the mean amplitudes were compared, amplitude fell from 189.53 ± 4.82 pA in control to 143.69 ± 3.17 in ACPA. The overall decrease in sIPSC amplitude was highly significant ($P \leq 0.0001$ ANOVA, n=5).

Fig 3.9D shows the cumulative probability for sIPSC IEI, the ACPA (10μM) (red) plot lies to a left of control (black) plot for IEI times between 50ms and 250ms. The separation between the two plots indicates a change in the distribution of sIPSC IEI between control and ACPA periods, and this change was highly significant ($P \leq 0.0001$ KS test). The change in IEI distribution is associated with a decrease in the mean median IEI, which fell from 67.69 ± 1.23 ms in control to 53.40 ± 0.85 ms in ACPA, this decrease in IEI times was highly significant and shows that the sIPSC frequency increased during ACPA application ($P \leq 0.0001$,

ANOVA). **Fig 3.9E** shows the cumulative probability plot for sIPSC areas. Here, the ACPA (red) plot lies to the left of the control (black) plot for the entire graph, the large gap shows that a shift in the distribution of sIPSC areas occurs and that this shift indicates a higher probability of larger sIPSC areas during ACPA compared to control. The change in distribution of sIPSC areas was highly significant ($P \leq 0.0001$, KS test).

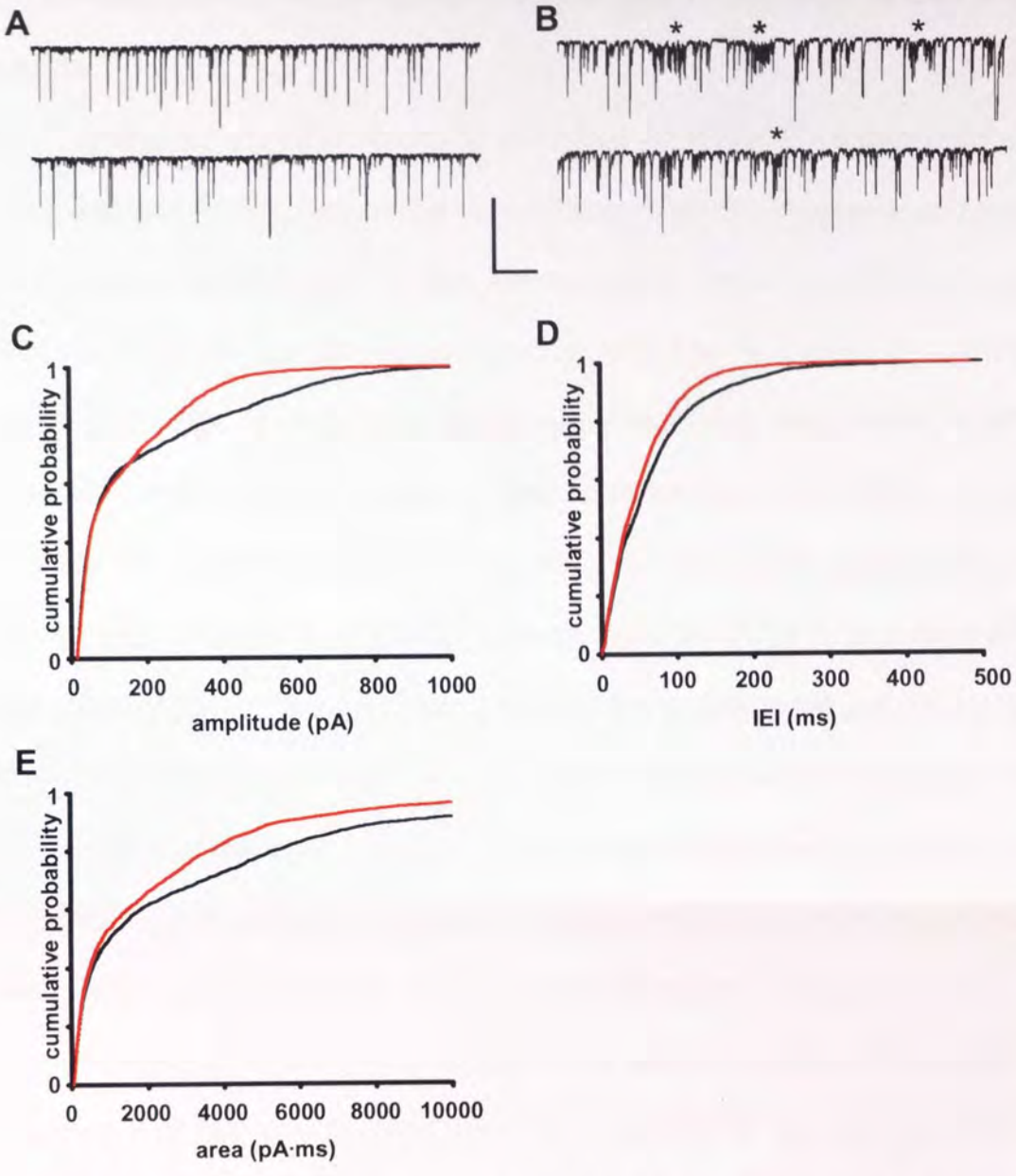

Fig 3.9 ACPA increases sIPSCs in layer II mEC in the presence of IEM
sIPSCs from a single layer II mEC neurone during **A.** Control and **B.** ACPA. Periods **C.** Pooled cumulative probability sIPSC amplitudes during control and ACPA **D.** Pooled cumulative probability sIPSC IEIs during control and ACPA, **E.** Pooled cumulative probability sIPSC areas during control and ACPA. All recordings done in the presence of IEM. Control = black ACPA = red scale **X** 2000ms **Y** 500pA, n=5

3.4 Normalised inhibitory charge transfer (NICT) analyses of CB1R agonist effects

Using our modified recording technique (IEM1460), we confirmed that the CB_1R agonist, ACPA, had similar dual effects on sIPSC frequency and amplitude as previously detailed in this thesis. As changes in frequency and amplitude were, in some cases, in opposite directions, it is difficult to determine the overall effect on phasic GABA release onto postsynaptic neurones, and hence whether the agonists would act to increase or decrease neuronal excitability. In order to address this issue, we calculated the NICT for 20 second epochs prior to and during drug application. Inhibitory charge transfer (ICT) is a measure of the amount of inhibitory charge passing across the postsynaptic membrane and, as such, is indicative of changes in GABA release and modulation thereof, independent of the specific direction of changes in frequency and amplitude of sIPSCs. We calculated NICT (using the mean area) for each individual recording, and then grouped these according to positive or negative changes in NICT.

We thought that NICT analyses would show a consistent decrease as it is expected that GABA signalling would be inhibited by the cannabinoid agonist ACPA. However, once again, we found dual effects of ACPA on NICT in recordings from layer II neurones of mEC. Application of ACPA caused a decrease in NICT (mean of 29.3 ± 6.37%, $P \leq 0.002$, ANOVA, n=5) in 5/9 recordings. The mean decrease in NICT in response in ACPA in the presence of IEM is shown in **Fig 3.10A**. ACPA caused an increase in NICT (mean 38.17 ± 17.61%, $P \leq 0.073$, ANOVA, n=4) in 4/9 recordings. The mean increase in NICT in response in ACPA in the presence of IEM is shown in **Fig 3.10B.** Both increased and decreased frequency and amplitude were seen in each NICT group.

When we reanalyzed the data recorded using ACPA in the presence of CNQX and 2-AP5, we found similar results. Here, a decrease in NICT occurred, in

4/11 recordings, (NICT decreased by mean -39.70 ± 13.71% in ACPA compared to control, $P \leq 0.026$, ANOVA, n=4), **Fig 3.10C** illustrates the mean decrease in NICT in response to ACPA application in layer II of the mEC in the presence of CNQX and 2-AP5. However in 7/11 recordings, NICT increased, (mean 59.32 ± 17.89% in ACPA, $P \leq 0.006$, ANOVA, n=7) compared to control. **Fig 3.10D** illustrates the mean increase in NICT in response to ACPA application in layer II of the mEC in the presence of CNQX and 2-AP5.

In summary, we found that structurally dissimilar CB1R agonists had two effects on GABA release from terminals onto neurones in layer II of the mEC. Using different recording techniques (including a completely novel method of blocking ionotropic glutamate receptors from inside the recorded cell) and analytical methods, we were unable to ascribe these dual effects to experimental artefact or analytical bias. These issues are discussed later, however, we next determined to investigate the effects of CB1R antagonists at layer II inhibitory terminals.

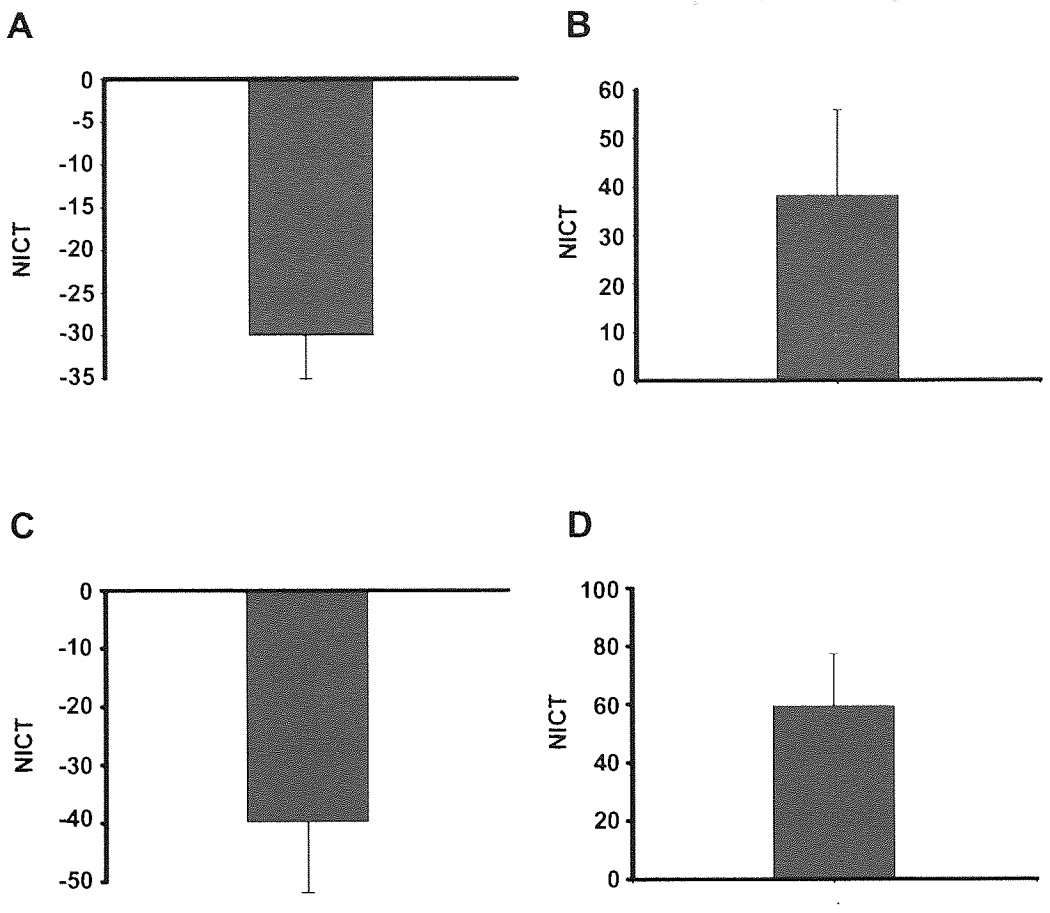

Fig 3.10 ACPA has duel effects on NICT whether experiments are carried out in the presence of CNQX and 2-AP5 or IEM 1460

bar charts illustrating that both **A.** Decreases in NICT (n=5) and **B.** Increases in NICT (N=4) with respect to control occurred in layer II mEC in response to ACPA (10μM) application in the presence of intracellular IEM 1460. **C.** Decreases in NICT during ACPA (10μM) application in layer II mEC in the presence of CNQX and AP-5 (n=4). **D.** Increases in NICT during ACPA (10μM) application in the presence of CNQX and 2-AP5 (n=7)

3.5 The CB1R antagonist AM-251 consistently increased sIPSC frequency and had mixed effect on amplitude and NICT.

In some areas of the brain it has been shown that cannabinoid signalling is tonically active, that is to say that endogenous cannabinoids are continually being released and suppressing GABA release (Oliet *et al.,* 2007), or that CBRs are constitutively active, with similar results (for review, see Pertwee, 2005). To investigate tonic endocannabinoid function in the mEC it was decided measure sIPSCs parameters when a CB_1R antagonist/inverse agonist was applied. AM-251 is a CB1R selective antagonist/inverse agonist and was identified as a CB1R ligand in 1996 by Gatley *et al.*

AM-251 (10μM) was bath applied to the slice and either the IEM1460 recording method was used, or block of NMDA and AMPA receptors as previously described. Since we observed little difference in cannabinoid modulation of GABA responses recorded using either method, all data were pooled. The data below are from 10 layer II mEC neurones all of which showed an increase in sIPSC frequency during AM-251 application.

Fig 3.11A & B show sIPSCs recorded from a single layer II mEC neurones during control (**A**) and AM-251 (10μM) (**B**) periods. When the AM-251 period is compared to control it appears to have a higher number of the larger sIPSCs than control, and this is notable as the larger sIPSCs in control are sparsely distributed while in AM-251 (10μM) the larger events are much closer together indicating an increase in frequency.

Fig 3.11C Shows the cumulative probability plot for sIPSC amplitudes. The AM-251 (red) plot lies to the right of control (black line) for amplitudes below 200pA suggesting that a change in the distribution of sIPSC amplitudes towards larger values occurs between control and AM-251 recordings. This change in distribution was highly significant ($P \leq 0.0001$, KS test). Although the change in

the distribution of sIPSC amplitudes occurred there was no significant change in the mean amplitude (mean control amplitude 140.80 ± 8.57pA versus 139.77 ± 8.82 in AM-251; $P \leq 0.86$ ANOVA), almost certainly reflecting the fact that mean sIPSC amplitude in layer II is dominated by the preponderance of low amplitude, AP-independent events.

Fig 3.11D Shows the cumulative probability plot for sIPSC IEIs. The AM-251 (red) plot lies to the left of control (black), indicating increased frequency, and this was true in 10/10 recordings. This shift in distribution towards lower IEI values was highly significant ($P \leq 0.0001$, KS test, n=10). In addition to a change in the distribution of sIPSC IEI there was also a significant decrease in the mean median IEI from 43.80 ± 1.43 ms in control to 35.68 ± 1.46ms ($P \leq 0.0001$, ANOVA), again confirming that the sIPSC frequency increased during AM-251 application.

Fig 3.11E Shows the cumulative probability plot for sIPSC area. The AM-251 (red) plot lies to the right of control (black) plot for areas up to 1000 pA·ms and the gap between the two plots shows a change in the distribution of sIPSC areas towards larger values occurs between control and AM-251 periods. This change in distribution was significant ($P \leq 0.001$ KS test, n=10). The mean area showed a slight increase rising from 318.96 ± 6.63 in control to 342.73 ± 7.34 pA·ms in AM-251.

When the effects of AM-251 on GABAergic signalling were considered in terms of NICT, we again observed two effects, consistent with the agonist data described above, and despite the consistent effect on frequency in all 10 recordings. As **Fig.12A** shows, in 5/10 recordings, NICT was reduced by 28.81 ± 9.35% of control ($P \leq 0.013$, ANOVA n=5), and, as **Fig 12B** shows, in 5/10 recordings NICT increased by 68.33 ± 26.86% of control ($P \leq 0.037$, ANOVA, n=5).

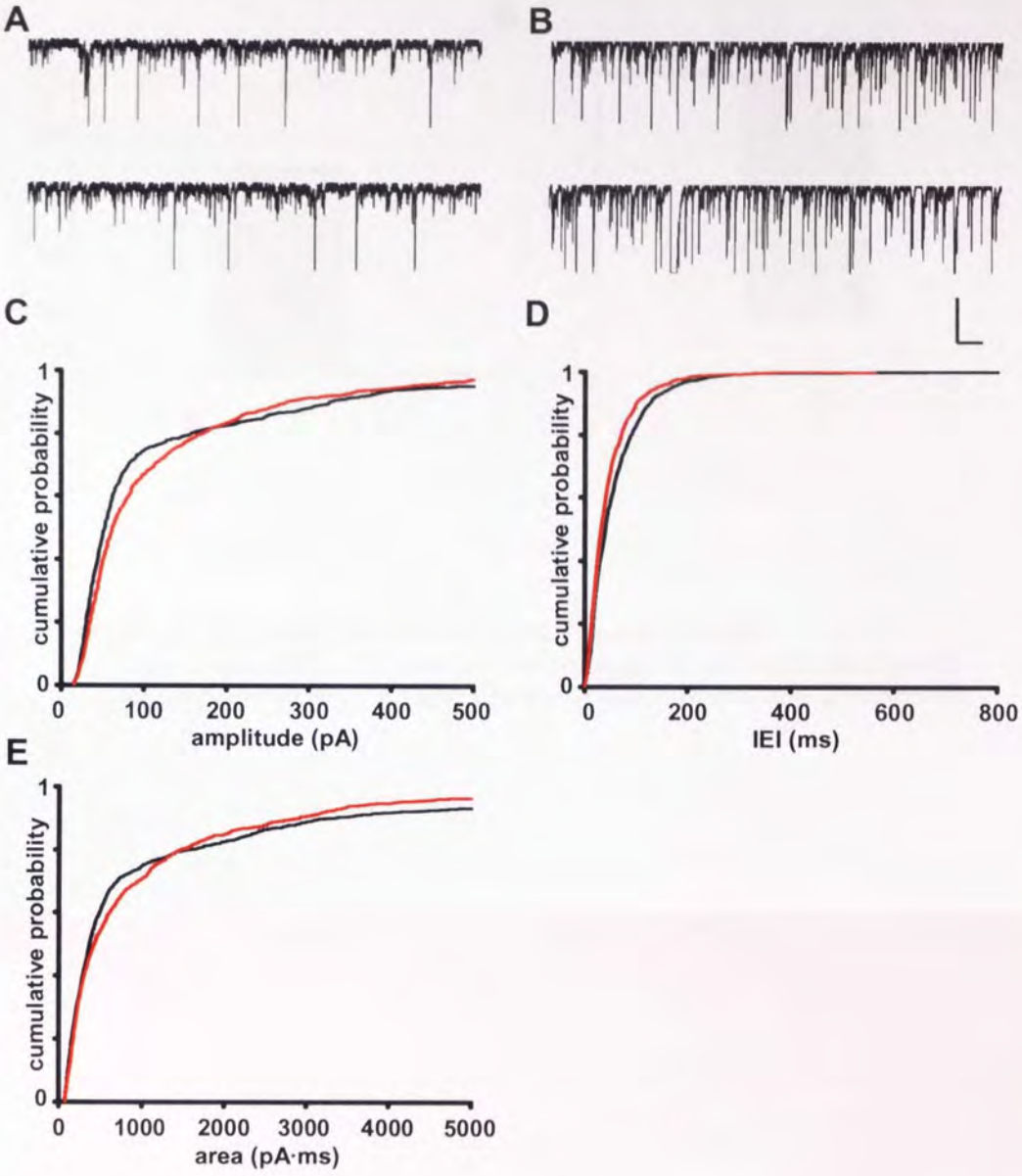

Fig 3.11 A&B Effects of AM-251 on layer II sIPSC kinetics.
sIPSCs from a single layer II mEC neuron during **A.** Control and **B.** AM-251 (10μM). **C.** Pooled cumulative probability sIPSC amplitudes in control and AM-251 (10μM) periods **D.** Pooled cumulative probability sIPSC IEIs in control and AM-251 periods. **E.** Pooled cumulative probability sIPSC areas in control and AM-251. **X** axes 1000ms **Y** 100pA, n=10. black = control, red = AM-251 (10μM)

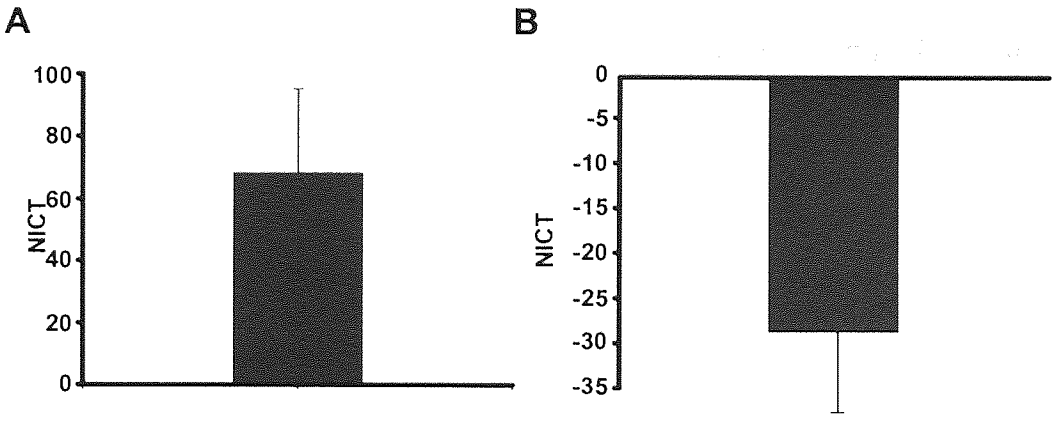

Fig 3.12 AM-251 has dual effects on NICT in layer II mEC.
A. mean increase in NICT in layer II in response to AM-251 application (n=5).
B. mean decrease in NICT in layer II in response to AM-251 application (n=5)

3.5 ACPA only has one effect on GABAergic signalling in layer V mEC

After seeing that the CB1R agonists WIN 55,212-2 and ACPA both had a dual effect on GABA release in layer II of the mEC, it was next decided to see how the deep layers (namely layer V) responded to CB1R agonist. As already discussed, layer V neurones have a much lower level of inhibitory activity than layer II neurones, as well as different connections within the PHR and it maybe that they respond differently to the cannabinoid agonist.

For these experiments, the IEM 1460 method of blocking excitatory signalling was used and ACPA was selected as the agonist to maintain consistency with previous experiments. 100% of neurones showed a decrease in sIPSC frequency during ACPA application.

Fig 3.13A&B show sIPSCs from a single layer V mEC neurone during control **(A)** and ACPA (10μM) **(B)** periods. The control trace illustrates the lower level of inhibitory activity that occurs in layer V of the mEC compared to layer II, as described by Woodhall *et al.* (2005). When the layer V control (**Fig 3.13A**) is compared to the ACPA record (**Fig 3.13B)** then it can be seen that the number of large sIPSCs has decreased. In addition to this, it appears that the number of smaller sIPSCs has also decreased as overall there are fewer downward deflections from the base line in ACPA compared to control.

Fig 3.13C Shows the cumulative probability plot for sIPSC amplitude. The ACPA (red) plot lies directly over the control (black) plot showing no shift in amplitude distribution. This was confirmed by a non significant KS test (P = 0.23). While there was no change in distribution of sIPSC amplitudes there was a slight increase in the mean amplitude which rose from 59.41 ± 7.33pA in control to 70.49 ± 8.89pA in ACPA this increase was not significant (P = 0.33, ANOVA, n=6).

Fig 3.13D shows the cumulative probability for sIPSC IEI. The ACPA (red) plot lies to the right of the control (black) plot for the duration of the graph, indicating a shift in distribution of sIPSC IEI towards much larger values (decreased frequency) between control and ACPA periods in layer V. The change in distribution was significant ($P \leq 0.0001$ KS test). In addition to a change in the overall distribution of sIPSC IEI, the mean median IEI was found to increase very significantly from 792.59 ± 41.12ms in control to 1317± 745.00ms in ACPA ($P \leq 0.0001$, ANOVA, n=6). This effect of ACPA on IEI in layer V was consistent in all recordings.

Fig 3.13E is the cumulative probability plot for sIPSC area the ACPA (10μM) (red) plot and the control (black) plot lie very close together suggesting no change in the distribution of sIPSC areas has occurred, and this was confirmed in statistical analysis ($P \geq 0.23$ KS test). The mean area showed a slight increase from 272.92 ± 7.51 pA·ms in control to 290.72 ± 8.03 pA·ms in ACPA (10μM) this increase in area was not significant ($P = 0.47$ ANOVA). **Fig 3.13F** shows a bar chart illustrating the slight increase in NICT that occurs in ACPA compared to control, and again this was not significant ($P \geq 0.51$, ANOVA, n=6).

Unlike layer II neurones sIPSCs recorded from layer V consistently showed a decrease in sIPSC frequency, therefore it was decided that we would not repeat the ACPA experiments in CNQX and 2-AP5 in addition to the IEM 1460 experiments described above. We next investigated the effects of the CB1R antagonist AM-251 in layer V of the mEC.

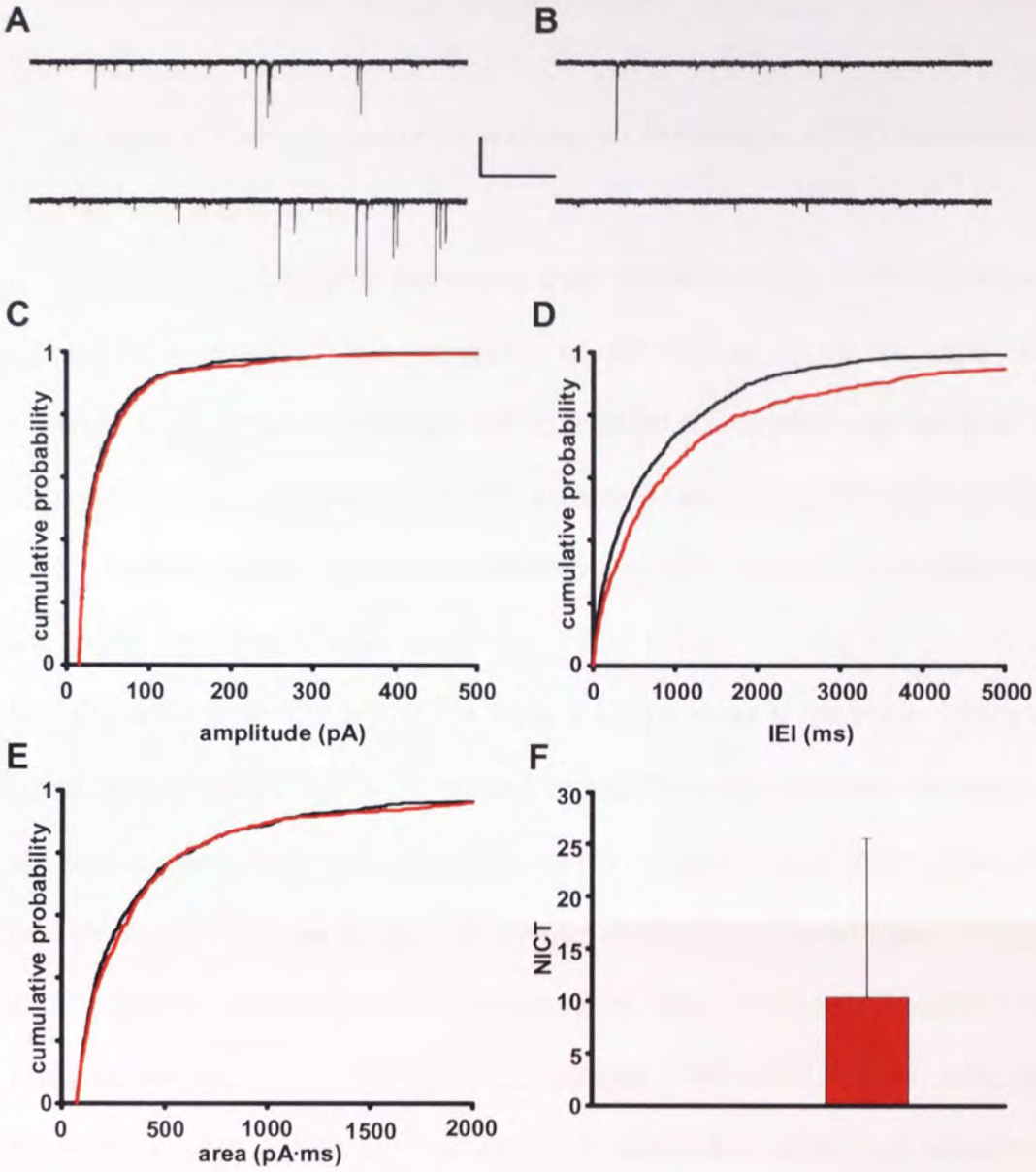

Fig 3.13 ACPA reduces sIPSCs in layer V mEC.
sIPSCs from a single layer V neuron during **A** control and **B** ACPA(10μM). **C.** Pooled layer V sIPSC amplitude in control and ACPA **D.** Pooled sIPSC IEIs in control and ACPA. **E** Pooled sIPSC areas during control and ACPA **F.** Change in NICT during ACPA application (red bar) layer V. Control = black, ACPA =red, Scale bar **X** 5000ms **Y** 200pA. n=6.

3.5.1 The CB_1R antagonist/ inverse agonist AM-251 increases sIPSC frequency.

In layer V 100% of neurones showed an increase in sIPSC frequency during AM-251 application.

Previous experiments indicated that ACPA reduced sIPSC frequency in deep mEC, suggesting the presence of CB1Rs at terminals onto layer V neurones. We decided to use AM-251 to explore the question of whether CB_1Rs at layer V terminals showed any tonic activity or were constitutively active, as in layer II. Results below were recorded from 4 layer V neurones using IEM1460 to block AMPA and NMDA receptors.

Fig 3.14 A&B Show sIPSCs from a single layer V neurone during control **(A)** and AM-251 **(B)** periods. In control the sIPSCs are sparsely distributed, and when this is compared to the AM-251 period it can be seen there more sIPSCs, with a tendency towards clusters of events. From these recordings it is apparent that AM-251 increased sIPSC frequency in layer V mEC. **Fig3.14C** is the cumulative probability plot for sIPSC amplitude. The AM-251 (red) plot lies very close to the control (black) plot, with a small shift in the distribution towards larger sIPSC amplitudes, and this was significant ($P \leq 0.019$, KS test, n=4). The mean amplitude showed a small non-significant decrease from 87.44 ± 5.79pA in control to 85.84 ± 4.65 pA ($P \geq 0.828$, ANOVA). **Fig 3.14D** Shows the cumulative probability plot for sIPSC IEI. The AM-251 (red) plot lies markedly to the left of control for the duration of the graph, and this indicates that a strong shift towards shorter IEI values (increased frequency) in the distribution of sIPSC IEI between the control period and the AM-251periods. This shift in IEI distribution was not significant ($P \geq 0.075$, KS test). Whilst the change in distribution of sIPSC IEI times was not significant, the overall decrease in the mean median IEI from 1003.2 ± 143.88ms in control to 349.2 ± 53.33ms in AM-251 was highly significant

($P \leq 0.002$, ANOVA, n=4). This decrease in IEI shows that AM-251 causes an overall increase in sIPSC frequency.

Fig 3.14E Shows the cumulative probability plot for sIPSC area. The AM-251 (red) plot and the control (black) plot lie close to together with no clear shift of the AM-251 plot to the left or right of the control. This indicates that there is no difference in the distribution of sIPSC areas between the two situations; the KS test confirms no significant change occurs in the area distribution ($P = 0.68$, KS test). The mean area showed a slight decrease from 336.40 ± 14.49 pA·ms in control to 318.54 ± 13.90 pA·ms in AM-251. This decrease was not significant ($P = 0.24$, ANOVA, n=4). When we measured NICT, AM-251 caused an increase in charge transfer with the inhibitory charge transfer rising from 0±0 in control to 39.55 ± 47.90 % in AM-251. Due to the high degree of variance in the NICT measurements, this did not reach statistical significance. **Fig 3.14F** is a bar chart illustrating the increase in NICT (red bar) in AM-251 compared to a control.

Thus we saw a significant change in IEI but while trends towards a larger amplitude and increased NICT were seen, these changes were not significant, it is felt that the lack of significant change in NICT and amplitude was due to the variance between the pooled numbers.

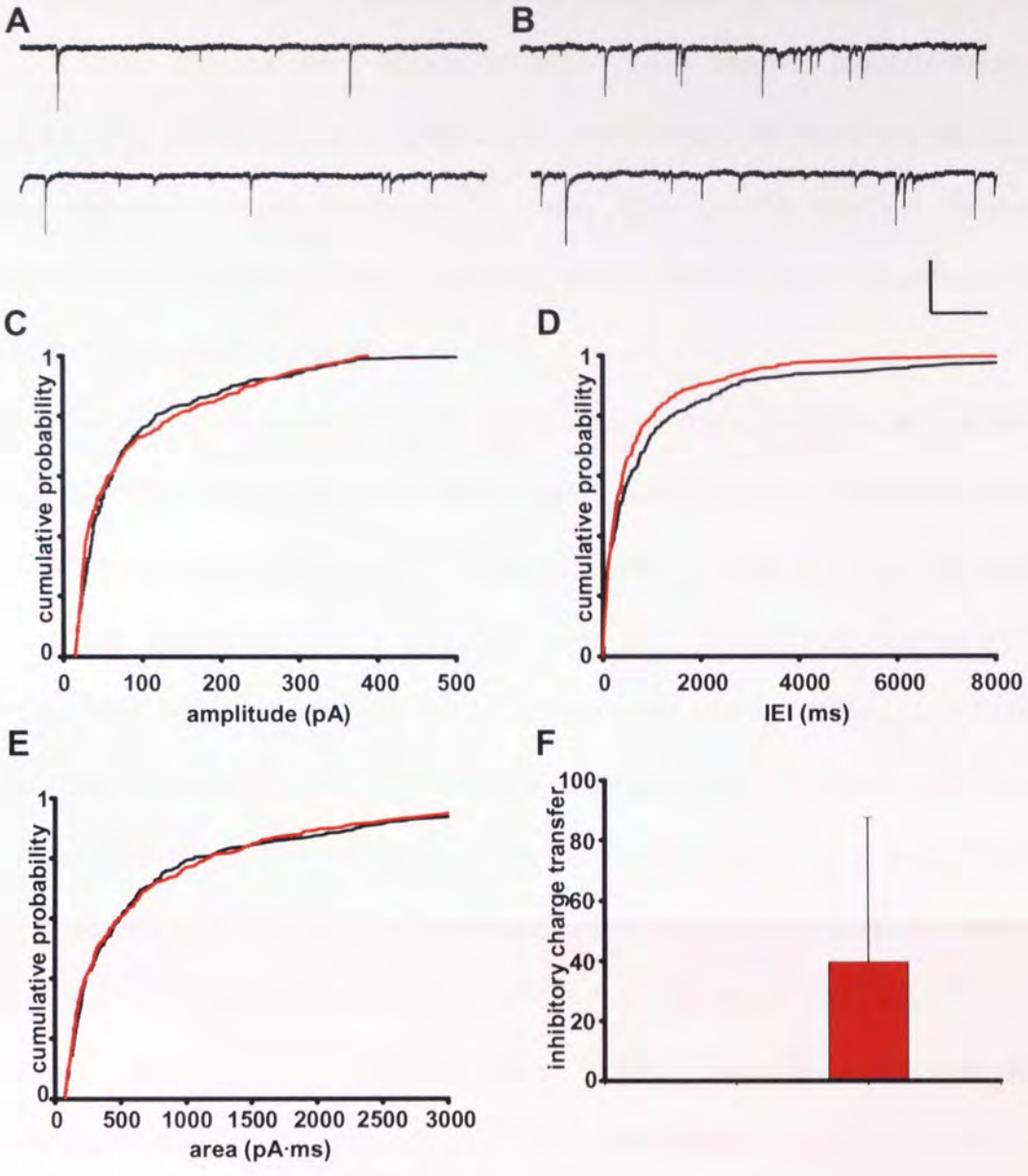

Fig 3.14 AM-251 increases sIPSCs in layer V mEC
sIPSCs from a single layer V mEC neurone during **A** Control **B** and AM-251(10μM) periods. **C.** Pooled sIPSC amplitudes in control and AM-251. **D**. Cumulative probability pooled sIPSC IEIs in control and AM-251.**E.** Cumulative probability for sIPSC areas in control and AM-251 in layer V Control =black AM-251=red. scale bar **X** 1000ms **Y** 200pA, n=4.

3.6 Tocrisolve ™ has no significant effects on layer II sIPSCs

Since two opposing effects of ACPA were seen in layer II neurones in response to ACPA (10μM) application it was decided to check the effects of the drug delivery vehicle Tocrisolve™ alone. The results outlined below were collected from 5 layer II mEC neurones where sIPSCs were recorded using the IEM methods already described.

When we measured mean amplitude in the presence and absence of Tocrisolve™, a slight decrease was noted, from 127.13 ± 7.56pA in control to 109.86 ± 6.60pA in Tocrisolve™. This decrease in amplitude was not significant ($P \geq 0.085$, ANOVA, n=5). Similarly, changes in IEI distribution was not significant ($P \geq 0.0646$ KS test) and nor was the increased mean median IEI (from 47.29 ±10.10ms in control to 56.25 ± 15.37ms in Tocrisolve™; $P = 0.29$, ANOVA, n=5). We did note a significant change in the distribution of sIPSC areas ($P \leq 0.0007$, KS test), however, mean area showed a slight, but non-significant decrease from 351.70 ± 8.63 pA·ms in control to 333.73 ± 1.91 pA·ms in Tocrisolve™ ($P \geq 0.10$, ANOVA). Once the area was converted to NICT, we noted no change in this parameter (-4.0 ± 9.3 % in Tocrisolve™; $P = 0.68$, n=5).

3.7 Discussion

3.7.1 Effects of WIN 55,212-2 and ACPA.

Data presented here using CB_1R agonists WIN 55,212-2 and ACPA agree in showing that application of CB_1R agonists cause a suppression of $GABA_A$ mediated sIPSCs shown by increased IEI and decreased NICT. These data agree with previous studies showing that application of a CB_1R agonist suppresses $GABA_A$ergic neurotransmission. For example, Nakatsuka *et al.,* (2003) showed WIN 55,212-2 suppressed both frequency and amplitude of sIPSCs and reduced the amplitude of eIPSCs in the human dentate gyrus. Katona *et al.,* (2001) in the amygdala showed WIN 55,212-2 and CP 55,940 (a CB_1R agonist) reduced the amplitude of both s & e IPSCs. In hippocampus, Katona *et al.,* (1999) reported WIN 55,212-2 reducing evoked GABA release in a dose dependent manner using concentrations from 0.01-3 μM. Furthermore these authors used TTX to show that their evoked GABA release was action potential-dependent (AP-dependent) and therefore that cannabinoids must be modulating AP-dependent events. Hájos *et al.,* (2000) further showed that WIN 55,212-2 specifically decreased Ca^{2+} dependent GABA release in the hippocampus. In the rat somatosensory cortex, application of WIN 55,212-2 suppressed the amplitude of eIPSCs (Bodin *et al.,* 2001) and Ohno-Shosaku *et al.,* (2001) showed WIN 55,212-2 (1-3 μM) suppressed IPSCs recorded from cultured hippocampal neurones.

As well suppressing inhibitory signalling it has also been shown that cannabinoid agonists are capable of suppressing excitatory signalling. With studies by Takahashi & Castillo 2006 showing a decrease in field excitatory post synaptic potentials in the presence of WIN 55,212-2 in the hippocampus and Kreitzer & Regehr (2001) showed depolarization-induced suppression of excitation (DSE) in Purkinje cells that could be prevented by the CB_1R antagonist AM-251 and occluded by WIN 55,212-2.

While we have presented data that broadly agrees with work done in previous studies that cannabinoid agonists suppress $GABA_A$ mediate IPSCs, this is not the whole story. We have also presented data above that indicates CB_1R agonists also promote increases in $GABA_A$ mediated neurotransmission in layer II mEC neurones. In 50% of neurones tested using WIN 55,212-2 (10μM) and 65% tested using ACPA (10μM); a decrease in IEI (indicating an increase in frequency) was seen, with mixed effects on amplitude. In addition to this when NICT was calculated in an attempt to make sense of the unexpected frequency increase neurones could still be split into two distinct groups those with an overall decrease in NICT and those with an increase in NICT. Hence, even while effects on IEI amplitude and area were complex, and often contradictory, it was not true that overall inhibitory neurotransmission was reduced. The increases in inhibitory signalling that we observed were unexpected, and we chose to investigate possible causes.

Firstly it was thought that it was possible that the drug delivery vehicle Tocrisolve™ was affecting signalling. To address this problem a control experiment was done using Tocrisolve™ with no ACPA in layer II neurones, however as described above application of Tocrisolve™ had no significant affects on sIPSCs in layer II mEC.

Next, we questioned if the IEM1460 recording method was causing the enhancement in inhibitory signalling. In using IEM1460, we were measuring $GABA_A$ mediated events, but in the context of intact excitatory network function - perhaps allowing excitatory signalling in the rest of the slice to give rise to the unexpected increase in NICT and decrease in IEI in some layer II neurones. By suppressing excitation elsewhere in the slice we may increase inhibition (e.g. through disinhibition) onto the postsynaptic neurone where recordings were being made.

It is known that cannabinoids modulate glutamate signalling and that there are CB_1Rs at excitatory presynaptic terminals (Domenici *et al.,* 2006). There is also plenty of electrophysiological evidence that cannabinoids can modulate excitatory signalling. For example, agonist-mediated suppression of spontaneous and/or evoked EPSC amplitude has been shown in nucleus accumbens (Robbe *et al.,* 2001), ventral tegmental area (Melis *et al.,* 2004), hippocampus and (Takahashi & Castilo, 2006). It was possible that CB_1R agonists acting to suppress excitatory signalling may have been reported as the decreased sIPSC IEI and increased NICT due to connectivity effects within the slice, e.g. disinhibition. However, picrotoxin experiments confirmed that we were exclusively measuring GABAergic events in the postsynaptic neurone, and application of glutamate receptor blockers (CNQX and 2-AP5) showed that two effects could be elicited by ACPA even when excitatory network function was abolished.

Once we had ruled out the IEM 1460 recording method, the drug delivery vehicle and actions of cannabinoid agonists on excitatory signalling as possible causes of the increase in inhibitory signalling reported here, we next looked at the cannabinoid agonists used. Both WIN 55,212-2 and ACPA were used at a bath concentration of 10μM, this was higher than that in previous studies where WIN 55,212-2 concentration ranges from 1μM-5μM. (Melis *et al.,* 2004; Hajos *et al* 2000;2001, Ohno-Shosaku *et al.,* 2001; Wilson & Nicoll., 2001; Kreitzer & Regehr 2001 and Hentges *et al.,* 2005), previous studies using ACPA selECted concentrations of 5 and 10μM (Newman *et al.*, 2007). Although the concentrations of CB_1R agonists used here are little higher than those used in other studies, they are not overly high, and furthermore it is believed that if the increases in inhibitory signalling in response to both WIN 55,212-2 and ACPA was due to overly high concentrations of the drug, then we would have expected to have seen mixed results in layer V neurones in addition to layer II. As this was not the case it would

appear that neither the drug used or the concentration of agonist bath applied was the cause of the increase in sIPSCs.

Finally we considered if the unexpected increase in inhibitory signalling was due to the viability of the slices. The recordings made were from various points within a day's research, but there was no trend of only seeing the agonist causing increased sIPSCs at either the end or start of the experimental day. Furthermore due to the lipophillic nature of the drugs used all recordings were a minimum of an hour which indicates that slice viability was good throughout. Finally, as with the drug concentrations, it would be expected that if the increase in sIPSCs was due to slice viability we would see similar results in layers V.

3.7.2 Hypothesis

Having ruled out the most obvious explanations for the unusual effects of CB_1R agonists ACPA and WIN 55,212-2 in layer II mEC we considered other possible explanations of the increase in inhibitory signalling in layer II mEC neurones.

Layer II of the mEC is a not a simple brain area, it consists of various cell types (see introduction for full overview) with the two main principal neurones being stellate and pyramidal cells (Alonso & Klink 1993; Klink & Alonso 1997; Buckmaster *et al.,* 2004). In addition to this, a range of inhibitory interneurones are also present within layer II of the mEC and it could be possible that it is this variation that accounts for the mixed responses to CB_1R agonists. Hence, when patching in layer II it is not always clear if we are recording from a pyramidal or stellate neurone and it maybe that these different neuronal types have different inhibitory inputs from different interneurones. While immunohistochemical studies such as those carried about by Moldrich & Wenger, (2000) and Tsou *et al.*, (1998) confirmed the presence of CB_1Rs on presynaptic GABAergic terminals. More

recent studies have shown that CB_1R expression can be further defined to specific subsets of interneurones. Four main different types of interneurones have been identified in the brain in general, two types of basket cell are seen, one positive for cholecystokinin (CCK) and one that is positive for parvalbumin (PV), and both these interneurones innervate the soma and proximal dendrites of principal cells. One further type of interneurone also innervates principal cells but not at the soma, instead calbindin positive (CD28k) interneurones innervate the mid-proximal dendrite of pyramidal cells. Finally, a fourth type of interneurone has been identified that specifically innervates other inhibitory interneurones, and these are identified by their positive staining with calretinin (CRT) (for a full review see Marsicano & Lutz 1999).

Marsicano & Lutz (1999) went on to show that in the mouse forebrain expression of CB_1Rs is restricted to specific subpopulations of inhibitory interneurones, with CB_1R expression highest in CCK-positive PV-negative GABAergic neurones, and that calbindin interneurones showed some co-expression with CB_1Rs but not to the same extent as the CCK-positive neurones. No co-expression of CB_1Rs and PV-positive or CRT- positive interneurones was found in this study. The specific localization of CB_1Rs on CCK-positive interneurones was confirmed in the human hippocampus, (Katona *et al.,* 2000) and the amygdala of the rat (Katona *et al.,* 2001). Katona *et al.,* (1999) also showed that in hippocampal networks of the rat, interneurones staining positive for CB_1Rs largely belonged to the CCK-positive basket cell subpopulation of interneurones while a very small percentage (4% of CB_1R positive cells) of the PV-positive neurones were also positive for CB_1Rs. Furthermore these authors demonstrated that in the rat hippocampus, when co-localization of CB_1R and PV did occur, this was not at terminals onto pyramidal neurones. In the rat somatasensory cortex Bodor *et al.*, (2005) concurred with the findings of

Marsicano & Lutz (1999) that CB_1R expression was localized to two specific subsets of interneurones, they identified that two thirds of the CB_1R expressing interneurones were CCK-positive while the remaining third of CB_1R expressing neurones were CD28k positive. Thus it appears that CB_1Rs are not present on all GABAergic interneurones, and subsets of theses cells differentially innervate principal cells.

Both PV-positive and CCK-positive basket interneurones have been shown to be present in the EC (Köhler & Chan-Palay 1982; and Wouterlood *et al.,* 1995 respectively). Within the PHR the EC has the highest proportion of CCK positive interneurones, and layer II of the EC has CCK-positive neurones with dendrites that extend within the layer and to all other layers of the EC. In addition to this layer II of the EC receives inputs from CCK-positive cells which originate from other layers of the EC (Köhler & Chan-Palay 1982). Layer II of the mEC (along with layer IV) appears to have the highest number of CCK-positive nerve terminals and the majority of these synapses are formed with the somata of principal cells (see Kohler & Chan-Palay, 1982 for full summary). Wouterlood *et al.,* (1995) showed PV-positive fibres formed symmetrical synapses with principal cells in layer II of the EC and these appeared to be arranged in basket formation. Niether Wouterlood *et al.*, (1995) and Köhler & Chan-Palay (1982) differentiates as to whether inhibitory synapses are formed with any specificity to stellate or pyramidal cells. However, if these inhibitory inputs to the principal cells could be linked to one specific principal neurone type, then it might help explain the unusual affects of CB_1R agonists in layer II. If we are to presume that the CCK positive synapses also express CB_1Rs and are only found at a subset of the principal neurones I layer II then these may be the neurones that show a decrease in inhibitory signalling in response to the cannabinoid agonists. Conversely, if another set of principal cells present in layer II of the mEC receive

the majority of their inhibitory input from the PV positive CB_1R negative interneurones, and these neurones are in turn subject to input from CCK and/or CB_1R positive interneurones, then conditions exist to support disinhibition and principal cells may report an increase in inhibitory signalling in response to CB_1R agonists. It is possible that this is a viable scenario, although Marsicano & Lutz (1999) showed in mouse forebrain that no CB_1Rs were co-expressed with calretinin, which is used as a marker for interneurones that specifically act to inhibit other interneurones. That is not to say that CB_1Rs are not present at the synapse of these interneurones elsewhere in the brain (e.g. mEC) or that species-specific differences might exist. Alternatively, other types of interneurone apart from the calretinin cells may form inhibitory synapses with other interneurones. Wouterlood *et al* (1995), looking at PV positive interneurones in the entorhinal cortex, identified a subset of interneurones within the PV positive group that formed synapses with the axon terminals, dendrites and somas of other PV positive interneurones. Further evidence to support this connectivity comes from work done in the neocortex by Galarreta *et al.,* (2008). Here the investigators looked the differences between fast spiking interneurones (FS) that showed no CB_1R expression and were insensitive to both DSI and bath applied WIN 55,121-2 and irregular spiking interneurones that were positive for CB_1R expression (CB_1-IS) and showed suppression of IPSCs during DSI and bath application of WIN 55,212-2. When CB_1-IS interneurones were further investigated they were shown not only to form synapses with the pyramidal neurones but that they also formed synapses with other CB_1-IS interneurones. Bath application of WIN 55,212-2 suppressed IPSCs at these CB_1-IS synapses. However, when these researchers tried to evoke DSI at these inhibitory to inhibitory synapses they saw no suppression of sIPSCs was observed, suggesting that while CB_1Rs are present at these CB_1-IS to CB_1-IS synapses they do not respond in the same way as the

CB_1-IS, pyramidal synapse. Lastly, a further complication is the report by Wouterlood et al., (2000), who identified *excitatory* interneuronal calretinin (CRT)-positive cells in layer I of mEC that may innervate principal and inhibitory neurones I layers II and III.

A further potential explanation of the dual effects of CB_1R agonists on sIPSCs in layer II mEC involves the possibility that the different neuronal targets synthesise different endogenous cannabinoids, which activate target and agonist-specific G-protein complexes. There is growing evidence that specific populations of neurones in different brain regions produce either AEA or 2AG in response to stimulus. Stella *et al.,* (1997) showed that high frequency stimulation in the hippocampus increased levels of the endogenous cannabinoid 2-AG, while AEA levels remained the same. Conversely, in dorsal striatum it was found that AEA was released in response to depolarization or in response to application of the D_2 like agonist quinpirole (Giuffrida *et al.*, 1999). Evidence such as this indicates that different neuronal subtypes produce specific endogenous cannabinoids in response to stimulation. Similarly, it has been shown that the CB_1R G-protein association may allow for differential signalling by CB_1R ligands. Although only one effect of cannabinoid ligands has been reported in inhibitory and excitatory signalling in neurones (namely a suppressive role). In other systems binding of agonists have been shown to have both inhibitory and stimulating effects. For example it has been shown that binding of cannabinoid agonists at CB_1R receptors can both inhibit and stimulate adenylyl cyclase activity, and it does so via different G_i protein isoforms (for a full review see Mukhopadhyay *et al.,* 2002). Rhee *et al.,* (1998) investigated this difference and found the effect CB_1R agonists in modulating adenylyl cyclase (i.e. inhibitory or stimulating) was dependent on the precise isoform of adenylyl cyclase present intracellularly. It was that found adenylyl cyclase isoforms I, V, VI and VIII were inhibited due to activation of CB_1

or CB_2 receptors while the adenylyl cyclase isoforms II, IV and VII were stimulated in response to CB receptor activation (Rhee *et al.,* 1998). It is believed that the stimulatory effects of CBRs on adenylyl cyclase isoforms II, IV and VII are due to them interacting with $\beta\gamma$ subunit that is liberated from the $G_{\alpha\ i/o}$ subunits on activation of the cannabinoid receptor. While the inhibitory effects of CBR activation on isoforms I, V, VI and VIII is due to the α i/o subunit of the G-protein complex (Rhee *et al.,* 1998). It is possible that are dual response to cannabinoid agonists WIN 55,212-2 and ACPA may therefore relate to different intracellular messenger activity in the pre-synaptic neurone as a result of receptor activation. Differential modulation of intracellular signalling mechanisms may tie in to different inhibitory innervations of principal cell types between terminals expressing mainly increased or decreased cAMP responses.

In addition to the possibility that activation of CB_1Rs in layer II of the mEC may stimulate different responses due to different neurones having different intracellular signalling cascades, it has also been shown that different agonist structures dock at different sites with in the CB_1R, and in so doing activate specific G-protein subtypes (e.g. G_i, G_0, G_q), leading to different intracellular signals being sent. It has been shown that different CB_1R agonists have different efficacies when it comes to activating different G-protein subunits. For example WIN 55,212-2 and AEA were equally efficacious in producing maximal stimulation of G_i proteins, but were both only partially active when it came to stimulating G_o proteins (for a full review of different CBR agonists and there ability to stimulation G-protein subunits see Mukhopadhyay *et al.,* 2002). It appears that the ability of a cannabinoid agonist to stimulate the various G-protein subunits depends on where it docks within the CB_1R. Different CB_1R agonists have different structural properties and as such they dock with the CB_1R at different sites depending on where the agonist docks the CB_1R undergoes different conformational change

and interacts with different G-protein subunits. Hence, depending on which cannabinoid agonist interacts with the receptor may determine which G-protein subunits are activated and thus which intracellular signalling mechanisms are activated. Lastly, it has also been demonstrated that CBR signalling may involve a 'chord', as opposed to a single 'note' played on G-proteins (Mukhopadhyay *et al.,* 2002). Here, ligands may activate, for example, 3 G-proteins, and be a full agonist, neutral antagonist or inverse agonist at any combination of these. Clearly, these signalling complexities mean that a given ligand is potentially capable of producing many effects that depend on ligand structure, downstream second messenger and effecter isoforms and multiple/differential pharmacological action at the G-protein level. Hence, if the postsynaptic cells in layer II of the mEC also release different endogenous cannabinoids, then these may modulate the intracellular signalling pathways differently to our bath applied agonists, and their presence may also modify exogenous agonist responses.

In addition to these factors, we must also consider the possibility that another CB receptor is present in layer II of the mEC in addition to CB_1Rs. It is possible that a CB_2R like receptor is present in layer II of the mEC alternately it may be an as yet unidentified receptor.

Finally the dual effects of CB_1R agonists in layer II of the mEC seen here may simply be due to poor drug access to the neurones. The cannabinoid drugs are highly lipophillic and there is a possibility that rather than reaching target neurones they become partitioned in the surrounding fatty tissues, thus giving mixed results due to the drug being not present at some of the CB_1R expressing sites so having no effect at all or the presynaptic targets may be being exposed to exceptionally high levels of the agonist due to build up in the tissue surrounding them thus giving unusual effects. Indeed Brown *et al.,* (2004) showed that cannabinoids were poor at penetrating slices and these researches showed that

recording at depth of more than 80μM below the surface of a slice result in unreliable recordings to drug penetration issues. This issue is considered further in Chapter 4.

In layer V, application of the CB_1R agonist ACPA significantly decreased sIPSC frequency, but had no significant effect on sIPSC amplitude and area. This decrease in frequency fits with the work previously done in the hippocampus and amygdala (Hajos *et al,*. 2000, Katona *et al.,* 1999 respectively). Because layer V of the mEC responded to bath application of the CB_1R agonist ACPA (10μM) in a consistent manner, and its response to ACPA was what would be predicted based on previous studies, it indicates that the dual response to ACPA (and WIN 55,212-2) seen in layer II neurones is not due to unreliable drugs or receptor independent effects, therefore it indicates that the effects seen in layer II are receptor-mediated and worthy of further investigation.

3.7.3 The effects of AM-251 in layer II and V

We have shown that application of the CB_1R antagonist AM-251 caused an increase in $GABA_A$ergic neurotransmission, shown by a decrease in IEI times and an increase in NICT.

The significant increase in sIPSC frequency in both layers II and V and the trend towards an increase in GABA release in both areas in response to the application of the CB_1R antagonist AM-251 indicates that in the mEC there is tonic endocannabinoid release. AM-251 is a known inverse agonist/antagonist of CB_1R, this means that it produces effects in some CB_1R containing systems that are opposite to the effects caused by CB_1R agonists (for a full over see Pertwee 2005).

Pertwee (2005) indicates that the effects of AM-251 could be due to 3 possible mechanisms:

1) AM-251 may be out-competing naturally occurring endocannabinoids, to say that in layer II and V of the mEC there is tonic activity of the car signalling system meaning that sIPSCs are already suppressed and appl AM-251 overcomes this to lead to an overall increase in GABA release.

2) Cannabinoid receptors may exist in 2 different states, constitutively Here, CB_1R in a constitutively "on" state are effectively active in spit absence of an agonist, and application of AM-251 switches them to or "off" states. Evidence for this is based on work done where tissues endogenous cannabinoid activity have been made to express forms of CE when the CB_1R antagonist SR141716A was applied it still elicited invers effects.

3) While it is thought that AM-251 is acting via CB_1Rs to increas frequency, from the experiments done here it is not possible to disce inverse effects of AM-251 are as a result of the antagonist blocking released endocannabinoids, or if the effects of AM-251 are due to co activity of CB_1Rs Hinges *et al.,* (2005) showed a continual (tonic) re endocannabinoids inhibited GABA release onto hypothalam opiomelanocortin (POMC) neurones and Slanina & Schweitzer (2005) evidence for tonic release of endocannabinoids controlling excitatory tran in CA1 of the hippocampus. Mato *et al.,* (2002) presented evidence in fa constitutively active CB_1R, while Savinainen *et al.,* 2003 argue that CB_1 no constitutive activity.

To further investigate the mechanism of action of AM-251 it v necessary to obtain a "neutral" antagonist, these are ligands for CBRs overcome any tonic activity by out competing the endocannabinoids bu interfere with constitutive activity of cannabinoids receptors.

3.7.4 Future experiments

In order to investigate at least some of these hypotheses outlined above for dual effects of cannabinoid agonists on inhibitory signalling in layer II of the mEC, we suggest a number of future experiments.

Firstly we suggest identifying if the dual affects of the bath applied CB_1R agonists can be split between the two different principal neurones (maybe stellate cells report the increase in inhibitory signalling while pyramidal cells report the decrease or vice versa.) Initially this will be done by filling the postsynaptic neurones with biocytin during recording and then seeing if there is any correlation between cell type and the effect of the agonist.

Secondly investigate the possibility of CB_2Rs or an as yet unidentified cannabinoid receptor being present in layer II of the mEC though use of more receptor specific drugs, and possibly staining with receptor specific antibodies.

Thirdly, we might investigate the effects of bath application of the endogenous agonist's 2-AG and AEA and ask - do they also have dual effects or are there affects more consistent?

Fourth, what happens if we minimize the issues of the penetration of the slice by the drugs by investigating their effects in juvenile animals? Is a more consistent affect seen?

Finally what happens to activity in the network when CBR agonists are bath applied to entorhinal slices? Are cannabinoids acting to modulate short-range signalling between the pre and postsynaptic neurones or can they have an larger effect on network activity, for example, do they significantly affect oscillations with in the EC?

One other factor that is not considered here is the effect that the efficacies of the cannabinoid ligands used may have on the results or indeed the effectiveness of the drugs. However it was not possible to consider this aspect as

it is yet to be decided on true efficacy values for the CBR ligands, with various researchers showing that the efficacy of ligands varied depending on the signalling system used to measure their affects, while others show that efficacy could vary depending on the region of the brain studied. For full reviews on CBR ligands efficacy see Howlett (2004), and Fowler (2007).

CHAPTER 4
Effects of cannabinoid ligands in the superficial layers of the mEC in P8-12 slices.

4.1 Introduction

After observing mixed results with the CBR agonist, ACPA, in layer II neurones at P30, it was decided to investigate this issue further. One possible explanation for the mixed results was poor penetration of the slice by cannabinoid drugs, which are highly lipophillic. Indeed, Brown *et al.,* (2004) concluded that it was "difficult to control the concentrations of lipophilic agonists such as WIN55, 212-2 within a brain slice". These authors found that recording at a depth of 80μm or more below the surface of the slice, low does (5-10μM) of WIN had no effect and even at high concentrations (>100μM) it took considerable time for a stable effect of WIN55,212-2 to be seen.

Given the strong likelihood that drug partition into myelin and other lipids within the P30 slice was significant, it was decided to investigate cannabinoid ligand activity in slices taken from animals aged from postnatal day 8-12 (P8-12). Young animals have less myelination and consequently lower levels of fat in the brain and we reasoned that this would enable easier access for the drug to the neurones.

For this series of experiments, male Wistar rats aged 8-12 days were used. This was selected as a suitable age, since studies by Morozov & Freund (2003), and Romero *et al.,* (1997) in the rat show that CB1Rs at present and functional in the hippocampus at this early developmental stage. Indeed, a secondary aim of these studies was to investigate the development of GABAergic inhibition in EC and the role that cannabinoid receptors might play in this.

Brains were extracted and stored using the methods already outlined in and slices were cut at 300 µm thickness. A thickness of 300µm was selected as this was the thinnest the slices could be made without losing connectivity within the slice (e.g. between hippocampus and EC). Within these constraints, however,

slices were made as thin a possible to minimise the amount non-target tissue that could take up the cannabinoid.

In addition to using P8-12 slices and cutting thin slices, some experiments were carried out in which the slice was placed on top of a piece of lens tissue in the bath. The aim of using the lens tissue was to try and prevent the slice adhering to the bottom of the recording chamber, thus allowing the drug to have access to both the top and bottom of the slice. We found that this made little or no difference to drug responses, but added considerable difficulty to experiments in terms of slice visualisation.

When the P8-12 slices were visualised under DIC optics, it was apparent that at this age, the mEC was not fully developed. The laminar structure described in the introduction was not as clearly defined as in the adults, and neurones in the juvenile slice had no characteristic morphology. Hence, in the superficial layers, at P8-12, neurones were large and rounded in appearance, compared to P30, where stellate and pyramidal morphology was readily apparent. In layer V, neurones were much smaller and similarly rounded, and it was also noted that the axonal bundle that marked the deep edge of layer V at P30 was not apparent in the younger animals.

For these experiments the P8-12 neurones were filled with the same mixture of IPSC solution + IEM1460 as used previously (see materials and methods for full description).

4.2 sIPSCs at P8-12 occur irregularly when compared to P30 in both deep and superficial layers of the mEC.

On performing whole-cell voltage clamp recording in layer II neurones in P8-12 animals it was notable that the pattern of GABA release was different to that seen at P30. In recordings from adult rats, sIPSCs in layer II are very frequent, with typically very low IEI values under control conditions (see table 4.1), such that little or no baseline is seen. In the P8-12 layer II neurones this was not the case. Whole-cell voltage clamp recordings in slices from layer II neurones at P8-12 revealed that the IEIs were very large, with quiescent periods interspersed by groups of closely spaced sIPSCs which we referred to as "bursts". Within bursts, we noted that sIPSCs were considerably larger than the individual sIPSCs that occurred infrequently during quiescent periods. We believe that these "bursts" are similar to be giant depolarising potentials (GDPs) first identified by Ben Ari *et al.,* (1989) in the CA3 region of the hippocampus. Using intracellular recording Ben Ari *et al.,* (1989) described the presence of spontaneous giant depolarizing potentials in rats from P0 to P18. These authors noted that GDPs were most frequent during the first 8 postnatal days, and then declined in frequency until no GDPs were seen in CA3 after postnatal day 12. While there are no specific studies of GDPs in layer II of the mEC the postnatal ages of the rats used in this study is similar to that used in the study of Ben Ari et al., (1989).

Fig 4.1A Shows sIPSCs recorded from a mEC layer II neurone in a slice taken from the brain of a P30 animal. This trace shows typical sIPSCs in a P30 layer II neurone, with a short IEI (mean median IEI 86.58 ± 15.84 ms) and variable amplitudes. Mean amplitude was 51.71 ± 3.55 pA. This IEI compares favourably with previously reported values in this area (mean median IEI 86.7 ± 2.0 ms Woodhall *et al.,* 2005), although amplitude was considerably higher than previously reported, perhaps reflecting the greater network activity (and hence

sIPSC summation) when IEM1460 is used in place of glutamate receptor blockade. Indeed, we often saw very large sIPSCs (>500 pA) using IEM1640, and these are not visible when recording in 2-AP5 and CNQX (Woodhall, personal communication). In contrast, **Fig 4.1B** shows sIPSCs recorded from a single mEC layer II neurone in a slice taken from the brain of a P8-12 animal. The GABA signalling in these neurones is characterised by long quiescent periods broken by complex bursts of GABA release. The mean median IEI for p8-12 sIPSCs was typically around 166.99 ± 49.78 ms while the mean amplitude was 83.08pA ± 3.61. Obviously, given the fact that we observed long periods of quiescence, the mean median values reported here are a poor reflection of the pattern of sIPSC activity. In the example neurone in **Fig. 4.1B** the mean inter-burst interval was 11,264 ± 2,390 ms while the mean peak amplitude was 737.8 ± 62.0 pA.

Fig 4.2A shows the cumulative probability plot for P8-12 sIPSC amplitude distribution (black) compared to P30 (red). The left shift of the P30 plot with respect to control for values between 0 and 500pA shows that the probability of these smaller amplitude sIPSCs occurring is higher in layer II neurones from P30 animals compared to P8-12. The KS test confirmed that the difference in sIPSC amplitude distribution between P8-12 and P 30 neurones was significant ($P \leq$ 0.0001, n=18). **Fig 4.2B** shows the cumulative probability plot for sIPSC IEI P8-12 (black) compared to P30 (red). Here, the P30 plot always lies to the left of the P10 plot, indicating that the probability of low IEIs is considerably higher in P30 layer II neurones than in P8-12. KS test showed the difference in IEI distribution between P30 and P8-12 neurones was significant ($P \leq 0.0001$, n=18).

Table 4.1 & 4.2, shows a comparison of kinetic parameters of sIPSCs between P30 and P8-12 animals. Since previous studies have reported a mixture of mean and mean median values, both have been included here. Again, kinetics of sIPSCs from P30 neurones were similar to previously reported values

(Woodhall *et al.,* 2005), however, it is clear that, compared to sIPSCs at P30, those recorded at P8-12 are slower to rise and decay, of greater amplitude, and show considerably greater charge-transfer.

When we examined GABA release in layer V neurones at P8-12, it was clear that very few sIPSCs occurred at all. In fact, the amount of GABA release in juvenile layer V neurones was so minimal that the effects of cannabinoid drugs on sIPSCs in neurones from P8-12 slices could not be investigated. **Fig 4.1C** illustrates the minimal GABA release in a layer V neurone from at P8-12. In this particularly active layer V neurone, the mean sIPSC frequency was 0.4 Hz and the mean amplitude was 27.2 pA. Often, control IEI values in layer V at P8-12 were of the order of 0.1 Hz or less, and given that cannabinoid agonists generally suppressed GABA release, the amount of recording time needed to collect sufficient sIPSCs for statistical analysis during pharmacological investigations was so long that whole-cell recordings became unviable. **Fig 4.1D** shows sIPSCs recorded from a single layer V neurone in a P10 slice, illustrating minimal GABA release.

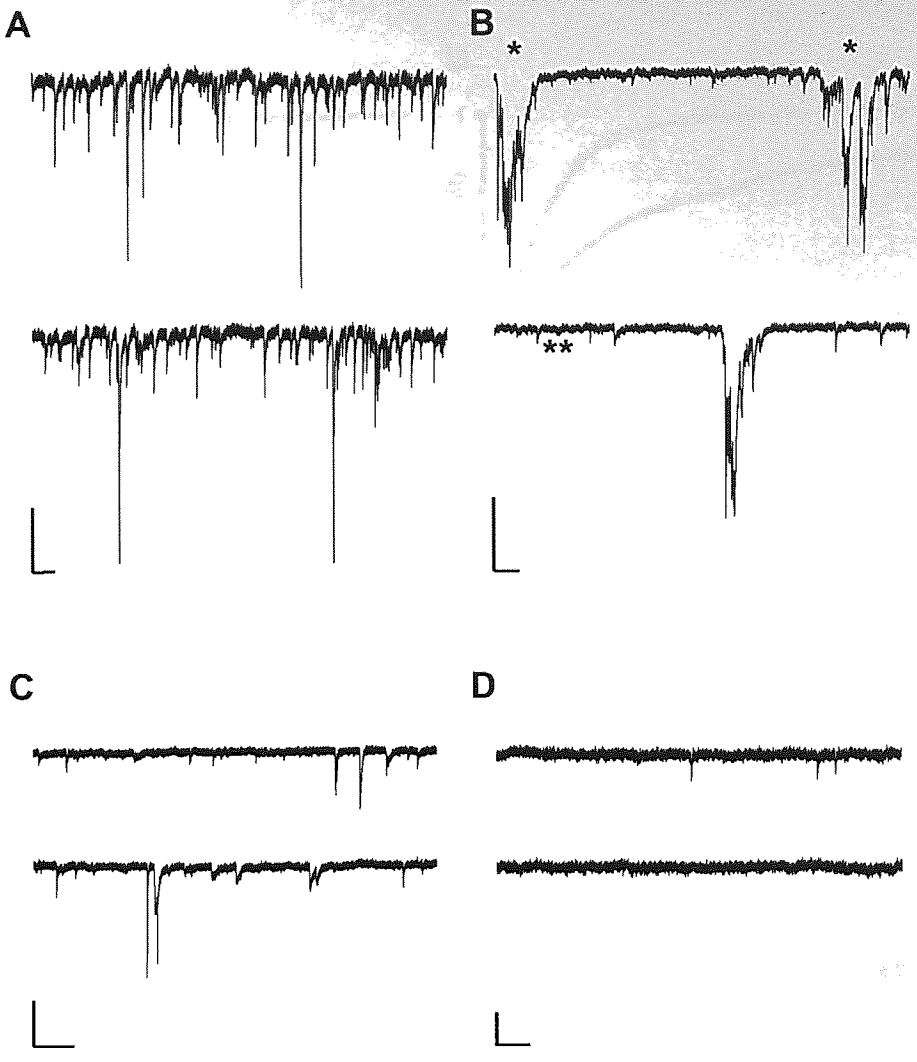

Fig 4.1 comparison of layer II sIPSCs between P8-12 and P30 animals.
A. sIPSCs from a single P30 layer II neurone. Scale bar **Y**100pA **X** 500ms. **B.** sIPSCs from a single layer II P8-12 neurone Scale **Y** 250pA **X** 2000ms.* Giant depolarising currents, ** quiescent period **C.** sIPSCs from a single layer V P30 neurone **Y** 200pA **X** 1000ms **D.** sIPSCs from a single layer V P10 neurone **Y** 50pA **X** 100ms.

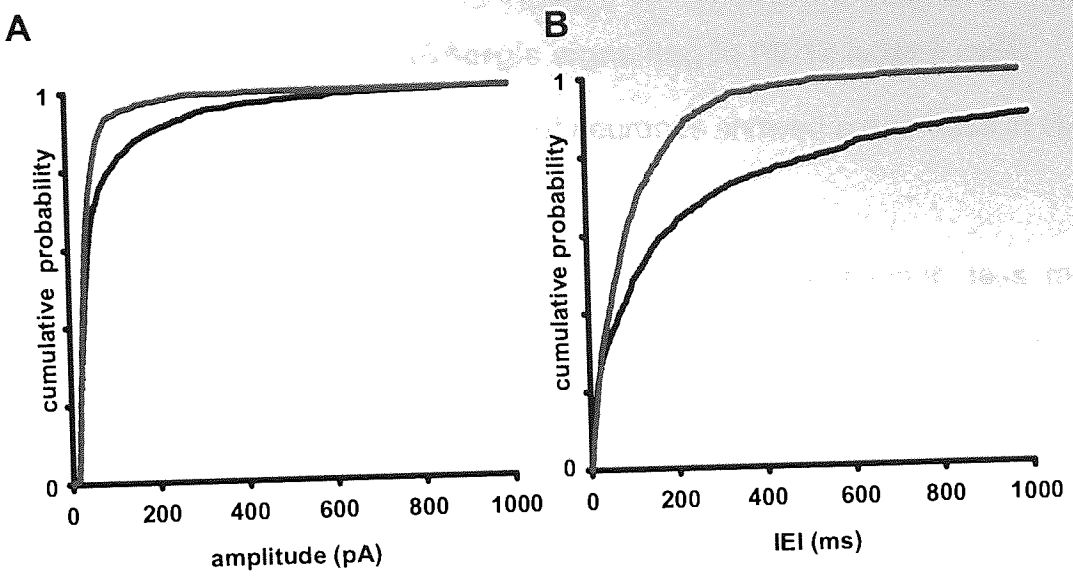

Mean Median Values	Layer II P8-12	Layer II P30
10-90Rise (ms)	3.24 ± 0.13	2.51 ± 0.15
Peak Amplitude (pA)	38.15 ± 1.26	33.98 ± 2.76
Decay Time (ms)	18.39 ± 1.35	8.9 ± 1.18
Area (pA·ms)	714.22 ± 52.35	299.47 ± 39.04
Half Width	11.27 ± 0.98	4.65 ± 0.70

Table 4.1

Mean Values	Layer II P8-12	Layer II P30
10-90 Rise (ms)	3.50 ± 0.05	2.43 ± 0.06
Peak Amplitude (pA)	83.08 ± 3.61	59.28 ± 3.08
Decay Time (ms)	20.78± 0.37	10.62 ± 0.31
Area (pA·ms)	385.78 ± 9.87	721.73 ± 52.81
Half Width	14.92 ± 0.36	6.93 ± 0.24

Table 4.2

Fig 4.2 Comparing layer II sIPSC kinetics for P30 and P8-12 neurones.
A. Cumulative probability for sIPSC amplitudes in P10 and P30. **B.** Cumulative probability for sIPSC IEIs at p8-12 and p30. P8-12=black, P30 =red
Table 4.1 mean median kinetics for layer II sIPSCs comparing P8-12 with P30.
Table 4.2 mean kinetics for layer II sIPSCs comparing P8-12 with P30.

4.3 Results

4.3.1 ACPA decreases GABAergic signalling in P8-12 layer II mEC.

In p8-12 layer II slices 100% of neurones showed a decrease in GABAergic signalling during ACPA application.

To investigate effects of cannabinoid drugs in thinner, less myelinated slices, it was decided to continue to use ACPA. ACPA (10μM) was bath applied to the juvenile slices in exactly the same way as it had been during previous experiments. However, unlike the experiments in P30 animals ACPA only had one effect on the frequency of the sIPSCs, acting to decrease both frequency and amplitude.

Fig 4.3A & B show example sIPSCs from a single layer II neurone in a P11 slice, during control **(A)** and ACPA application **(B)**. **Fig 4.3A** illustrates the characteristic GABA release already described in layer II neurones from P8-12 slices (quiescent periods punctuated with bursts of sIPSCs). When **Fig 4.3A** is compared to **Fig 4.3B** which shows sIPSCs from the same neurone during ACPA application, a decrease in sIPSC frequency can be seen. Both the number of individual sIPSCs, and the number of sIPSC bursts have fallen.

4.3.2 ACPA decreases sIPSC amplitude in p8-12 layer II mEC

During application of ACPA (10μM) the mean amplitude decreased from 96.37 ± 4.56pA in control to 79.30 ± 3.56pA, this decrease in sIPSC amplitude between control and ACPA periods was significant. ($P \leq 0.004$ ANOVA, n=5). **Fig 4.3C** shows the pooled cumulative probability plot for sIPSC amplitude in layer II at P8-12. The red plot indicates sIPSC amplitude during ACPA application, and the black plot shows sIPSC amplitudes in control. The plots indicate that a change in the distribution of sIPSC amplitudes towards lower values has occurred

between control and ACPA periods, and this change in distribution was significant ($P \leq 0.001$ KS test, n=5).

4.3.3 ACPA decreases sIPSC frequency in P8-12 layer II mEC

The mean median IEI for P8-12 sIPSCs was found to increase during ACPA application from 84.41 ± 31.19ms to 184.83 ± 70.08ms. An increase in the IEI time shows that a decrease in sIPSC frequency has occurred and the increase in IEI was significant ($P \leq 0.0001$, ANOVA, n=5). **Fig 4.3D** shows the cumulative probability plot for pooled layer II sIPSC IEIs in P8-12 neurones, during control (black) and ACPA (red) periods. The ACPA plot lies to right of control for the duration of the plot indication a change in the distribution of sIPSC IEI times has occurred. The change in sIPSC IEI distribution was significant ($P \leq 0.001$, KS Test).

4.3.4 ACPA decreases sIPSC NICT in P8-12 layer II mEC

Fig 4.3E shows the cumulative probability plot for sIPSC areas during control (black) and ACPA (red) application. The ACPA plot lies to the right of control for the entire plot, indicating that sIPSC area is always smaller in ACPA. The change in distribution of sIPSC area between control and ACPA periods is significant ($P \leq 0.001$, KS test). **Fig 4.3F** Illustrates the decrease in NICT when compared to a normalized control of 1 ACPA caused the mean inhibitory charge transfer to decrease by -18.99 ± 7.81% of control. The decrease in inhibitory charge transfer was found to be significant. ($P \leq 0.034$, ANOVA, n=5).

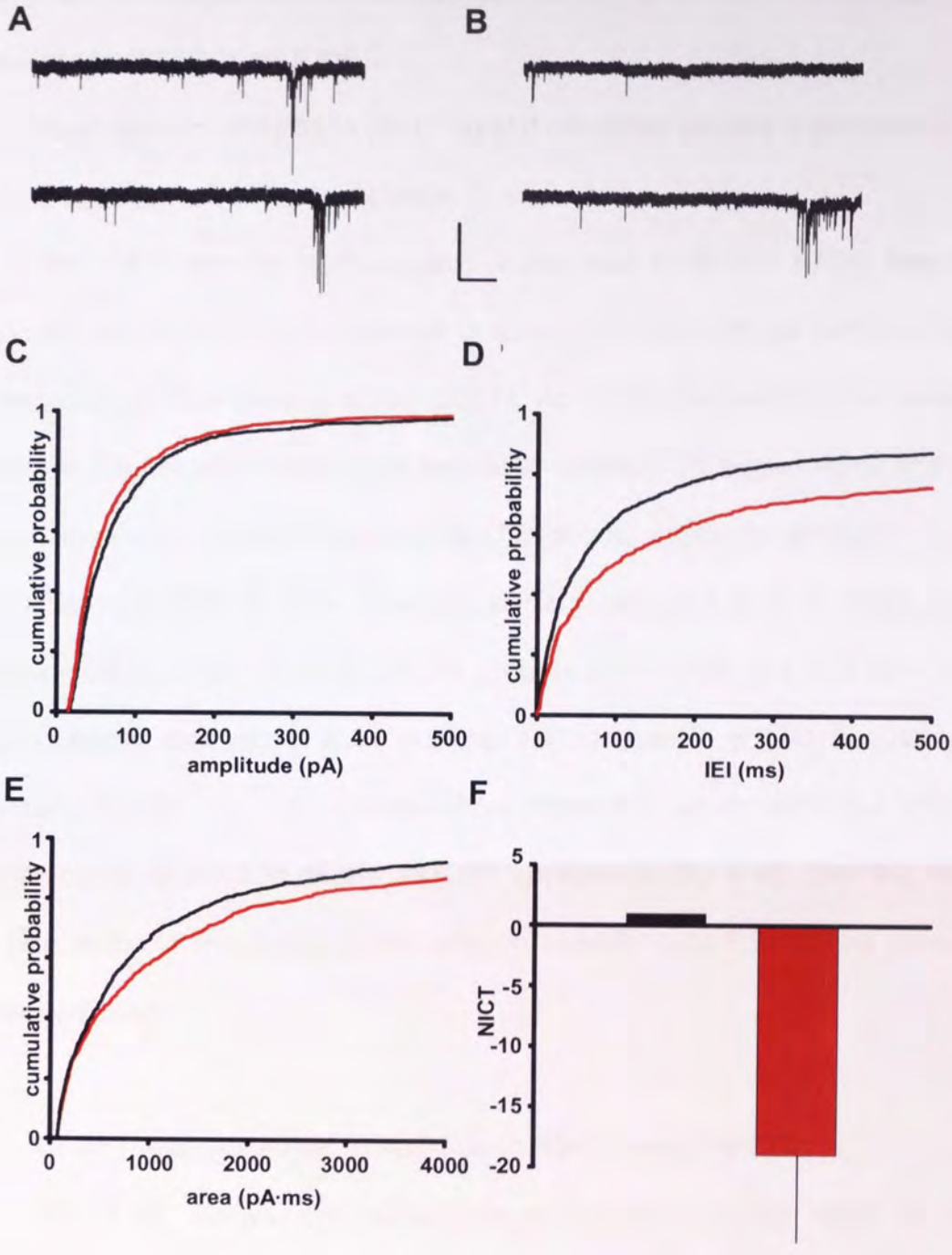

Fig 4.3 Effects of CB1 agonist ACPA on P8-12 sIPSCs
sIPSCs from a single Layer II mEC neurone in a P8-12 slice during **A.** Control and **B.** ACPA (10μM) application. Scale **Y** 250pA **X** 2500ms. **C.** Pooled cumulative probability plot for sIPSC amplitude. **D.** Pooled cumulative probability plot for sIPSC IEI during control and ACPA application. **E** Pooled cumulative frequency plot of layer II sIPSC area in p8-12 neurones control and ACPA. **F** Bar chart depicting change in NICT during ACPA application compared to control of 0. n=5 Control=black, ACPA=red **C-F** pooled data, n=4

4.4 The CB_1R antagonist/inverse agonist AM-251 decreases GABAergic signalling in P8-12 layer II mEC.

Application of AM-251 to p8-12 layer II neurones caused a decrease in sIPSC frequency in 100% of neurones.

The CB_1R agonist ACPA caused a decrease in layer II sIPSC frequency, amplitude and NICT in P8-12 animals in a manner that might be expected based on previous studies (Hajos *et al.,* 2001). As ACPA behaved in a consistent manner in the juvenile slices it was decide to continue the experiments and see if a CB_1R antagonist would increase sIPSC frequency, amplitude and NICT.

Fig 4.4A and B show example sIPSCs recorded from a single layer II neurone during control (**A**) and AM-251 (10μM) (**B**) periods, in a P10 slice. These traces suggest that rather than causing an increase in sIPSC frequency and amplitude AM-251 had the opposite effect. When the control sIPSCs in **Fig 4.4A** are compared to sIPSCs during AM-251 application **Fig 4.4B** then the number and size of the characteristic bursts seen in juvenile layer II neurones appears to have decreased.

4.4.1 AM-251 reduces sIPSC amplitude in P8-12 layer II mEC.

Fig 4.4C shows the cumulative probability plot for layer II sIPSC amplitudes during control (black) and AM-251 (10μM; red) periods. The AM-251 plot lies to the left of control plot, suggesting that there is a higher probability of lower amplitude sIPSCs. More importantly, the gap between the control and AM-251 plot suggests that a notable change in distribution of sIPSC amplitudes has occurred and this change in the distribution of sIPSC amplitude was significant ($P \leq 0.002$, KS test). Application of AM-251 not only altered the distribution of sIPSC amplitudes it also reduced the mean amplitude from 106.49 ± 7.39pA in control to

74.63 ± 5.75pA in AM-251, this decrease in amplitude was again significant ($P \leq$ 0.0007, ANOVA, n=4).

4.4.2 AM-251 reduces sIPSC frequency P8-12 layer II mEC.

Fig 4.4D shows the cumulative probability plot for layer II sIPSC IEIs during control (black) and AM-251 (10μM; red) periods. The AM-251 plot lies to the right of control for the duration of the graph; the gap between the two plots indicates that a change in the distribution of sIPSC IEI times has occurred between control and AM-251 periods. This change in distribution was found to be significant ($P \leq$ 0.0001, KS test). In addition to a change in the distribution of sIPSC IEIs the mean median IEI was found to increase from 58.81 ± 13.93ms in control to 96.12 ± 17.73ms showing that a overall decrease in sIPSC frequency had occurred during AM-251 application. The increase in IEI was significant ($P \leq 0.0001$, ANOVA, n=4).

4.4.3 Effects of AM-251 on NICT in P8-12 layer II

Fig 4.4E shows the cumulative probability plot for sIPSC areas in control (black) and AM-251(red) periods. The AM-251 plot lies to the right of control for the duration of the graph the gap between the two plots shows that a change in the distribution of sIPSC area has occurred between the control and the AM-251 periods, this change in sIPSC area distribution was just significant ($P \leq 0.04$ KS test n=4). **Fig 4.4F** shows the change in NICT during AM-251 (red bar) application compared to a normalised control of 1. NICT increased by 105.29 ± 156.93% of control in AM-251, n=4 however the increase in NICT was not significant ($P \geq 0.53$ ANOVA, n=4). It was felt that the lack of significance maybe due to one cell, which showed a massive increase in NICT compared to the other 3 cells which showed

consistent decreases in NICT in response to AM-251 application. When this cell was removed from the pooled data then NICT decreased by 54.47 ± 10.19 % of control and this decrease was statistically significant ($P \leq 0.007$ ANOVA, n=3).

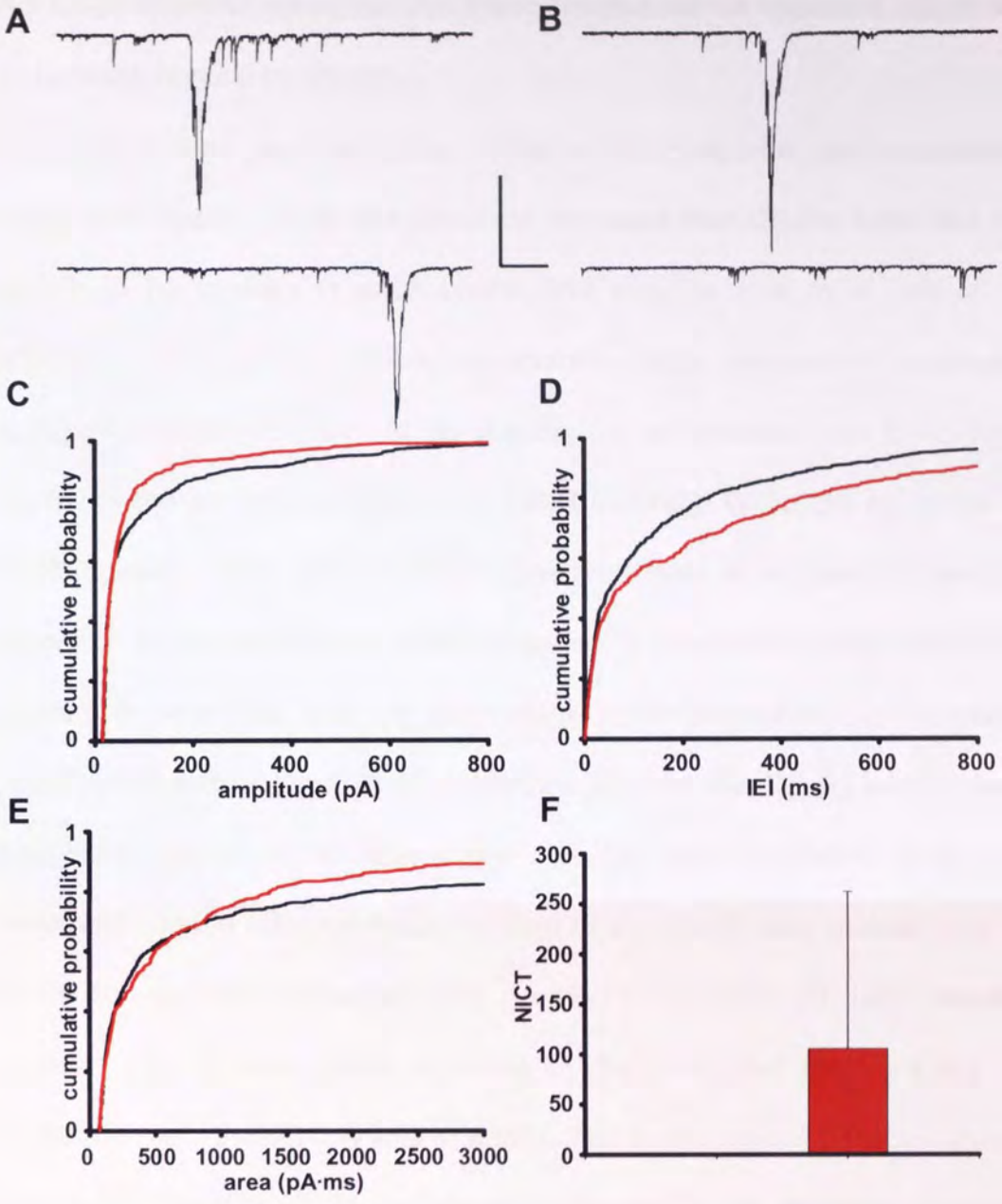

Fig 4.4 Comparing control to AM-251 periods for layer II sIPSCs
Example layer II sIPSCs from a p10 neurone during **A**.Control and**B**. AM-251 (10μM) application Scale **X** 1000ms **Y** 100pA. **C.**& **D.** Show the cumulative probability plots for layer II sIPSC amplitude and IEIs respectively during control (black) and AM-251 (red) periods. **E.** Cumulative probability plot for sIPSC areas during control (black) and AM-251(red) periods.
F. Plots the change in inhibitory charge transfer compared to a control of 1. **C-F** Pooled data n=4.

4.5 CB_2R Specific agonists and antagonists/inverse agonists effect sIPSCs in juvenile layer II neurones.

Up to this point, only the effects of CB_1R agonist and antagonists have been investigated. While the literature indicates that CB_2Rs have not yet been shown to be present in adult brains, this may be due to a lack of antibody specificity, as available antibodies against CB_2Rs are derived against human epitopes, and hence may not be specific for rat proteins (see Discussion for a review of the available evidence for CB_2R in CNS). While the evidence for adult CNS indicates there are no CB_2Rs present, there is no specific work on their presence in the developing brain. However, it has been shown that CB_1Rs are present in neurones from an early stage in development, e.g. Romero *et al.,* (1997) used autoradiographical techniques to show that CB_1Rs were present from gestational day 21 in rat fetuses and that they were present in similar areas to those identified in adult rat brain. Romero *et al.,* (1997) also showed that the level of CB_1Rs present increased from gestation day (GD) 21 until adulthood. In addition, CB_1Rs were found in areas of the brain that they are not normally associated with these receptors in adults. The expression of CB_1Rs in these areas was at its highest at GD21 and starts to decrease at P5, reaching a nadir at P30. This developmental change in CB_1R distribution indicates that changes in CB_1R expression do occur during development, and so we should not rule out the possibility of the presence of CB_2Rs in a developing brain. For example, amongst the G-protein coupled receptors, metabotropic glutamate receptors show a high degree of developmentally regulated expression (e,g, Defagot *et al.,* 2002). We therefore decided to investigate the effects of CB_2R agonists and antagonists on P8-12 layer II neurones. The cannabinoid ligands chosen for this set of experiments were

6-Iodo-2-methyl-1-[2-(4-morpholinyl)ethyl]-1H-indol-3-yl](4-methoxyphenyl) methanone (AM-630) and (6aR,10aR)-3-(1,1-Dimethylbutyl)-6a,7,10,10a-tetrahydro-6,6,9-trimethyl-6H-dibenzo[b,d]pyran (JWH-133).

AM-630 is a CB_2R antagonist/inverse agonist with a K_i of 31.2 nM at CB_2Rs (K_i for CB1 5-10μM). Pertwee *et al.,* (1995) confirmed that AM-630 was a novel cannabinoid receptor antagonist, and Ross *et al.,* (1999) confirmed that AM-630 was a CB_2R-specific ligand and acted as an inverse agonist at CB2Rs, with weak partial agonist activity at CB_1Rs but a far higher affinity for CB2Rs (for K_i values see table 2.1 in material and methods). JWH-133 is a CB_2 specific agonist with a K_i of 3.4nM at CB_2Rs and its K_i at CB1 receptors is >700 nM (Huffman *et al.,* 1999)

4.5.1 AM-630 decreases sIPSC amplitude in P8-12 layer II mEC.

Fig 4.5A & B show sIPSCs recorded from a single layer II neurone in a P8-12 slices. **Fig 4.5A** shows the control period consisting of a few isolated sIPSCs in the quiescent period punctuated by large bursts of sIPSCs (see earlier descriptions.) **Fig 4.5B** shows sIPSCs from the same neurone as **4.5A** but this time in the presence of 50 nM AM-630, these examples show how AM-630 greatly diminished sIPSCs activity, leaving a few low amplitude, isolated sIPSCs and no sIPSC bursts. 100% of neurones showed a decrease in GABAergic signalling during AM-630 application.

Application of AM-630 caused a significant decrease in sIPSC amplitude. The mean amplitude fell from 71.9 ± 4.18 pA in control to 52.87 ± 5.0 pA in AM-630 ($P \leq 0.008$, ANOVA, n=4). **Fig 4.5C** Shows the cumulative probability plot for sIPSC amplitude, and compares control (black) with AM-630 (red) sIPSC amplitudes. The left shift of the AM-630 plot indicates that smaller amplitude sIPSCs are more likely to occur during AM-630 application when compared to

control. This change in distribution of sIPSC amplitudes was significant ($P \leq$ 0.0001, KS test).

4.5.2 AM-630 decreases sIPSC frequency in P8-12 layer II mEC.

Fig 4.5D Shows the cumulative probability plot for sIPSC IEIs comparing control (black) and AM-630 (red) periods. The AM-630 plot lies to the right of control; furthermore this right shift is present for the entire length of the plot indicating a profound shift in IEI distribution. The right shift indicates that there is a lower probability of a small IEI during application of ACPA this change in distribution was significant ($P \leq 0.0001$, KS test). When the mean median IEI was studied it was found to increase from 189.55 ± 39.75ms in control to 643.93 ± 98.26ms during application of AM-630, although this increase was not significant ($P = 0.191$ ANOVA, n=4).

4.5.3 AM-630 decreases NICT in P8-12 layer II mEC.

As with the ACPA and AM-251 experiments the effects of AM-630 application on NICT in P8-12 layer II mEC neurones was also investigated. The combination of a decrease in frequency and decrease in amplitude made it likely that a decrease in NICT would be seen in response to AM-630 application.

Fig 4.6A shows the pooled cumulative probability plot for sIPSC areas during control (black) and AM-630 (red) periods. The AM-630 plot shifts to the right of the control plot, indicating a lower probability of events with large areas this change in distribution was significant ($P \leq 0.0001$, KS test). NICT decreased by -30.09 ± 15.39 % of control, this decrease was not quite significant ($P \geq 0.08$ ANOVA, n=4). ***Fig* 4.6B** shows the decrease in NICT during AM-630 application (red bar) compared to normalized control of 1 (black bar).

The changes in the distributions of sIPSC frequency, amplitude and inhibitory charge transfer were unexpected. AM-630 is a CB_2R antagonist/inverse agonist and as such if it had any effect then it would be expected to increase sIPSC frequency and amplitude, similar to that seen in response to CB_1R antagonists. To investigate this phenomenon further we decided to apply a CB_2R specific agonist while recording from P8-12 neurones in layer II.

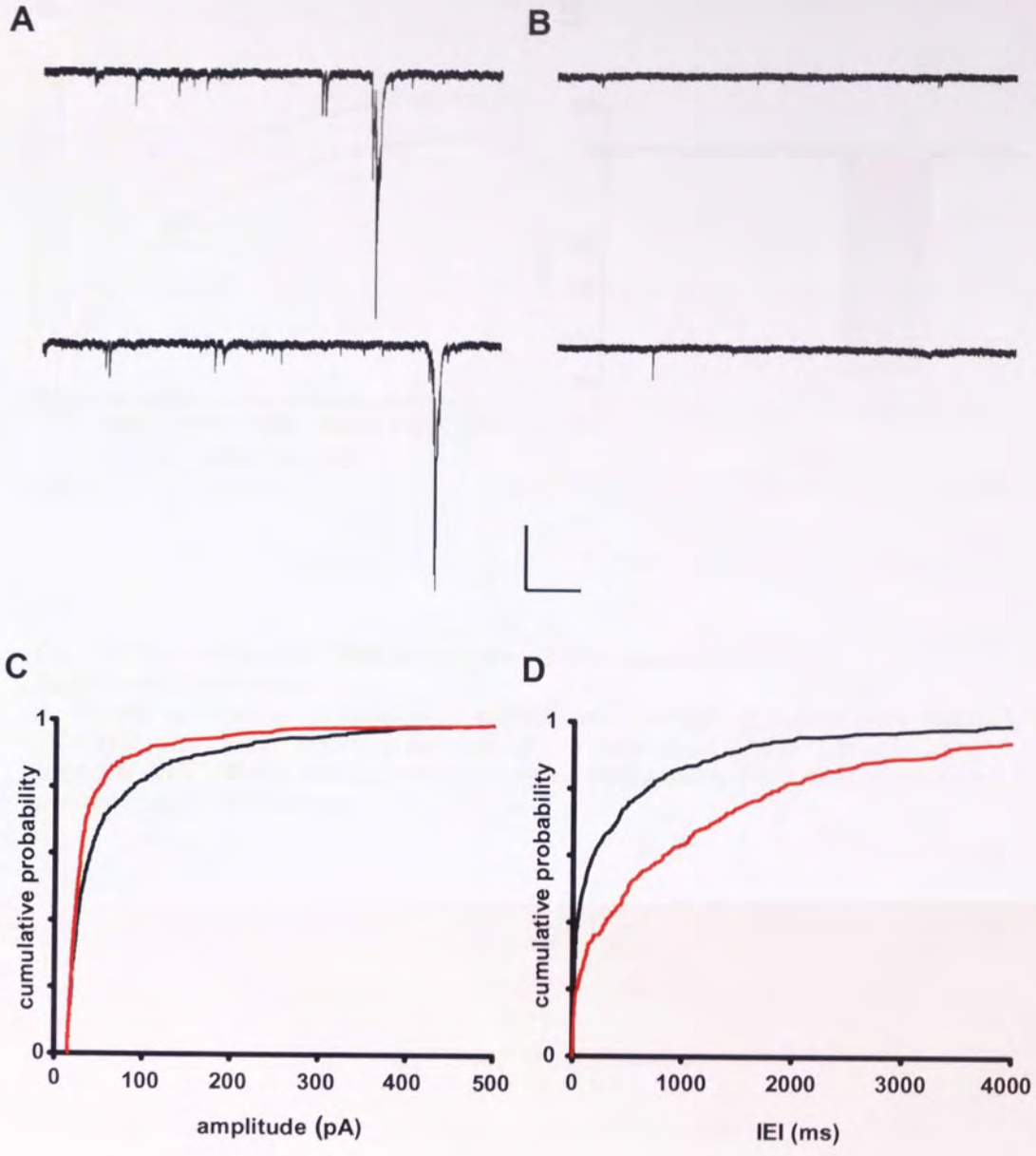

Fig 4.5 the effects of AM-630 on layer II sIPSCs in p8-12 slices
sIPSCs from a single layer II neurone in a P8-12 slice during **A** control and **B** AM-630. **C** cumulative probability sIPSC amplitude cumulative probability plot sIPSC IEI control (black) AM-630 (50nM) (red) Scale **Y** 250pA **X** 2500ms. **C-D** Pooled data, n=4.

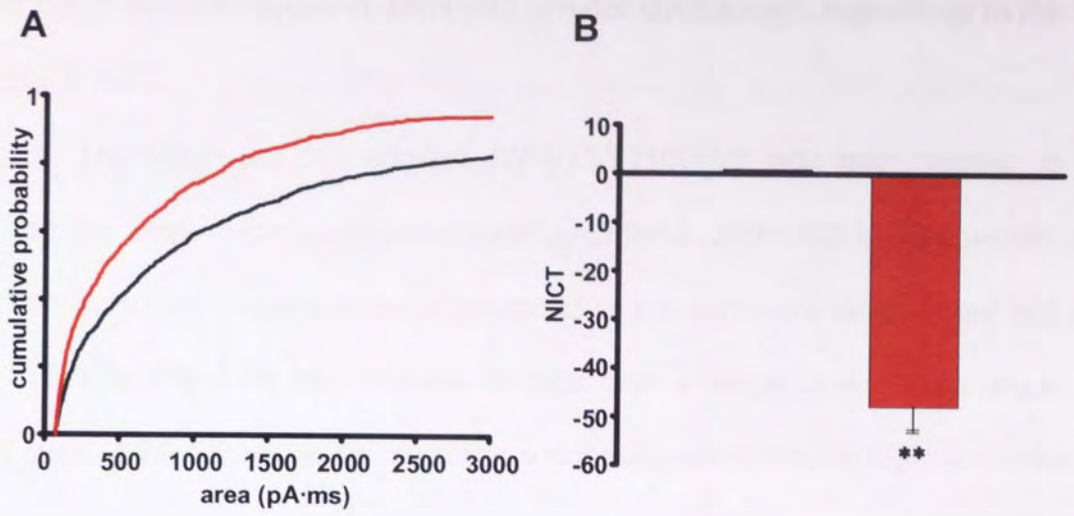

Fig 4.6 CB_2R antagonist AM-630 reduces GABA release in P8-12 layer II mEC neurones.

A. Pooled cumulative probability of sIPSC area comparing control with AM-630 (50nM) **B.** Bar chart comparing the decrease in normalised inhibitory charge transfer during AM-630 (50nM) application compared to control of 0 in P8-12 layer II neurones. Control=black, AM-630 =red, ** $P \leq 0.01$, n=4.

4.6 CB_2R specific agonist JWH-133 affects GABAergic signalling in P8-12 layer II mEC.

The CB_2R specific agonist JWH-133 (100nM) was bath applied to slices using the same techniques previously described. JWH-133 is light sensitive and so drug delivery reservoirs were wrapped in foil and work was carried out at low light levels. **Fig 4.7A and B** show sIPSCs from a single layer II neurone in a P8-12 slice. **4.7A** Shows sIPSCs during a control period, displaying the combination of quiescent periods with bursts of sIPSCs as already discussed. **Fig 4.7B** shows sIPSCs from the same layer II neurone during JWH-133 application. It is readily apparent that the frequency and amplitude of sIPSCs and bursts in the two JWH-133 traces is markedly decreased.

Application of JWH-133 lead to a decrease in GABAergic signalling in 100% of neurones, tested.

4.6.1 JWH-133 decreases sIPSC amplitude in P8-12 layer II mEC.

Fig 4.7C shows the cumulative probability plot for sIPSC amplitude in P8-12 layer II neurones. The JWH-133 plot (red) shifts to the left of the control plot (black.) The left shift indicates that there is a higher probability of a low amplitude sIPSCs occurring during JWH-133 application this change in distribution was significant ($P \leq 0.0001$, KS test). The mean amplitude decreased from 83.1 ± 3.6 pA in control to 49.6 ± 2.4 pA in JWH-133 and this decrease in amplitude was significant ($P \leq 0.002$, ANOVA, n=9).

4.6.2 JWH-133 decreases sIPSC frequency in P8-12 layer II mEC.

Fig 4.7D shows the pooled cumulative probability for layer II IEIs. The JWH-133 red) plot shifts to the right of the control (black) plot indicating that during JWH-133 application the probability of larger IEIs was greater than control.

This change in the distribution was significant ($P \leq 0.0001$ KS test). In addition to the significant change in the IEI distribution there was also an increase in the mean median IEI. The mean median IEI rose from 166.66 ± 23.99ms in control to 576.33 ± 73.67ms in JWH-133 and this increase was significant ($P \leq 0.047$ ANOVA, n=9).

4.6.3 JWH-133 reduces NICT P8-12 layer II mEC.

Fig. 4.8A Shows the pooled cumulative probability plot of sIPSC area in control (black) and in the presence of JWH-133 (red). The JWH-133 plot lies to the right of the control indicating a shift towards lower area values. The gap between the two plots shows a change in distribution of sIPSC areas occurs between control and JWH-133 periods this change in distribution was significant ($P \leq 0.0001$, KS test). In addition to changing the distribution of sIPSC area application of JWH-133 caused NICT to decrease by 47.92 ± 6.06% of control, this decrease in NICT represents an overall decrease in GABAergic signalling and this decrease was significant ($P \leq 0.0001$, ANOVA, n=9) **FIG 4.8B** Shows the decrease in NICT during JWH-133 application (red bar) compared to normalised control of 1 (black bar).

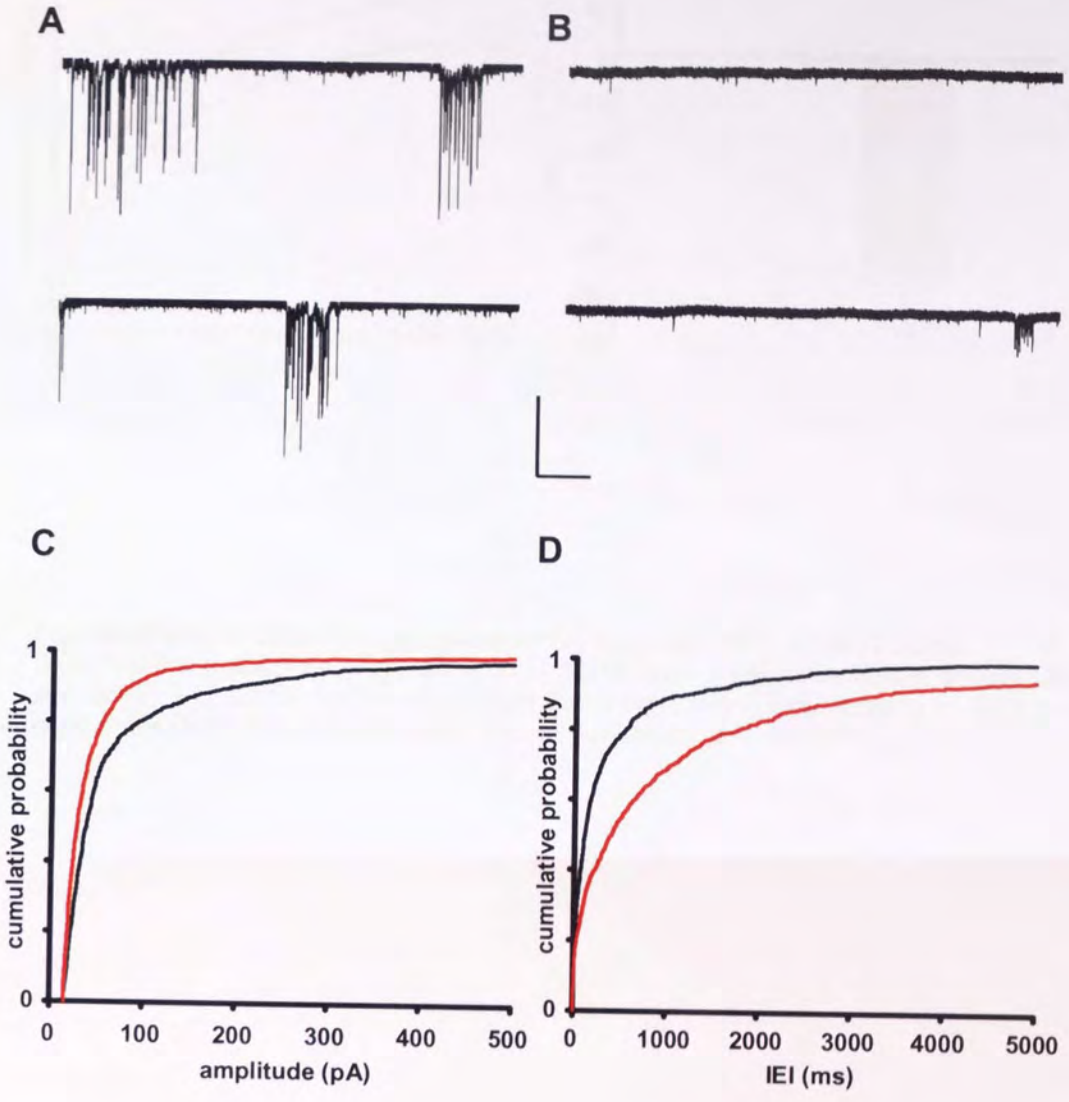

Fig 4.7 effects of JWH-133 on layer II sIPSCs in p8-12 slices.
sIPSCs recorded from a single layer II neurone in a P8-12 slice during **A.** control and **B.** JWH-133 application. **C.** Cumulative probability for amplitude during control (black) and JWH-133 (red) periods. **D.** Cumulative probability for IEIs in layer II during control and JWH-133. **C-D** Pooled data, n=9

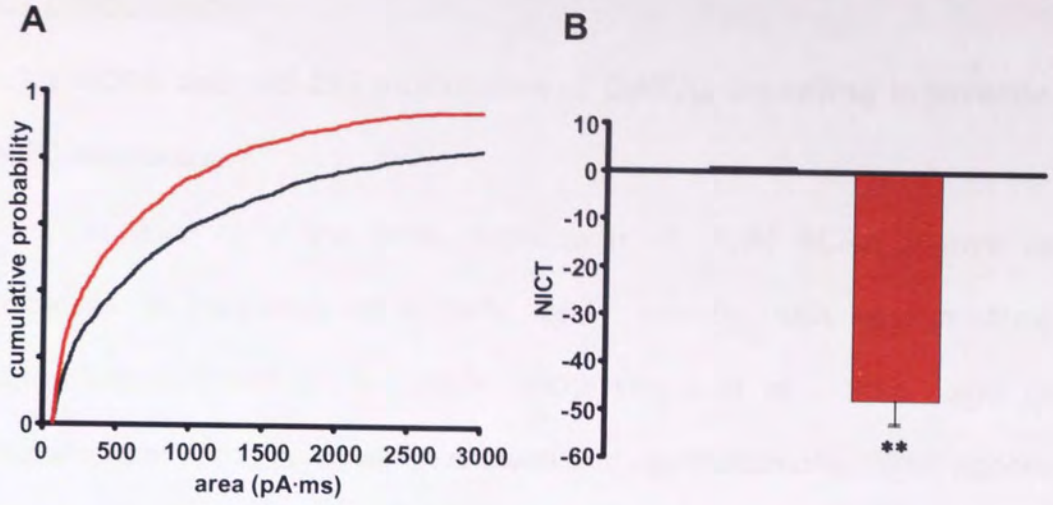

Fig 4.8 effects of JWH-133 on layer II sIPSC area and NICT in p8-12 slices
A cumulative probability for sIPSC area in p8-12 layer II neurones during control (black) and JWH-133 (100nM; red) application. **B** Bar chart showing the decrease in NICT during control and JWH-133 compared with normalised control of 1. Pooled data, n=9.

4.7 DISCUSSION

4.7.1 ACPA and AM-251 modulation of $GABA_A$ signalling in juvenile layer II mEC neurones.

In layer II of the mEC, application of 15μM ACPA always caused a decrease in frequency of sIPSCs, and this fits with studies done in the hippocampus (Hoffman & Lupica, 2000; Hajos *et al.*, 2000) and amygdala (Katona et al 2001), all of which showed that application of a CB1R agonist (WIN 55,212-2) reduced both sIPSC frequency and amplitude.

There are several possible explanations as to why ACPA produces a consistent effect of sIPSC frequency in the P8-12 layer II mEC neurones, while in P30 layer II mEC neurones we have found ACPA to both increase and decrease sIPSC frequency. The first of these explanations is simply that of the drugs accessing the neurones. In the P30 slices the levels of fatty tissue present in the brain is far greater than that found in the P8-12 slices. ACPA, along with the other CB1R agonists, is a highly lipophillic and it may be sequestered into lipids surrounding the neurones of layer II of the mEC, making access to CB1Rs variable and inconsistent. The lack of myelination in P8-12 animals means that the partitioning of drug is less likely, and so ACPA is seen to have a more consistent effect on sIPSC frequency and amplitude in layer II mEC neurones of juvenile animals. However, this explanation is unlikely as in the adults the same slices were used to study sIPSC signalling in layer V mEC neurones, and a consistent effect on sIPSC frequency and amplitude by ACPA was seen. As such the only role the lack of myelin in the P8-12 slices may be that the CBR drugs act faster due to fact that their access to neurones is less impeded. Another possible answer ACPA only having one effect on sIPSC frequency in the juvenile layer II neurones is related to differentiation of neurones and connectivity of the slice. As already discussed in chapter 3, the different responses seen in layer II neurones n

P30 animals may be due to the type of postsynaptic cell patched or differential inputs onto principal cells in the slice.

The differences observed in the patterns of spontaneous GABA release when sIPSCs from P8-12 layer II mEC neurones are compared to P30 layer II mEC neurones (**Fig 4.1 A&B)** shows that the adult connections and signalling are not yet in place in these juvenile brains.

While application of ACPA gave the predicted outcome of decreasing sIPSC frequency and amplitude when AM-251 was bath applied to P8-12 slices and layer II sIPSC were recorded it was found to have the opposite effect to that which was expected. It was predicted that AM-251 application would lead to an increase in sIPSC frequency and amplitude similar to that seen in layer II and V mEC neurones in P30 slices. However it was found when applied to the juvenile neurones the CB_1R antagonist acted in the same way as the agonist causing a decrease in sIPSC amplitude and frequency. When inhibitory charge transfer for layer II neurones in P8-12 slices was calculated with a statistical outlier excluded, then an overall decrease in inhibitory charge transfer was also seen. These effects of AM-251 were unexpected, since in the P30 animals all inconsistent effects had been due to CB_1R agonists, while AM-251 had shown a robust increase in sIPSC frequency and amplitude in layers II and V.

4.7.2 AM-630 and JWH-133 modulation of sIPSCs in p8-12 layer II mEC neurones.

Both AM-630 and JWH-133 are CB_2R specific cannabinoids, while in these experiments they were used at a concentration above their Ki values for CB_2Rs they were still under the *Ki* level for CB_1 receptors.

For a long time it was believed that CB_1Rs were located primarily in the CNS and peripheral nervous system, while the other known CBR (CB_2R) was

believed to only be expressed in the peripheral nervous system and the immune system. While various immunohistochemical and autoradiographical studies showed the presence of CB_1Rs in the brain no such data could be produced for CB_2R (although it could be located else where in the body). However, while this distribution of CBRs is considered to be the standard the presence of CB_2Rs on CNS neurones is still a hotly debated subject. In 2004 Derbenev *et al.,* showed using Western blot techniques that no CB_2 protein was present in the rat dorsal motor nucleus of the vagus (DMV). However, in 2005 Van Sickle *et al.,* showed a positive western blot for CB_2 proteins in the DMV (as well as other areas of the brain). In addition to the western blot, Van Sickle *et al.,* (2005) showed that there was mRNA expression for CB_2Rs using reverse transcription polymerase chain reaction techniques (RT-PCR). This is in contrast to Derbenev *et al.,* (2004), who also used RT-PCR techniques but got negative results for CB_2R mRNA. It is worth nothing that van Sickle *et al.,* 2005 attribute their success in using RT-PCR to show the presence of CB_2R mRNA to using a different Primer to Derbeneve *et al.,* (2004). While the evidence for CB_2Rs in healthy adult neurones is limited, there is an increasing amount of work that shows the presence of CB_2Rs associated with glial cells in diseased brains. Miklaszewska *et al.,* (2007) have shown that CB_2Rs are expressed in certain types of adult and paediatric brain tumours (namely malignant gliomas). While Benito *et al.,* (2003) have shown that CB_2Rs are expressed in neuritic plaque-associated astrocytes and microglia in the brains of patients suffering from Alzheimer's disease.

It is apparent that both the CB_2R specific drugs had an effect on sIPSCs and GABA release, but again it was unexpected to see and agonist and an antagonist having the same overall effect, namely decreasing overall GABA release. These results tell us that both CB_1R and CB_2R agonists and antagonists can modulate sIPSCs in layer II mEC neurones, and that while both the CB_1 and

CB_2R agonists have the predicted effect of reducing sIPSCs frequency amplitude and inhibitory charge transfer, both CB_1& CB_2R antagonists act to decrease sIPSC frequency, amplitude and inhibitory charge transfer in developing brain.

A possible explanation in the similarity of the effects of both the CB_1R and CB_2 R antagonists compared to the agonists is that at this age signalling systems in the brain are not yet fully developed and so although the drugs have an effect it is not yet specific.

It has been shown that different agonist for CB_1Rs have different docking sites within the receptor, and in addition to this it would appear that depending on the docking site, the receptor undergoes conformational changes and interacts with specific G-protein subunits to different degrees. For example WIN 55,212-2 and ananadmide produced a maximal stimulation with equal efficacy at CB_1Rs that mediated interaction with G_i proteins, however at CB_1Rs that mediated interaction with G_o proteins, WIN 55,212-2 and anandamide were only partially active. In addition to this, when the role of CB_1Rs in cellular signalling pathways other than GABA release was investigated it was found that different cannabinoid agonists affected the process in different ways. For example CB_1Rs have been shown to play a role in regulating adenylyl cyclase and, different CB_1R agonists regulated adenylyl cyclase with different potencies correlated with the agonists' affinity for the receptor. Furthermore depending on the isoform of adenylyl cyclase present, then CBR agonists have different effects. The calmodulin regulated isoforms of adenylyl cyclise, 1, 3 and 8 and the hormone stimulated isoforms, 5 and 6, were all inhibited in response to cannabinoid agonists, but isoforms 2, 4 and 7 were all stimulated in response to cannabinoid agonists. For a full review of cannabinoid docking sites and interactions with G-proteins see Mukhopadhyay *et al.,* (2002). It maybe that in our P8-12 slices the neurones, CBRs and or the G-proteins they are coupled to, are not yet differentiated enough to be able to

respond to cannabinoid agonists and antagonists in different ways. It is possible that cannabinoid agonists and antagonists have different docking sites within the CBR and that they interact with different G-protein subunits to bring about their overall effect on GABA signalling. When calcium responses to CB_1 agonists were investigated in neuronal cell modals it was found responses changed depending on the state of differentiation of the cell lines. Mukhopadhyay *et al.,* (2002). In terms of our P8-12 experiments, Ihanatovych *et al.,* (2002) showed that during postnatal development, the various Gα subunits are differentially expressed, while the Gβ subunit remains relatively unchanged. If the cannabinoid agonists and antagonist do indeed have different docking sites within the CBR and do cause conformational changes that lead to interactions with different G-protein subunits, then it is possible that the consistent response seen to both CB_1R and CB_2R agonist and antagonists used with the P8-12 experiments, is due to that fact that at this developmental stage, the Gα subunits are not yet showing the expression seen in adults and therefore not able to regulate the different responses of GABA signalling expected from cannabinoid agonists and antagonists.

CHAPTER 5

Pharmacological evidence for CB_2 receptors in the entorhinal cortex

5.1 Introduction

After observing that CB_2R-specific agonists and antagonists had effects on layer II neurones in P8-12 slices, it was decided to investigate the effect of these drugs in layers II and V of adult (P30) animals. While a CB_2R-specific agonist and an antagonist (JWH-133 and AM-630 respectively) altered GABA release in juvenile animals, it does not follow that CB_2 receptors are present in developed brain, since other receptors undergo changes in expression during development, for example, metabotropic glutamate receptors Defagot *et al.,* (2002). Similarly, G-proteins linked to G-coupled receptors are differentially expressed during development (Ihnatovych *et al.,* 2001).

Slices were prepared and stored in the same manner as used throughout. Drug delivery was also carried out using methods previously outlined. The aim of this section of work was to establish if sIPSCs in deep and superficial layers of the adult mEC were sensitive to CB_2R specific agonists and antagonists in a similar manner to that seen in juvenile mEC. This would constitute the first direct pharmacological evidence for CB_2R in the mature CNS *in vitro*.

For these experiments, data were analysed in 10 second and 20 second blocks (layers II and V respectively). Data from individual neurones was then pooled to give a clear picture of the effects of the CB1 and CB2 agonists and antagonists on inhibitory charge transfer which is an indirect indicator of total GABA release. Frequency and amplitude of sIPSCs were also analysed to see if use of the specific drugs gave more defined results than those seen with ACPA and WIN 55, 212-2.

5.2 RESULTS

5.2.1 Blockade of CB_1Rs does not prevent suppression of GABAergic signalling by the non-specific agonist 2-arachidonylglycerol.

In this series of experiments, we blocked CB_1R using the highly selective (see methods for K_i values) antagonist/inverse agonist LY320135 (500 nM). LY320135 was added to the slice and after a suitable interval (usually 20-30 minutes) the CBR agonist 2-arachidonylglycerol (2-AG; 500nM) was added to the slice in addition to LY320135. 2-AG is a naturally occurring agonist (endocannabinoid) and it is non-specific for CB1 and CB2 receptors at this concentration (again, see table materials and methods for individual receptor K_i values). Hence, if no CB_2Rs were present in the slice then application of an agonist should have little or no effect on inhibitory signalling when added in addition to the CB_1R antagonist LY320135. Finally we added a CB_2R specific antagonist, AM-630 to attempt to reverse any effects of 2-AG.

Fig 5.1 Shows sIPSCs recorded from a single layer II neurone during the various stages of drug application. **Fig 5.1A** shows typical layer II sIPSCs with a high frequency of events with mixed amplitudes. When **A** is compared to sIPSCs during application of 500nM LY320135 (**Fig 5.1B**) then it appears that the number of larger amplitude events has increased, however, there is no obvious difference in the frequency of sIPSCs between the two periods. **Fig 5.1C** shows sIPSCs recorded from the same layer II neurone during LY320135 + 2-AG. When compared to the previous condition (**Fig 5.1 B**), then a marked decrease in the number of large sIPSCs is clearly visible, while the number of smaller amplitude sIPSCs does not appear to have altered dramatically. **Fig 5.1 D** shows sIPSCs recorded during LY320135 +2-AG + AM-630 (50nM). Compared to **Fig 5.1 C**, it can be seen that the number of larger amplitude sIPSCs has increased, many of

the largest amplitude sIPSCs appear to occur in complex groups (bursts denoted by *) not seen in the LY320135+2-AG period.

5.2.2 Effects of LY320135 on sIPSCs in layer II mEC.

As with previous experiments, changes in frequency and amplitude of sIPSCs and inhibitory charge transfer were analysed during each successive drug application. Application of LY320135 (500nM) caused a small increase in mean sIPSC amplitude from 59.3 ± 3.1 pA in control to 67.4 ± 4.87 pA although this increase was non-significant ($P \leq 0.163$, ANOVA, n=6). **Fig 5.2 A** shows the cumulative probability plot, for layer II sIPSC amplitude during control (black) and LY320135 (red plot) periods. The two plots lie close together indicating no difference in distribution of sIPSC amplitude; this is supported by non-significant KS test ($P \geq 0.37$). Application of LY320135 only had a small effect on sIPSC frequency in these experiments with the mean median IEI increasing from 44.4ms ± 2.31ms to 47.7ms ± 2.14ms this increase in IEI was non-significant ($P = 0.97$, ANOVA, n=6). **Fig 5.2 B** shows the cumulative probability plots for sIPSC IEI in layer II neurones, the control (black) and LY320135 (500nM; red) plots show little separation indicating very little change in the distribution of sIPSC IEI has occurred between control and LY320135, this is confirmed by a non-significant change in the distribution ($P= 0.572$, KS test). **Fig 5.2C** shows the cumulative probability plots for layer II sIPSC areas. The LY320135 plot (red) lies slightly to the right of the control plot (black); this change in distribution of sIPSC area was significant. ($P \geq 0.005$ KS test) the overall change in area was also significant ($P \leq 0.013$ ANOVA). When NICT was calculated it was found to have increased by 76.47 ± 20.93% during LY320135 application, and this increase was highly

significant ($P \geq 0.005$ ANOVA). **Fig 5.2 D** illustrates the increase in NICT during LY320135 application (red bar) compared to normalised control (black bar).

5.2.3 2-AG reduces sIPSC amplitude, frequency and NICT in layer II mEC neurones in the presence of CB_1R antagonist LY320135.

Application of 2-AG (500nM) caused a decrease in the mean sIPSC amplitude, from 67.40 ± 4.87pA in LY320135 to 47.14 ± 1.29pA, in LY320135 +2-AG, this decrease was significant ($P \leq 0.03$, ANOVA, n=6). **Fig 5.2A** shows the cumulative probability plot for layer II sIPSC amplitudes during different stages of drug application. The LY320135 +2-AG plot (grey) shows a slight shift to the left of the LY320135 (red) plot. However this change in distribution of sIPSC amplitudes between the two drug periods was not significant ($P = 0.256$, KS test). **Fig 5.2B** shows the cumulative probability plot for layer II sIPSC IEIs. The LY320135 +2-AG plot (grey) lies to left of the LY320135 plot (red). However this change in distribution was not significant ($P \geq 0.1780$, KS test). When the mean median IEIs for LY320135 and LY320135+2-AG periods were compared then a decrease from 47.67 ± 2.14ms to 43.70 ± 1.91ms was found, this decrease was significant ($P \geq 0.03$, ANOVA, n=6).

Fig 5.2C shows the cumulative probability plot for sIPSC areas. The LY320135+2-AG plot (grey) lies to the left of LY320135 plot (red) however this change in distribution was not significant ($P \geq 0.178$ KS test). During LY320135 +2-AG NICT decreased to -20.1 ± 16.8% of control when the NICT for LY320135+2-AG was compared to NICT for the previous condition of LY320135 alone then it could be seen that a highly significant decrease had occurred ($P \leq 0.005$ ANOVA) with NICT decreasing from 76.5 ± 20.9% in LY320135 alone to -20.1 ± 16.8% in LY320135+2-AG. **Fig 5.2 D** illustrates the changes in NICT during

different periods of the experiment, black bar represents control, red bar representing LY320135 period, and the grey bar representing the LY320135 + 2-AG period. Overall there was a 96.5% net decrease in NICT between the LY320135 and LY320135 + 2-AG periods and this indicates a profound decrease in GABAergic transmission.

While a decrease in GABAergic activity is what might be expected if 2-AG had been applied alone to the slice, such an effect in the presence of a CB_1R antagonist at >3 x its K_i value suggested that 2-AG was acting at a site other than CB_1Rs. As it is known 2-AG can act as an agonist at both CB_1 and CB_2 receptors it was possible that the decrease in inhibitory charge transfer was due to 2-AG acting at CB_2Rs within layer II of the mEC.

5.2.4 AM-630 reversed the effects of 2-AG on sIPSC amplitude, frequency and NICT.

Given the evidence that 2-AG had an affect on amplitude and NICT in layer II of the mEC in the presence of a CB_1R antagonist, it was reasoned that it may be acting at non-specific sites or possibly at CB_2Rs or at an as yet unidentified cannabinoid receptor. To investigate these possibilities a CB_2R antagonist/inverse agonist, AM-630 (50nM), was bath applied to the slices in addition to the LY320135 and 2-AG that were already present.

Application of AM-630 (50nM; again 1.5 x K_i) caused an increase in mean sIPSC amplitude from 47.138 ± 1.29pA in LY320135 + 2-AG to 67.43 ± 4.29 pA in LY320135 + 2-AG + AM-630 this increase was significant ($P \leq 0.0001$, ANOVA, n=4). **Fig 5.2 A** shows the cumulative probability plot for sIPSC amplitudes the LY320135 + 2-AG + AM-630 plot (light blue) lies to the right of the LY320135+2-AG plot (grey) and this change in amplitude distribution between these two periods was significant ($P \leq 0.003$, KS test). **Fig 5.2 B** shows the cumulative

probability plot for sIPSC IEIs during different drug periods with in the experiments. The LY320135 + 2-AG + AM-630 plot (light blue) has shifted to the right of the LY320135 + 2-AG plot (light grey) this change in distribution was significant ($P \leq 0.003$, KS Test). When the mean median IEI for LY320135+2-AG+AM-630 was compared to the previous condition of LY320135 + 2-AG then a decrease was seen to occur from 43.7 ± 1.91ms in LY320135 + 2-AG to 35.4 ± 2.19ms in LY320135+ 2-AG + AM-630 this decrease in mean median IEI was not quite significant ($P = 0.066$, ANOVA), but does suggest an overall increase in sIPSC frequency.

In **Fig 5.2 C** it can be seen that the LY320135+2-AG +AM-630 plot (light blue) has shifted to the right of the LY320135+2-AG plot (grey) this change in distribution of sIPSC amplitudes between the two consecutive drug periods was significant ($P \leq 0.0007$, KS Test). In addition to the effects described above, application of AM-630 (50nM) in the presence of LY320135 and 2-AG caused an increase in NICT. Application of LY320135 + 2-AG + AM-630 increased NICT by 89.5 ± 27.8% compared to a control, a net increase of 109% in GABAergic signalling compared to LY320135+2-AG. This increase was very significant ($P \leq 0.007$, ANOVA). **Fig 5.4 D** illustrates the increase in NICT during LY320135 + 2-AG + AM-630 (light blue) compared to the control (black) and to LY320135 + 2-AG (grey).

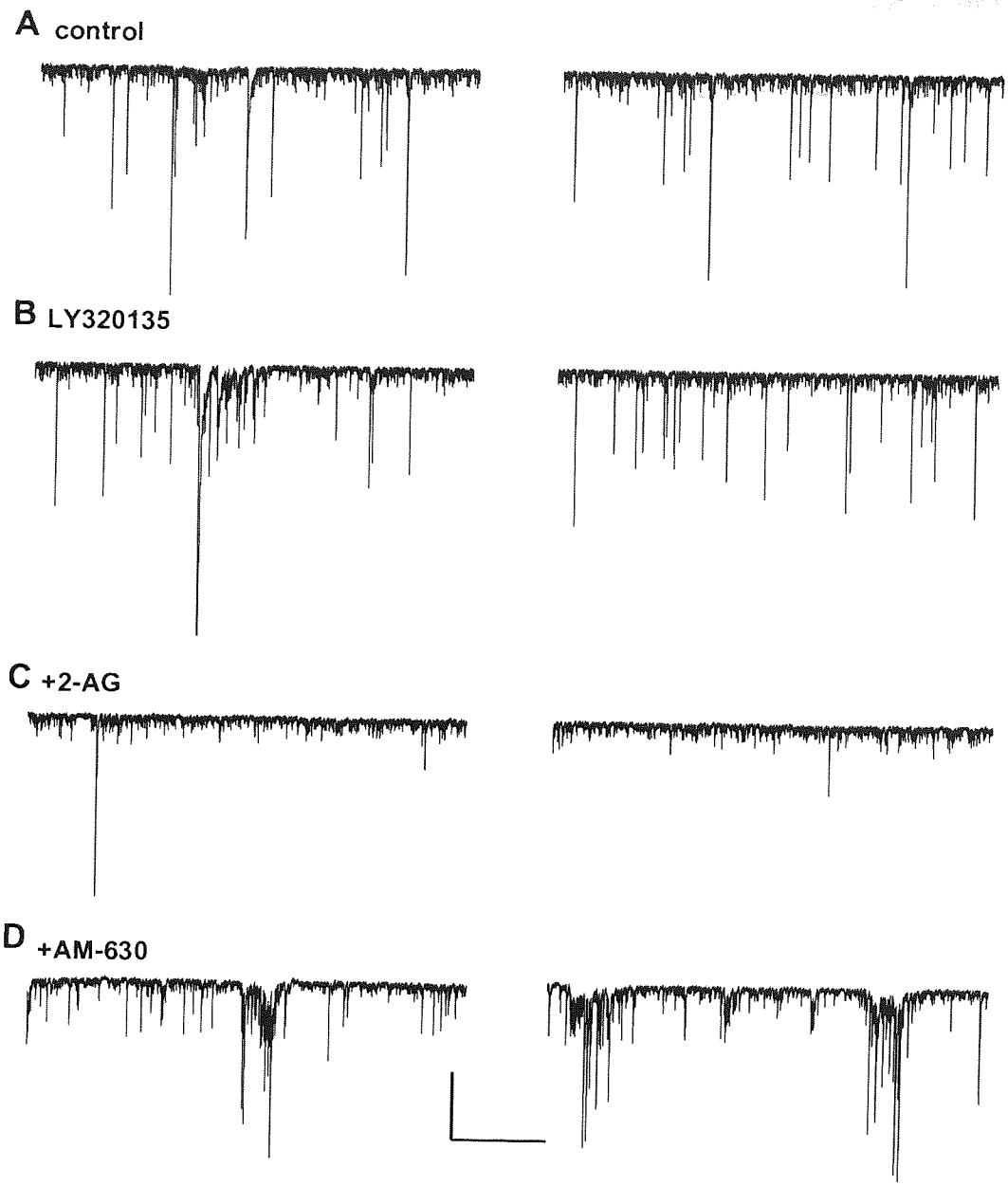

Fig 5.1 Layer II sIPSCs during control and additional drug application periods. Layer II sIPSCs from a single layer II neurone, during **A.** Control, **B.** LY320135 **C.** LY320135+2-AG and **D** LY320135+2-AG+AM-630 LY320135 (500nM), 2-AG (500nM) AM-630 (50nM) Scale **X** 5000ms **Y** 500pA.

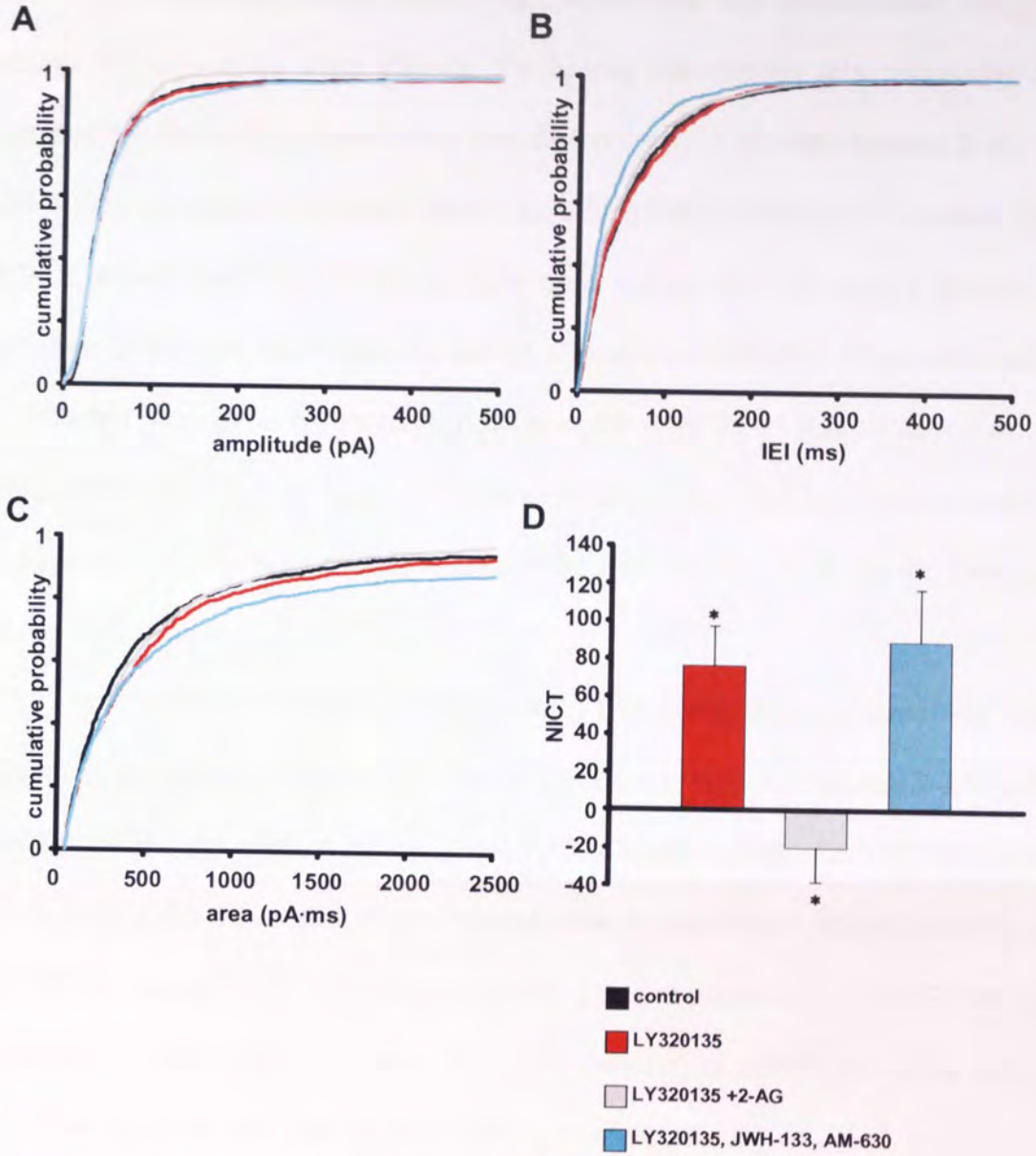

Fig 5. 2 effects of LY320135, 2-AG and AM-630 on layer II sIPSCS
Cumulative probability plots (for layer II) for the different periods of drug application during the experiment **A.** Cumulative probability for amplitude **B.** Cumulative probability for IEIs, **C.** Cumulative probability for area. **D.** Illustrates the changes in NICT with respect to normalised control of 1 and the other drug periods. Pooled data n= 6 LY320135 (500nM) 2-AG (500nM) AM-630 (50nM) * $P \leq 0.05$

This combination of results suggested that the cannabinoid drugs were acting at sites other than CB_1Rs. To further investigate this possibility it was decided to repeat the experiments but switch the non-specific agonist 2-AG with a CB_2R specific agonist, namely JWH-133, which had previously been used with the P8-12 slices. Use of a CB_2R specific drug would allow a clearer picture as to whether 2-AG and AM-630 were acting at a specific CB_2R or if the were acting in a different manner such as have non-receptor specific effects or acting on an as yet unidentified CB receptor. Recent studies have indicated a possible third subtype of cannabinoid receptor within the brain (Hajos *et al.*, 2001; Breivogel *et al.*, 2001).

In the following set of experiments the same drug protocol as outlined earlier in the chapter was used, the only change was to replace 2-AG with the CB_2R specific agonist JWH-133. JWH-133 is highly specific for CB_2Rs (see table 2.1 in methods) thus using it at a suitably low concentration should avoid it acting at CB_1Rs when added to the slice in the presence of a CB_1R antagonist (LY320135). JWH-133 was used at a concentration of 66nM (ten times below the K_i for rat CB_1R of 677 nM) in the following experiments.

5.3 A CB_2R-specific agonist replicates the effects of 2-AG in the presence of LY320135

Fig 5.3 shows sIPSCs recorded from a single layer II neurone during the various stages of drug application. **Fig 5.3A** shows sIPSCs from the control period, with the typically layer II pattern of high frequency mixed amplitude events. When the control period is compared to the LY320135 (500nM) period **Fig 5.3B** it appears that large amplitude events have increased in size and number, however, the number of intermediate amplitude sIPSCs seems to have decreased compared to the control period. **Fig 5.3C** shows sIPSCs recorded during

LY320135 +JWH-133 period, when these traces are compared to the LY320135 traces then it is apparent that the number of large amplitude events has been greatly reduced. Finally, **Fig 5.3D** shows sIPSCs recorded during LY320135 + JWH-133 +AM-630 application, when compared to the traces for the LY320135 + JWH-133 period it can be seen that the number of larger amplitude sIPSCs has once again increased.

5.3.1 LY320135 increased sIPSC amplitude and NICT in layer II mEC.

As with the previous set of experiments in layer II mEC neurones, bath application of LY320135 (500nM) caused an increase in sIPSC amplitude, and NICT. The mean amplitude increased from 51.7 ± 3.6 pA in control to of 69.0 ± 5.9 pA in LY320135, and this was significant ($P \leq 0.013$, ANOVA, n=6). **Fig 5.4A** shows the cumulative probability plot for sIPSC amplitudes in various stages of the experiment. The LY320135 (red) plot lies to the left of the control plot (black) indicating a change in the distribution of sIPSC amplitudes, this change in distribution was significant. ($P \leq 0.002$, KS test).

The mean median IEI showed a slight decrease from 86.6 ± 4.38ms in control to 80.6 ± 3.61ms in LY320135, this decrease in IEI time was not significant ($P \geq 0.116$, ANOVA, n=6). The cumulative probability plot in **Fig 5.4 B** shows that no change occurred in the overall distribution of sIPSC IEI in layer II neurones with the LY320135 plot (red) lying on top of the control plot (black) and this was confirmed by the KS test ($P \geq 0.40$).

Fig 5.4 C shows the cumulative probability plots for sIPSC areas during the various drug periods of the experiment, the LY320135 plot remains close to the control plot (black) suggesting that little change in sIPSC area distribution occurs between these two periods this is confirmed by a non-significant KS test ($P \geq 0.188$ KS test). During LY320135 application there was an overall increase in

NICT 62.5 ± 27.1% with respect to control this increase was just significant ($P \leq$ 0.048, ANOVA, n=6) **Fig 5.4D** illustrates the increase in NICT during LY320135 application (red bar) compared to normalised control (black bar).

5.3.2 Addition of JWH-133 (66nM) in the presence of LY320135 caused a decrease in sIPSC amplitude and NICT in layer II mEC.

During application of LY320135 + JWH-133 (66nM) the mean sIPSC amplitude decreased from 69.0 ± 5.9 pA to 44.9 ± 1.4 pA, ($P \leq 0.0001$, ANOVA, n=6). **Fig 5.4A** shows the cumulative probability plot for the distribution of sIPSC amplitudes the plot for LY320135 + JWH-133 (grey) lies to the left of the LY320135 plot (red) however this change in distribution was not significant ($P \geq$ 0.10, KS test). During application of LY320135+JWH-133 the mean median IEI was found to have decreased from 80.6 ± 3.61ms in LY320135 to 78.5 ± 3.89ms in LY320135 + JWH-133, and this decrease was not significant ($P \geq 0.534$, ANOVA, n=6). **Fig 5.4 B** shows the distribution of IEIs during various drug periods. The LY320135 + JWH-133 plot (grey) lies right next to the LY320135 (red) plot showing no change in IEI distribution has occurred. This is confirmed by a non-significant KS test ($P \geq 0.085$). The application of JWH-133 (66nM) in addition to LY320135 caused a decrease in GABAergic signalling. NICT decreased to -27.6 ± 9.5% of control during LY320135 + JWH-133 application. This decrease was significant ($P \leq$ 0.013, ANOVA, n=6), furthermore when the increased inhibitory charge transfer seen during the LY320135 period (62.0 ± 27.1%) was compared to the decreased inhibitory charge transfer of the LY320135 + JWH-133 (-27.6 ± 9.5%) it was found that this decrease significant ($P \leq$ 0.011, ANOVA, n=6). **Fig 5.4C** shows the cumulative probability plots for sIPSC areas during the various drug application periods. The LY320135 + JWH-133 plot

(grey) lies slightly to the left of the LY320135 plot (red) for values over 750pA·ms however this change in distribution was not significant ($P \geq 0.258$ KS test). During LY320135+JWH-133 application NICT decreased by -27.56 ± 9.46 % of control, when the decrease in NICT during LY320135 + JWH-133 application was compared to the previous drug period of LY320135 then a net decrease in NICT of 89% occurred, this decrease in NICT shows that a decrease in GABAergic signalling has occurred during LY320135 + JWH-133 application, this decrease was significant ($P \leq 0.025$ ANOVA n=6). **Fig 5.4D** (blue bar) compares the change in inhibitory charge transfer to normalised control as well as with the increase and decreases seen in response to the various drug applications.

The decrease in inhibitory charge transfer as well as changes seen in sIPSC frequency in response to LY320135 +JWH-133 application suggested that JWH-133 is acting on the neurones at sites other than CB_1Rs. To further investigate the possibility the JWH-133 may be acting at CB_2Rs AM-630, a CB_2R specific antagonist, was added to the bath in addition to the LY320135 and JWH-133.

5.3.3 AM-630 reversed the effects of JWH-133.

In the presence of LY320135 + JWH-133, application of AM-630 (50nM) caused an increase in the mean amplitude of sIPSCs. The mean amplitude increased markedly from 44.96 ± 1.35 pA in LY320135 + JWH-133 to 72.5 ± 4.7 pA in LY320135 + JWH-133 + AM-630. This increase in amplitude was found to be significant ($P \leq 0.0001$, ANOVA, n=6). The distribution of sIPSC amplitudes also changed. **Fig 5.4A** shows that the cumulative probability plot for LY320135+ JWH-133 + AM-630 (light blue) has shifted the right of the LY320135 + JWH-133

plot (grey), This change in the distribution of amplitudes was significant ($P \leq$ 0.0001, KS test).

AM-630 application also increases sIPSC frequency. In **Fig 5.4B** it can be seen that the cumulative probability plot for sIPSC IEIs in LY320135+JWH-133+AM-630 (light blue) lies just to the left of the LY320135+JWH-133 plot (grey) indicating a change in distribution of IEIs between the two drug periods. This change in distribution was significant ($P \leq 0.0001$, KS test). The mean median IEI also decreased from 78.52 ± 3.89ms in LY320135 + JWH-133 to 58.06 ± 2.75ms in LY320135 + JWH-133 + AM-630 this decrease was significant ($P \leq 0.0001$, ANOVA, n=6). **Fig 5.4 C** shows the cumulative probability plot for sIPSC areas during the different drug periods of the experiment the LY320135+JWH-133+AM-630 plot (light blue) has shifted notably to the right of the LY320135+JWH-133 plot (grey) showing a change in distribution of areas has occurred, this change in distribution was confirmed by a significant ($P \leq 0.0007$, KS test). Application of AM-630 caused an increase in GABAergic signalling with the NICT increasing by 108.630 ± 50.848% in LY320135 +JWH-133 + AM-630 with respect to control. The increase was not quite significant ($P \geq 0.06$, ANOVA, n=6). However, when NICT for LY320135 + JWH-133+ AM-630 (108.63 ± 50.85%) was compared to LY320135 + JWH-133 (-27.6 ± 9.5%) then it can be seen that a net increase of 136% in GABAergic signalling occurred, and this increase was significant ($P \leq$ 0.025 ANOVA). **Fig 5.4 D** illustrates the increase in NICT during LY320135+JWH-133+AM-630 application (light blue bar) compared to the changes in NICT during control and the other drug periods. The increase in inhibitory charge transfer indicated that there was an increased GABA release when the CB_2 antagonist AM-630 was applied to the slice in the presence of LY320135 and JWH-133,

adding support to the hypothesis that the cannabinoid agonist and antagonist are acting at a receptor-specific site.

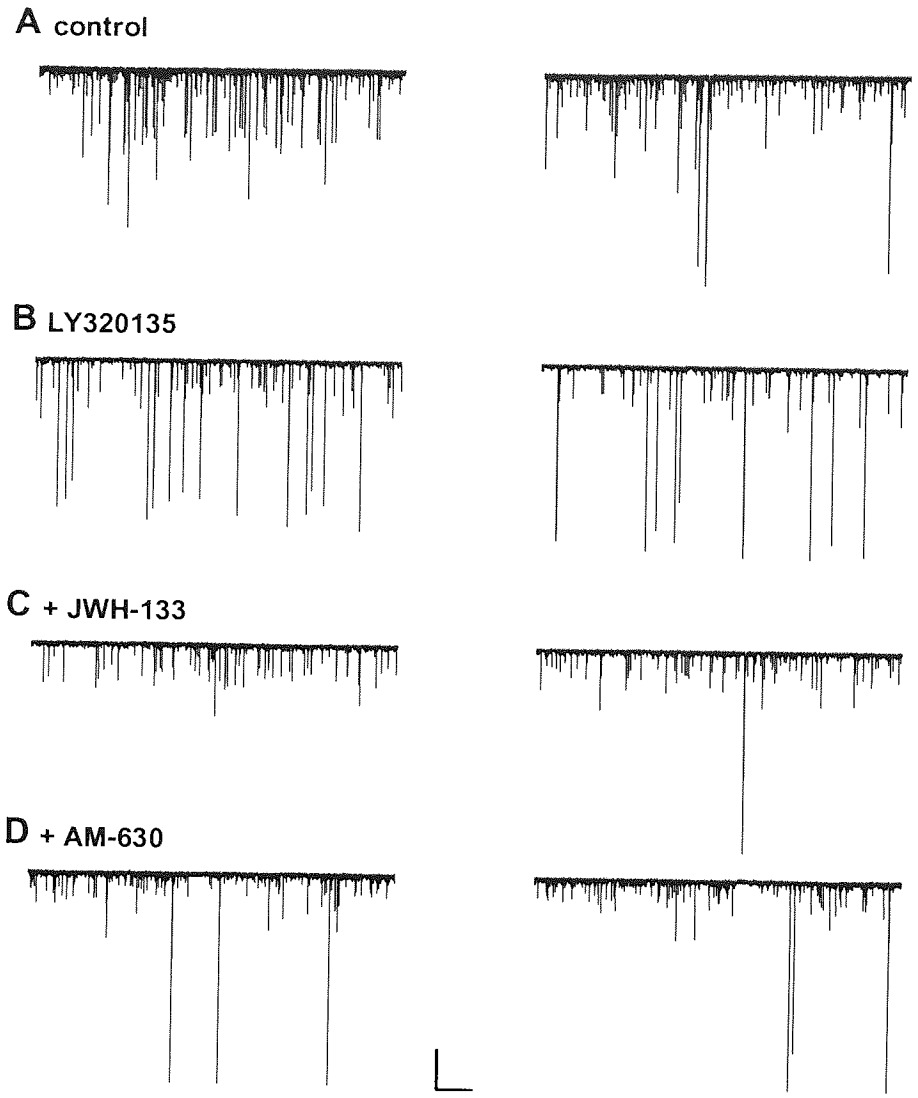

Fig 5.3 Layer II sIPSCs during control and consecutive drug application periods. Layer II sIPSCs from a single layer II neurone, during **A.** Control **B.** LY320135 **C.** LY320135 + JWH-133 and **D.** LY320135 + JWH-133 + AM-630: LY320135 (500nM) JWH-133 (66nM) AM-630 (50nM) Scale **X** 1000ms **Y** 500pA.

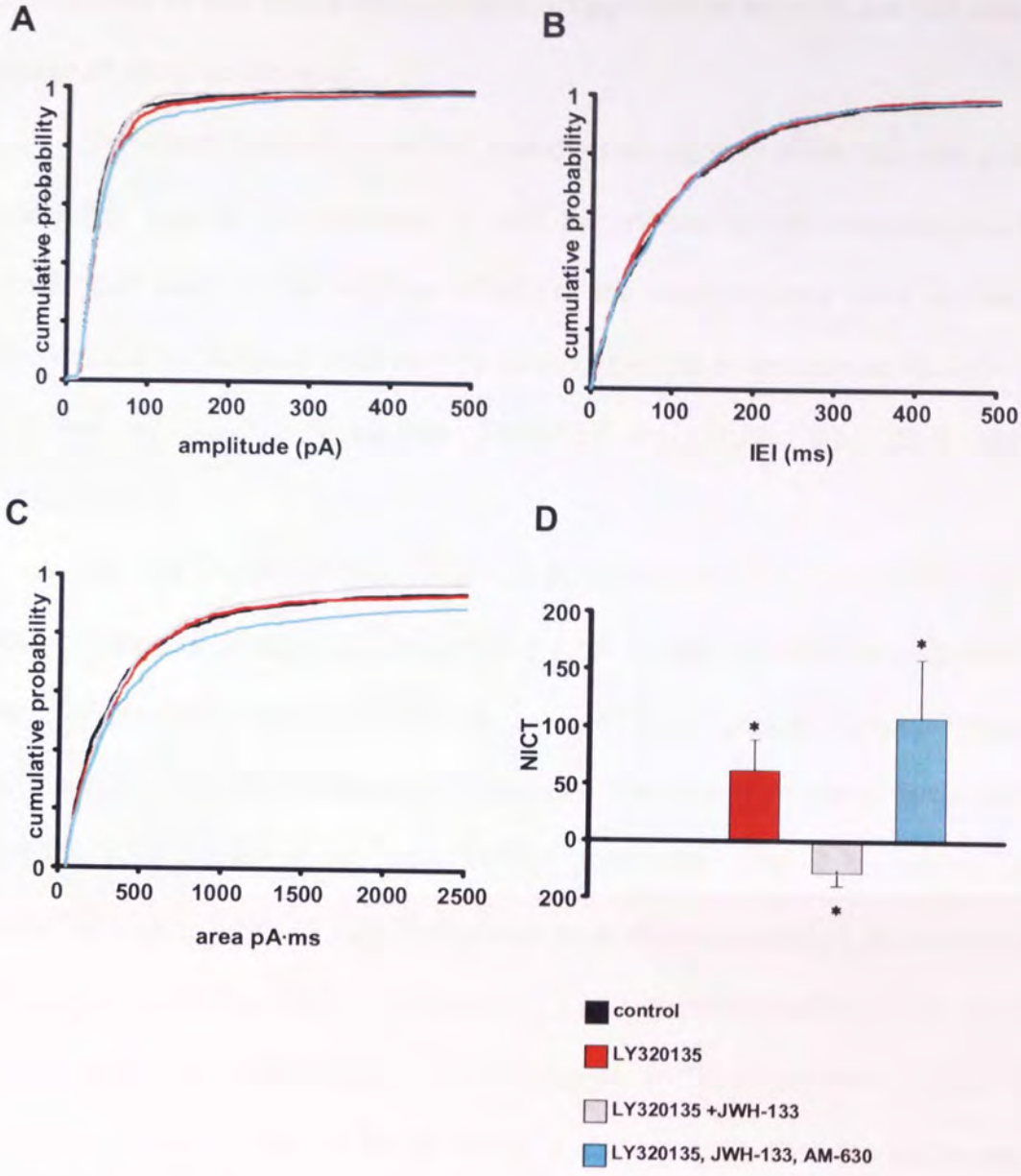

Fig 5. 4 effects of LY320135, JWH-133 and AM-630 on layer II sIPSCS
Cumulative probability plots (for layer II) for the different periods of drug application during the experiment **A.** Cumulative probability for amplitude **B.** Cumulative probability for IEIs, **C.** Cumulative probability for area. **D.** Illustrates the changes in NICT with respect to normalised control of 1 and the other drug periods. Pooled data n= 6, LY320135 (500nM) JWH-133 (66nM) AM-630 (50nM). * $P \leq 0.05$

5.4 Effects of the CB_2R agonist and antagonist in layer II are not due to the order of drug application.

To investigate the possibility that the CB_2 agonist JWH-133 was acting at a site other than a CB_2 receptor or that the effects see in response to AM-630 application were due to additive effects of the drug protocol used we decided to reverse the experiment and start by adding the CB_2R antagonist AM-630 (50nM) followed by the CB_2R agonist JWH-133 and finally the CB_1R antagonist LY320135.

Fig 5.5 shows sIPSCs recorded from a single layer II neurone during the different stages of drug application. **Fig 5.5A** shows the sIPSCs recorded during the control period, when these traces are compared to those recorded during AM-630 application (**Fig 5.5B**) then it appears that the number of large amplitude sIPSCs has increased during AM-630 application. **Fig 5.5C** shows sIPSCs recorded during AM-630 +JWH-133 period of drug application, compared to AM-630 alone it can be seen the number of large amplitude sIPSCs has decreased during AM-630 + JWH-133. **Fig 5.5D** shows sIPSCs recorded during AM-630 +JWH-133 +LY320135. In these traces it can be seen that the large amplitude sIPSCs that were all but lost during AM+JWH-133 application have returned in response to LY320135 application.

5.4.1 AM-630 alone increases sIPSC amplitude and NICT in layer II mEC

When AM-630 (50nM) was applied to the bath, the mean amplitude of layer II sIPSCs increased from 72.8 ± 4.7 pA in control to 89.4 ± 5.5 pA (n=7). The increase in mean sIPSC amplitude was significant ($P \leq 0.023$, ANOVA, n=7). **Fig 5.6A** shows the cumulative probability plot for sIPSC amplitudes during the different drug periods of the experiment. The AM-630 plot (light blue) shifts to the

right of the control plot (black); this change in distribution of sIPSC amplitudes was not significant ($P \geq 0.10$, KS test).

During AM-630 application the mean median IEI decreased from 63.7 ± 3.04ms in control to 56.3 ± 2.90ms. This decrease in the mean median IEI was non-significant ($P = 0.705$, ANOVA, n=7) **Fig 5.6 B** shows the cumulative probability plot for IEIs during various stages of the experiment. The AM-630 plot (light blue) lies on top of the control plot (black) indicating no change in IEI distribution has occurred and this is confirmed by a non-significant KS test ($P \geq 0.10$).

Fig 5.6 C shows the cumulative probability for sIPSC areas during the various stages of the experiment. The AM-630 plot (light blue) lies to the right of the control plot (black) indicating a change in the distribution of sIPSC amplitudes towards larger values in AM-630, and this was confirmed by a significant KS test ($P \leq 0.005$). Application of AM-630 caused NICT to increase by 41.46 +15.50 % of control this increase in NICT was significant ($P \leq 0.025$, ANOVA, n=7), **Fig 5.6 D** illustrates the increase in NICT with control represented by the black bar and AM-630 the light blue bar.

Having established the fact that AM-630 caused an increase in inhibitory charge transfer along with altering sIPSC frequency and amplitude when added to the slice alone, the next step was to see if adding JWH-133 had any effect on the response elicited by AM-630.

5.4.2 JWH-133 decreases sIPSC amplitude and NICT in layer II mEC.

JWH-133 (66nM), a CB_2R-specific agonist was applied to the slice in addition to AM-630 (50nM). During application of JWH-133 the mean sIPSC amplitude fell from 95.28 ± 6.27 pA in AM-630 to 68.7 ± 5.0 pA in AM-630 + JWH-

133. This decrease in sIPSC amplitude was significant ($P \leq 0.02$, ANOVA, n=7). **Fig 5.6A** Is the cumulative probability plot for sIPSC amplitudes during the different drug applications the AM-630 + JWH-133 plot (grey) shows a notable left shift with respect to the AM-630 plot (light blue), this change in distribution of sIPSC amplitude between AM-630 and AM-630 + JWH-133 periods was significant ($P \leq 0.003$, KS test). **Fig 5.6B** shows the cumulative probability plot, comparing layer II sIPSC IEI times during the different drug periods of the experiment. The AM-630+JWH-133 plot (grey) is intertwined with the AM-630 plot (light blue) for the duration of the graph showing no change has occurred in the distribution of IEIs between AM-630 and AM-630+JWH-133 periods. This is confirmed by a non-significant KS test ($P \geq 0.799$). The mean median IEI showed a slight increase from 58.34 ± 2.90ms in AM-630 to 64.65 ± 3.27ms in AM-630+JWH-133 but this decrease was not significant indicating no overall change in the frequency of sIPSCs occurred ($P \geq 0.673$ ANOVA) .

Fig 5.6C shows the cumulative probability plot for sIPSC area distribution during the different stages of the experiment. The AM-630+JWH-133 plot (grey) shows a large shift to the left of the AM-630 plot (light blue) for the duration of the graph, showing a change in distribution of sIPSC areas occurs between these two drug periods, this change in distribution is confirmed by a very significant KS test ($P \leq 0.0001$). Inhibitory charge transfer decreased to -11.8 ± 21.6 % of control in AM-630+JWH-133, when compared to NICT for AM-630 (41.46 + 15.50 %) then a net decrease of 52.54 % in GABAergic signalling occurred, this decrease was just significant ($P \leq 0.049$, ANOVA, n=7) **Fig 5.6 D** illustrates the change in NICT with respect to control and the other drug periods, the change in NICT during AM-630+JWH-133 application is illustrated by the grey bar. When we subsequently

added the CB1R antagonist LY320135 (500 nM), we again observed an increase in GABAergic neurotransmission.

5.4.3 LY320135 increases GABAergic neurotransmission in the presence of AM-630 and JWH-133

Fig 5.6A shows the cumulative probability plot for sIPSC amplitudes during the various stages of the experiment. The AM-630+JWH-133+LY320135 plot (red) lies to the right of the plot for the previous drug application of AM-630+JWH-133 (grey). Pointing towards a lower probability of smaller amplitude events in LY320135+JWH-133+AM-630 compared to the AM-630+JWH-133 application period. This change in distribution was not significant ($P \leq 0.113$ KS test). The mean amplitude increased during AM-630+JWH-133+LY320135 application from 68.72 ± 5.00pA in AM-630+JWH-133 to 73.43 ± 4.71pA in AM-630. However this increase in amplitude was not significant ($P \geq 0.398$, ANOVA, n=6).

Fig 5.6 B shows the cumulative probability for sIPSC IEIs during the various stages of the experiment, The AM-630+JWH-133+LY320135 plot (red lies very close to the AM-630+JWH-133 plot (grey) pointing towards no change in distribution of IEI times, this was confirmed by a non-significant KS test ($P \geq 0.440$). The mean median IEI showed an increase from 64.64 ± 3.27ms in AM-630+JWH-133 to 73.31 ± 3.69ms in AM-630+JWH-133+LY320135. This increase in IEI was not significant ($P \geq 0.119$, ANOVA, n=6).

Fig 5.6 C shows the cumulative probability for sIPSC areas during the different stages of the experiment, the AM-630+JWH-133+LY320135 plot (red) lies to the right of the AM-630+JWH-133 plot (grey), showing a lower probability of smaller areas in AM-630+JWH-133+LY320135. This change in distribution was not significant ($P \geq 0.279$, KS test). During AM-630+JWH-133+LY320135

application NICT increased by 41.67 ± 30.96% of control, when the increase in NICT was compared with the decreased NICT value for the previous drug period of AM-630+JWH-133 then a net increase of 52% in NICT occurred this shows that during AM-630+JWH-133+LY320135 application GABAergic signalling increased. However this increase in NICT was not significant ($P \geq 0.153$, ANOVA, n=6).

The above series of experiments showed that in P30 layer II nurones the CB_1R antagonist LY320135 acted as expected based on previous work. However, the effects of the CB_1R antagonist could not prevent the effects of a non-specific CBR agonist and a CB_2R specific agonist. The effects of the non-specific agonist and the CB_2R agonist were reversed by application of a CB_2R specific antagonist. Finally, the effects of the CB_2R antagonist are not due to the order of application of the drugs to the slice as the CB_2R antagonist (AM-630) caused an increase in GABA release when added to the slice alone, as well as when it was added in the presence of a CB_1R antagonist plus a non-specific CBR agonist or a CB_2R specific agonist.

It might be expected that the CB_2R specific agonist (JWH-133 66nM) should have no affect on GABAergic signalling when added to the slice in the presence of the CB_2R antagonist AM-630, if both ligands are presumed to be acting at CB_2Rs. There are two potential explanations for these data: 1) 50nM AM-630 is unable to fully compete with JWH-133 for binding sites in the receptors, thus JWH-133 is still able to have an effect, or 2) unidentified CBR present in layer II of the mEC that is capable of interacting with JWH-133. These possibilities will be discussed later.

Having established that CB_2R specific agonists and antagonists affect GABAergic signalling in P30 layer II neurones it was decided to see if they had the same effects in layer V P30 neurones.

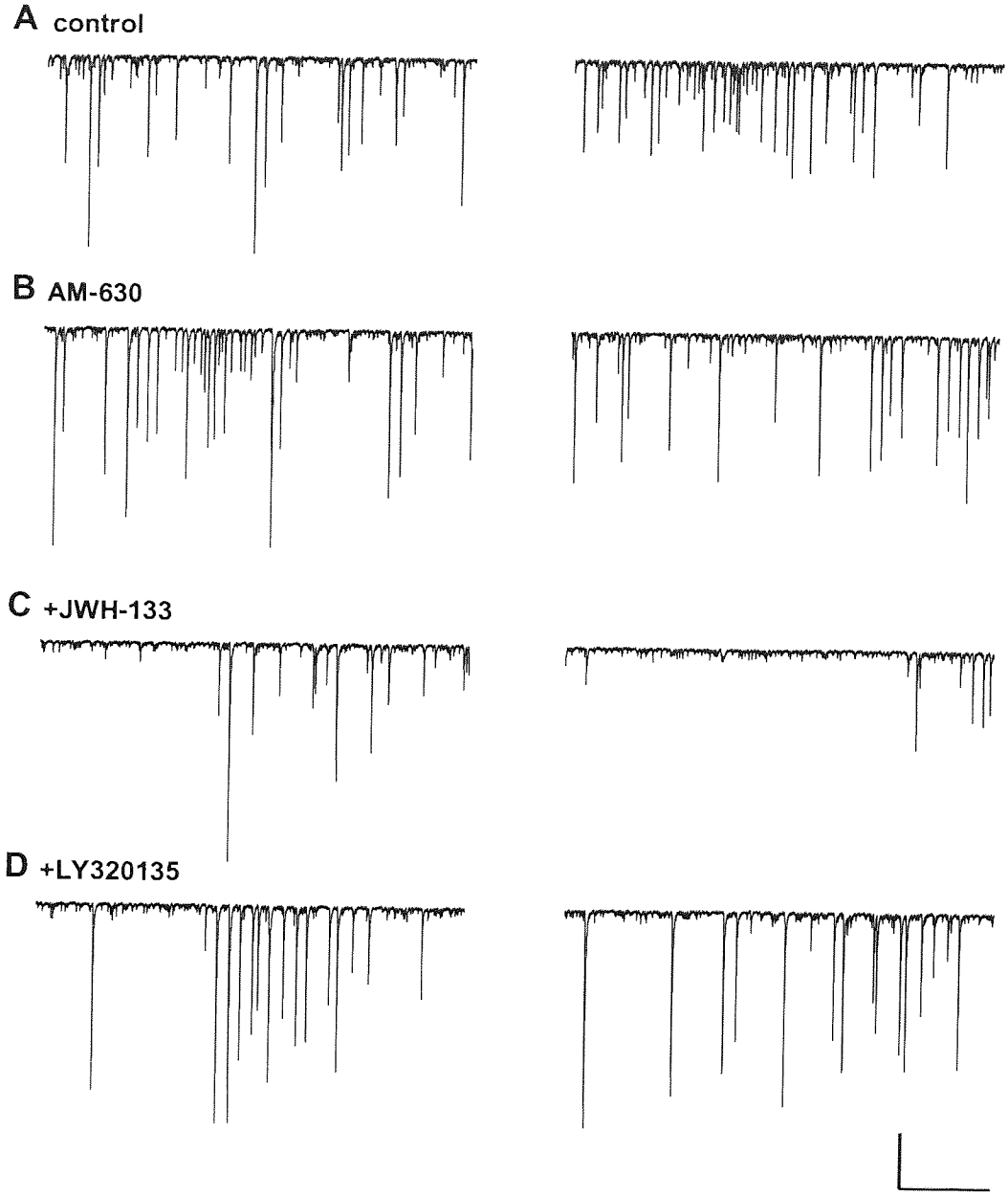

Fig 5.5 layer II sIPSCs during control and consecutive drug application periods

Layer II sIPSCs from a single layer II neurone, during **A.** Control, **B.** AM-630 **C.** AM-630 + JWH-133 and **D.** AM-630 + JWH-133 + LY320135; AM-630 (50nM), JWH-133 (66nM) and LY320135 (500nM) Scale **X** 2000ms **Y** 500pA.

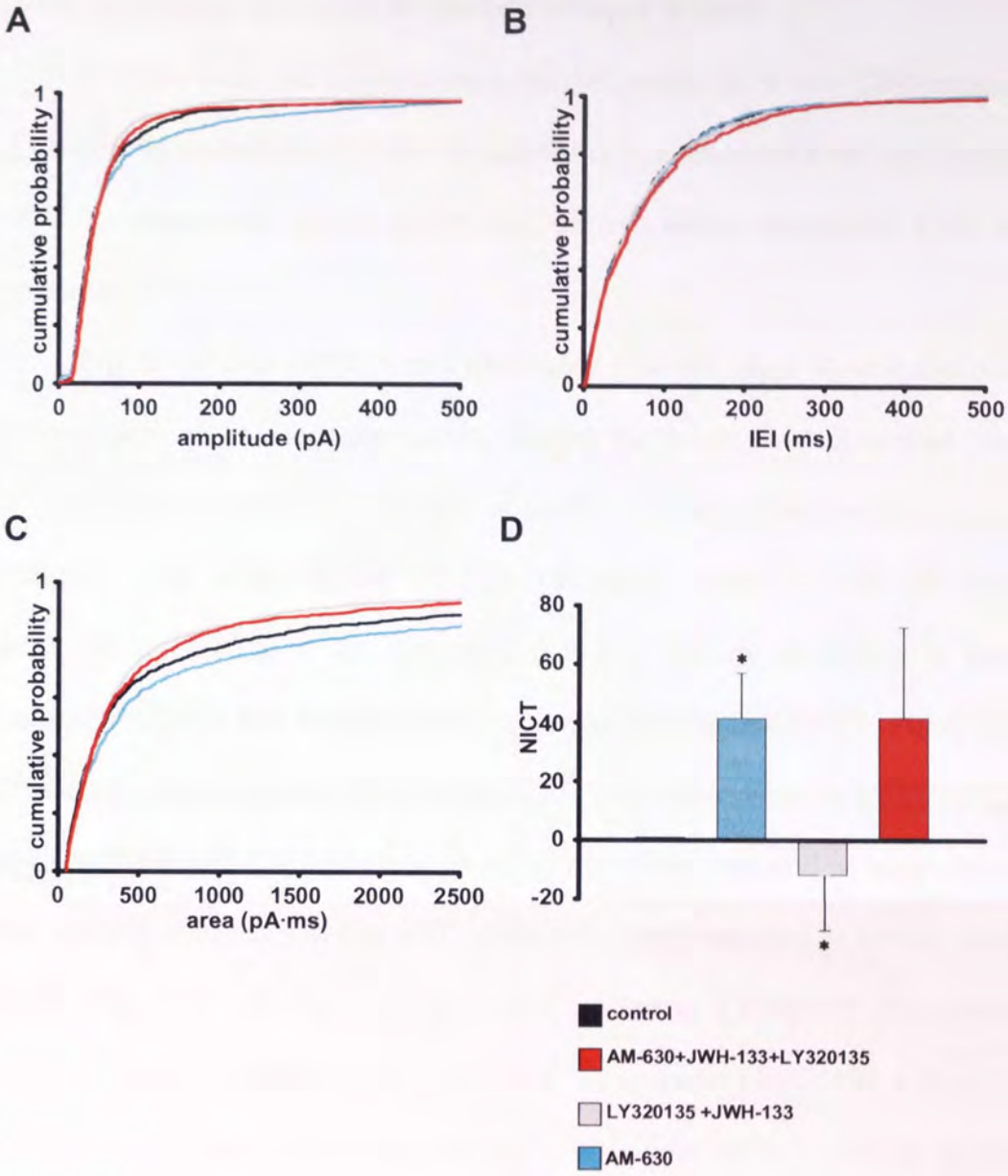

Fig 5. 6 Effects of LY320135, 2-AG and AM-630 on layer II sIPSCS
Shows the cumulative probability plots (layer II data) for the different periods of drug application during the experiment **A.** Cumulative probability for amplitude **B.** Cumulative probability for IEIs, **C.** Cumulative probability for area. **D.** Illustrates the changes in NICT with respect to normalised control of 1 and the other drug periods. Pooled data n=6, AM-630 (50nM) JWH-133 (66nM) LY320135 (500nM). * $P \leq 0.05$

5.5 CB_2R Responses to CB_2R ligands in layer V mEC

In order to further explore the potential presence of non-CB_1R responses in mEC, and to investigate lamina-specificity of our observations, we repeated the entire experimental series described above whilst recording from layer V pyramidal neurones.

Fig 5.7 shows sIPSCs recorded from a single layer V neurone during the different periods of drug application. During the control we observed the typical low frequency low amplitude pattern of sIPSCs already described for layer V mEC sIPSCs. **Fig 5.7B** shows sIPSCs recorded during LY320135 application compared to control it can be seen that the number and size of the larger amplitude sIPSCs has increased during application of LY320135. **Fig 5.7C** shows sIPSCs recorded during LY3201352 + 2-AG when compared to LY320135 alone it appears that the large amplitude events have been reduced in both number and size, making the traces in **Fig 5.7C** resemble those recorded in control (**Fig 5.7A**). Finally **Fig 5.7D** shows sIPSCs recorded during LY320135 (500nM) +2-AG (500nM) + AM-630 (50nM), compared to the traces for LY320135 + 2-AG then an increase in the size and number of larger amplitude sIPSCs can be seen during LY320135 + 2-AG + AM-630 application, indicating that AM-630 has to some extent reversed the suppressing effects of 2-AG.

5.5.1 LY320135 increased amplitude and NICT in layer V mEC

Application of the CB_1R specific antagonist LY320135 (500nM) caused the mean amplitude of layer V sIPSCs to increase from 42.1pA ± 3.1 to 79.5pA ± 7.3 and this increase was significant ($P \leq 0.003$, ANOVA n= 6). **Fig 5.8A** shows the cumulative probability plot for sIPSC amplitudes during the various stages of the experiment. The LY320135 plot (red) shows a large right shift with respect to the control plot (black). As well as shifting to the right of control the LY320135 plot

also continues along the X axis after the control plot has finished. This shows that during LY320135 application sIPSC with amplitudes larger than anything seen in the control period occur. The change in distribution of sIPSC amplitude was significant ($P \leq 0.0004$, KS test).

Addition of LY320135 caused a decrease in the mean median IEI from 448.7 ± 75.73ms in control to 325.9 ± 67.15 in LY320135. This decrease in the mean median IEI was not significant ($P = 0.989$, ANOVA, n=6). **Fig 5.8 B** shows the cumulative probability for sIPSC IEIs during the different drug periods of the experiment. The control plot (black) and the LY320135 plot (red) remain intertwined with the LY320135 plot showing no clear shift to the right or left of the control indicating the distribution of sIPSC IEIs does not change significantly between control and LY320135 application. This is confirmed by a KS test ($P \geq 0.985$).

Fig 5.8C Shows the cumulative probability for sIPSC areas during the various drug periods of the experiment, the LY320135 plot (red) shows a large leftward shift with respect to the control plot (black) this change in sIPSC area distribution was very significant ($P \leq 0.0001$). During LY320135 application NICT increased to 132.35 ± 68.02% of control. This net increase in GABAergic signalling just failed to reach significance ($P \leq 0.082$ ANOVA), presumably due to the large variance in area in this series of recordings.

5.5.2 The CBR non-specific agonist 2-AG reversed the effects of LY320135.

Just as the previous experiments in layer II, after LY320135 application we added the non-specific agonist 2-AG (500nM) to the slice in addition to the LY320135 (500nM). Here, the mean amplitude decreased from 79.52 ± 7.32pA in LY320135 to 45.2pA ± 3.2 in LY320135+2-AG. This decrease was significant ($P \leq$

0.0001, ANOVA, n=6). **Fig 5.8A** shows the cumulative probability plot for sIPSC amplitudes during the different drug periods in the experiment. The LY320135+2-AG plot (grey) lies to the left of the LY320135 plot (red), showing a change in distribution of sIPSC amplitudes between the two drug periods. This change in distribution was very significant ($P \leq 0.0001$, KS test).

Fig 5.8B shows the cumulative probability plot for sIPSCs IEIs during the different drug application periods of the experiment. The LY320135+2-AG lies slightly to the right of the LY320135 plot (red) showing a change in distribution this change in the IEI between LY320135 and LY320135+2-AG periods was significant ($P \leq 0.0001$, KS Test). The mean median IEI time increased between LY320135 and LY320135+2-AG application, rising from 325.9 ± 67.5ms in LY320135 to 1426.1 ± 75.74ms in LY320135+2-AG (an increase in the mean median IEI is linked to a decrease in sIPSC frequency), however this increase in mean median IEI was not significant ($P \geq 0.140$, ANOVA, n=6).

Fig 5.8C shows the cumulative probability plots for sIPSC areas during the various drug application periods. The LY320135+2-AG plot (grey) shows a marked shift to the right of the LY320135 plot (red) the gap between the two plots suggest that a change in IEI distribution has occurred between the two drug periods this was confirmed by a significant KS test ($P \leq 0.0004$). Application of LY320135+2-AG caused NICT to increase by 5.03 ± 22.99 % of control. However when NICT for LY320135+2-AG was compared to NICT for the previous condition of LY320135 then a net decrease of -127% was seen, this decrease in NICT shows a decrease in GABAergic signalling in response to LY320135+2-AG, the decrease in NICT between LY320135 and LY320135+2-AG periods was not significant ($P \leq 0.107$, KS ANOVA, n=6). **Fig 5.8D** represents the change in NICT with respect to a normalised control (black bar) and the other drug periods of the

experiment. The change in NICT during LY320135+2-AG application is represented by the grey bar.

5.5.3 AM-630 reverses the effects of 2-AG in layer V mEC.

AM-630 was added to the bath in addition to LY320135 and 2-AG to see if the effects of 2-AG could be reversed by this CB_2R specific antagonist in layer V.

During application of LY320135+2-AG+AM-630, the mean amplitude increased from 45.2 ± 3.2pA in LY320135+2-AG to 82.3 ± 4.0pA in LY320135+2-AG+AM-630 this increase in mean amplitude was highly significant ($P \leq 0.0001$, ANOVA). **Fig 5.8A** shows the cumulative probability plots for layer V sIPSC amplitude during the various drug periods through out the experiment. The LY320135+2-AG+AM-630 plot (light blue) shifts to the right of the LY320135+2-AG plot (grey). In addition to the right shift the LY320135+2-AG+AM-630 plot extends along the X axes beyond the point which the LY320135+2-AG plot stops. This shows that in LY320135+2-AG+AM-630 sIPSCs occur that have larger amplitudes than anything seen in LY320135 + 2-AG and this change in the distribution of sIPSC amplitude between control and LY320135+2-AG+AM-630 periods was significant ($P \leq 0.0001$, KS test).

The addition of AM-630 to LY320135+2-AG caused the mean median IEI in layer V to decrease from 1426.1 ± 75.74ms in LY320135+2-AG to160.5 ± 26.50ms in LY320135+2-AG+AM-630 this decrease in IEIs shows that an overall increase in sIPSC frequency occurred during LY320135+2-AG+AM-630 this increase was significant ($P \leq 0.0001$, ANOVA, n=6). **Fig 5.8B** shows the cumulative probability plot for sIPSCs IEIs during the various stages of the experiment. The LY320135 + 2-AG + AM-630 plot (light blue) lies to the right of the LY320135 + 2-AG plot (grey) showing higher probability of smaller IEIs during

LY320135+2-AG+AM-630 application, this change in IEI distribution between LY320135+2-AG and LY320135+2-AG+AM-630 periods was significant ($P \leq$ 0.0008 KS test).

Fig 5.8C shows the cumulative probability plots for sIPSC areas during the different stages of drug application. The LY320135 + 2-AG + AM-630 plot (light blue) shifts to the left of the LY320135+2-AG plot (light grey) the large gap between the two plot shows a marked change in the distribution of sIPSC areas occurs between the two drug periods, this is confirmed by a significant KS test ($P \leq 0.0001$). **Fig 5.8D** is the bar chart illustrating the changes in NICT during the different drug periods. During LY320135 + 2-AG + AM-630 application (light blue bar) NICT increased by 64.9 ± 54.3% of control. When the increase in NICT during LY320135+2-AG+AM-630 was compared to NICT for LY320135+2-AG (5.03 ± 22.99) then a net increase of 60% in GABAergic signalling is seen. However this increase in NICT was not significant ($P \geq 0.333$, ANOVA, n=6).

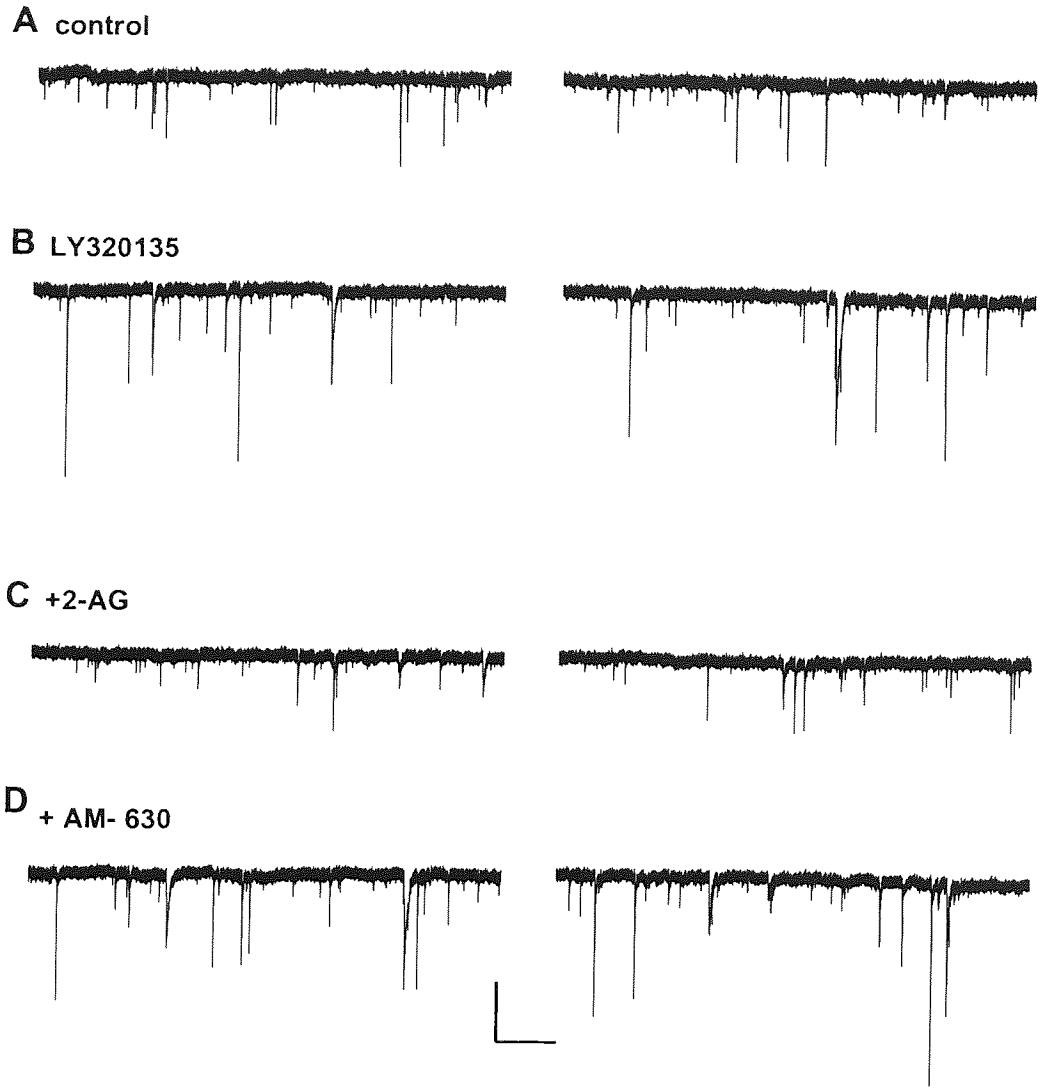

Fig 5.7 layer V sIPSCs during control and consecutive drug application periods
Layer V sIPSCs from a single layer II neurone, during **A.** Control, **B.** LY320135, **C.** LY320135+2-AG and **D.** LY320135+2-AG+ AM-630. LY320135 (500nM) 2-AG (500nM) AM-630 (50nM), Scale **X** 2000ms **Y** 100pA.

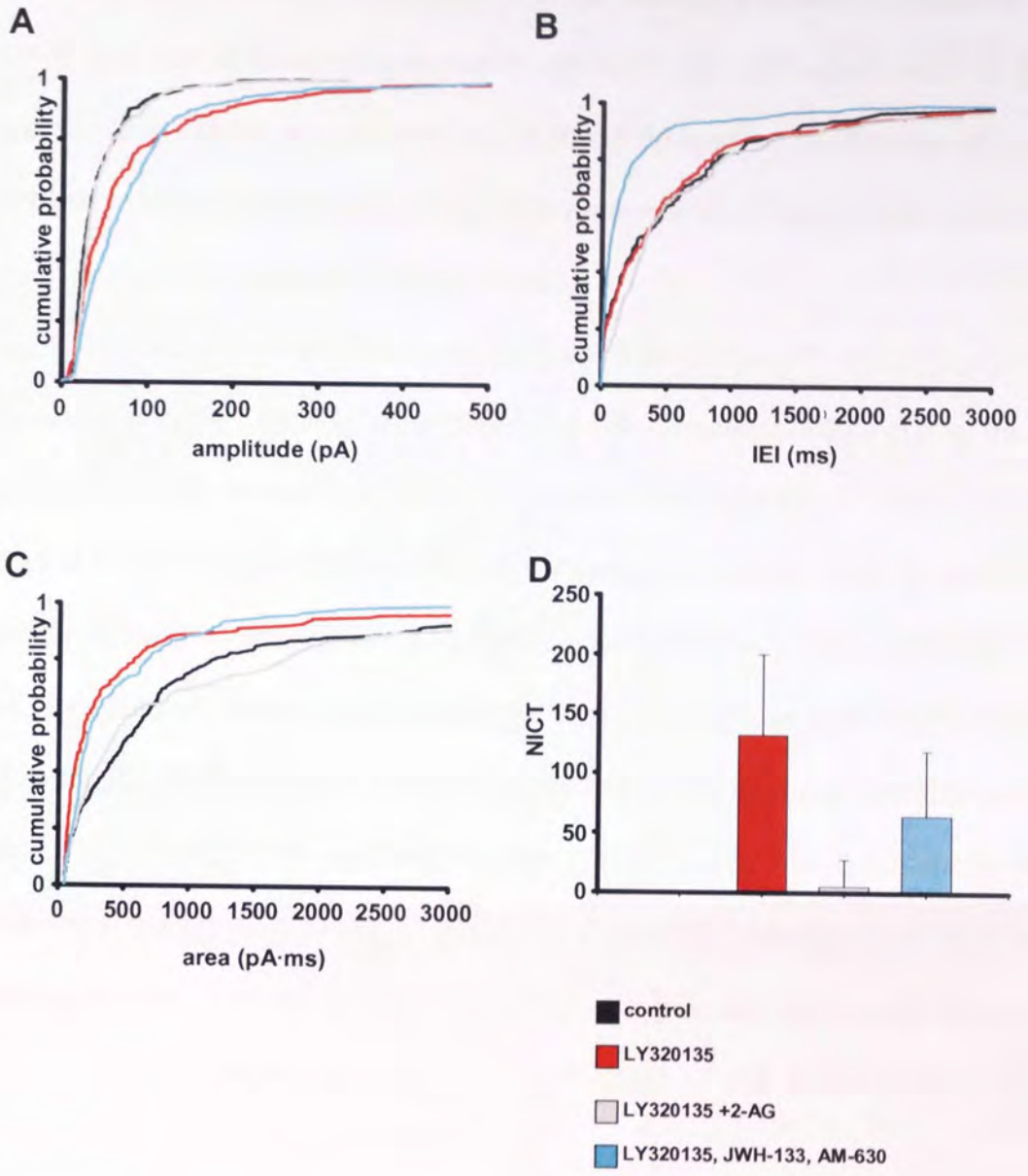

Fig 5. 8 Effects of LY320135, 2-AG and AM-630 on layer V sIPSCS
Cumulative probability plots (for layer V) for the different periods of drug application during the experiment **A.** Cumulative probability for amplitude **B.** Cumulative probability for IEIs, **C.** Cumulative probability for area. **D.** Illustrates the changes in NICT with respect to normalised control of 1 and the other drug periods. Pooled data n=6.

Having established that layer V mEC neurones show increases to both the CB_1R and CB_2R antagonists/inverse agonists and that application of the non-specific 2-AG (500nM) reversed the increase caused by application of LY320135 (500nM) alone. The next stage was to investigate the effects of the CB2R specific agonist JWH-133 (66nM), in place of 2-AG.

Fig 5.9 shows sIPSCs recorded from a single layer V mEC neurone during the various stages of drug application. **Fig 5.9 A** shows sIPSCs during the control period **Fig 5.9B** shows sIPSCs during LY320135 application when compared to control it can be seen that the number of larger amplitude sIPSCs has increased during LY320135 application. **Fig 5.9C** shows sIPSCs during LY320135 + JWH-133 application, during JWH-133 application the number and size of the larger amplitude sIPSCs appears reduced compared to the increase that had previously seen during LY320135 application (**Fig 5.9B).** Finally **Fig 5.9D** shows sIPSCs recorded during LY320135 (500nM) + JWH-133 (66nM) + AM-630 (50nM) application the number of larger amplitude sIPSCs has increased, showing that AM-630 has managed to reverse at least some of the suppression caused by LY320135 + JWH-133 application.

5.6 LY320135 increases sIPSC amplitude, frequency and NICT in layer V mEC

During application of LY320135 the mean amplitude of layer V sIPSCs rose from 47.0pA ± 3.0 to 87.9pA ± 7.4 pA This increase in amplitude was significant ($P \leq 0.0001$, ANOVA). **Fig 5.10A** shows the cumulative probability plots for layer V sIPSC amplitudes during the different stages of drug application. The LY320135 plot (red) shifts to the right of the control plot, (black).This right shift indicates that the probability of a sIPSC with amplitude between 0 and 300pA is lower in LY320135 than in control. In addition to the right shift the LY320135 plot continues

along the X axis past the 300pA point, whereas the control plot stops at around 300pA, indicating that in the control period no sIPSCs with a amplitude larger than 300pA occurred however in LY320135 sIPSCs occurred that had amplitudes larger that any seen in control. The change in sIPSC amplitude distribution between control and LY320135 application is significant ($P \leq 0.005$, KS test).

During LY320135 application the mean median IEI decreased from 477.1 ± 54.18ms in control to 300.0 ± 39.09ms in LY320135 showing that an overall increase in sIPSC frequency has occurred. The decrease in mean median IEI between control and LY320135 periods was significant ($P \leq 0.014$ ANOVA, n=7). **Fig 5.10B** plots the cumulative probability for the sIPSC IEIs during the different stages of drug application. The LY320135 plot (red) shifts to the left of the control plot (black) for IEI times that lie between 0ms and 2000ms this shows that the probability for the smaller IEI times is higher in LY320135 than in control. The increased probability of a smaller IEI in LY320135 suggests that a change in IEI distribution in layer V neurones occurs between control and LY320135, this change in distribution was significant ($P \leq 0.016$, KS test).

Fig 5.10C shows the cumulative probability plots for sIPSC areas during the different drug application periods. The LY320135 plot (red) shows no clear shift to the left or right of the control plot (black). From the graph it is hard to discern if any overall change in area distribution has occurred between control and LY320135 application. However the KS test gave a significant P of ≤ 0.02 showing that overall a change in distribution of sIPSC areas had occurred between control and LY320135 application. **Fig 5.10D** plots the changes in NICT during the different drug periods compared to a normalised control of 1 (black bar) and to the preceding drug application period. The red bar represents the increase in NICT in response to LY320135 application. NICT increased by 406.8 ± 170.2%

of control and this increase in GABAergic signalling was significant ($P \leq 0.034$ ANONA, n=7).

5.6.1 JWH-133 reverses the effects of LY320135 in layer V mEC.

Mirroring the previous experiments in layer II the next stage was to see if JWH-133 (the CB_2R specific agonist) had a similar effect on layer V sIPSCs as that caused by the non-specific CBR agonist 2-AG.

During LY20135+JWH-133 application the mean amplitude fell from 87.86 ± 7.37pA in LY320135 to 38.1pA ± 2.4 in LY320135 + JWH-133 this decrease in the mean amplitude highly significant ($P \leq 0.0001$, ANOVA n=7). **Fig 5.10A** shows the cumulative probability plots for layer V sIPSC amplitudes during the different stages of drug application. The LY320135 + JWH-133 plot (grey) shifts to the left of the LY320135 plot (red) indicating that for smaller amplitudes the probability is higher during LY320135 + JWH-133 application. In addition to this the LY320135 + JWH-133 plot stops at approximately 400pA while the LY 320135 plot continues beyond this point. This shows that during LY320135 + JWH-133 application no sIPSCs occurred with amplitude greater than 400pA. The change in sIPSC amplitude distribution was significant ($P \leq 0.0001$, KS test).

Fig 5.10B shows the cumulative probability plots for layer V sIPSC IEIs during the various stages of drug application. The LY320135 + JWH-133 plot (grey) remains intertwined with the LY320135 plot (red) for the entire plot the lack of a gap between the two plots shows no change in the distribution of IEIs has occurred this is confirmed by a non-significant KS test ($P \geq 0.761$). When we compare the mean median IEI times for LY320135 alone with that for LY320135 + JWH-133 then it can be seen that addition of JWH-133 has increased the mean median IEI, from 300.0 ± 39.09ms in LY320135 to 427.63 ± 43.39ms in LY320135

+ JWH-133 this increase in IEI times (and thus a decrease in sIPSC frequency) was not significant ($P \geq 0.896$, ANOVA, n=7). Thus, while JWH-133 did reverse some of the effects on frequency caused by LY320135 application it was not able to total overcome the LY320135 effects.

Fig 5.10C shows the cumulative probability plots for sIPSC areas in layer V during the various stages of drug application. The LY320135 + JWH-133 plot (grey) shows a large shift to the left of the LY320135 plot (red) this left shift shows a marked change in the distribution of sIPSC areas between the two drug periods, this change in distribution was significant ($P \leq 0.0001$, KS test). During LY320135+JWH-133 application NICT decreased by -19.67 ± 31.54% of control when this was compared to the increase in NICT seen during LY320135 application then a net decrease of 425% in GABAergic signalling occurred, this decrease was significant ($P \leq 0.03$, ANOVA, n=7). **Fig 5.10D** is a bar char illustrating the change in NICT compared to a normalised control of 1 (black bar) and to the other drug application periods. The decrease in NICT during LY320135 + JWH-133 is represented by the grey bar.

5.6.2 AM-630 reverses the effects of JWH-133 in layer V mEC

The final stage in this set of experiments in layer V was to see if application of the CB_2R antagonist AM-630 (50nM) could reverse the effects of JWH-133.

Fig 5.10A shows the cumulative probability plots for layer V sIPSC amplitudes during the various stages of drug application. The LY320135 + JWH-133+AM-630 plot (light blue) lies to the right of the LY320135 + JWH-133 plot (grey) further more while the LY320135 + JWH-133 plot stops at 400pA while the LY320135 + JWH-133 + AM-630 plot continues beyond this point showing that during LY320135 + JWH-133 + AM-630 sIPSC amplitudes increased beyond any

seen during LY320135 + JWH-133 application. The change in sIPSC amplitude distribution between LY320135 + JWH-133 and LY320135 + JWH-133 + AM-630 application was highly significant ($P \leq 0.0001$, KS test). When the mean sIPSC amplitudes were compared it was found that they increased from 38.09 ± 0.36pA in LY320135 + JWH-133 to 80.0 ± 7.2 pA during LY320135 + JWH-133 + AM-630 application, this increase in amplitude was highly significant ($P \leq 0.0001$, ANOVA, n=7)

Fig 5.10B shows the cumulative probability plot for layer V IEIs. The LY320135+JWH-133+AM-630 plot (light blue) does not appear to make a clear shift away from the LY320135+JWH-133 plot (grey) this lack of difference in IEI distribution between the two drug periods is confirmed by a non-significant KS test ($P \geq 0.402$). The mean median IEI was found to decrease from 427.6± 43.39ms in LY320135+JWH-133 to 211.5ms ± 37.76ms during LY320135+JWH-133+AM-630 application. This decrease was not significant ($P \geq 0.692$, ANOVA n=7).

Fig5.10C shows the cumulative probability plot for layer V sIPSC areas. The LY320135 + JWH-133 + AM-630 plot (light blue) lies to the right of the LY320135 + JWH-133 plot (grey) the marked gap between the two plots shows a change in sIPSC area distribution has occurred between the LY320135 + JWH-133 and LY320135 + JWH-133 + AM-630 periods, this change in distribution was significant ($P \leq 0.0001$, KS test). During LY320135+JWH-133+AM-630 application NICT increased by 172.5 ± 83.1% of control. When NICT for LY320135 + JWH-133 was compared to NICT for LY320135 + JWH-133 + AM-630 then a net increase of 190% occurred. This increase in NICT and thus GABAergic signalling was significant ($P \leq 0.05$, ANOVA, n=7). **Fig 5.10D** illustrates the changes in NICT during the different stages of drug application the increase in NICT during LY320135+JWH-133+AM-630 is illustrated by the light blue bar. AM-630 was not

able to return NICT to the level achieved when LY320135 was applied to the layer V neurones alone. This suggests that in this set of experiments AM-630 could overcome some but not all of the effects of JWH-133.

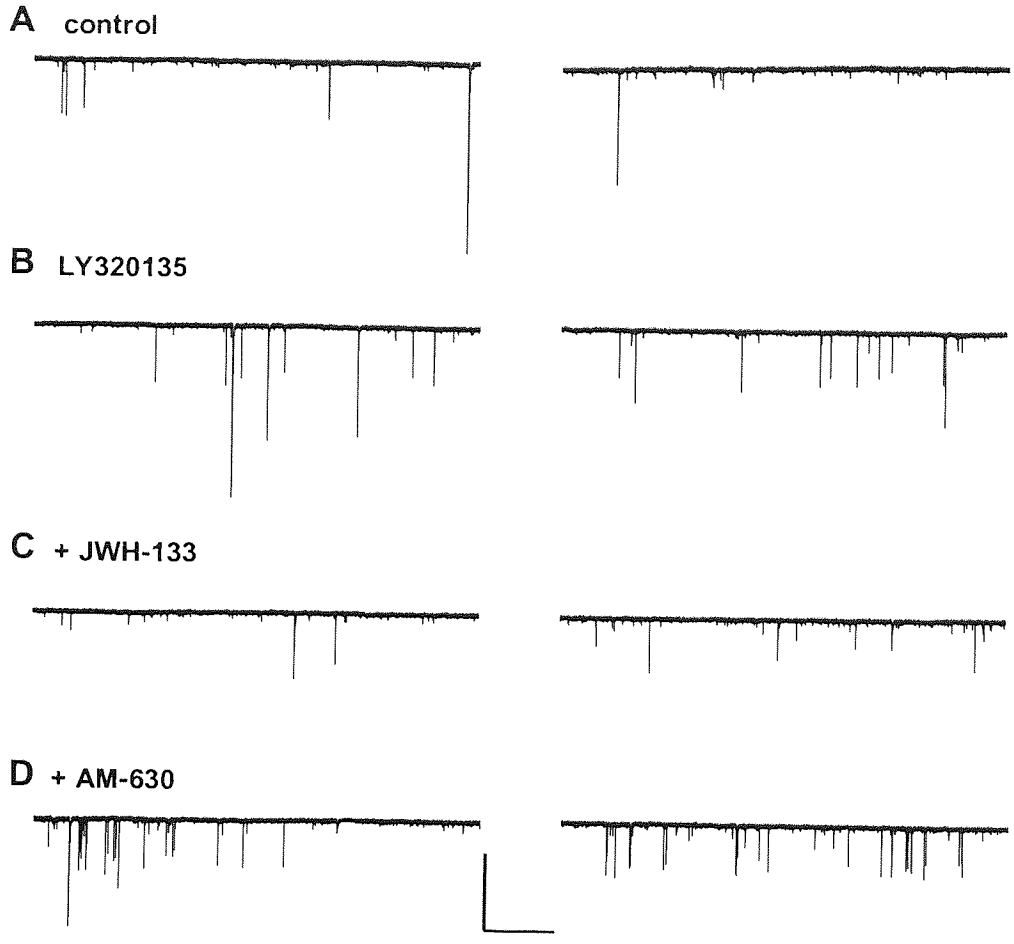

Fig 5.9 Effects of LY320135, JWH-133 and AM-630 on layer V sIPSCs
Layer V sIPSCs from a single layer II neurone, during **A.** Control, **B.** LY320135, **C.** LY320135 + JWH-133, and **D.** LY320135 + JWH-133 + AM-630 + LY320135 (500nM) JWH-133 (66nM) AM-630 (50nM) Scale **X** 2000ms **Y** 500pA.

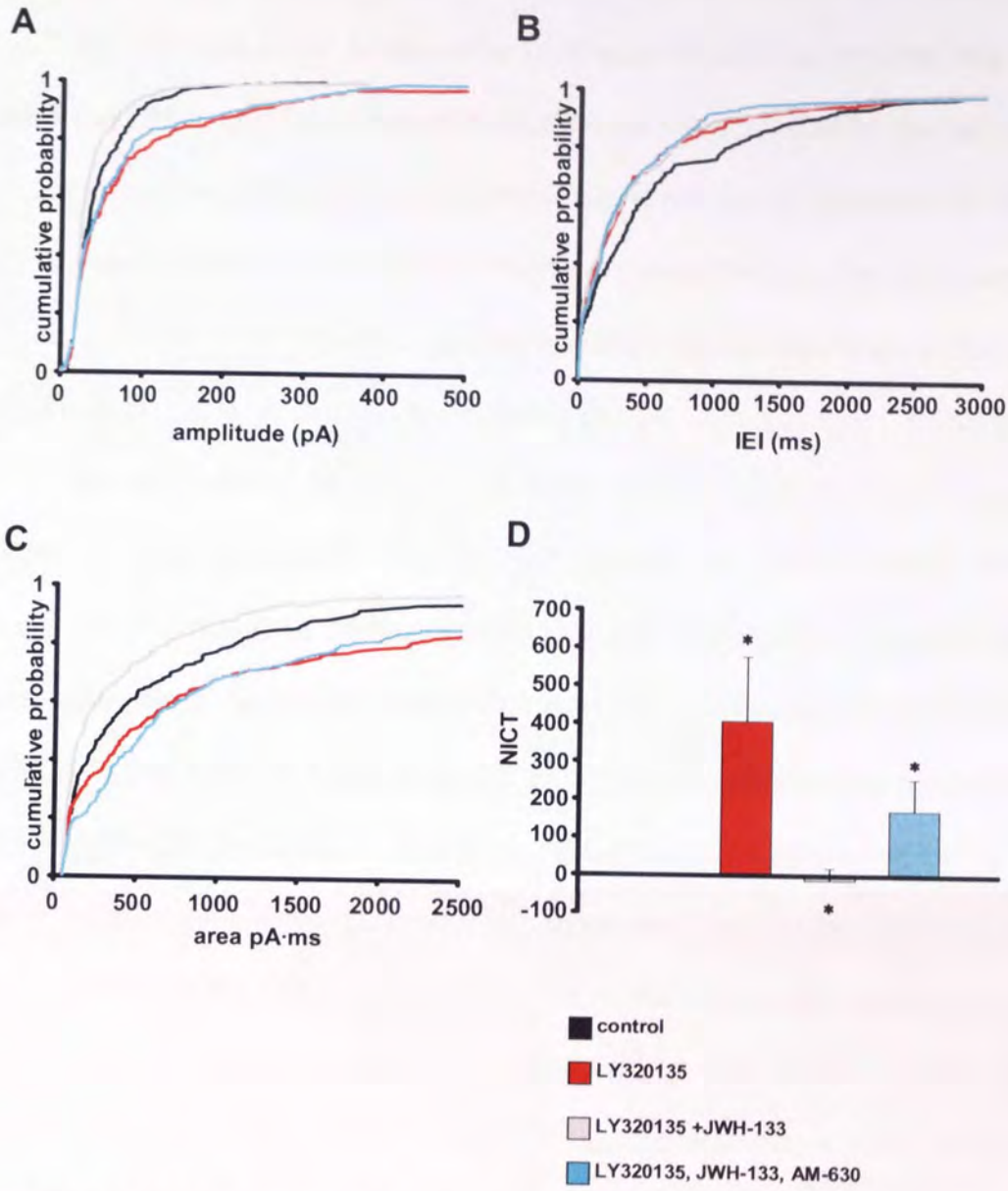

Fig 5. 10 Effects of LY320135, JWH-133 and AM-630 on layer V sIPSC kinetics
Cumulative probability plots for layer V for the different periods of drug application during the experiment **A.** Cumulative probability for amplitude **B.** Cumulative probability for IEIs, **C.** Cumulative probability for area. **D.** Illustrates the changes in NICT with respect to a normalised control of 1 and the other drug periods pooled data n= 7. LY320135 (500nM) JWH-133 (66nM) AM-630 (50nM). * $P \leq 0.05$

5.7 Effects of the CBR ligands are not due to the order of application.

As with the layer II experiments it was decided to reverse the order in which the CB_2R and CB_1R specific antagonists were applied to the slice in order to check that the effects described above were not due to the order in which the drugs were applied to the slices. For these experiments the first cannabinoid added was the CB2R specific agonist AM-630(100nM) this was followed by the CB_2R specific agonist JWH-133 and finally the CB1R antagonist LY320135.

Fig 5.11 shows sIPSCs from a single layer II neurone during the different stages of drug application. **Fig 5.11A** illustrates the control period. **Fig 5.11B** shows sIPSCs recorded during AM-630 (100nM) application, compared to control there appears to be an increase in the size and number of the larger amplitude sIPSCs during AM-630 application. **Fig 5.11C** shows sIPSCs recorded during AM-630 + JWH-133 application. There appears to be little difference in the sIPSCs recorded during this period compared to those recorded during application of AM-630 alone, indicating that adding JWH-133 to the slice in the presence of a AM-630 blocks the effects of JWH-133. Finally **Fig 5.11D** shows sIPSCs recorded during AM-630 + JWH-133 + LY320135 application the number of the larger amplitude sIPSCs appears to have increased even further in response to LY320135.

5.7.1 AM-630 increases sIPSC amplitude and NICT in layer V mEC

Fig 5.12A shows the cumulative probability plots for sIPSC amplitudes The AM-630 (100nM) plot (light blue) lies to the right of control indicating a lower probability of sIPSCs with lower amplitudes occurring during AM-630 application in addition to this the AM-630 plot extends beyond the point on the X axis where the control plot stops showing that during AM-630 application sIPSCs with amplitudes larger than any seen in control occur, these changes in sIPSC

amplitude distribution between control and AM-630 application were significant ($P \leq 0.0003$, KS test). The changes in distribution point towards larger amplitude sIPSCs occurring during AM-630 application this was shown to be the case with the mean amplitude increasing from 50.67 ± 3.71pA in control to 72.31 ± 4.91pA in AM-630 this increase in amplitude was significant ($P \leq 0.0008$, ANOVA, n=7).

Fig 5.12B shows the cumulative probability plot for layer V sIPSC IEIs. The AM-630 plot (light blue) shows no clear shift to the left or the right of the control plot (black) this shows no change in IEI distribution has occurred, the lack of change is confirmed by a non-significant KS test ($P \geq 0.216$). When the mean median IEI times were compared it was found to have decreased from 1149.0 ± 68.98ms to 367.7 ± 50.49ms this decrease in IEI time was not significant ($P \geq 0.255$, ANOVA, n=7).

Fig 5.12C shows the cumulative probability plot for sIPSC areas in layer V. The AM-630 plot (light blue) lies to the right of the control plot for the entire graph this change in distribution was significant ($P \leq 0.22$, KS test). When NICT was calculated it was found to increase by 71.63 ± 16.5% of control showing an increase in GABAergic signalling during AM-630 application, this increase in NICT was significant ($P \leq 0.001$, ANOVA, n=7). The increase in NICT compared to a normalised control (black bar) and the other drug periods in the experiment are illustrated in **Fig 5.12D** the increase in NICT during AM-630 application is shown by the light blue bar.

5.7.2 CB_2R agonist JWH-133 has no effect in the presence of 100nM AM-630

Next the CB_2R agonist JWH-133 (66nM) was applied to the slices in addition to the already present CB_2R antagonist AM-630, this allowed us to investigate whether the effects of the CB_2R agonist could be blocked if it was

applied after the antagonist at a higher concentration than used in layer II where only a partial block of JWH-133 was seen when AM-630 was applied at 50nM).

Fig 5.12A shows the cumulative probability plots for layer V sIPSC amplitude The AM-630 + JWH-133 plot (grey) lies to the lift of the AM-630 plot (light blue) this left shift indicates a change in sIPSC amplitude distribution towards slightly smaller amplitudes during AM-630 + JWH-133 application compared to AM-630 alone, this change in distribution was significant ($P \leq 0.0003$ KS test). The mean amplitude showed a decrease during AM-630+JWH-133 application from 72.31 ± 4.91pA in AM-630 to 55.83 ± 3.89pA in AM-630+JWH-133 this decrease was significant ($P \leq 0.003$, ANOVA, N=7).

Fig 5.12B shows the cumulative probability for layer V sIPSC IEIs. The AM-630+JWH-133 plot (grey) lies directly next to the AM-630 plot (light blue) showing no change in IEI distribution occurred, however a KS test showed that a significant change in IEI distribution did occur ($P \leq 0.004$ KS test). When the mean median IEIs for AM-630 + JWH-133 was compared to AM-630 alone then a increase was seen to occur from 367.72 ± 50.49ms in AM-630 to 842.56 ± 53.434ms in AM-630+JWH-133. However this increase was not significant ($P \geq 0.353$, ANOVA, N=7)

Fig 5.12C Plots the cumulative probability for layer V sIPSC areas. The AM-630 + JWH-133 plot (grey) shows a shift to the right of control for lower amplitude sIPSCs indicating that there is a shift towards larger sIPSC areas during AM-630 + JWH-133 application the change in distribution is confirmed by a significant KS test ($P \leq 0.0001$). During AM-630+JWH-133 application NICT increased by 114.31 ± 39.36% of control, this increase in NICT shows that an overall increase in GABAergic signalling has occurred during AM-630+JWH-133 application. When compared to AM-630 alone then a net increase in NICT and

thus GABAergic signalling of 40% is seen the increase in NICT between AM-630 and AM-630+JWH-133 is not significant ($P \geq 0.338$, ANOVA n=7). However, this is not surprising as NICT is increasing which indicates that JWH-133 has not been able to suppress GABAergic signalling in the presence of the increased concentration of AM-630. **Fig 5.12D** illustrates changes in NICT AM-630+JWH-133 application (grey bar) compared to control and the other drug periods of the experiment.

5.7.3 LY 320135 increases amplitude and NICT in the presence of AM-630 and JWH-133 in layer V mEC.

To complete the reversed drug protocol LY320135 (500nM) was added to the slice in addition to AM-630 (100nM) and JWH-133 (66nM).

Fig 5.12A shows the cumulative probability for sIPSC amplitudes. The AM630 + JWH-133 + LY320135 plot (red) lies to the right of the AM-630 + JWH-133 plot (grey) for the lower amplitudes in addition to a decreased probability of small amplitude sIPSCs during AM-630 + JWH-133 + LY320135. The AM-630 + JWH-133 + LY320135 plot extends beyond 350pA while the AM-630 + JWH-133 plot stops at this point. These changes show that during AM-630 + JWH-133 + LY320135 there is a change in sIPSC amplitude distribution towards large amplitude sIPSCs this change in distribution was significant ($P \leq 0.0004$, KS test). The mean amplitude increased from 55.83 ± 3.89 pA in LY320135+JWH-133 to 86.72 ± 6.58 pA in AM-630 + JWH-133 + LY320135. This increase was significant ($P \leq 0.0004$).

Fig 5.12B shows the cumulative probability for layer V sIPSC IEIs. The AM-630 + JWH-133 + LY320135 plot (red) lies on top of the AM-630 + JWH-133 plot (grey) showing no change in IEI distribution occurred between these two drug

periods this was confirmed by a non-significant KS test ($P \geq 0.887$ n=7). The mean median IEI showed a decrease during AM-630 + JWH-133 + LY320135 application going from 842.56 ± 53.43ms in AM-630 + JWH-133 to 316.11 ± 41.24ms this decrease in IEI was not significant ($P \geq 0.358$, ANOVA, N=7).

Fig 5.12.C shows the cumulative probability for layer V sIPSC areas the AM-630+JWH-133+LY320135 plot (red) shifts to the right of the AM-630+JWH-133 (grey plot) the gap between the two plots remains for the duration of the plot showing a marked change in sIPSC area distribution occurs between the AM-630 + JWH-133 and AM-630 + JWH-133 + LY320135 periods this is confirmed by a significant KS test ($P \leq 0.005$, KS test). NICT increased by 279.40 ± 160.79 % of control, there was a net increase in NICT of 165% between AM-630+JWH-133 and AM-630 + JWH-133 + LY320135 periods, showing an increase in GABAergic signalling, this increase was not significant (probably due to the trend towards increases in NICT throughout all the drug application periods). **Fig 5.12D** illustrates the changes in NICT during the different drug periods compared with control and with each other, the increase in NICT during AM-630 + JWH-133 + LY320135 application is represented by the red bar.

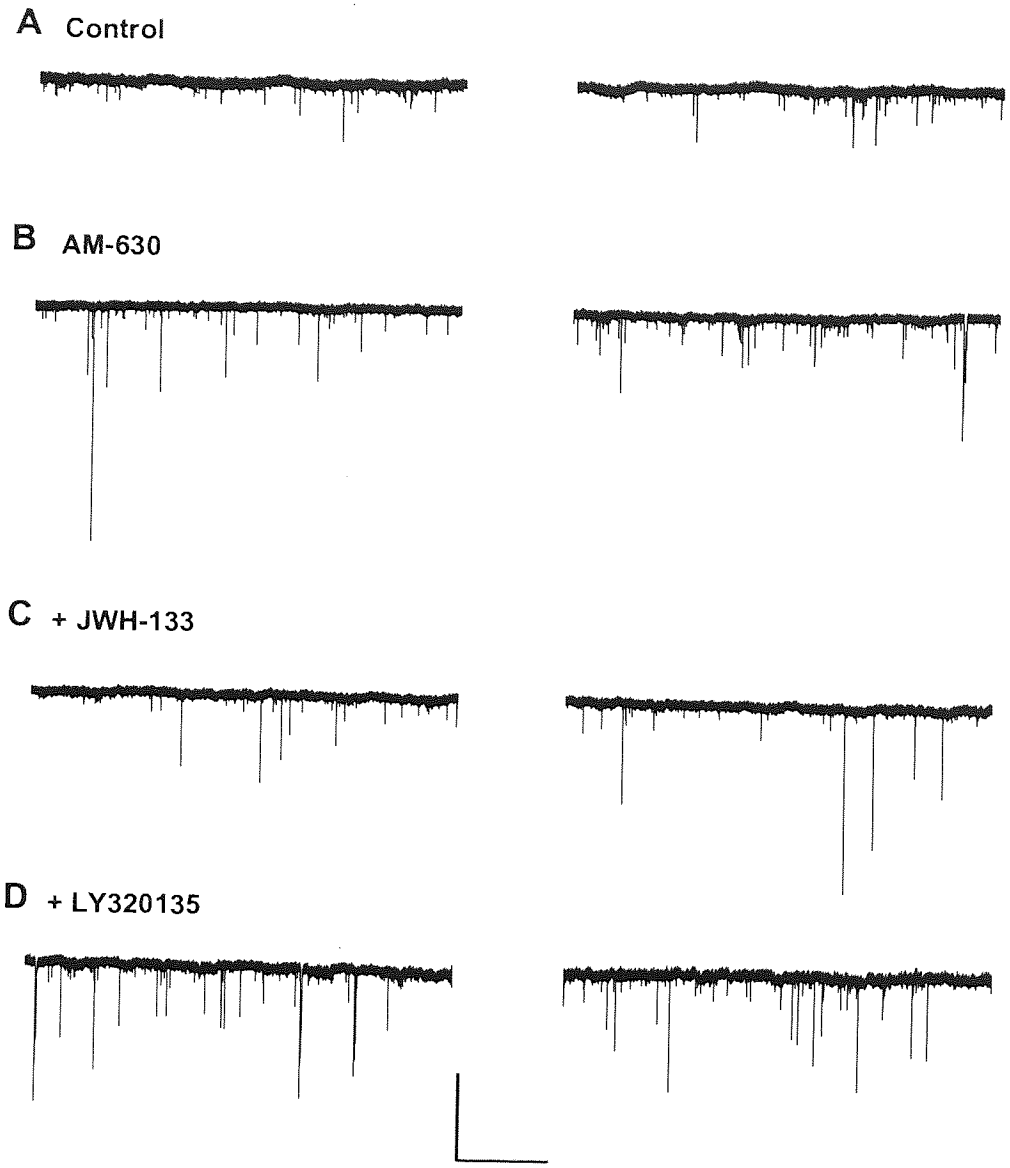

Fig 5.11 layer V sIPSCs during control and consecutive drug application periods
Layer V sIPSCs from a single layer II neurone, during **A.** Control, **B.** AM-630 **C.** AM630+JWH-133 and **D.** AM-630+JWH-133+ LY320135. AM-630 (100nM) JWH-133 (66nM) LY320135 (500nM) Scale **X** 20000ms **Y** 200pA.

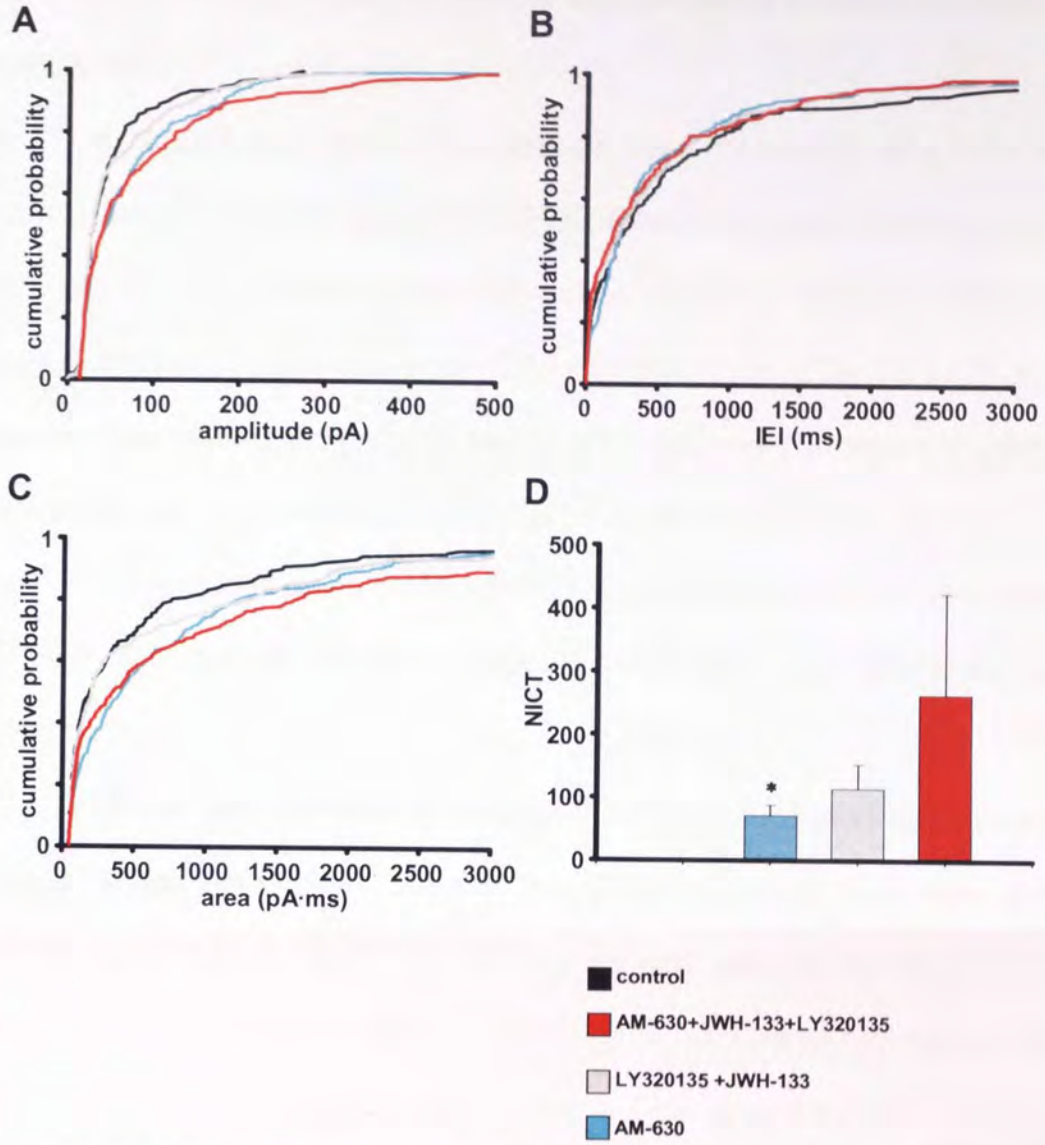

Fig 5.12 Effects of AM-630, JWH-133 and LY320135 on layer V sIPSC kinetics
Cumulative probability plots for layer V for the different periods of drug application during the experiment **A.** Cumulative probability for amplitude **B.** Cumulative probability for IEIs, **C.** Cumulative probability for area. **D.** Illustrates the changes in NICT with respect to normalised control of 1 and the other drug periods. Pooled data N= 7. AM-630 (100nM), JWH-133 (66nM), LY320135 (500nM). * $P \leq 0.05$

5.8 JTE-907 a CB_2R selective inverse agonist alters GABAergic signalling in layer II mEC.

As there were various possibilities open to explain why both a CB_2R agonist and antagonist modulated sIPSC frequency and amplitude and overall inhibitory charge transfer it was decided to see what affects a different CB_2R antagonist would have on layer II sIPSCs in p30 slices. JTE-907 a CB_2R specific inverse agonist/antagonist was selected. JTE-907 was chosen as it belongs to a different group of cannabinoid ligands, and its structure is very different to that of AM-630. This should mean that if AM-630 is acting at a receptor other than a CB_2 JTE-907 is unlikely to be able to interact in the same way due to its structural differences.

JTE-907 was identified as a novel CB_2R receptor ligand by Iwamura *et al.*, (2001). These researchers showed that JTE-907 bound to human and mice CB_2Rs expressed in CHO cell membranes and also to CB_2Rs found on rat splenocytes. The Ki for rat CB_2Rs was found to be 0.38nM furthermore Iwamura *et al.*, (2001) showed that JTE-907 had a high selectivity ratio for rat CB_2R compared to rat CB_1R when these receptors were expressed in CHO cells. The inverse agonist/antagonist properties of JTE-907 were shown when its effects on forskolin-stimulated cAMP production in CHO cells expressing CB_2Rs were investigated. Iwamura *et al* 2001 showed that JTE-907 increased cAMP production while the CB agonist WIN 55,2-212 decreased cAMP production.

Fig 5.13 A&B is sIPSCs recorded from a single P30 layer II neurone during **(A)** control and **(B)** JTE-907(1nM) periods. The control period has the frequent sIPSCs already described as characteristic in layer II that are interspersed with much larger amplitude sIPSCs. In JTE-907 traces it is clear that the number of the large amplitude events has increased in frequency but from the traces alone it is hard to comment whether a change in frequency has occurred.

Fig 5.14A is the cumulative probability plot for sIPSC amplitude during control (black) and JTE-907(purple) periods. The JTE-907 plot lies to the right of control suggesting a lower probability of the sIPSCs with small amplitudes. This change in distribution of sIPSC amplitudes was significant ($P \leq 0.026$, KS test) The mean amplitude increased from 61.82 ± 4.03pA on control to 86.70 ±6.77pA this increase in sIPSC amplitudes was significant ($P \leq 0.002$, ANOVA n=5).

Fig 5.14 B shows the cumulative probability plot for sIPSC IEIs during control (black) and JTE-907 (purple) periods. The JTE-907 plot lies to the right of control for showing an overall increase in IEI times during JTE-907 application, which shows that a decrease in frequency has occurred. This change in distribution of sIPSC IEIs is just significant ($P \leq 0.05$, KS test, n=5). However when the mean median IEI times was compared it was found to have increased from 57.43 ± 2.60ms to 63.74 ± 3.11ms this increase in IEI was significant ($P \geq 0.002$, ANOVA n=5).

Fig 5.14 C shows the cumulative probability plot for sIPSC area in control (black) and JTE-907 (1nM; purple) periods. The JTE-907 plot lies to the right of the control plot for the duration of the graph showing that a change in area distribution has occurred. This change in distribution was very significant ($P \leq 0.0005$, KS test). In addition to the change in distribution of sIPSC areas when NICT was calculated to was found to increase to 119.86 ± 77.98% of control, however due to the variance this increase was not significant ($P \geq 0.166$, ANOVA n=5). The overall increase in NICT compared to control is illustrated in **Fig 14 D** which plots NICT in control (black bar) and in JTE-907 (purple bar).

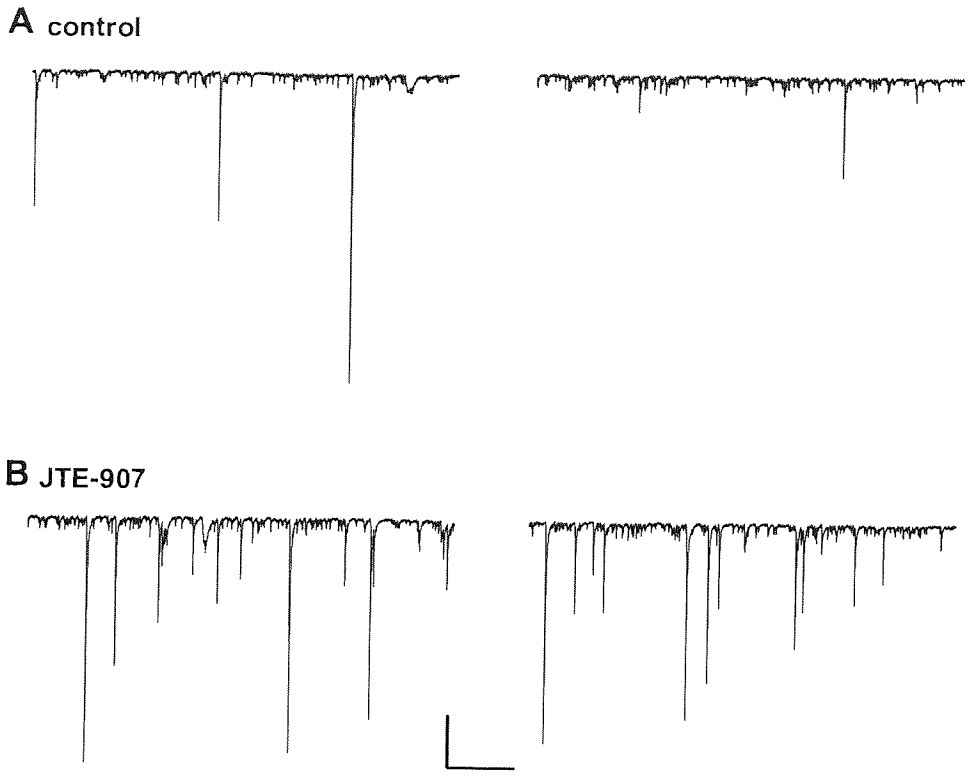

Fig 5.13 Example layer II sIPSCs in control and JTE 907
Layer II sIPSCs from a single layer II neurone, during **A**. Control, and **B.** JTE-907(1nM) Scale **X** 1000ms **Y** 500pA.

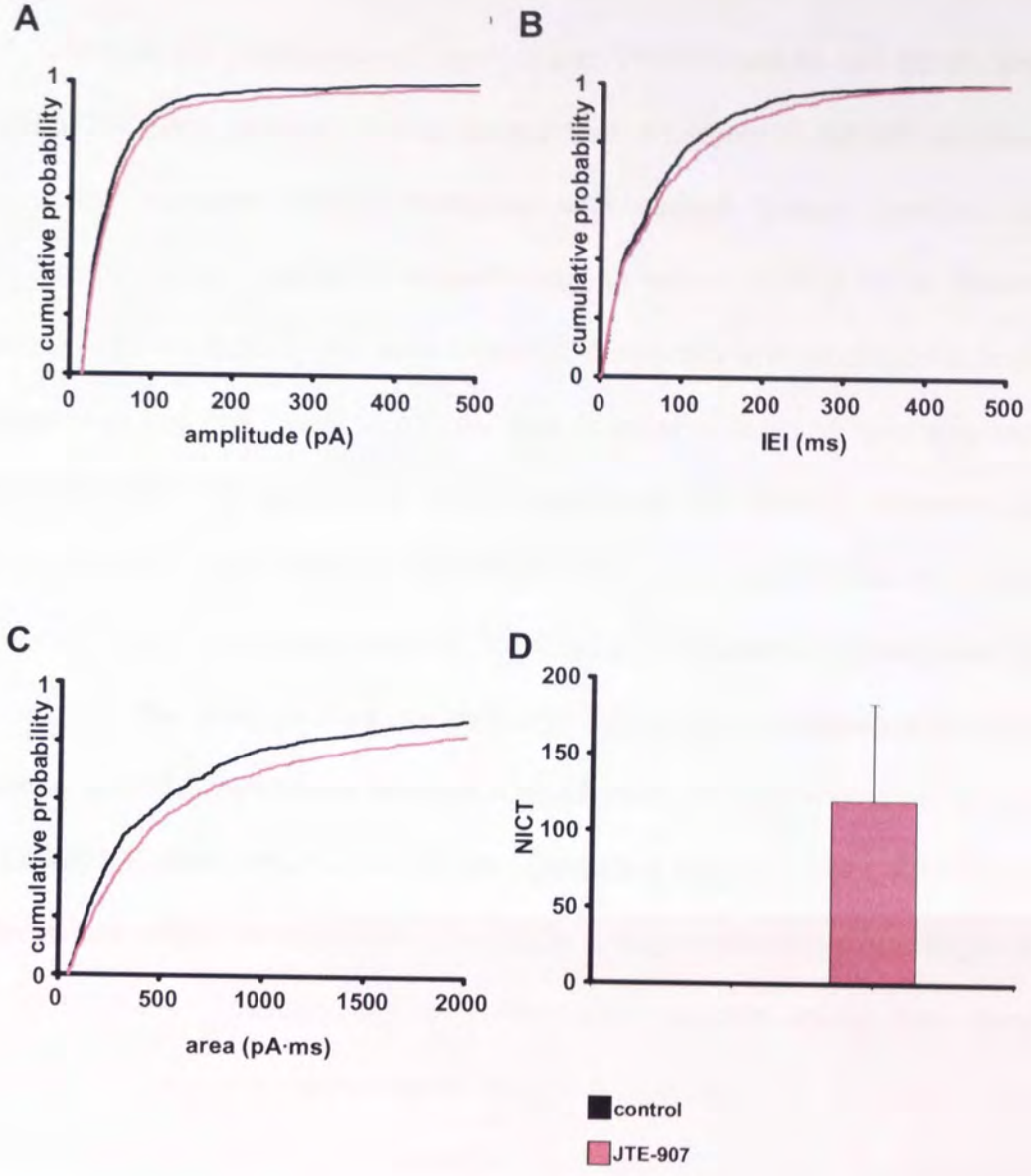

Fig 5. 14 Effects of JTE-907 on layer II sIPSCs
A. Cumulative probability for layer II sIPSC amplitudes, during control and JTE 907(1nM) periods. **B.** Cumulative probability sIPSC IEIs during control and JTE-907 periods. **C.** Cumulative probability sIPSC areas during different stages of the experiment. **D.** Bar chart, showing changes in NICT with respect to normalised control of 1. **A-D** pooled data, n=5.

5.9 Discussion.

When the responses of layer II and V neurones to the CB1R antagonist LY320135 were studied, it was found that changes in sIPSC amplitude and frequency occurred. When compared with control, these changes were not significant in every series of experiments, in either layer II or V. However, an overall trend towards an increase in sIPSC frequency and amplitude in both layers II and V of the mEC was apparent, and at least in layer V, this was significant when all LY320135 recordings were pooled (data not shown). However, the most consistent and clear effect of LY320135 in layers II and V was to increase the inhibitory charge transfer (NICT). As already discussed, an increase in NICT shows that the total amount of GABA signalling has increased. This makes the change in inhibitory charge transfer a much more reliable indicator of the effects of LY320135 than amplitude and IEIs. Overall, it appears that LY320135 has the effects that might be expected of a CB_1R antagonist/inverse agonist, increasing GABA-mediated inhibition in the postsynaptic neurone, rather than decreasing inhibition as has been demonstrated for CB_1R agonists.

When we applied a non-specific CBR agonist or a specific agonist at CB_2R in the presence of LY320135, we observed suppression of GABAergic inhibitory signalling, even whilst CB_1R were blocked. Application of 2-AG (500nM) (K_i CB_1 472nM, K_i CB_2 1400nM), in the presence of the CB_1R antagonist LY320135 should have had little or no effect on layer II or V sIPSCs and inhibitory charge transfer. Hajos *et al.,* (2001) show that the CB_1R antagonist SR141716A totally blocks the effects of WIN 55,212-2 while Hentges *et al.,* (2005) and showed that the CB_1R antagonist AM-251 blocked the effects of continuously released endocannabinoids in hypothalamic propiomelanocortin (POMC) neurones, and Kreitzer and Regehr (2001) showed AM-251 blocked DSI. These data indicate that in other situations, CB_1R antagonists can completely block the effects of

CB_1R agonists. In the current experiments, application of 2-AG to the bath in addition to LY320135 decreased inhibitory charge transfer in both layer II and V of the mEC. As 2-AG was added at a concentration just above the K_i for CB_1Rs, and LY320135 was present at 3 x its K_i value, it seems unlikely that 2-AG was out-competing LY320135 at the CB_1R itself. We hypothesised that 2-AG was acting at CB2 type receptors, and this seems to be supported by our data showing that in both layers II and V, the CB_2R-specific agonist JWH-133 mimicked the effects of 2-AG, and in both cases, this was reversed by the CB_2R-specific antagonist AM-630. When we reversed the experiments, using AM-630 alone, we saw significant increases in GABAergic activity. In layer II, AM-630 did not prevent the effects of JWH-133, but in layer V (at a higher dose of AM-630) JWH-133 was ineffective in decreasing GABAergic signalling when AM-630 was pre-applied. In addition to these data, a novel, selective CB2R antagonist/inverse agonist, JTE907 also increased GABAergic signalling in layer II. Taken together, these data indicate that CB2R-like response can be found in both layers of the mEC, using a variety of specific and selective ligands, and as such, this is the first report of CB_2R-mediated effects on inhibitory function in the CNS.

It is possible that the effects of 2-AG and JWH-133 were due to actions at non-receptor sites. 2-AG, along with other endogenous cannabinoids such as AEA, has been shown to have a range of non-CBR specific effects. For example, in addition to interacting with CB_1R and CB_2Rs it has been shown endogenous cannabinoids can modulate properties of voltage-gated ion channels such as calcium, sodium and potassium channels. In addition to this, endogenous cannabinoids have also been shown to interact with ligand-gated ion channels such as nicotinic acetylcholine receptors, glycine receptors and ionotropic glutamate receptors. For a full review of non-CBR effects of the endogenous cannabinoids see (Oz, 2006). However, non-CBR effects have not been clearly

demonstrated for synthetic cannabinoids, and given that the effects we have described are repeatable using a variety of structurally dissimilar agents, and are reversible using specific antagonists, it seems unlikely that non-receptor effects can account fully for our data.

Apart from non-receptor specific affects of endogenous cannabinoids another site of action for 2-AG is a putative novel (CB_3) cannabinoid receptor. Hajos *et al.,* (2001) and Breivogel *et al.,* (2001) have reported evidence in the brain for a non-CB_1 non-CB_2 cannabinoid receptor to be present, using CB1R knockout mice and immunocytochemistry for CBRs. More recently, one possible candidate for the role of a new cannabinoid receptor is the orphan receptor GPR55. Baker *et al.,* (2006) first promoted GPR55 as a potential cannabinoid receptor and Ryberg *et al.,* (2007) confirmed that GPR55 is a G-protein coupled receptor, and that it responds to cannabinoids. Interestingly while GPR55 showed binding and responses to some cannabinoids it did not respond to WIN 55,212-2 and when the response of GPR55 to AM-251 (a CB_1R antagonist) was tested, it was found to behave as an agonist.

While Ryberg *et al.,* (2007) have strongly suggested that GPR55 is novel cannabinoid receptor, it is unlikely that that it is responsible for the effects we see in these experiments, although GPR55 does respond to 2-AG there is no evidence to suggest that it is also capable of being activated by the CB_2R specific ligands JWH-133 and AM-630, or that it has other pharmacological properties in common with the CB2R. In addition to this, the presence of GPR55 would not explain the dual effects seen in layer II of the mEC (Chapter 3). According to Ryberg *et al.,* (2007), GPR55 shows no response to WIN 55, 212-2, and while both Hajos *et al.,* (2001) and Breivogel *et al.,* (2001) show that there is a potential novel CB receptor in the hippocampus, the receptor they identified responded to

WIN 55, 212.-2. This would suggest that they are as yet unidentified cannabinoid receptors in the CNS, or that CB_2R are indeed present.

While it is possible that the results presented here can be explained by non-receptor specific effects of the CB_2R ligands or that the CB_2R ligands are acting at an as yet unidentified receptor, this researcher would argue that when the literature is considered together with the data above, they point to a CB_2R like receptor being present within the mEC of the rat.

The presence of CB_2Rs with in the immune system is well documented with CB_2R mRNA being found in immune tissue such as the spleen and bone marrow; CB_2Rs are also expressed by many immune specific cells (see Cabral & Dove-Pettit 1998 for a full review). However their presence in the CNS has always been debated. While various immunohistochemical and autoradioagraphical studies (such as the work of Tsou *et al.,* 1988 and Glass *et al.,* 1997) have been done that show the presence of CB_1Rs in the CNS, no such studies showing CB_2Rs in the CNS existed, moreover researchers such as Schatz *et al.,* (1997) and Griffin *et al.,* (1999) have been unable to show the presence of CB_2Rs in the CNS, and thus it was concluded that CB_2Rs were not present in the CNS. However in more recent years the development of more specific CB_2R antibodies has led to the discovery of functional CB_2R on neurones of the brain stem (Van Sickle *et al.,* 2005). In 2006 Gong *et al.,* produced the first immunohistochemical evidence for CB_2R expression in the rat brain, using a combination of RT-PCR and immunohistochemical techniques. These researchers showed that not only is CB_2R mRNA in the rat brain but that CB_2Rs are expressed on neurone cell bodies and process through out the brain. The work of Gong *et al.,* (2006) is supported by the *in vivo* work of Onaivi *et al.,* 2006, who showed that the CB_2R agonist JWH-015 caused a decrease in locomotor activity in mice and also had affects on behaviour, which the researchers argued showed a functional role for CB_2Rs.

CB_2Rs have also been shown to be expressed on microglia and astroglia cells in Down's syndrome (Núñez *et al.,* 2007). CB_2Rs have also been shown to be expressed in disease states such as Alzheimer's disease where (Benito *et al.,* 2003) where the glial cells associated with the neuritic plaques express CB_2Rs. CB_2Rs have also been shown to be expressed in certain types of brain tumour Miklaszewska *et al.,* 2007 showed that adult and paediatric malignant gliomas express CB_2Rs.

Further evidence to support the argument that the CBR ligands used in these experiments were acting at a receptor as opposed to having non-specific receptor effects is the low concentrations of the receptor specific ligands used, most notably the 1nM JTE-907 that still caused an increase in GABAergic signalling in layer II. Furthermore, when AM-630 was increase to 100nM in layer V application of JWH-133 (66nM) failed to suppress GABAergic signalling. The fact that the effects of JWH-133 could be over by prior application of AM-630 suggests that this two cannabinoid ligands are acting at the same site, rather than having more random non-receptor specific effects.

3.9.1 Future Work

While the data presented here presents a strong argument for pharmacological evidence of CB_2Rs in both deep and superficial layers of the mEC further work can still be done to confirm the data. This researcher recommends: 1. carrying out immunohistochemical studies using species specific CB_2R antibodies. To see if CB_2Rs staining can specifically be identified in the mEC and if so if the CB_2Rs are located on a specific sub-set of synapse and to what level they show co-localisation with CB_1Rs. 2. Repeating the reversed drug protocol in layer II this time using AM-630 at 100nM to see if it can block all the effects of JWH-133, and 3. Investigating the effects of these receptor specific

ligands in terms of a more physiological role by seeing if they are capable of altering network activity by studying their effects on oscillations in both deep and superficial layers of the mEC.

Chapter 6
Differential effects of CB_1R and CB_2R activity on network oscillations in deep and superficial layers of the mEC.

6.1 Introduction

Up to this point, this thesis has considered cannabinoid receptor mediated modulation of inhibitory function at the level of synapses and individual IPSCs. However, while this is an indicator of receptor function, it does not reflect more physiologically relevant neuronal activity in the CNS, for example neuronal network activity. We decided to investigate the functional effects of CBRs on neuronal network activity modelled *in vitro* by kainate (KA) induced persistent oscillations (Whittington *et al.,* 1995). Persistent oscillatory activity in the gamma frequency band (30-80 Hz) has been the most commonly reported and studied form of network activity in the *in vitro* slice preparation, and can be elicited by metabotropic glutamate receptors (Whittington et al., 1995) or application of kainic acid (Hajos *et al.,* 2000; Hormuszdi *et al.,* 2001) and/or the muscarinic agonist carbachol (Fisahn *et al.,* 1998). Neuronal network oscillatory activity reflects the phasic inhibition of principal cells by GABAergic interneurones, which act to entrain and synchronize principal cell activity (Cobb *et al.,* 1995). The mEC has been reported to express gamma oscillations (30-80 Hz) in response to application of nanomolar concentrations of kainate (Cunningham *et al.,* 2003). Oscillatory power was greatest in superficial layers II/III (Cunningham *et al.,* 2003), and it depended on $GABA_A$ receptors, AMPA receptors and gap junction activity.

Cannabinoid receptors have been shown to modulate oscillatory activity in hippocampus (Hajos *et al.,* 2000) and hippocampus and EC (Hajos *et al.,* 2008), mostly using CB1R agonists such as WIN 55,212-2 and CP55940 and the antagonist AM-251. We prepared slices in a similar manner to that described above, but increased slice thickness to 450 μm and stored them in and recorded activity using interface chambers (for details see Methods, Chapter 2 above). Briefly, field recordings were made using low impedance electrodes (5-10 MΩ)

and oscillations elicited using 300-400 nM kainate (KA). Cannabinoid ligands were applied for 40-60 minutes, after oscillatory activity had been assessed to have stabilised (measured by minimal change in the power spectra generated using Clampfit software). We analysed oscillations at beta (15-29 Hz) and gamma (30-90 Hz) bands, using band-pass filters (Clampfit 10.1) and measurement of the area under the power spectrum curve in Sigmaplot 8.0.

6.2 The effects of cannabinoids on oscillatory activity in layer II

We applied the CBR agonist ACPA at 10 μM, as previously described, onto slices from which stable gamma activity had been induced by 300-400nM kainate. As **Fig.6.1A A** shows, KA induced gamma oscillations in layer II were broadly similar to those reported by Cunningham *et al.,* (2003). Hence, mean area power in the γ-band was 561 ± 179 μV^2. Mean control gamma frequency was 40.7 ± 2.4 Hz. Area power values were normalised for each recording, and percentage change in area power is used in all following data. Paired t-tests were used to compare area power and frequency between conditions. **Fig 6.1 B** shows the power spectral density of activity band pass filtered between 2-100 Hz, and **Fig. 6.1C** shows similar data filtered at gamma frequency (30-90 Hz). As **Fig.6.1** shows, there was a tendency towards an increase in gamma power in ACPA in some recordings, but this was not significant overall ($P \geq 0.19$, n=9,). ACPA did, however, significantly reduce mean peak gamma frequency to 35.6 ± 1.8 Hz ($P \leq 0.04$, n=9).

We next applied the CB_2R-specific inverse agonist/ antagonist AM-630 (250nM) to slices previously exposed to ACPA. In the presence of AM-630, there was a significant decrease in normalised gamma power (**Fig. 6.6A**, red bar), which was reduced to 61.4 ± 13.3 % of control ($P \leq 0.014$, n=9) and peak gamma frequency returned to control levels 40.4 ± 3.8 Hz ($P \geq 0.4$, n=9). No further

change in frequency was seen. When we added the CB_1R-specific inverse agonist / antagonist LY320135, however, there was a marked, further reduction in normalised gamma power to 39.4 ± 10.1 % of control, and this was highly significant ($P \leq 0.0006$, n=9).

When we measured beta power in layer II, we noted a similar pattern of drug responses to that observed for gamma activity. Mean area power in the beta band was lower than that of gamma activity at 26 ± 6 μV^2 and mean peak beta frequency in control conditions was 25.6 ± 1.4 Hz. **Fig 6.2 B** shows the power spectral density of activity band pass filtered between 2-100 Hz, and **Fig. 6.1C** shows similar data filtered at beta frequency (15-29 Hz). As **Fig.6.2** shows, there was a slight tendency towards a decrease in beta power in ACPA in some recordings, but this was not significant overall (81.4 ± 15 % of control, $P \geq 0.14$, n=9). ACPA had no significant effect on mean peak beta frequency (27.6 ± 1.43 Hz, $P \geq 0.25$, n=9).

We next applied the CB_2R-specific inverse agonist/ antagonist AM-630 (250nM) onto slices previously exposed to ACPA. In the presence of AM-630, there was a decrease in normalised beta power (**Fig. 6.6A**, red bar), which was significant (67.3 ± 14.1 % of control, $P \leq 0.02$, n=9). When we added the CB1R-specific inverse agonist LY320135, there was a further reduction in normalised beta power to 57 ± 13 % of control, and this was highly significant ($P \leq 0.008$, n=9). Neither AM-630 nor LY320135 altered mean peak frequency (25.8 ± 1.66 Hz, $P \geq 0.9$, n=9 in AM-630 and 27.9 ± 0.52 Hz, $P \geq 0.4$, n=9 in LY320135).

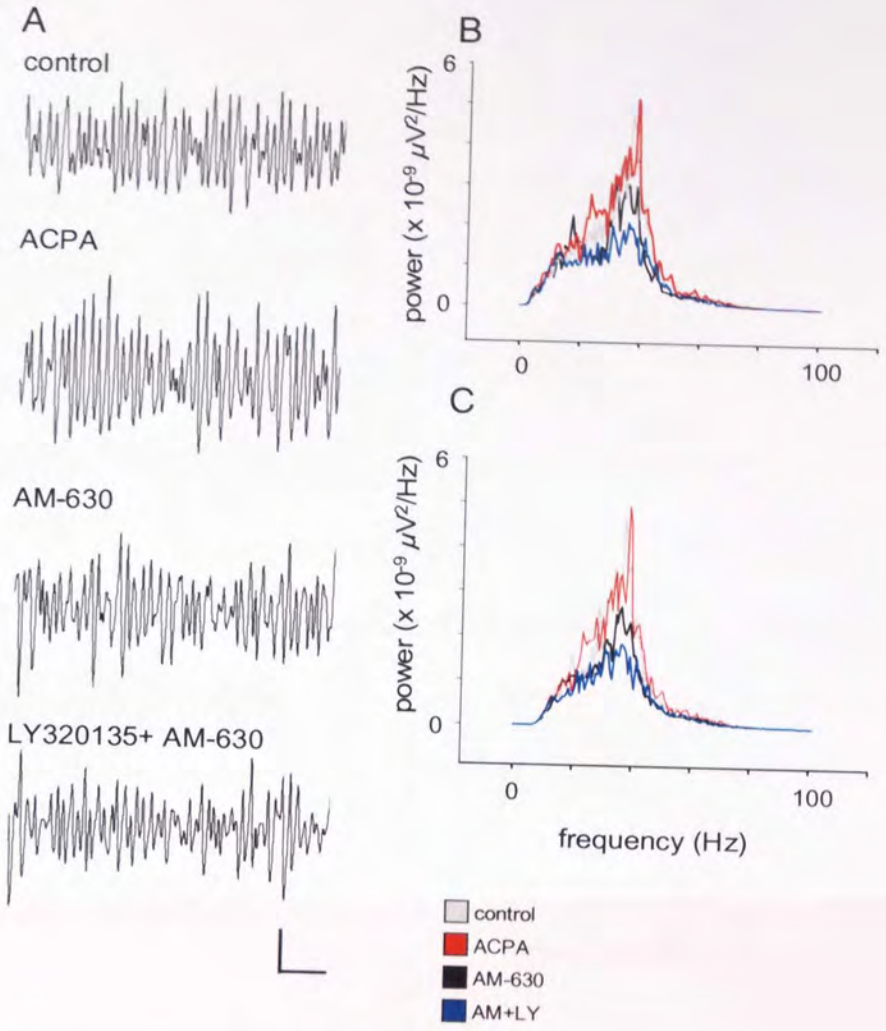

Fig. 6.1 The effects of cannabinoid ligands on γ-band activity in mEC layer II.
A. Example traces from layer II showing γ-oscillations under conditions in which ACPA (10μM), AM-630 (250nM) or LY320135 (1μM) were applied. **B.** Plot of power spectral density during drug application (filtered between 2-100 Hz). Control (black line), ACPA (red line), AM-630 (grey line) LY320135 (blue line). **C.** Similar plot to **B.** band pass filtered between 30-90 Hz. Scale bar = 200 ms x 100 μV.

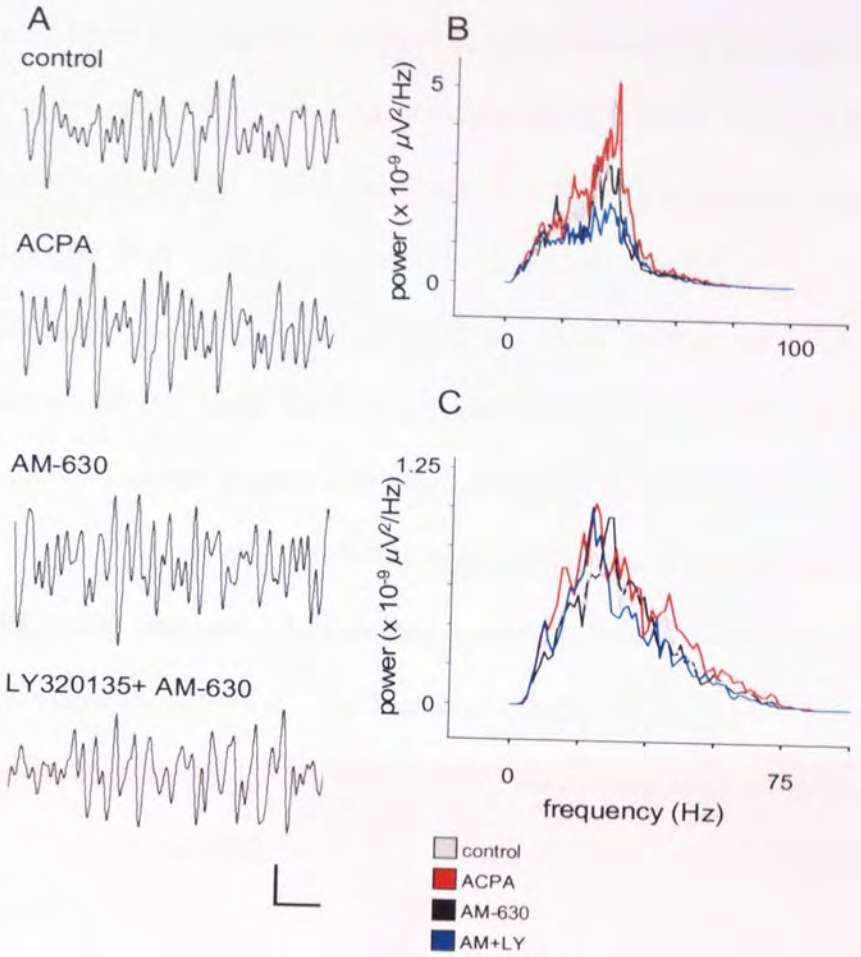

Fig. 6.2 The effects of cannabinoid ligands on β-band activity in mEC layer II.
A. Example traces from layer II showing β -oscillations under conditions in which ACPA (10μM), AM-630 (250nM) or LY320135 (1μM) were applied. **B.** Plot of power spectral density during drug application (filtered between 2-100 Hz). Control (black line), ACPA (red line), AM-630 (grey line) LY320135 (blue line). **C.** Similar plot to **B.** band pass filtered between 15-29 Hz. Scale bar = 200 ms x 50 μV.

6.2.1 The effects of cannabinoids on oscillatory activity in layer V mEC

During the above experiments, we simultaneously recorded oscillatory activity in deep entorhinal cortex (layer V). Oscillatory activity in layer V was lower in power in layer V compared to layer II, with mean area gamma power just 60 ± 10 μV^2. Mean peak frequency was similar to layer II at 39.19 ± 3.1 Hz.

When we applied ACPA there was a small but significant increase in mean gamma power (**Fig.6.3A-C**), by 38.1 ± 13.4 % of control ($P \leq 0.03$, n=9). Peak frequency was again slightly reduced to 36.01 ± 2.4 Hz, but this was not significant ($P \geq 0.31$, n=9). On subsequent addition of AM-630, a further increase in normalised gamma power was seen (**Fig. 6.7A**, red bar), by 80.4 ± 39 % of control ($P \leq 0.04$, n=9). When we added the CB1R-specific inverse agonist LY320135, there was yet a further increase in normalised gamma power to 108.4 ± 58 % of control, and this just reached significance ($P = 0.049$, n=9). Again, neither AM-630 nor LY320135 significantly altered mean peak gamma frequency (35.6 ± 3.24 Hz in AM-630, $P \geq 0.29$, n=9; 35.7 ± 2.41 Hz in LY320135, $P \geq 0.45$, n=9).

When we measured beta power in layer V, we noted a similar pattern of drug responses to that observed for gamma activity. Mean area power in the beta band was lower than that of gamma activity at 9.6 ± 0.6 μV^2 and mean control beta frequency was 27.9 ± 0.52 Hz (**Fig. 6.4B and C**). **Fig 6.4 B** shows the power spectral density of activity band pass filtered between 2-100 Hz, and **Fig. 6.4C** shows similar data filtered at beta frequency (15-29 Hz). As **Fig.6.4** shows, there was a slight tendency towards an increase in beta power (by 27 ± 14 %) in ACPA in some recordings, but this was not significant overall ($P \geq 0.06$, n=9). ACPA had no significant effect on mean peak beta frequency (28.4 ± 0.7 Hz, $P \geq 0.5$, n=9).

We next applied the CB_2R-specific inverse agonist AM-630 (250nM) onto slices previously exposed to ACPA. In the presence of AM-630, there was a

significant increase in normalised beta power (**Fig. 6.7A**, red bar), which was increased by 90.8 ± 53 % of control, but this did not quite reach significance ($P \leq$ 0.07, n=9). When we added the CB1R-specific inverse agonist LY320135, there was a further increase in normalised beta power by 142.4 ± 88 % of control, and this again failed to reach significance ($P \leq 0.07$, n=9). Neither AM-630 (27.9 ± 1.15 Hz, $P \geq 0.4$, n=9) nor LY320135 (26.3 ± 1.5 Hz, $P \geq 0.3$, n=9) altered peak frequency.

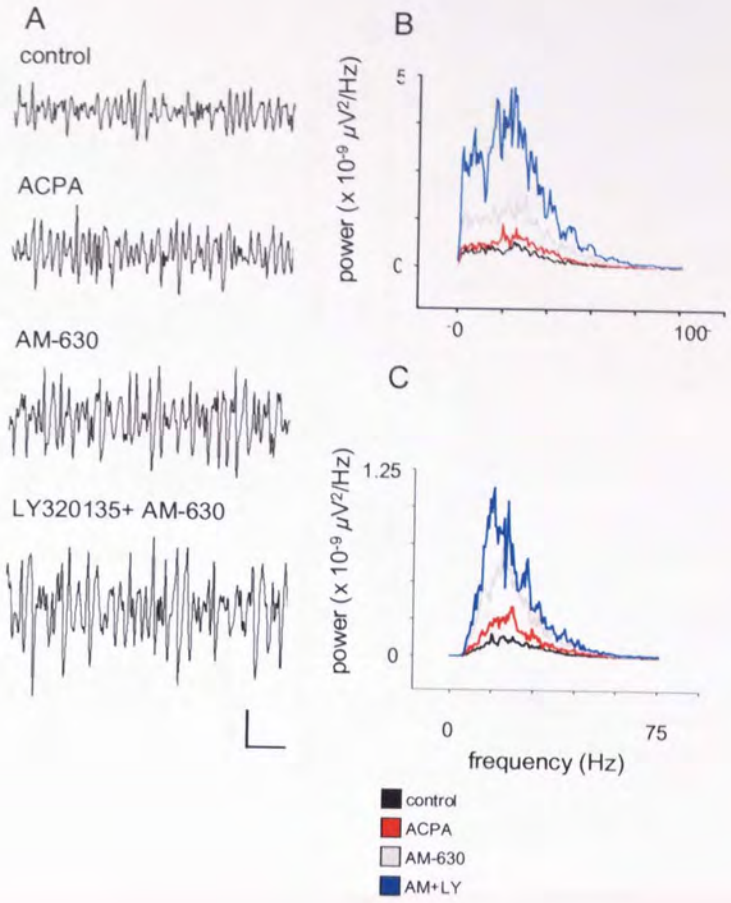

Fig. 6.3 The effects of cannabinoid ligands on γ-band activity in mEC layer V.
A. Example traces from layer II showing γ-oscillations under conditions in which ACPA (10μM), AM-630 (250nM) or LY320135 (1μM) were applied. **B.** Plot of power spectral density during drug application (filtered between 2-100 Hz). Control (black line), ACPA (red line), AM-630 (grey line) LY320135 (blue line). **C.** Similar plot to **B.** band pass filtered between 30-90 Hz. Scale bar = 200 ms x 50 μV.

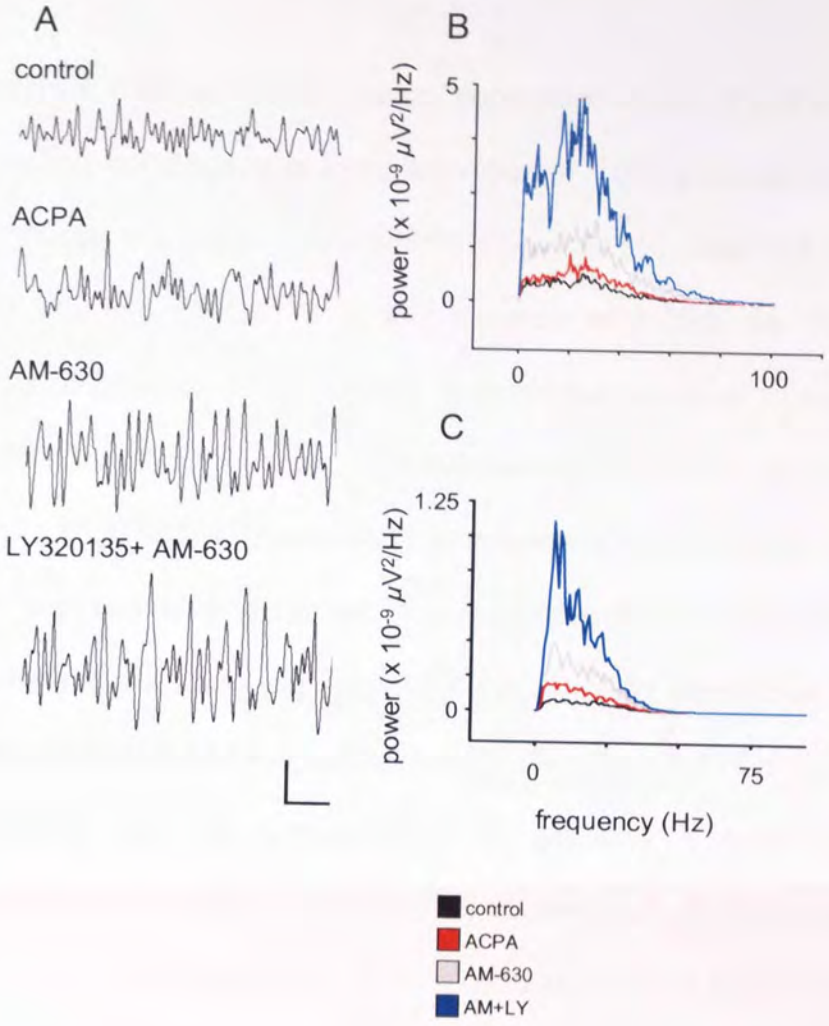

Fig. 6.4 The effects of cannabinoid ligands on β-band activity in mEC layer V
A. Example traces from layer II showing β-oscillations under conditions in which ACPA (10μM), AM-630 (250nM) or LY320135 (1μM) were applied. **B.** Plot of power spectral density during drug application (filtered between 2-100 Hz). Control (black line), ACPA (red line), AM-630 (grey line) LY320135 (blue line). **C.** Similar plot to **B.** band pass filtered between 15-29 Hz. Scale bar = 200 ms x 50 μV.

6.2.2 The effects of inverse agonists alone on oscillatory activity in layers II and V

We hypothesised that the lack of consistent effects of ACPA in layers II and V might reflect constitutive or tonic activation of CBR, perhaps due to persistent kainate-induced activation of pyramidal neurones. To test this hypothesis, we used AM-630 and LY320135 in the absence of ACPA. As **Fig.6.6B** shows, application of AM-630 alone caused a decrease in mean normalised gamma power by 64.3 ± 22 % of control, and this was significant ($P \leq 0.02$, n=9). Further addition of LY320135 enhanced the suppression of gamma band activity down to 19.5 ± 11 % of control, and this was highly significant ($P \leq 0.01$, n=9). When beta activity was measured, it was apparent that AM-630 alone had no statistically significant effect on mean normalised beta power (85 ± 6.1 % of control; $P \geq 0.4$, n=9). However, when we added LY320135, we noted a significant reduction in mean normalised beta power (58.4 ± 12 % of control; $P \leq 0.04$, n=9), compared to both control and AM-630 conditions ($P \leq 0.03$ AM-630 *Vs* LY320135).

Similar experiments in layer V showed that neither AM-630, nor LY320135 had significant effects on beta or gamma power or frequency.

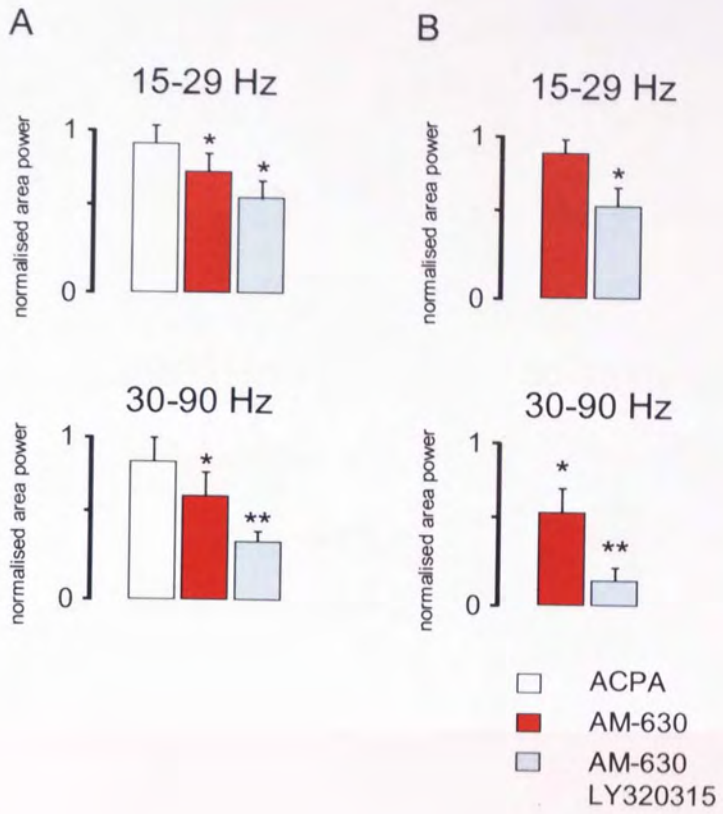

Fig. 6.5 Summary of the effects of cannabinoid ligands on oscillatory activity in mEC. **A.** Bar charts showing the effects of cannabinoid ligands in layer II on normalised area power at γ and β frequencies. **B.** Bar charts showing the effects of inverse agonists alone in layer II on normalised area power at γ and β frequencies.

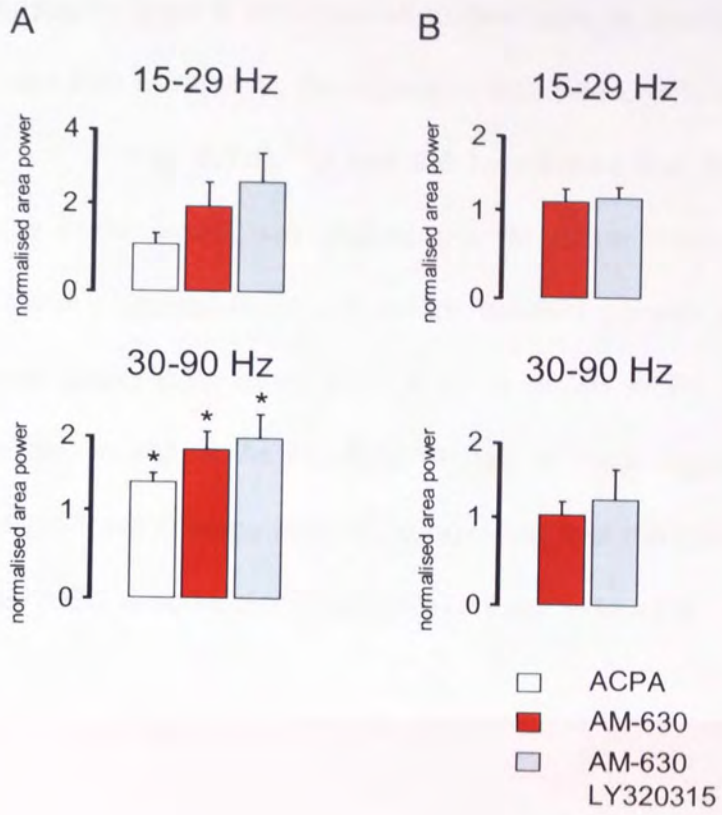

Fig. 6.6 Summary of the effects of cannabinoid ligands on oscillatory activity in mEC. **A.** Bar charts showing the effects of cannabinoid ligands in layer V on normalised area power at γ and β frequencies. **B.** Bar charts showing the effects of inverse agonists alone in layer V on normalised area power at γ and β frequencies.

6.2.3 Differential effects of cannabinoids on oscillatory activity in layers II and V

The data presented up to this point indicated that, in general, gamma and beta power decreased in layer II in response to blockade or inverse agonism of CB_1 and CB_2Rs, and that in layer V, the opposite was seen, with an increase in gamma and beta power (**Fig. 6.7A**). To test the hypothesis that these opposing changes may have been linked, we plotted the fractional decrease in mean gamma power in layer II against the fractional increase in gamma power in layer V, using mean data taken from the experiments in which ACPA, AM-630 and LY320135 were added in series. As **Fig.6.7B** shows, a linear regression fits the plot with a highly significant r^2 value of 0.93, suggesting that the increase gamma band power in deep mEC is correlated with the decrease in layer II.

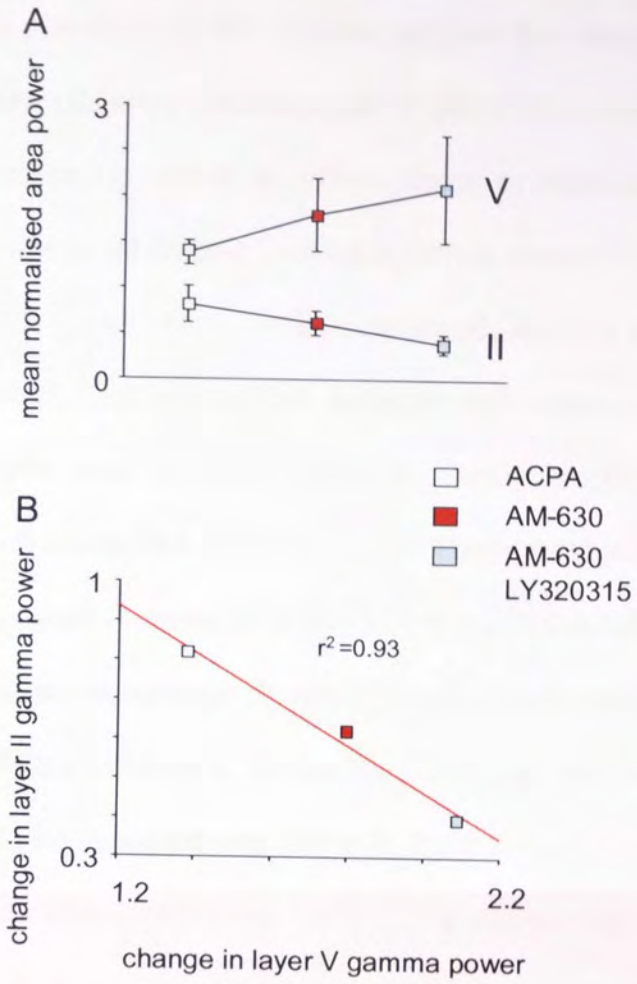

Fig. 6.7 Correlation between the effects of cannabinoid ligands on γ-band activity in layer II and V.
A. Plot of mean normalised γ-band power in layers II and V under various drug conditions. **B.** Plot of fractional normalised area power in the gamma band in layer II during drug application, versus similar data in layer V. Linear regression analysis (red line) indicates $r^2 = 0.93$.

6.3 Discussion

The data presented in this chapter suggest that cannabinoid receptors are tonically activated under conditions used to generate network oscillations, since ACPA had little or no effect in either deep or superficial layers of mEC. Experiments in which we utilised inverse agonists showed that in layer II, gamma and beta frequency oscillations were suppressed, and the opposite was found in layer V. In general, it appeared that antagonism/inverse agonism of CB_2R with AM-630 alone was only weakly effective in altering oscillatory activity, but that subsequent CB_1R block had marked effects. These data suggest that CB_1R may be the most important in terms of network activity in the mEC. When we applied inverse agonists alone, effects of oscillatory function were much weaker, and were only significant in layer II. These data suggest that cannabinoid receptors are more likely to be constitutively active in layer II than in layer V, which agrees well with previous observations we have made concerning the actions of ACPA and other agonists on sIPSCs in layers II and V.

Cannabinoid receptors exert powerful control over GABA release from presynaptic terminals, with CB1 receptors having been shown to suppress both IPSPs and IPSCs in pyramidal neurones (IPSPs, Freund *et al.,* 2003; Piomelli *et al.,* 2003; IPSCs, Hajos *et al.,* 1999; 2001). Endocannabinoids, such as 2-arachidonyl glycerol (2-AG, Jones et al., 2003) and anandamide (AEA, Davis et al., 1991) also suppress inhibition in CNS (Woodhall et al., 2005). Cannabinoids are also believed to mediate the phenomenon of depolarisation-induced suppression of inhibition (DSI; Llano et al., 1991; Alger and Pitler 1992; Wilson & Nicoll 2002; Freund et al., 2003). Recently, studies have suggested that CB1R are present at terminals from specific subsets of inhibitory interneurones. For example, fast spiking (FS) inhibitory neurons in neocortex express parvalbumin (PV) but not CB1R, and by contrast, irregular spiking (IS) neurones express CB_1R

but not PV (Galaretta et al., 2004; Bodor et al., 2005). Recently, Galaretta et al., (2008) have demonstrated that synapses between IS neurons and pyramidal cells express CB_1R and show DSI, whereas synapses between FS neurons and pyramidal cells show neither CB_1R nor DSI. FS cells are thought to pace fast oscillatory network rhythms such as gamma activity (Bartos *et al.,* 2000; Traub et al., 2003), and IS cells are thought to possess properties that predispose towards non-rhythmic activity (Gibson et al., 1999; Galaretta et al., 2004). A subset of neurons that express CB_1R but not PV expresses cholecystokinin (CCK), and these neurons have been suggested to act, through DSI, to differentiate subgroups of pyramidal cells into neuronal assemblies which are then entrained by FS cells ('sparse coding', Klausberger *et al.,* 2005). In this scenario, pyramidal cell activation leads to endocannabinoid synthesis and release, which inhibits IS-cell inputs to the somata and proximal dendrites of active cells, but allows IS-cell mediated inhibition to remain intact (and ongoing) at less active pyramids. This effect, in turn, allows FS-cells to entrain oscillatory activity only at the disinhibited population of pyramidal cells, effectively selecting that subset for rhythmic activity.

It seems possible that PV-/CCK+/CB_1R+ inhibitory interneurones might similarly select populations of pyramidal cells involved in rhythmogenesis in the mEC, which contains both PV+ and PV- neurones (Wouterlood *et al.,* 1995) and CCK+ interneurones (Kohler & Chan-Palay, 1982), which also express CB_1R (Marsicano and Lutz, 1999). We used cannabinoid receptor inverse agonists to globally inhibit CBRs, presumably at IS-cell terminals during persistent gamma and beta band oscillations in brain slices from the mEC. Under conditions in which both CB_1 and CB_2R were subject to blockade or inverse agonist effects, we observed a decrease in oscillatory power in gamma and beta bands in layer II. This is consistent with the literature described above (Klausbgerger *et al.,* 2005; Galaretta *et al.,* 2008): we propose that, in layer II, blockade or inverse agonism

of CBRs results in increased phasic inhibition from IS-cells onto pyramidal cells, decreasing the population available to participate in network oscillations and hence reducing field oscillatory power. This appears to be supported by our recordings (Chapter 5) showing that AM-630 and LY320135 increase phasic GABAergic inhibition at principal cells.

When we measured oscillatory activity in layer V, inverse agonists at CBR *increased* gamma and beta power and this was correlated with decreased superficial beta and gamma power. At first, this appears paradoxical, however, oscillatory activity in specific laminae does not exist in isolation, and we might expect interactions between, as well as within networks of neurons. Bragin *et al.,* (1995) have demonstrated that, *in vivo*, bilateral ablation of the EC suppresses gamma activity in the dentate gyrus (DG), but augments gamma oscillations in CA3-CA1. As previously discussed (Introduction), superficial mEC projects to DG, and CA1 projects to deep mEC layers. Given that in our experiments, oscillatory activity in superficial mEC was suppressed, it is reasonable to suggest that this may depress gamma and/or beta activity in DG and enhance such activity in CA3-CA1. This, in turn, would feed through to layer V, where increased gamma and beta power is seen.

6.3.1 Further experiments

To test the above hypotheses, further recordings would need to be performed, in which a series of lesions (cuts) were placed at strategic loci along the hippocampal-entorhinal loop(s). For example, we would predict that, a cut between superficial mEC and DG would enhance power in layer V, but prevent further enhanced power when oscillatory activity in layer II was suppressed with cannabinoid inverse agonists. Similarly, and cut between CA3-CA1 and layer V would decrease gamma and beta power in deep mEC, and this would not then be

enhanced by cannabinoid inverse agonists/antagonists. Finally, to test the hypothesis that IS-cell disinhibition allows a larger number of principal neurones to be recruited into oscillatory activity, we would apply a cannabinoid agonist alone while recording in superficial mEC, and it seems possible that oscillations might arise spontaneously, or at much lower doses of kainate.

Chapter 7
General Discussion

7.1 Discussion

In this thesis, I have investigated the role cannabinoid receptors play in modulating $GABA_A$ inhibitory signalling in deep and superficial layers of the mEC.

It is well established through both labelling and physiological studies that CB_1Rs play a role in modulating inhibitory signalling in many brain regions. In this study I have shown that within the medial entorhinal cortex (mEC) cannabinoids appear to modulate inhibitory signalling in both deep and superficial layers. In layer V, the effects of both the agonists and antagonists were consistent, with agonists causing a decrease in normalised inhibitory charge transfer (NICT) and antagonists increasing NICT. In layer II, when using the agonists ACPA and WIN 55,121-2 and the antagonist, AM-251, the picture was less clear as these drugs gave mixed results showing both increases and decreases in NICT. These early experiments showed that functional CB_1Rs were present at inhibitory terminals in both deep and superficial mEC, and that in layer V at least, these behaved as might be expected based on previous studies. In layer II it is harder to draw any conclusions due to the dual affects both the agonists and antagonists had on NICT.

While the effects of ACPA and AM-251 were unclear in P30 layer II neurones in P8-12 slices a consistent effect of CB_1R agonist ACPA and the CB_1R antagonist AM-251 was seen in both layers II and V. However this effect was not wholly expected as both ACPA and AM-251 caused a decrease in GABAergic signalling. In addition to the effects of the CB_1R ligands in juvenile mEC the CB_2R agonist JWH-133 and antagonist / inverse agonist AM-630 also both suppressed GABAergic signalling in both deep and superficial layers of the mEC. While application of both CB_1R and CB_2R specific ligands altered inhibitory signalling, the effects of the agonists and antagonists were apparently non-specific. That is to say that both CB_1R and CB_2R agonists and antagonists served to decrease

inhibitory signalling. This result points towards CBRs being present in the juvenile brain but suggests that the subtleties of CBR linked signalling are not fully developed at this stage, such that binding of the ligand to the receptor is only able to elicit one type of response.

Having seen that CB_2R specific ligands altered GABAergic signalling in the P8-12 neurones, I used the same receptor-specific ligands to investigate the possibility that CB_2Rs are present in the mEC.

In layer II of the P30 slices the CB_1R specific antagonist / inverse agonist LY320135 consistently increased GABAergic signalling and this affect could be reversed by both 2-AG and JWH-133 indicating that these CBR agonists were acting at somewhere other than CB_1Rs. Use of a CB_2R specific antagonist/ inverse agonist AM-630 overcame the suppressing effects of 2-AG and JWH-133. These results were clearest in layer V of the mEC. Further evidence to support the argument that functional CB_2Rs were present in P30 mEC was that by reversing the experiment and starting with the CB_2R antagonist/ inverse agonist AM-630, I was able to prevent the suppressing effects in layer V and layer II of the CB_2R agonist JWH-133. Finally, I showed that a structurally unique CB_2R specific antagonist/ inverse agonist, JTE-907, increased GABAergic signalling in layer II at a concentration of 1nM. These results are the first pharmacological demonstration of functional CB_2Rs in the CNS. While there was little evidence to support the idea that CB_2Rs are present within the CNS, I feel that the lack of positive immunohistochemical evidence for CB_2Rs may be due to the fact that there were no suitable species-specific antibodies for these studies. In support of this view, some studies have shown CB_2R mRNA in CNS, and others have shown behavioural effects of CB_2R-specific ligands *in vivo*.

In addition to using pharmacological investigations to establish the presence of CB_2Rs within the mEC, use of the CB_1R specific ligand LY320135

removed any of the dual effects that had been seen earlier with both WIN 55,212-2 and ACPA in layer II of the mEC. The dual effects of ACPA and WIN 55,212-2 could be due a lack of specificity for cannabinoid receptors, or it may be that bath application of the drugs does not replicate what would happen physiologically.

Having established that both CB_1R and CB_2Rs are present at inhibitory terminals in the mEC I investigated what role these receptors may play in a more complete physiological situation by studying the effects of the CBR agonist, ACPA, CB2R antagonist AM-630 and CB1R antagonist LY320135 on oscillations in both deep and superficial layers of the mEC. It appeared that application the CB_1R agonist ACPA had little effect on the oscillations; however application of the CB_2R antagonist AM-630 increased the power of both gamma and beta frequency oscillations in layer II and when the CB_1R antagonist/ inverse agonist further increased the power of these oscillations. Interestingly, while the power of gamma and beta oscillations increased in layer II in layer V of the mEC application of AM-630 and LY320135 decreased the power of gamma and beta oscillations. This balanced effect of the cannabinoid antagonists/ inverse agonists in the deep and superficial layers of the mEC suggests that layer II may have some influence over oscillations in layer V.

While I have established that functional cannabinoid receptors are present within the mEC, the mixed results seen in layer II depending on the ligand used suggest that we do not fully understand the role these receptors are playing in modulating inhibitory signalling within the EC. Endogenous cannabinoids are synthesised on demand and, as discussed earlier, there is some evidence to suggest that specific stimuli activate production of different endocannabinoids. This, combined with the different docking sites for different ligands within the CBRs, may allow elicitation of different, ligand-specific conformational changes in the receptor, activating different signalling cascades. Hence, cannabinoid

signalling may be highly specific and designed to act over a short range, and bath application of CBR ligands may not illustrate the true physiological roles of cannabinoid signalling. This argument is further supported by the work of Hentges *et al.*, (2005) who showed that bath application of a synthetic cannabinoid produced different effects to the naturally released endocannabinoids and also Galarreta *et al.*, (2008) who showed that while bath application of cannabinoids suppressed inhibitory synaptic activity between inhibitory to inhibitory synapses of irregular bursting inhibitory interneurones, activation of these same synapses using stimulation protocols could not elicit DSI, a physiologically relevant measure of cannabinoid-mediated suppression of inhibition.

References

References

Akil, M and Lewis, D. A(1997) Cytoarchitecture of the entorhinal cortex in schizophrenia. American Journal of Psychiatry **154**:1010-1012

Alger, B.E and Pitler, T.A Wagner, J J., L A Martin, L.A., Morishita, W., Kirov, S A and Lenz, R A (1996). Retrograde signalling in depolarization-induced suppression of inhibition in rat hippocampal CA1 cells. Journal of Physiology **496:** 197-209

Alonso, A and Klink, R (1993) Differential electroresponsiveness of stellate and pyramidal-like cells of medial entorhinal cortex layer II. Journal of Neurophysiology **70**:128-143.

Ameri A., Wilhelm A., Simmet T (1999). Effects of the endogenous cannabinoid anandamide on neuronal activity in rat hippocampal slices. British Journal of Pharmacology **126**:1831-1839

Ameri, A., Wilhelm, A., Simmet, T (1999) Effects of the endogenous cannabinoid, anandamide, on neuronal activity in rat hippocampal slices. British Journal of Pharmacology **126**:1831-1839

Arai, Y., Fukushima, T., Shirao, M., Yang, X and Imai K. (2000). Sensitive determination of anandamide in rat brain utilizing a coupled-column HPLC with flurimetric detection. Biomedical Chromatography **14**: 118-124

Azad S.C., Eder M., Marsicano G., Lutz B., Zieglgansberger W., Rammed G.L (2003). Activation of the cannabinoid receptor type 1 decreases glutamatergic and GABAergic synaptic transmission in the lateral amygdale of the mouse. Learning and Memory **10**: 116-128

Bai, D., Zhu, G., Pennefather, P., Jackson, M.F., Macdonald, J.F and Orser, B.A (2001). Distinction functional and pharmacological properties of tonic and quantal inhibitory postsynaptic currents mediated by γ-Aminobutyric Acid $_A$ receptors in hippocampus neurons. Molecular Pharmacology 59:814-824

Baker D., Pryce G., Davies W.L., Hiley C.R. (2006) In silico patent searching reveals a new cannabinoid receptor. Trends in Pharmacology Science **27**:1-3.

Bartos, M., Vid, I., Frotscher, M., Meyer, A., Monyer, H., Geiger, J.R.P and Jonas, P. (2002). Proceedings of the National Academy of Sciences **99**:13221-13227

Bazinet RP, Lee HJ, Felder CC, Porter AC, Rapoport SI, Rosenberger TA. (2005) Rapid high-energy microwave fixation is required to determine the anandamide (N-arachidonoylethanolamine) concentration of rat brain. Neurochemistry Research **30**: 597-601

Beltramo, M and Piomelli, D (2000). Carrier-mediated transport and enzymatic hydrolysis of the endogenous cannabinoid 2-arachidonylglycerol. Neuroreport **11**:1231-1235

Beltramo, M., Stella, N., Calignano, A., Lin, S.Y., Makriyannis, A., and D. Piomelli, (1997) Functional role of high-affinity anandamide transport, as revealed by selective inhibition Science **22**:1094-1097.

Ben-Ari, Y., Cherubini, E., Corradetti, R., and Gaiarsa, J.L (1989) Giant synaptic potentials in immature rat CA3 hippocampal neurones. Journal of Physiology **416:** 303-325.

Benito, B., Núñex, E., Tolón, R.M., Carrier, E.J., Rábano, A., Hillard, C.J and Romero, J (2003) Cannabinoid CB_2 receptors and fatty acid hydrolase are selectively over expressed in neuritic plaque associated glia in Alzheimer's disease brains. The Journal of Neuroscience **3**: 11136-11141

Berretta, N., Jones, R.S.G (1996). Tonic facilitation of glutamate release by presynaptic N-methyl-D-aspartate autoreceptors in the entorhinal cortex. Neuroscience 75:339-344

Bettler, B and Mulle. C (1995) AMPA and Kianate receptors Neuropharmacology **344**:123-139.

Bettler, B., Egebjerg, J., Sharma, G., Pecht, G., Hermans-Borgmeyer, I., Moll, C., Stevens, C.F and Heinemann, S (1992) Cloning of a putative glutamate receptor: A low affinity kainate-binding subunit. Neuron, **8:** 257-62

Billinton, A., Antoinette O. Ige' A.O., Bolam, J,P.,. White[c], J.H., Marshall, F.H and Piers C. Emson, P.C. (2001). Advances in the molecular understanding of $GABA_B$ receptors Trends in Neuroscience **24**: 277-282

Bisogno, T., Howell, F., Williams, G., Minassi, A., Cascio, M.G., Ligresti, A., Matias, I., Schiano-Moriello, A., Paul, P., Williams, E.J., Gangadharan,U., Hobbs, C., Di Marzo, V and Doherty, P (2003) Cloning of the first sn1-DAG lipases points to the spatial and temporal regulation of endocannabinoid signaling in the brain Journal of Cell Biology (2003) **163**: 463-468.

Bodor AL, Katona I, Nyiri G, Mackie K, Ledent C, Hajos N, Freund TF. (2005) Endocannabinoid signaling in rat somatosensory cortex: laminar differences and involvement of specific interneuron types. Journal of Neuroscience. **25**: 6845-56.

Bracey, M.H., Hanson, M.A., Masuda, K.R., Stevens, R.C and Cravatt. B.F (2002) structural adaptations in a membrane enzyme that terminates endocannabinoid signalling. Science **298**:1793-1796

Bragin, A., Jando, G., Nadasdy, Z., Hetke, J and Buzsaki, G. (1995) γ (40-100 Hz) oscillation in the hippocampus of the behaving rat. Journal of Neuroscience **15**: 47-60

Breivogel CS., Griffin G., Di Marzo V., Martin BR. (2001) Evidence for a new G protein-coupled cannabinoidr in mouse brain. Molecular Pharmacology **60**:155-163.

Brown, S.P., Safo, P.K., and Regehr, W.G (2004). Endocannabinoids inhibit transmission at granule cell to purkinje cell synapses by modulating three types of presynaptic calcium channels Journal of Neuroscience **24**:5623 – 5631.

Brun,V.H., Otnæss, M.K., Molden, S., Steffenach, H.A., Witter M.P, Moser,M.B., and Moser, E.I (2002) Place Cells and Place Recognition Maintained by Direct Entorhinal-Hippocampal Circuitry. Science **296**: 2243-2246

Brun,, V.H., Leutgeb,S., Wu, H.Q., Schwarcz, R., Witter, M.P., Moser, E.I and Moser, M.B (2008) Impaired spatial representation in CA1 after lesion of direct input from entorhinal cortex. Neuron **57**: 290-302

Buckmaster, P.S., Alonso,A., Canfield, D.R and Amaral, D.G (2004). Dendritic morphology, local circuitry, and intrinsic electrophysiology of principal neurons in the entorhinal cortex of macaque monkeys. The Journal of Comparative Neurology **470**: 317-329

Buldakova, S.L., Vorobjev, V.S., Sharonova, I.N., Samoilova, M.V and Magazanik, L.G (1999) Characterization of AMPA receptor populations in rat brain cells by the use of subunit-specific open channel blocking drug, IEM-1460. Brain Research, **846:** 52-58

Burwell, R (2000). The parahippocampal region: Corticocortical connectivity. Annals of the New York Academy of Sciences. 911: 25-42

Burwell, R.D and Amaral D.G (1998). Cortical afferents of the perirhinal, postrhinal, and entorhinal cortices of the rat. The Journal of Comparative Neurology **398**: 179-205.

Burwell, R.D and Amaral, D.G (1998). Perirhinal and postrhinal cortices of the rat: Interconnectivity and connections with the entorhinal cortex. The Journal of Comparative Neurology **391**: 293-321

Cabral, G.A and. Dove Pettit, D. A (1998) Drugs and immunity: cannabinoids and their role in decreased resistance to infectious disease. The Journal of Neuroimmunology, **83**:116-123

Cintra, L., Aguilar, A., Granados, L., Galván, A., Kemper, T., DeBassio, W., Galler, J., Morgane, P., Durán, P and Díaz-Cintra, S. (1997) Effects of prenatal protein malnutrition on hippocampal CA1 pyramidal cells in rats of four age groups Hippocampus **7**: 192-203

Cobb SR, Buhl EH, Halasy K, Paulsen O, Somogyi P. (1995) Synchronization of neuronal activity in hippocampus by individual GABAergic interneurons. Nature. **378**: 75-8.

Conn, P.J & Pin, J-P (1997) Pharmacology and functions of metabotropic glutamate receptors. Annual Review Pharmacology Toxicology **37**: 205-237

Couve, A., Moss, S.J and Pangalos, M.N (2000) GABAB receptors: a new paradigm in G protein signalling. Molecular Cell Neuroscience **16**: 296-312

Cravatt, B.F., Demarest, K., Patricelli, M.P., Bracey, M.H., Giang, D.K., Martin, B.R and Lichtman, A.H (2001). Supersensitivity to anandamide and enhanced endogenous cannabinoid signaling in mice lacking fatty acid amide hydrolase PNAS **98**: 9371-9376

Cravatt, B.F., Giang, D.K., Mayfield, S.P., Boger, D.L., Lerner, R.A and Gilula. N.B (1996) Molecular characterization of an enzyme that degrades neuromodulatory fatty-acid amides Nature **384**: 83-87

Cunha, R.A., João, C Malva, O and Ribeiro, J.A (1999) Kainate receptors coupled to G_i/G_o proteins in the rat hippocampus. Molecular Pharmacol **56**: 429-433

Cunningham, M.O., Davies, C.E., Buhl, E.H., Kopell, N and Whittington, M.A (2003) Gamma oscillations induced by kainate receptor activation in the entorhinal cortex in vitro. The Journal of Neuroscience 23:9761-9769

Cunningham, M.O., Hunt, J., Middleton,S., LeBeau, F.E.N., Gillies, M.G., Davies, C.H., Maycox, P.R., Whittington, M.A and Racca, C. (2006) Region specific reduction in entorhinal gamma oscillations and parvalbumin-immunreactive neurons in animal models of psychiatric illness. Neurobiology of Disease **26**:2767-2776.

Defagot M.C Villar M.J, Antonelli M.C (2002) Differential localization of metabotropic glutamate receptors during postnatal development. Developmental Neuroscience. **24**:272-82.

Degn, M., Lambertsen, K.L., Petersen, G., Meldgaard M., Artmann, A., Clausen B.H., Hansen, S.H., Finsen, B., Hansen, H.S., and Lund T.M (2007) Changes in brain levels of N-acylethanolamines and 2-arachidonoylglycerol in focal cerebral ischemia in mice. Journal of Neurochemistry **103**:1907-1916

Derbenev, A.V., Stuart, T.C and Smith, B.N (2004) Cannabinoids suppress synaptic input to neurones of the rat dorsal motor nucleus of the vagus nerve Journal of Physiology **559**: 923-938

Devane., W.A, Hanus, L., Breuer, A., Pertwee, RG., Stevenson, LA., Griffin, G ., Gibson,D., Mandelbaum, A., Etinger, A and Mechoulam, R (1992) Isolation and structure of a brain constituent that binds to the cannabinoid receptor. Science **18:**1946-1949.

Devane, W.A.,Dysar, F.A.,Johnson, M.R.,Melvin, L.S., and Howlett, A.C (1988)Determination and characterization of A cannabinoid receptor in rat brain. Molecular Pharmacology. **34:** 605-613

Di Marzo, V., Melck, D., Bisogno, T and De Petrocellis, L (1998) Endocannabinoids: endogenous cannabinoid receptor ligands with neuromodulatory action. Trends in Neuroscience **21:**521-528

Di Marzo, V., Fontana, A., Cadas H., Schinelli, S., Cimino G., Schwartz J.C. & Piomelli D. (1994) Formation and inactivation of endogenous cannabinoid anandamide in central neurons. Nature **372:** 686–691.

Didelon, F., Sciancalepore, M., Savic.N., Mladinic, M., Bradbury, A., and Cherubini, E (2002) Ɣ-Aminobutyric acid ρ receptor subunits in the developing rat hippocampus. Journal of Neuroscience Research 67:739-744

Dingledine, R., Borges, K., Bowie, D and Traynelis, S.F. (1999).The Glutamate Receptor Ion Channels. Pharmacology Reviews **51**:7-62

Dinh, T. P., Carpenter, D., Leslie, F. M., Freund, T. F. Katona, I Sensi, S. L., Kathuria, S and Piomelli, D. (2002) Brain monoglyceride lipase participating in endocannabinoid inactivation PNAS **99**:10819-10824;

Doherty, J., and Dingledine, R (2003) Functional interactions between cannabinoid and metabotropic glutamate receptors in the central nervous system Current Opinion in Pharmacology **3**:46-53

Dolorfo, C.L and Amaral, D.G (1998) Entorhinal cortex of the Rat: Topographic organization of the cells of origin of the perforant path projection to the dentate gyrus. The Journal of Comparative Neurology **398:** 25-48

Domenici, M.R., Azad, S.C., Marsicano, G., Schierloh, A., Wotjak,C.T., Dodt, H.U., Zieglgänsberger, W., Lutz, B and Rammes, G (2006). Cannabinoid receptor type 1 located on presynaptic terminals of principal neurons in the forebrain controls glutamatergic synaptic transmission The Journal of Neuroscience, **26**:5794-5799

Edwards D.A., Kim, J and Bradley E. Alger, B.E (2006) Multiple mechanisms of endocannabinoid response initiation in hippocampus. Journal of Neurophysiology **95**:67-75,

Edwards, D.A., Kim, J., Alger, B.E (2005) Multiple mechanisms of endocannabinoid response initiation in hippocampus. The Journal of Neurophysiology 95:67-75

Egebjerg, J., Bettler, B., Hermans-Borgmeyer, I and Heinemann. S. Cloning of a cDNA for a glutamate receptor subunit activated by kainate but not AMPA. Nature **351**:745-748

Ellert-Miklaszewska, A., Grajkowska, W., Gabrusiewicz, K., Kaminska, B and Konarska, L (2007). Distinctive pattern of cannabinoid receptor type II (CB2) expression in adult and pediatric brain tumours. Brain Research **1137**:161-169

Endoh, T (2006) Pharmacological characterization of inhibitory effects of postsynaptic opioid and cannabinoid receptors on calcium currents in neonatal rat nucleus tractus solitarius. British Journal of Pharmacology **147** 391-401

Enz, R and Cutting, G,R (1999) $GABA_C$ receptor ρ subunits are heterogeneously expressed in the human CNS and form homo- and heterooligomers with distinct physical properties. European Journal of Neuroscience **11**:41-50

Enz, R and Cutting, G.R (1998) Molecular composition of $GABA_C$ receptors. Vision Research **38**:1431-1441

Evans D.I.P 2000 The role of metabotropic glutamate receptors in controlling neurotransmission in the rat entorhinal cortex in vitro. Dissertation University of Bristol Department of Physiology)

Evans, D.I.P., Jones, R.S.G. and Woodhall, G.L. (2000) Activation of group III metabotropic receptors enhances glutamate release in rat entorhinal cortex. Journal of Neurophysiology. **83:** 2519-2525

Farooqui, A.A., Rammohan, K.W and Horrocks, L.A (1989). Isolation, characterization and regulation of diacylglycerol lipases from bovine brain. Ann. NY. Acad. Sci. **559**:25-36

Finch, D.M., Tan, A.M., and Isokawa-Akesson, M (1988). Feed forward inhibition of the rat entorhinal cortex and subicular complex. Journal of Neuroscience. **8**:2213-2226

Fowler, C.J. (2007) The pharmacology of the cannabinoid system- A question of efficacy and selectivity. Molecular Neurobiology **36**: 15-25

Freund, T.F., Katona, I and Piomelli, D (2003) Role of endogenous cannabinoids in synaptic signaling. Physiological Reviews **83**:1017-1066

Galarreta M, Erdelyi, F., Szabo, G and Hestrin, S. (2004) Electrical coupling amoung irregular-spiking GABAergic interneurones expressing cannabinoid receptors. Journal of Neuroscience **24**: 9770-9778.

Galarreta, M., Erdelyl, F., Szabo, G and Hestrin S (2008). Cannabinoid sensitivity and synaptic properties of 2 GABAergic networks in the neocortex. Cerbral cortex advanced access published January 17 2008.

Gately, S.J., Gifford, A.N., Volkow, N.D., Lan, R and Makriyannia, A (1996). 123I-labled AM-251: a radioiodinated ligand which binds in vivo to mouse brain cannabinoid CB1 receptors. European Journal of Pharmacology. **307**: 331-338

Germroth P., Schwerdtfeger WK., Bühl EH (1989). Morphology of identified entorhinal neurons projecting to the hippocampus. A light microscopical study combining reterograde tracing and intracellular injection. Neuroscience **30**:683-691.

Germroth, P., Schwerdtfeger, W.K., Buhl, E.H. (1991) Ultrastructure and aspects of functional organization of pyramidal and nonpyramidal entorhinal projection neurons contributing to the perforant path. Journal of Comparative Neurology , **305**:215 231.

Gibson, J.R., Beierlein, M and Connors, B.W (1999) Two networks of electrically couple inhibitory neurones in neocortex. Nature 402: 75-79

Giuffrida, L. H. Parsons, T. M. Kerr, F. Rodríguez de Fonseca, M. Navarro & D. Piomelli (1999). Dopamine activation of endogenous cannabinoid signaling in dorsal striatum. Nature Neuroscience 2 358-363

Glass M., Dragunow M., Faull R.L.M (1997) Cannabinoid receptors in the human brain: A detailed anatomical and quantitative autoradiographic study in the fetal, neonatal and adult human brain. Neuroscience **77**:299-318

Gloveli T., Egorov AV., Schmitz D., Heinmann U, Müller W (1999). Charbachol-induced changes in excitability and [Ca 2+]I siginalling in projection cells of the medial Entorhinal cortex layers II and III. European Journal Neuroscience **11**:3626-3636

Gloveli,T., Dugladze,T., Schmitz, D., Heinemann, U. (2001) Short communication properties of the entorhinal cortex deep layer neurons projecting to the dentate gyrus. European Journal of Neuroscience **13**: 413-420

Gloveli, T., Schmitz, D., Empson, R.M, Dugladze, T and Heinemann, U (1997) Morphological and electrophysiological characterization of layer III cells of the medial entorhinal cortex of the rat. Neuroscience **77**: 629-648.

Gong,J.P., Onaivi, E.S., Ishiguro, H., Liu, Q.R., Tagliaferro, P.A., Brusco, A., and Uhl, G.R (2006) Cannabinoid CB_2 receptors: immunhistochemical localization in rat brain. Brain Research **1071**: 10-23

Goparaju, K.S., Ueda, N., Taniguchi, K and Yamamoto, S (1999). Enzymes of porcine brain hydrolyzing 2-arachidonoylglycerol, an endogenous ligand of cannabinoid receptors. Biochemical Pharmacology **57**: 417-423

Griffin,G., Wray, E.J., Tao, Q., McAllister D., Rorrer, W.K., Aung, M., Martin, B.R., and Abood, M.E.(1999) Evaluation of the cannabinoid CB_2 receptor-selective antagonist, SR144528: further evidence for cannabinoid CB_2 receptor absence in the rat central nervous system. European Journal of Pharmacology **377**: 117-125

Hajos N., Katona I., Naiem S.S., Mackie K., Ledent C., Moody, I., Freund T.F (2000). Cannabinoids inhibit hippocampal GABAergic transmission and network oscillations. European Journal of Neuroscience **12**: 3239-3249

Hajos N., Ledent, C and Freund,T.F. (2001) Novel cannabinoid sensitive receptor mediates inhibition of glutamatergic synaptic transmission in the hippocampus. Neuroscience **106**:1-4

Hájos N.; Kathuria S.; Dinh T.; Piomelli D.; Freund T.F.(2004) Endocannabinoid transport tightly controls 2-arachidonoyl glycerol actions in the hippocampus: effects of low temperature and the transport inhibitor AM404. European Journal of Neuroscience **19**: 2991-2996

Haller, J., Mátyás, F., Soproni, K., Varga, B., Barsy, B., Németh, B., Mikics, É., Freund, T.F and Hájos, N (2007). Correlated species differences in the effects of cannabinoid ligands on anxiety and on GABAergic and glutamatergic synaptic transmission. European Journal of Neuroscience **25**: 2445–2456

Hansen, H.H., Hansen, S.T., Schousboe, A & Hansen, H.S (2000) Determination of the phospholipid precursor of anandamide and other N-Acylethanolamine phospholipids before and after sodium azide-induced toxicity in cultured neocortical neurons Journal of Neurochemistry **75**: 861–871

Harris, K.M., Marshall, P.E and Landis, D.M.D (1985). Ultra structure study of cholecystokinin- immunoreactive cells and processes in area CA1 of the rat hippocampus. The Journal of Comparative Neurology **233**:147-158

Hentges, S.T., Low, M.J and Williams, J.T (2005). Differential regulation of synaptic inputs by constitutively released endocannabinoids and exogenous cannabinoids. The Journal of Neuroscience **25**: 9746-9751

Herkenham,M., Lynn,A.B., Johnson,M.R., Melvin,L.S., de Costa. B.R., Rice,K.C (1991). Characterization and localisation of cannabinoid receptors in rat brain: A quantative in vitro autoradiographic study. The Journal of Neuroscience, **11**: 563-583.

Herkenham.M., Lynn, A.B., Little,M.D., Johnson M.R., Melvin L.S., De Costa B.R., Rice K.C. (1990) Cannabinoid receptor localisation in Brain. Proc.Natl.Acad.Sci.USA, Neurobiology. **87**:1932-1936

Higgs, H.N and Glomset, J.A (1994) Identification of a phosphatidic acid-preferring phospholipase A_1 from bovine brain and testis PNAS **91**: 9574-9578

Hill, D.R and Bowery, N.G (1981) ^{3}H-baclofen and ^{3}H-GABA bind to bicuculline insensitive $GABA_B$ sites in rat brain Nature **298**:149-152

Hillard, C.J., Edgemond, W.S., Jarrahian A., and Campbell W.B., (1997) Accumulation of N-Arachidonoylethanolamine (Anandamide) into Cerebellar Granule Cells Occurs via Facilitated Diffusion. Journal of Neurochemistry **69**: 631-638

Hillard, C.J., Manna, S., Greenberg, M.J., DiCamelli, R., Ross, R.A., Stevenson, L.A., Murphy, V., Pertwee, R.G and Campbell, W.B. (1999). Synthesis and characterization of potent and selective agonists of the neuronal cannabinoid receptor (CB_1). Pharmacology and Experimental Teraputics **289:** 1427-1433.

Ho, S.Y., Delgado, L and Storch, J (2002). Monoacylglycerol metabolism in human intestinal caco-2 cells. Evidence for metabolic compartmentation and hydrolysis. Journal of BiologicalChemistry **277**: 1816 – 1823

Hoffman A.F., Riegal A,C and Lupica.,C.R (2003) Functional localization of cannabinoid receptors and endogenous cannabinoid production in distinct neuron populations of the hippocampus. European Journal of Neuroscience **18**: 524-534

Hoffman, A.F & Lupica, C.R (2000). Mechanisms of cannabinoid inhibition of GABA(A) synaptic transmission in the hippocampus. The Journal of Neuroscience **20:** 2470-2479

Hohmann, A.G., Briley, E.M and Herkenham, M (1999). Pre- and postsynaptic distribution of cannabinoid and mu opiod receptors in rat spinal cord. Brain Research **822**: 17-25.

Hollrigel, G.S., Soltesz, I (1997) Slow kinetics of miniature IPSCs during early postnatal development in granule cells of the dentate gyrus. The Journal of Neuroscience **17**: 5119-6128

Hormuzdi, S.G., Pais, I., LeBeau, F.E.N., Towers, S.K., Rozov, A., Buhl, E.H., Whittington, M.A and Monye, H (2001). Impaired Electrical Signaling Disrupts Gamma Frequency Oscillations in Connexin 36-Deficient Mice. Neuron **31:** 487-495

Howlett, A.C (2002). The cannabinoid receptors. Prostaglandins & Other Lipid Mediators 68-69:619-631.

Howlett, A.C (2004). Efficacy in CB_1 receptor-mediated signal transduction. British Journal of Pharmacology **142**: 1209-1218

Huffman, J.W., Liddle, J., Yu, S., Aung, M., Abood, M.E., Wiley, J.L., and Martin, B.R. (1999) 3-(1,1-Dimethylbutyl)-1-deoxy- D-THC and related compounds: Synthesis of selective ligands for the CB_2 receptor. Bioorganic & Medicinal Chemistry **7**: 2905-2914

Ihanatovych, I., Novotny J., Haugvicova, R., Bourova, L., Mares, P and Svoboda, P (2002) Opposing changes of trimeric G protein levels during ontogentic development of rat brain. Developmental Brain Research **133**: 57-67.

Insausti R., Amaral DG., Cowan WM 1987 The entorhinal cortex of the monkey III subcortical afferents Journal of Comparative Neurology **264**: 396-408

Insausti R., Herro MT & Witter MP 1997 Entorhinal cortex of the Rat: cytoarchitectonic subdivisions and the origin and distribution of cortical efferents. Hippocampus **7:** 146-183.

Insausti, R., Marcos, P., Arroyo-Jiménez, M.M., Blaizot, X and Martínez-Marcos, A (2002) Comparative aspects of the olfactory portion of the entorhinal cortex and its projection to the hippocampus in rodents, nonhuman primates, and the human brain Brain Research Bulletin **57**: 557-560

Iwamura H., Suzuki H., Ueda Y., Kaya T and Inaba T (2001). In vitro and in vivo pharmacological characterization of JTE-907, a novel selective ligand for the CB_2 receptor.The Journal of Pharmacology and Experimental Theraputics **296**:420-425

Johnston, G.A.R (1996 a) $GABA_A$ receptor pharmacology. Pharmacology Theraputics **69**: 173-198

Johnston, G.A.R (1996b). $GABA_C$ receptors: Relatively simple transmitter- gated ion channels. Trends in Pharmaceutical Sciences **17**: 319-323

Jones, K.A., Borowsky, B.,.Tamm, J.A., Craig, D.A., Durkin, M.M., Dai, M., Yao, W.J., Johnson, M., Gunwaldsen, C., Huang, L.Y., Tang, C., Shen, Q., . Salon, J.A., Morse, K., Laz, T., Smith, K.E., Nagarathnam, D., Noble, S.A., Branchek, T.A and Gerald, C (1998) $GABA_B$ receptors function as a heteromeric assembly of the subunits $GABA_BR1$ and $GABA_BR2$. Nature **396**: 674-679

Jones, K.A., Tamm, J.A., Craig, D.A., Yao, W.J and Panico, R. (2000) Signal Transduction by $GABA_B$ Receptor Heterodimers. Neuropsychopharmacology **23,** S41-S49

Jones, R.S and Bühl, E.H (1993). Basket-like interneurones in layer II of the entorhinal cortex exhibit a powerful NMDA-mediated synaptic excitation. Neuroscience Letters.**149**: 35-9.

Katona I., Rancz E.A., Acsady L., Ledent C., Mackie K., Hajos N., Freund T F (2001). Distribution of CB_1 cannabinoid receptors in the Amygdala and their role in the control of GABAergic transmission. The Journal of Neuroscience **21**: 9506-9518

Katona I., Sperlagh, B., Sik A., Kafalvi, A., Sylvester, E., Mackie, K., and Freund T.F(1999) Presynaptically located CB_1 cannabinoid receptors regulate GABA release from axon terminals of specific hippocampal interneurons. The Journal of Neuroscience **19**: 4544-4558

Katona, I., Sperlágh, B., Maglóczky, Z. E., Sántha, A., Köfalvi, S., Czirják K., Mackie, E. Vizi S and Freund, T. F. (2000) GABAergic interneurons are the targets of cannabinoid actions in the human hippocampus. Neuroscience **100**: 797-804

Keinänen, K., Wisden, W., Sommer, B., Werner, P., Herb, A., Verdoorn, T.A., Sakmann, B., and Seeberg, P.H. (1990) A family of AMPA selective glutamate receptors. Science **249**: 556-560

Kim, J and Alger, B.E (2004). Inhibition of cyclooxgenase-2 potentiates retrograde endocannabinoid effects in hippocampus. Nature Neuroscience **7:** 697-698

Kirby, M. T., Hampson, R.E & Deadwyler, S.A (1995) Cannabinoids selectively decrease paired-pluse facilitation of perforant path synaptic potentials in dentate gyrus in vitro Brain Research **688**: 114-20

Klausberger, T., Marton, L.F., O'Neill, J., Huck, J.H.J ., Dalezios, Y ., Fuentealba, P., Suen,W.Y., Papp, E., Kaneko, T., Watanabe, M., Csicsvari, J. and Somogyi, P. (2005) Complementary roles of cholecystokinin-and parvalbumin-expressing GABAergic neurons in hippocampal network oscillations. The Journal of Neuroscience **25**: 9782-9793

Klink, R and Alonso, A (1997). Morphological characteristics of layer II projection neurons in the rat medial entorhinal cortex. Hippocampus **7:** 571-583

Kloosterman, F., Witter, M.P and Van Haeften, T (2003). Topographical and laminar organization of subicular projections to the parahippocampal region of the rat. The Journal of Comparative Neurology **455:**156-171

Köhler C (1986) Intrinsic connections of the retrohippocampal region in the rat brain II The medial entorhinal area. Journal of Comparative Neurology **246:** 149-169

Köhler, C & Chan-Palay, V (1982). The distribution of cholecystokinin-like immunoreactive neurons and nerve terminals in the retrohippocampal region in the rat and guinea pig. The Journal of Comparative Neurology **210:** 136-146

Kreitzer A.C & Regehr W.G (2001). Retrograde inhibition of presynaptic calcium influx by endogenous cannabinoids at excitatory synapses onto purkinje cells Neuron **29:** 717-727

Kreitzer, A.C and Regehr, W.G (2001) Cerebellar Depolarization-Induced Suppression of Inhibition Is Mediated by Endogenous Cannabinoids. Journal of Neuroscience **21**:RC174:1-5

Krimer, L.S., Herman, M.M., Saunders, R.C., Boyd, J.C., Hyde, T.M., Carter, J.M., Kleinman, J.E and Weinberger, D.R (1997) A qualitative and quantitative Analysis of the entorhinal cortex in schizophrenia. Cerebral Cortex **7**: 732-739

Liao C., Zheng J., David L.S., Nicholson R.A (2004). Inhibition of voltage-sensative sodium channels by the cannabinoid receptor antagonist AM-251 in mammalian brain. Basic and Clinical Pharmacology and Toxicology **94:** 73-78

Lichtman, A.H., Hawkins, E.G., Griffin, G and Cravatt, B.F (2002) Pharmacological activity of fatty acid amides is regulated, but not mediated, by fatty acid amide hydrolase in *vivo*. Journal of. Pharmacology Experimental. Theraputics **302:** 73-79

Ligresti, A., Morera, E., Van Der Stelt, M., Monory, K., Lutz, B ., Ortar, G and Di Marzo, V (2004). Further evidence for the existence of a specific process for the membrane transport of anandamide. Biochemistry Journal. **380** :265-272

Lingenhöhl, K and Finch, D.M (1991). Morphological characterization of rat entorhinal neurons in vivo: soma-dendritic structure and axonal domains. Experimental Brain Research **84:** 57-74

Llano, I., Leresche, N., Marty, A. (1991) Calcium entry increases the sensitivity of cerebellar Purkinje cells to applied GABA and decreases inhibitory synaptic currents. Neuron, **6:** 565 574.

Lopes da Silve, F.H., Witter, M.P., Boeijinga, P.H and Lohman, A.H.M (1990). Anatomical organisation and physiology of the limbic cortex. Physiological Reviews **70:** 453-511

López-Chávez, A., Miledi, R and Martínez-Torres, A (2005) Cloning and functional expression of the bovine $GABA_C$ ρ2 subunit Molecular evidence of a widespread distribution in the CNS. Neuroscience Research **53**: 421-427

Lorente de Nó, R (1933). Studies on the structure of the cerebral cortex I.The area entorhinalis. Journal psychol. Neurology 45: 381-438

MacDermott, A.B., Mayer, M.L ., Westbrook, G.L., Smith, S.J and Barker, J.L (1986). NMDA-receptor activation increases cytoplasmic calcium concentration in cultured spinal cord neurons. Nature **321**: 519-522

Mackie K & Hille B (1992) Cannabinoids inhibit N-type calcium channels in neuroblastoma-glioma cells. Proceedings of the National Academy of Sciences. USA **89**: 3825-3829

Maejima,T., Oka, S., Hashimotodani, Y., Ohno-Shosaku, T., Aiba, A., Wu, D., Waku, K., Sugiura,T and Kano, M (2005). Synaptically driven endocannabinoid release requires Ca^{2+}-assisted metabotropic glutamate receptor subtype 1 to phospholipase C β4 signaling cascade in the cerebellum. The Journal of Neuroscience, **25:** 6826-6835

Magazanik, L.G., Buldakova, S., Samoilova, M.V., Gmiro, V.E., Mellor, I.R and Usherwood, P.N. (1997) Block of open channels of recombinant AMPA receptors and native AMPA/ kainate receptors by adamantane derivatives. Journal of Physiology **505:** 655-663.

Marsicano G, Lutz B. (1999). Expression of the cannabinoid receptor CB1 in distinct neuronal subpopulations in the adult mouse forebrain. European Journal of Neuroscience **11:**4213-4225

Mato, S., Pazos, A and Valdizán, E.M (2002) Cannabinoid receptor antagonism and inverse agonism in response to SR141716A on cAMP production in human and rat brain European Journal of Pharmacology **443**: 43-46

Matsuda,L.A., Lolait S.J., Brownstein M.J., Young A.C., & Bonner T.I (1990) Structure of a cannabinoid receptor and functional expression of the cloned cDNA. Nature **346**: 561-564

Mayer , M.L., Westbrook, G.L and Guthrie, P.B (1984). Voltage dependent block by Mg^{2+} of NMDA responses in the spinal cord neurons. Nature **309**: 261-263

McAllister and Glass M (2002). CB1 and CB2 receptor-mediated signalling: A focus on endocannabinoids. Prostaglandins, Leukotrienes & Essential Fatty Acids. 66:161-171

McBain, C.J and Mayer, M.L (1994) N-methyl-D-aspartic acid receptor structure and function. Physiology Review. **74:** 723-760,

Mechoulam, R., Ben-Shabat, S., Hanus, L., Ligumsky, M., Kaminski, N.E., Schatz, A.R., Gopher, A., Almog, S., Martin, B.R., Compton, D.R., Pertwee, R.G., Griffin, G., Bayewitch, M., Barg, J and Vogel, Z. Identification of an endogenous 2 monoglyceride, present in canine gut, that binds to cannabinoid receptors Biochemical Pharmacology **50:** 83-90

Melis M, Pistis M, Perra S, Muntoni AL, Pillolla G, and Gessa GL. (2004) Endocannabinoids mediate presynaptic inhibition of glutamatergic transmission in rat ventral tegmental area dopamine neurons through activation of CB_1 receptors.Journal of Neuroscience **24**: 53-62

Meunier M, Cirilli L, Bachevalier J. (2006) Responses to affective stimuli in monkeys with entorhinal or perirhinal cortex lesions. The Journal of Neuroscience **26:** 7718-7722

Meunier, M and Bachevalier, J (2002). Comparison of emotional responses in monkeys with rhinal cortex or amygdala lesions. Emotion **2:** 147-161

Mikkonen M (1999) The human entorhinal cortex anatomic organisation and its alteration in Alzheimer's disease and temporal lobe epilepsy. doctoral dissertation University of Kuopia department of neuroscience and neurology and Al Virtanen institute.)

Miklaszewska, A.E., Gaubrusiewilz, K., Kaminska, B and Konarska, L. (2007) Distinctive pattern of cannabinoid receptor type II (CB_2) expression in adult and paediatric brain tumours. Brain Research **1137:** 161-169

Moldrich G., Wenger T. (2000). Localisation of the CB1 Cannabinoid Receptor in the rat brain an immunohistochemical study. Peptides **21**:1735-1742

Morozov YM, Freund TF. (2003) Post-natal development of type 1 cannabinoid receptor immunoreactivity in the rat hippocampus. European Journal of Neuroscience. **18:**1213-22.

Mukhopadhyay, S., Shim JY., Assi AA., Norford, D., Howlett, A.C (2002) CB1 cannabinoid receptor-G protein association: a possible mechanism for differential signalling. Chemistry and physics of Lipids. **121**: 91-109

Nakatsuka T., Chen H.X., Roper S.N., Gu J.G (2003). Cannabinoid receptor-1 activation suppresses inhibitory synaptic activity in human dentate gyrus. Neuropharmacology **45:** 116-121

Newman, Z., Malik, P., Wu, T.Y., Ochoa, C., Watsa, N and Lindgren, C.A (2007). Endocannabinoids mediate muscarine-induced synaptic depression at the vertebrate neuromuscular junction. European Journal of Neuroscience **25**:1619-1630.

Nowak, L., Bregestovski, P., Ascher, P., Herbert, A and Prochiantz, A (1984) Magnesium gates glutamate-activated channels in mouse central neurones. Nature **307**: 462-465

Núñez, E., Benito, C., Tolón, R.M., Hillard, C.J., Griffin, W.S.T and Romero, J. (2008) Glial expression of cannabinoid CB_2 receptors and fatty acid amide hydrolase are beta amyloid-linkked events in Down's syndrome. Neuroscience **151**: 104-110

Ohno-Shosaku T, Tsubokawa H, Mizushima I, Yoneda N, Zimmer A, Kano M. (2002 a) Presynaptic cannabinoid sensitivity is a major determinant of depolarization-induced retrograde suppression at hippocampal synapses. The Journal of Neuroscience **22**:3864-3872.

Ohno-Shosaku, T., Maejima, J., and Kano, M (2001) Endogenous cannabinoids mediate signals from depolarized post synaptic neurones to presynaptic terminals. Neuron **29**: 729-738

Ohno-Shosaku, T., Matsui, M., Yuko Fukudome, Jumpei Shosaku, Hiroshi Tsubokawa, Makoto M. Taketo, Toshiya Manabe and Masanobu Kano (2003) Postsynaptic M_1 and M_3 receptors are responsible for the muscarinic enhancement of retrograde endocannabinoid signalling in the hippocampus. European Journal of Neuroscience **18**: 109-116

Ohno-Shosaku,T., Shosaku, J., Tsubokawa, H., Kano, M (2002 b) Co-operative enddocannabinoid production by neuronal depolarisation and group I metabotropic glutamate receptor activation. European Journal of Neuroscience **15** 953-961

Okamoto, Y., Morishita, J., Tsuboi, K., Tonai, T and Ueda, N (2004). Molecular characterization of a phospholipase D generating anandamide and its congeners. Journal of Biological Chemistry. **279**: 5298-5305

Oliet S.H, Baimoukhametova D.V, Piet R, Bains J.S. (2007) Retrograde regulation of GABA transmission by the tonic release of oxytocin and endocannabinoids governs postsynaptic firing. Journal of Neuroscience **27**:1321333

Onaivi, E.S., Ishiguro, H., Gong, J.P., Patel, S., Perchuk, A., Meozzi, P.A., Myers, L., Mora, Z., Tagliaferro, P., Gardener, E., Bruscho, A., Akinshola, B.E., Liu, Q.R., Hope, B., Iwasaki, S., Arinami, T., Teasenfitz, L and Uhl, G.R (2006). Discovery of the presence and functional expression of cannabinoid CB_2 receptors in brain. Annals New York Academy of Sciences.**1074**:514-536

Oz, M (2006) Receptor-independent actions of cannabinoids on cell membranes: focus on endocannabinoids. Pharmacological Therapeutics. **111**: 114-44.

Ozawa,S., Kamiya, H and Tsuzuki, K (1998). Glutamate receptors in the mammalian central nervous system. Progress in Neurobiology **54**: 581-618

Pakkanen, J.S., Jokitalo, E., and Tuominen, R.K (2005) Up-regulation of $\beta 2$ and $\alpha 7$ subunit containing nicotinic acetylcholine receptors in mouse striatum at cellular level European Journal of Neuroscience **21**:2681–2691.

Pertwee R.G (2005) Inverse agonism and neutral antagonism at cannabinoid CB_1 receptors. Life Science **76**:1307-1324

Petralia, R.S., Wang, Y. X., Wenthold, R.J (1994) Histological and ultra structural localization of the kainate receptor subunits, KA2 and GluR6/7, in the rat nervous system using selective antipeptide antibodies. The Journal of Comparative Neurology **349**: 85-110

Pettit D.A.D., Harrison M.P., Olson J,M., Spencer R.F., Cabral G.A. (1998) Immunhistochemical localisation of the neural cannabinoid receptor in rat brain. Journal of Neuroscience Research **51**: 391-402

Piomelli D. 2003 The molecular logic of endocannabinoid signalling. Nature Reviews Neuroscience **4:** 873-884

Represa, A., Tremblay, E and Ben-Ari, Y (1987). Kainate binding sites in the hippocampal mossy fibers: Localization and plasticity. Neuroscience20: 739-748

Rhee, M.H., Bayewitch M., Avidor Reiss T., Levy R., Vogel Z (1998) Cannabinoid receptor activation differentially regulates the various adenylyl cyclase isoenzymes Journal of Neurochemistry **71**:1525-1534

Robbe D., Alonso G., Duchamp F., Bockaert J., Manzoni OJ (2001) Location and mechanisms of action of cannabinoid receptors at glutamatergic synapses of the mouse nucleus accumbens. Journal of Neuroscience **21**:109-116

Rodriguez-Mureno, A & Lerma, J (1998) Kainate receptor modulation of GABA release involves a metabotropic function. Neuron **20**: 1211-1218

Romero, J., Garcia-Palomero, E., Berrendero, F., Garcia-Gil, L., Hernandez, M.L., Ramos, J.A and Fernandez-Ruiz, J.J. (1997) Atypical location of cannabinoid receptors in white matter areas during rat brain development Synapse **26**: 317 – 323

Room & Groenewegen (1986) Study in the cat showing projections to the EC Journal of Comprative Neurology **251:** 415-450

Ross, R.A., Brockie, H.C., Stevenson, L.A., Murphy, V.L., Templeton, F., Makriyannis, A and Pertwee R.G (1999) Agonist-inverse agonist characterization at CB_1 and CB_2 cannabinoid receptors of L759633, L759656 and AM630 British Journal of Pharmacology **126**: 665-672

Ryberg, E., Larsson, N., Sjögren, S., Leonova, J., Elebring, T., Nilsson, K., Drmota, T and Greasley, P.J. (2007) The orphan receptor GPR55 is a novel cannabinoid receptor. British Journal of pharmacology **152**: 1092-1101.

Salio, C., Fischer, J., Franzoni, F and Conrath, M (2002). Pre-and postsynaptic localisations of the CB1 cannabinoid receptor in the dorsal horn of the rat spinal cord. Neuroscience **110**: 755-764

Sánchez-Pastor E, Trujillo X, Huerta M, Andrade F.(2007) Effects of cannabinoids on synaptic transmission in the frog neuromuscular junction. Journal of Pharmacological Experimental Theraputics. **32**: 439-44.

Sargolini F., Fyhn, M., Hafting, T., MaNaughton, B.L., Witter, M.P., Moser, M.B., Moser, E.I (2006) Conjunctive Representation of position, Direction and velocity in entorhinal cortex Science **312**: 758-762

Satake, S.I., Saitow, F., Yamada, J and Konishi, S (2000) Synaptic activation of AMPA receptors inhibits GABA release from cerebellar interneurons. Nature Neuroscience **3**: 551 – 558

Savinainen, J.R., Saario, S.M., Niemi, RJarvinen, T and Laitinen, J.T (2003). An optimized approach to study endocannabinoid signaling: evidence against constitutive activity of rat brain adenosine A_1 and cannabinoid CB_1 receptors. British Journal of Pharmacology **140**:1451-1459

Schatz, A.R., Lee, M., Condie, R.B., Pulaski, J.T., Kaminski, N.E (1996) Cannabinoid receptors CB_1 and CB_2: A characterization of expression and Adenylat Cyclase modulation with in the immune system.(1996)Toxicology and Applied Pharmacology **142**:278-287

Schlesinger, F., Tammena, D., Krampfl, K and Bufler, J. (2005). Two mechanisms of action of the adamantane derivative IEM-1460 at human AMPA-type glutamate receptors. British Journal of Pharmacology **145**: 656-663

Schwerdtfeger, W.K., Buhl,E.H and Germroth, P. (1990). Disynaptic olfactory input to the hippocampus mediated by stellate cells in the entorhinal cortex. The Journal of Comparative Neurology **292**: 163-177.

Sjöström, P.,Turrigiano, G., Nelson, S (2003). Neocortical LTD via coincident activation of presynaptic NMDA and cannabinoid receptors. Neuron, 39 641-654

Slanina, KA., Roberto, M and Schweitzer, P.(2005) Endocannabinoids restrict hippocampal long-term potentiation via CB1. Neuropharmacology **49**: 660-668

Soriano, E., Martinez, A., Fariñas, I and Frotsche, M (1993). Chandelier cells in the hippocampal formation of the rat: The entorhinal area and subicular complex. The Journal of Comparative Neurology **337**:151-167

Spencer, S.S and Spencer, D.D (1994) Entorhinal-Hippocampal Interactions in Medial Temporal Lobe Epilepsy. Epilepsia **35:** 721–727.

Steffenach, H.A Witter, M., Moser, M.B and Edvard I. Moser, E.I (2005) Spatial Memory in the rat requires the dorsolateral band of the entorhinal cortex. Neuron **45:** 301-313

Stella, N., Schweitzer, P and Piomelli, D (1997) A second endogenous cannabinoid that modulates long-term potentiation Nature **388**: 773-778

Steward, O and Scoville, S.A (1976). Cells of origin of entorhinal cortical afferents to the hippocampus and fascia dentate of the rat. The Journal of Comparative Neurology **169**: 347-370

Sugiura, T., Kodaka, T.,Nakane, S.,Miyashita, T.,Kondo, S., Suhara, Y., Takayama, H., Waku, K., Seki, C., Baba, N., and Ishima, Y (1999) Evidence That the Cannabinoid CB1 Receptor Is a 2-Arachidonoylglycerol Receptor. Structure-activity relationship of 2-arachidonylglycerol, ether-linked analogues and related compounds. Journal. Biological. Chemistry., 274: 2794 – 2801

Sugiura, T., Kondo, S., Kishimoto, S., Miyashita, T., Nakane, S., Kodaka, .Suhara, Y., Takayama, H and Waku, K (2000) Evidence that 2 arachidonoylglycerol but not N-Palmitoylethanolamine or anandamide Is the physiological ligand for the cannabinoid CB_2 receptor. Comparison of the agonist activities of various cannabinoid receptor ligands in HL-60 cells. Journal of Biological Chemistry. **275**: 605-612.

Sugiura, T., Kondo, S., Sukagawa, A., Tonegawa, T., Nakane, S., Yamashita, A., Ishima, Y. and Waku, K. (1996) Transacylase-mediated and phosphodiesterase-mediated synthesis of N-arachidonoylethanolamine, an endogenous cannabinoid-receptor ligand, in rat brain microsomes. Comparison with synthesis from free arachidonic acid and ethanolamine. European Journal of Biochemistry. **240**: 53–62.

Takahashi, K.A., Castillo, P.E (2006) The CB_1 cannabinoid receptor mediates glutamatergic synaptic suppression in the hippocampus Neuroscience **139:** 795-802

Takashi Maejima, Kouichi Hashimoto, Takayuki Yoshida, Atsu Aiba, and Masanobu Kano (2001) Presynaptic Inhibition Caused by Retrograde Signal from Metabotropic Glutamate to Cannabinoid Receptors. Neuron **31**: 463-475

Traub RD, Buhl EH, Gloveli T, Whittington MA. (2003). Fast rhythmic bursting can be induced in layer 2/3 cortical neurons by enhancing persistent Na+ conductance or by blocking BK channels. Journal of Neurophysiology. **89**: 909-21

Tsou K., Brown S., Sañudo-peña M.C., Mackie K., and Walker J.M. (1998) Immunohistochemical distribution of cannabinoid CB1 receptors in the rat rentral nervous system. Neuroscience **83**: 393-411

Tsou K., Mackie, K., Sañudo-Peña*, M. C. and Walker J. M (1999) Cannabinoid CB_1 receptors are localized primarily on cholecystokinin-containing GABAergic interneurons in the rat hippocampal formation Neuroscience **93:** 969-975

Twitchell, W., Brown, S., and Mackie K (1997) Cannabinoids Inhibit N- and P/Q-type calcium channels in cultured rat hippocampal neurons. The Journal of Neurophysiology **78:**43-50

Van Haeften T, Baks-te-Bulte, L., Goede, P., Wouterlood, F.G., and Witter, M.P (2003). Morphological and numerical analysis of synaptic interactions between neurons in deep and superficial layers of the entorhinal cortex of the rat. Hippocampus **13**: 943-952

Van Hoesen, G.W and Pandya, D.N (1975). Some connections of the entorhinal (area 28) and perirhinal (area 35) cortices of the rhesus monkey. I. Temporal lobe afferents. Brain Research **95**: 1-24

Van Hoesen, G.W., Pandya, D.N. and Butters, N. (1972). Cortical afferents to the entorhinal cortex of the rhesus monkey Science **175**: 1471-1473

Van Sickle, M.D., Duncan, D., Kingsley, P.J., Mouihate, A., Urbani, P., Mackie, K., Stella, N., Makriyannis, A., Piomelli, D., Davison, J.S., Marnett, L.J., Di Marzo,V., Pittman,Q.J., Patel, K.D and Sharkey, K.A (2005). Identification and Functional Characterization of Brainstem Cannabinoid CB_2 Receptors. Science **310**:329-332

Varma, N., Carlson, G.C., Ledent, C and. Alger B.E (2001) Metabotropic glutamate receptors drive the endocannabinoid system in hippocampus. The Journal of Neuroscience **21**: RC188:1-5

Wang,H., Dey, S.K and Maccarrone, M., (2006) Jekyll and Hyde: Two faces of cannabinoid signalling in male and female fertility. Endocrine Reviews **27**; 427-448

Werner, P., Voigt, M., Keinänen, K., Wisden, W & Seeburg, P.H (1991) Cloning of a putative high-affinity kainate receptor expressed predominantly in hippocampal CA3 cells. Nature **351**: 742-744

Whittington MA, Traub RD, Jefferys JG. (1995) Synchronized oscillations in interneuron networks driven by metabotropic glutamate receptor activation. Synchronized oscillations in interneuron networks driven by metabotropic glutamate receptor activation. Nature **373**: 563-4

Wilson R.I., Nicoll R.A. (2001). Endogenous cannabinoids mediate retrograde signaling at hippocampal synapses. Nature **410**: 588-592

Wilson, R.I & Nicoll R.A (2002) Endocannabinoid signalling in the brain. Science **296:** 678-82.

Wilson, R.I., Kunos, G and Nicoll, R.A (2001) Presynaptic specificity of endocannabinoid signaling in the hippocampus. Neuron **31**: 453-462.

Witter MP & Groenewegen HJ 1984 Laminar origin and septotemporal distribution of Entorhinal and perirhinal projections to hippocampus in cat. The Journal of Comparative Neurology 224: 371-385

Witter, M.P., Groenewegen, H.J., Lopes da Silva, F.H and Lohman, A.H.M. (1989) Functional organization of the extrinsic and intrinsic circuitry of the parahippocampal region Progressive Neurobiology. 33:161-253.

Woodhall, G.L., Bailey, S.J., Thompson, S.E.,Evans, D.I.P and Jones, R.S.G (2005) Fundamental differences in spontaneous synaptic inhibition between deep and superficial layers of the rat entorhinal cortex. Hippocampus **15**: 232 – 245

Woodhall, G.L., Evans, D.I., Cunningham, M.O and Jones, R.S.G (2001). NR2B-containing NMDA autoreceptors at synapses on entorhinal cortical neurones. Journal of Neurophysiology **86**: 1644-1651

Wouterlood FG., Härtig W., Brückner G., Witter MP (1995). Parvalbumin immunoreactiv neurones in the Entorhinal cortex of the rat: localization, morphology, connectivity and ultrstrucure. Journal of Neurocytology **24**: 153-143

Wouterlood FG., van Denderen J., van Haeften T., Witter MP (2000) Calretinin in the entorhinal cortex of the rat: distribution, morphology, ultra structure of neurons and co-localisation with γ-amino butyric acid and parvalbumin. Journal of Comparative Neurology **425**:177-192

Wouterlood, F.G., Mugnaini, E and Nederlof, J. (1985) Projection of olfactory bulb efferents to layer I GABAergic neurons in the entorhinal area. Combination of anterograde degeneration and immunoelectron microscopy in rat. Brain Research, **343**: 283-296

Wóznicka A., Malinowska M and Kosmel A 2006. Cytoarchitectonic organisation of the entorhinal cortex of the canine brain. Brain Research **52:** 346-367